

Endocannabinoid regulation of gastric vagal
afferent signalling

Stewart Christie

A thesis submitted for the degree of
Doctor of Philosophy



Adelaide Medical School
Faculty of Health and Medical Sciences
The University of Adelaide

Australia

May 2020

Contents

Abstract.....	iv
Statement of Declaration	vi
Acknowledgements.....	vii
Publications.....	viii
Conference Proceedings	x
List of Figures	xi
List of Tables	xiii
List of Abbreviations	xiv
Chapter 1 : General Introduction	1
1.1 Obesity.....	2
1.1.1 Bariatric Surgery	5
1.2 Regulation of Food Intake	7
1.2.1 Central Food Intake Regulation.....	7
1.2.2 Peripheral Food Intake Regulation	11
1.2.2.1 Gastrointestinal signals	14
1.3 Vagal Nerve.....	22
1.3.1 Gastrointestinal Vagal Afferents	23
1.3.3 Vagal Afferents and Diet-Induced Obesity	30
1.4 Endocannabinoid System	31
1.5 Growth Hormone Secretagogue Receptor.....	47
1.6 Transient receptor potential channels.....	50

1.6.2 TRPV1 and Food Intake.....	55
1.7 TRPV1 and the Endocannabinoid System	58
1.9 Thesis Outline.....	63
Chapter 2 : Materials and Methods.....	64
Chapter 3 : Biphasic effects of methanandamide on murine gastric vagal afferent mechanosensitivity.....	92
Chapter 4 : Modulatory effect of methanandamide on gastric vagal afferents depends on nutritional status.....	121
Chapter 5 : A high fat diet alters endocannabinoid and ghrelin mediated regulation of endocannabinoid pathway expression in nodose ganglia	155
Chapter 6 : General Conclusions	177
Chapter 7 : References	188
Chapter 8 Appendix: Published Literature Review	261

Abstract

Background: Gastric vagal afferents (GVAs) play a role in peripheral appetite control. Tension sensitive GVAs respond to stretch or distension of the stomach sending signals to the hindbrain to produce feelings of fullness and satiety. The sensitivity of tension sensitive GVAs is reduced in diet-induced obesity which may contribute to increased meal size. Further, transient receptor potential vanilloid 1 (TRPV1) knockout mice also show decreased GVA tension receptor sensitivity.

Endocannabinoids (ECs) regulate appetite via cannabinoid 1 (CB1) receptors and are also endogenous ligands for TRPV1. The CB1 receptor and TRPV1 are expressed on GVAs and the CB1 receptor is also expressed on gastric ghrelin cells. Further, the endocannabinoid anandamide (AEA; ligand for CB1) is expressed in the stomach. However, it is not known if ECs, ghrelin, and TRPV1 interact to regulate GVA sensitivity.

Aims: To determine in lean and diet induced obese mice:

1. The co-expression of CB1, TRPV1, and ghrelin receptor (growth hormone secretagogue receptor; GHSR) in individual GVA cell bodies.
2. The effect of AEA on GVA sensitivity and secondary messenger pathways involved.
3. The effect of AEA and ghrelin on the expression of orexigenic receptors in nodose ganglia.

Methods: Retrograde tracing was used to identify single GVA cell bodies in the nodose ganglia which was then combined with single cell QRT-PCR. An *in vitro* electrophysiology preparation was used to determine the effects of methanandamide (mAEA; stable analogue of AEA) on the sensitivity of GVAs in C57BL/6 mice fed *ad*

libitum with either a standard laboratory diet (SLD) or high fat diet (HFD). This was performed with mAEA alone or in combination with antagonists to determine possible secondary messenger pathways. Nodose ganglia were cultured for 14 hours in a medium containing mAEA or ghrelin and then analysed via QRT-PCR for changes in receptor or ion channel expression.

Results: CB1, TRPV1, and GHSR were expressed and co-expressed in individual tension sensitive GVA neurons in a diet-dependent manner. In SLD-mice mAEA exhibited concentration-dependent dual inhibitory and excitatory effects on the mechanosensitivity of tension sensitive GVAs. This was abolished to a single inhibitory effect regardless of concentration in HFD-mice.

In cultured vagal afferent cell bodies, exposure to mAEA and ghrelin altered the expression of CB1, TRPV1, and GHSR mRNA in a diet dependent manner.

Conclusions: ECs, acting through CB1 and TRPV1, have a pivotal role in modulating GVA satiety signals depending on the second messenger pathway utilised. In HFD-mice only an inhibitory effect is observed. These changes may contribute to the development and/or maintenance of obesity.

Statement of Declaration

I certify that this work contains no material which has been accepted for the award of any other degree or diploma in my name, in any university or other tertiary institution and, to the best of my knowledge and belief, contains no material previously published or written by another person, except where due reference has been made in the text. In addition, I certify that no part of this work will, in the future, be used in a submission in my name, for any other degree or diploma in any university or other tertiary institution without the prior approval of the University of Adelaide and where applicable, any partner institution responsible for the joint-award of this degree.

I acknowledge that copyright of published works contained within this thesis resides with the copyright holder(s) of those works.

I also give permission for the digital version of my thesis to be made available on the web, via the University's digital research repository, the Library Search and also through web search engines, unless permission has been granted by the University to restrict access for a period of time.

I acknowledge the support I have received for my research through the provision of an Australian Government Research Training Program Scholarship.

Stewart Christie

Acknowledgements

I would first like to thank my supervisors Amanda Page and Hui Li for their guidance and support during my candidature. I would also like to thank Gary Wittert for his intellectual input and guidance in paper writing. To the members of the vagal afferent research group, Rebecca O’Rielly, Maria Nunez, Yoko Wang and Prem Shakya, I would like to thank you for your help at various stages with my experiments.

I would also like to thank my parents, Susan and Darren Christie who have encouraged me across my education from my bachelors to my PhD. Lastly, I would like to thank my partner Jamie Ramsay, and my mother in-law, Fiona Ramsay, for their support during my PhD.

Publications

Publications from thesis

Christie S., Wittert GA., Li H., Page AJ., 2018. The Involvement of TRPV1 Channels in Energy Homeostasis. *Frontiers in Endocrinology.* **9**:420, DOI: 10.3389/fendo.2018.00420

Christie S., O'Reilly R., Li H., Wittert GA., Page AJ., 2019. Biphasic effects of methanandamide on murine gastric vagal afferent mechanosensitivity. *Journal of Physiology.* DOI: 10.1113/JP278696

Christie S., O'Reilly R., Li H., Nunez-Salces M., Wittert GA., Page AJ., 2020. Modulatory effect of methanandamide on gastric vagal afferent satiety signals depends on nutritional status. *Journal of Physiology*

Christie S., O'Rielly R., Li H., Wittert GA., Page AJ., (Pending). High fat diet induced obesity alters endocannabinoid and ghrelin mediated regulation of components of the endocannabinoid system in nodose ganglia. *Submitted to Peptides*

Additional publications

Christie S., Li H., Frisby CL., Kentish SJ., O'Reilly R., Wittert GA., Page AJ., 2018. A rotating light cycle promotes weight gain and hepatic lipid storage in mice. *American Journal of Physiology: Gastrointestinal and Liver Physiology.* DOI: 10.1152/ajpgi.00020.2018

Li H., Buiman-Pijlman FTA., Nunez-Salces M., **Christie S.,** Frisby CL., Inserra A., Hatznikolas G., Lewis MD., Kritas S., Wong ML., Page AJ. 2019. Chronic stress induces hypersensitivity of murine gastric vagal afferents. *Neurogastroenterology and Motility.* DOI: 10.1111/nmo.13669

Kentish SJ., **Christie S.**, Vincent A, Li H., Wittert GA., Page AJ. 2019. Disruption of the light cycle ablates diurnal rhythms in gastric vagal afferent mechanosensitivity. *Neurogastroenterology and Motility*. DOI: 10.1111/nmo.13711

Page, A.J., Li, H., **Christie, S.**, Symonds, E. 2020. Circadian regulation of appetite and the benefits of time restricted feeding. *Submitted to Physiology and Behaviour*

Conference Proceedings

O’Rielly R., **Christie S.**, Flach C., Hatznikolas G., Li H., Thompson N., Wittert G., Page A, (2017). Restricted feeding restores circadian rhythmicity of hepatic metabolic markers and reduces weight gain in high fat diet-induced obese mice. (Oral presentation) ANZOS and Obesity Surgery Society of Australia and New-Zealand Joint Meeting, Adelaide, Australia.

Christie S., Li H., O’Rielly R., Wittert G., Page A., (2018), Modulation of gastric vagal afferents by endocannabinoids (Poster). Australian and New Zealand Obesity Society 2018, Melbourne, Australia

Christie S., Li H., O’Rielly R., Wittert G., Page A., (2018), Modulation of gastric vagal afferents by endocannabinoids (Poster). The Obesity Society 2018, Nashville, Tennessee, USA

Christie S., Li H., O’Rielly R., Nunez M., Wittert G., Page A., (2019). Modulatory effects of methanandamide on gastric vagal afferents depend on nutritional status (Poster). The Society for the Study of Ingestive Behaviour 2019, Utrecht, Netherlands

Christie S., Li H., O’Rielly R., Nunez M., Wittert G., Page A., (2019). Modulatory effects of methanandamide on gastric vagal afferents depend on nutritional status (Oral presentation). Australian and New Zealand Obesity Society 2019, Sydney, Australia

Christie S., Li H., O’Rielly R., Nunez M., Wittert G., Page A., (2019). Modulatory effects of methanandamide on gastric vagal afferents depend on nutritional status (Oral presentation). The Obesity Society 2019, Las Vegas, Nevada, USA

List of Figures

Figure 1.1: Different bariatric surgeries.	6
Figure 1.2: Hypothalamic nuclei involved in appetite regulation.	10
Figure 1.3 Peripheral regulation of appetite.	17
Figure 1.4: Typical response of mechanosensitive mucosal or tension gastric vagal afferent receptors to mucosal stroking or circular tension [215].	26
Figure 1.5: The structure and vagal afferent innervation of the gastrointestinal wall.	27
Figure 1.6: Generalised structure of the cannabinoid receptors.	34
Figure 1.7: Cellular localisations of the cannabinoid receptors [252].	35
Figure 1.8: Different signalling pathways utilised by cannabinoid receptors.	37
Figure 1.9: Synthesis and degradation of endocannabinoids.	43
Figure 1.10: Structural components of a TRPV1 subunit [399].	53
Figure 1.11: Interactions between endocannabinoids and TRPV1.	60
Figure 2.1: Retrogradely traced tension sensitive gastric vagal afferent cell bodies in mouse nodose ganglia.	67
Figure 2.2: Immunolabelling of TRPV1, CB1, and GHSR in nodose ganglia cell bodies.	72
Figure 2.3: In vitro gastric vagal afferent preparation [215].	74
Figure 2.4: Mechanosensitivity of tension and mucosal gastric vagal afferents over time.	77
Figure 2.5: Response of tension sensitive gastric vagal afferents to antagonists.	81
Figure 2.6: Response of tension sensitive gastric vagal afferents to ethanol.	81
Figure 2.7: Standard curve of ELISA kits.	85
Figure 3.1: CB1, TRPV1, and GHSR are co-expressed in tension sensitive gastric vagal afferent neurons.	107

Figure 3.2: Methanandamide has dose-dependent biphasic effects on tension sensitive but not mucosal gastric vagal afferents.....	110
Figure 3.3: The inhibitory and excitatory effects of methanandamide on gastric vagal afferent mechanosensitivity, are mediated by CB1 and TRPV1.	111
Figure 3.4: The inhibitory effect of methanandamide on gastric vagal afferent mechanosensitivity is mediated by $G\alpha_{i/o}$ – PKA, and GHSR pathways.	113
Figure 3.5: The excitatory effect of methanandamide is mediated by $G\alpha_q$ and PKC pathways.	114
Figure 3.6: Schematic of the possible pathways for the inhibitory and excitatory effects of methanandamide on gastric vagal afferent mechanosensitivity.	119
Figure 5.1: High fat diet fed mice gained more weight than standard laboratory diet fed mice.....	165
Figure 5.2: Methanandamide exposure alters TRPV1, GHSR, CB1, and FAAH expression.	169
Figure 5.3: Ghrelin exposure alters TRPV1, GHSR, CB1, and FAAH expression.....	172
Figure 6.1: Overall schematic of the peripheral vagal afferent system linking together the studies in this thesis.	184
Figure 8.1: Structure of a TRPV1 subunit.	269
Figure 8.2: Schematic of the synthesis, degradation and action of endocannabinoids at cannabinoid receptors.	272
Figure 8.3: Interaction between endocannabinoids, TRPV1 and CB1.	275
Figure 8.4: Browning of WAT by TRPV1 activation.	285
Figure 8.5: TRPV1 mediated activation of thermogenic activity in BAT.	286

List of Tables

Table 1.1 History of weight loss drugs	4
Table 1.2: Gastrointestinal hormone functions and their regulation by nutrients.	22
Table 1.3: Human studies of capsaicin supplementation on food intake.....	57
Table 2.1: Details of housekeeping genes tested in single nodose neurons	69
Table 2.2: Details of the antagonists used in electrophysiology studies	79
Table 2.3: Details of housekeeping genes tested in gastric mucosa scrapings	83
Table 2.4: Details of housekeeping genes tested in cultured nodose neurons	88
Table 8.1: Effects of Capsaicin Supplementation on food intake and metabolism in Humans	278

List of Abbreviations

Δ^9 -THC	Δ^9 -Tetrahydrocannabinol
2-AG	2-Arachidonoylglycerol
AEA	Anandamide
AgRP	Agouti Related Peptide
ARC	Arcuate Nucleus
BIS-II	Bisindolylmaleimide 2
BKCa	Calcium Activated Potassium Channel
BMI	Body Mass Index
cAMP	Cyclic Adenosine Monophosphate
CART	Cocaine and Amphetamine Regulated Transcript
CB	Cannabinoid
CCK	Cholecystokinin
CNS	Central Nervous System
CRH	Corticotrophin Releasing Hormone
DAG	Diacylglycerol
DAGL	Diacylglycerol Lipase
DMN	Dorsal Medial Nucleus
DMV	Dorsal Motor Nucleus of the Vagus
FAAH	Fatty Acid Amide Hydrolase

FABP	Fatty Acid Binding Protein
FFA	Free Fatty Acid
GPCR	G-Protein Coupled Receptor
GHSR	Growth Hormone Secretagogue Receptor
GLP-1	Glucagon Like Peptide-1
GVA	Gastric Vagal Afferent
IGLE	Intraganglionic Lamina Ending
IMA	Intramuscular Array
IP ₃	Inositol Triphosphate
LHA	Lateral Hypothalamic Area
mAEA	Methanandamide
MAG	Monoacylglycerol
MAGL	Monoacylglycerol Lipase
MAPK	Mitogen Activated Protein Kinase
MCH	Melanin Concentrating Hormone
MCR	Melanocortin Receptor
MSH	Melanocyte Stimulating Hormone
NAE	N-Acylethanolamine
NAPE	N-acylphosphatidyl Ethanolamine
NAPE-PLD	NAPE hydrolysing phospholipase D

NPY	Neuropeptide Y
NTS	Nucleus Tractus Solitarius
OLDA	N-Oleodopamine
PI3K	Phosphoinositide 3 Kinase
PIP ₂	Phosphatidylinositol 4,5-bisphosphate
PLA-AT	Phospholipase A-Acyltransferase
PLC	Phospholipase C
PKA	Protein Kinase A
PKA-IFA	PKA Inhibitor Fragment (6-22) Amide
PKC	Protein Kinase C
PNS	Peripheral Nervous System
POMC	Proopiomelanocortin
PtdEtn	Phosphatidyl Ethanolamine
PtdIn	Phosphatidyl Inositol
PVN	Paraventricular Nucleus
PYY	Peptide Tyrosine-Tyrosine
TRP	Transient Receptor Potential
TRPV1	Transient Receptor Potential Vanilloid 1
VMN	Ventral Medial Nucleus

Chapter 1 : General Introduction

1.1| Obesity

Generally, obesity develops when energy intake outweighs energy expenditure leading to excessive accumulation of adipose tissue. For adults obesity is defined by a body mass index (BMI; kg/m²) of 30 or higher [1]. Differently, for children obesity is determined by the child's age and sex on a percentile scale [2]. Currently, world-wide it is estimated that approximately 604 million adults and 108 million children are obese; figures that have tripled since 1980 [3]. This increase is likely a result of society adopting a more sedentary life style with an increase in consumption of caloric dense foods [4].

Coupled with obesity is the development of several co-morbidities including cardiovascular disease, type 2 diabetes, and certain types of cancer [5]. It is estimated that the risk of death associated with obesity and its related disorders increases nearly 3-fold with the life span of obese individuals being 7 to 14 years less than that of those with a healthy weight [6]. Further, obese individuals spend 36% more on healthcare [7]. In Australia annual obesity related health care costs are over \$130 billion [8], placing significant strains on healthcare systems.

Prevention and treatment strategies

Current prevention or treatment strategies for obesity include behavioural, pharmacological, and surgical interventions.

Behavioural interventions attempt to reduce weight by decreasing caloric dense foods and increasing physical activity. Whilst behavioural methods have proven effective in reducing weight, adherence to this life style typically diminishes over time with individuals regaining weight [9]. Further, the post-obese metabolic state differs to a never obese metabolic state which can contribute to weight regain. For example, rates of fat

oxidation are significantly lower in post-obese compared to never obese individuals [10]. Governments have attempted to aid in behavioural interventions by introducing policies such as the sugar sweetened beverage tax and comprehensive nutritional labelling of food products [11, 12]. However, the efficacy of these is not currently known.

Details of pharmacological interventions are illustrated in Table 1.1. Pharmacological interventions target both the central and peripheral systems. Short-term use drugs such as phentermine and mazindol are derivatives of amphetamine [13]. This class of drugs suppresses appetite and increases lipolysis by increasing the release, or preventing the reuptake, of norepinephrine from central neurons, [13, 14]. However, their effectiveness diminishes after one month, and can cause several unwanted side effects including high blood pressure and restlessness [15]. Other drugs such as Orlistat target the periphery, inhibiting gastrointestinal lipases and decreasing lipid absorption [16] However, Orlistat has unwanted side effects including steatorrhea [17] and risk of acute kidney disease [18]. Recent drugs such as liraglutide were approved for the control of blood glucose levels in diabetics, and are also approved as weight loss drugs [19]. Data on the side effects of liraglutide are limited, however, there is a possible increased risk of pancreatitis [19].

Table 1.1 History of weight loss drugs

Drug name	Approval year	Metabolic effects	Mechanism of action	Adverse side effects	Current status
Phentermine	1959	Increased lipolysis Decreased appetite [20]	Norepinephrine release [20]	Tachycardia [21] Insomnia [22] Urinary retention [15]	Available controlled [23]
Mazindol	1960	Increased lipolysis Decreased appetite [24]	Norepinephrine reuptake inhibitor [13]	Hypertension [25]	Available controlled [13]
Fenfluramine	1963	Decreased appetite [26]	Serotonin release [26]	Pulmonary hypertension [27] Cardiac fibrosis [28]	Withdrawn [15]
Aminorex	1965	Decreased appetite [29]	Catecholamine release [29]	Pulmonary hypertension [30]	Withdrawn [31]
Sibutramine	1995	Decreased appetite [32]	Monoamine reuptake inhibitor [32]	High stroke risk [32] High blood pressure [33] Cardiac arrhythmia [34]	Withdrawn [35]
Orlistat	1999	Prevent fat absorption [36]	Pancreatic lipase inhibitor [36]	Steatorrhea [37] Kidney injury [18] Colonic lesions [38]	Available controlled [39]
Rimonabant	2006	Decreased appetite [40]	CB1 receptor antagonist [40]	Depression [41] Suicidal thoughts [42] Fatty acid reflux [43]	Withdrawn [44]
Bupropion/natrxone	2010	Decreased appetite Increased energy output [45]	Norepinephrine release POMC neuron activation [45]	Mood changes [46]	Available controlled [47]
Lorcaserin	2012	Decreased appetite [48]	Serotonin receptor agonist [48]	Hallucinogen at high doses [49]	Available controlled [50]
Liraglutide	2014	Decreased appetite [51]	GLP-1 agonist [51]	Pancreatitis risk [19]	Available controlled [52]

1.1.1| Bariatric Surgery

Surgical interventions such as gastric banding, sleeve gastrectomy, and roux en-y bypass aim to promote weight loss by reducing gastric capacity and/or nutrient absorption.

Gastric banding involves the placement of an inflatable silicone band around the upper portion of the stomach to create a small pouch (Figure 1.1). This method decreases the amount of food consumed without affecting nutrient absorption, and is completely reversible [53]. However, gastric banding may not be suitable for individuals who have had previous abdominal surgery that may impact band placement [54].

A sleeve gastrectomy involves the removal of a large portion of the stomach along the greater curvature (Figure 1.1) [55]. This procedure reduces food consumption, however, a sleeve gastrectomy is irreversible and can cause deficiencies in folate and iron [56, 57]. This procedure is suitable for morbidly obese individuals, however, it is not suitable for individuals that have inflammatory bowel disease or portal hypertension [58].

A roux en Y gastric bypass involves the creation of a small gastric pouch from the upper stomach which is then connected to the small intestine (Figure 1.1) [59]. Variations of this procedure exist depending on which portion of the small intestine (i.e. proximal or distal) is connected to the small pouch [60]. This procedure reduces gastric capacity, however, it also reduces nutrient absorption causing nutrient deficiencies [61]. Further, a roux en Y gastric bypass also causes vagal denervation [62], and alters endocrine responses, although this is conflicting. For example, some studies indicate that, in roux en Y gastric bypass patients, the post prandial decrease of ghrelin is attenuated [63, 64], whilst a different study indicates it is exaggerated [65].

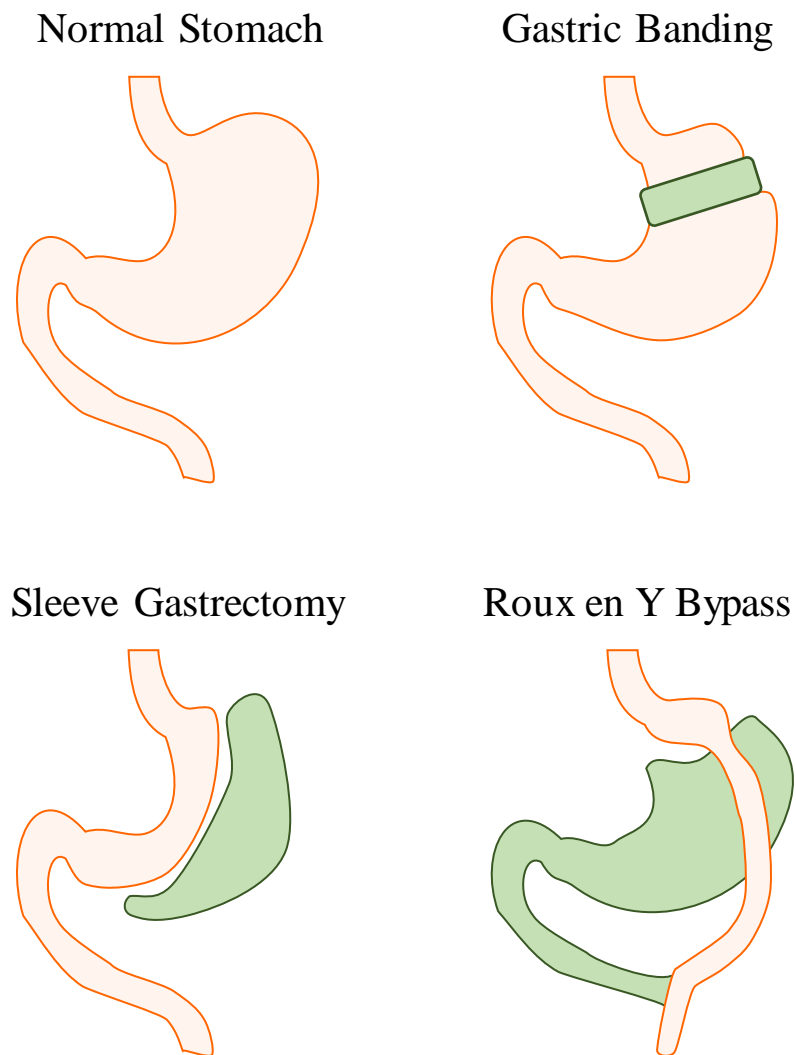


Figure 1.1: Different bariatric surgeries.

Gastric banding is a reversible procedure aimed at reducing food intake via the application of a band around the upper stomach. A sleeve gastrectomy is an irreversible procedure aimed at reducing stomach capacity by removing a large portion of the stomach along the greater curvature. A roux en Y bypass also reduces stomach capacity via the formation of a small gastric pouch that is directly connected the small intestine. This procedure bypasses the stomach and part of the duodenum, which can lead to malabsorption of nutrients.

Recent Progress

Recently, research has turned to appetite regulation in the gastrointestinal system. Aside from the digestion and absorption of nutrients, the gastrointestinal tract secretes hormones that can influence food intake via the circulation or vagal afferent nerves. Further, vagal afferent neurons are also mechanosensitive and can be regulated by food intake. Improving our understanding of the gastrointestinal appetite signalling pathways will provide potential targets for the treatment of obesity. Peripheral approaches without disturbing the CNS may induce less side effects.

1.2| Regulation of Food Intake

Energy intake is essential for life and as a consequence evolution has developed an intricate multilevel system to control food intake and energy expenditure to maintain life. This is particularly important for the maintenance of a healthy body weight. Signals from energy stores (e.g. adipose tissue) serve as long term regulators of food intake. Conversely, for the short term regulation of food intake, upon food ingestion the central nervous system (CNS) receives a multitude of signals to integrate and process, eventually producing feelings of fullness and satiety leading to meal termination. However, in obesity these signals become dysregulated leading to an increased appetite or latency in meal termination.

1.2.1| Central Food Intake Regulation

The central regulation of food intake is complex with the CNS receiving a variety of peripheral hormonal and neural inputs. Central areas involved in appetite regulation

include the hypothalamus, brain stem, and telencephalic areas such as the amygdala and nucleus accumbens.

Hypothalamus

The hypothalamus is composed of many nuclei with various functions directed towards one goal, homeostasis [66]. The medial aspect of the hypothalamus has a weak blood brain barrier and can therefore transmit blood borne signals to other hypothalamic nuclei. Conversely, the lateral aspect of the hypothalamus does not interact with blood borne signals but has extensive intra and extra hypothalamic connections [66]. In relation to food intake the most relevant hypothalamic areas include the arcuate nucleus (ARC), paraventricular nucleus (PVN), lateral hypothalamic area (LHA), ventral medial nucleus (VMN) and dorsal medial nucleus (DMN; Figure 1.2).

The ARC is located in the mediobasal hypothalamus and therefore can be regulated by blood borne signals; however it also receives neuronal inputs from the brainstem. Within the ARC there are two distinct opposing populations of nuclei: those that express pro-opiomelanocortin (POMC) [67] and cocaine and amphetamine regulated transcript (CART) [68], and those that express neuropeptide Y (NPY) and agouti-related peptide (AgRP) [69].

POMC/CART neurones are considered anorexigenic with their activation reducing food intake. These neurons can be stimulated by leptin and insulin, and indirectly inhibited by ghrelin via increased AgRP neuron signalling [70]. POMC is a precursor for many peptides, among which is α -melanocyte stimulating hormone (α -MSH) [71]. α -MSH binds to the melanocortin 3 receptor (MC3R) or MC4R to inhibit food intake [72, 73].

The receptor for CART is yet to be identified, however, chronic CART administration decreases food intake [74].

Conversely, NPY/AgRP neurones are considered orexigenic with their activation increasing food intake [75, 76]. These neurons can be stimulated by ghrelin and inhibited by leptin and peptide tyrosine-tyrosine (PYY) [77]. NPY binds to Y1 receptors [78] and AgRP antagonises MC3R and MC4R to prevent α -MSH binding and inhibition of food intake.

POMC/CART and NPY/AgRP neurons in the ARC project heavily to other hypothalamic nuclei including the PVN, LHA, VMN, and DMN [79]. The PVN is considered anorexigenic [80], being stimulated by POMC/CART neurons and inhibited by NPY/AgRP neurons [66]. Further, the PVN also receives inputs from the amygdala for stress and reward related regulation of food intake [81]. Conversely, the LHA is considered orexigenic and contains two populations of neurons expressing either orexin or melanin concentrating hormone (MCH) [82, 83]. These subsets of neurons are stimulated by NPY/AgRP neurons and inhibited by POMC/CART neurons [66]. Further, the LHA also receives projections from the nucleus accumbens and amygdala to regulate reward related food intake behaviour [84].

Lastly, the VMN and DMN also receive projections from the ARC where they are stimulated by POMC/CART neurons and inhibited by NPY/AgRP neurons [66].

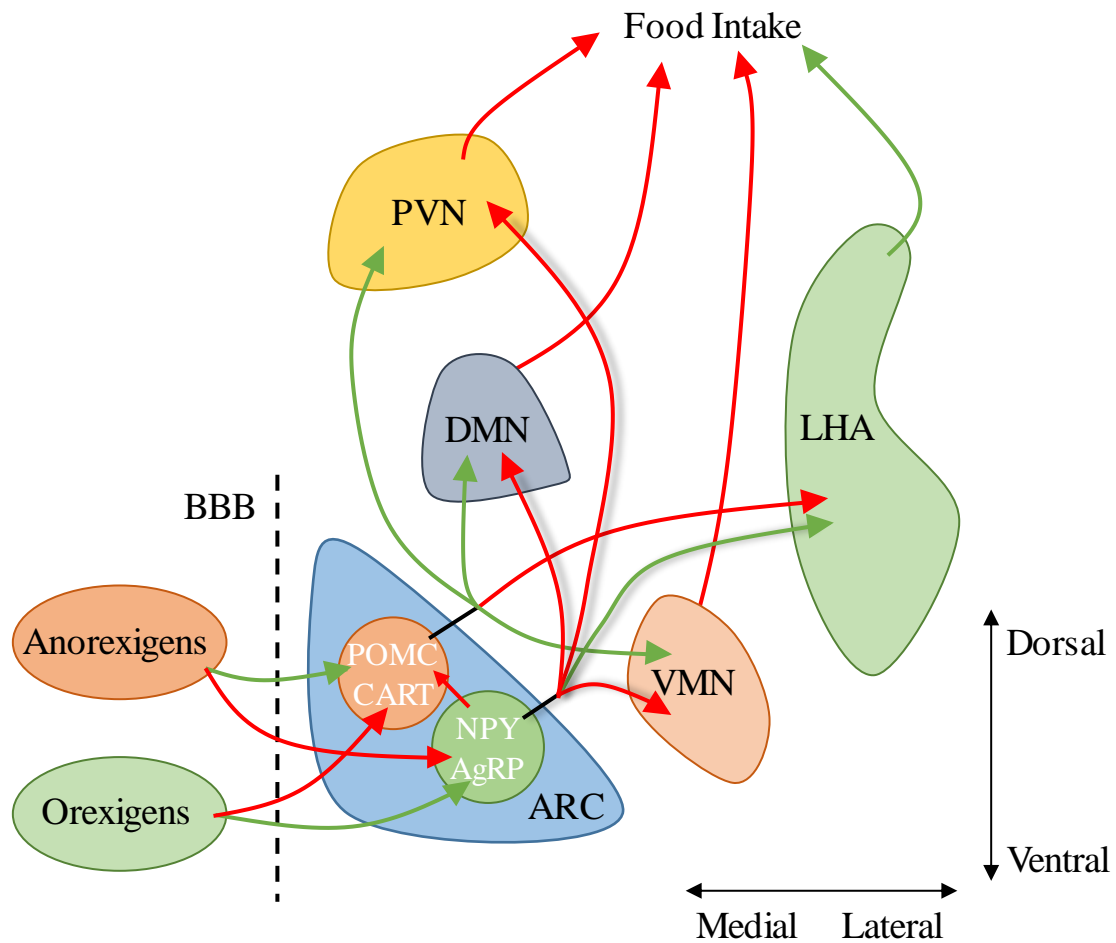


Figure 1.2: Hypothalamic nuclei involved in appetite regulation.

The major hypothalamic nuclei involved in appetite regulation are the arcuate nucleus (ARC), dorsal medial nucleus (DMN), ventral medial nucleus (VMN), paraventricular nucleus (PVN), and lateral hypothalamic area (LHA). Green lines represent activation, red lines represent inhibition. The ARC contains two opposing nuclei expressing either: neuropeptide Y (NPY) and agouti-related peptide (AgRP) or pro-opiomelanocortin (POMC) and cocaine and amphetamine related transcript (CART). NPY/AgRP neurons from the ARC inhibit the PVN, DMN, and VMN, and stimulates the LHA to increase food intake. POMC/AgRP neurons from the ARC inhibit the LHA and stimulate the PVN, DMN, and VMN to inhibit food intake. The ARC is adjacent to a weak blood brain barrier

(BBB) and is therefore capable of being regulated by blood borne signals such as orexigens and anorexigens.

Brainstem

The brainstem contains nuclei with extensive projections connecting the peripheral nervous system (PNS) to the CNS. Among the many nuclei, the nucleus tractus solitarius (NTS) and dorsal motor nucleus of the vagus (DMV) are involved in food intake regulation and gastrointestinal function.

The NTS is a vertical section of grey matter in the caudal brainstem at the level of the medulla oblongata [85]. It receives sensory projections from many cranial nerves including vagal afferents from visceral organs. The NTS also projects via second order neurons to various brain regions including the hypothalamus, and to other brainstem nuclei including the DMV. Further, the NTS also contains POMC and NPY expressing neurons to regulate appetite signalling at the level of the brainstem [86].

The DMV is located in the medulla oblongata adjacent to the fourth ventricle. It contains vagal efferent neurons that project to the thoracic and visceral organs to regulate motor activity. Notably, the DMV is involved in reflexes such as the vagovagal reflex to regulate gastrointestinal motility [87].

1.2.2| Peripheral Food Intake Regulation

Hormones secreted from white adipose tissue are basally active signals, providing information relating to energy stores, and thus serve as regulators of long term food intake. Conversely, hormones from the gastrointestinal tract serve as signals relating to

food intake and regulate short term satiety signals. These peripheral hormones can regulate appetite via the vagal afferent nerves or the CNS [88].

Energy store signals

White adipose tissue generally serves as the body's energy store where it can be utilised when energy intake is low. It secretes many peptides that can regulate energy balance and metabolism such as leptin and adiponectin.

Leptin is a 16 kDa adipokine and is typically secreted in proportion to adipocyte size and adipose mass [89]. It enters the circulation and, via a saturable transport protein [90], can cross the hypothalamic blood brain barrier. Here it binds to its receptor in many different hypothalamic neurons where it inhibits NPY and activates POMC neurones resulting in reduced food intake [91] and increased energy expenditure [92, 93]. A deficiency of leptin, or genetic mutation of the leptin receptor, induces hyperphagic behaviour and the development of obesity [94, 95]. Interestingly, genetic deletion of the leptin receptor in specific hypothalamic POMC neurons only induces a modest body weight increase compared to whole body genetic deletions [96]. This suggests that multiple sites of leptin actions are needed to control appetite and body weight.

Obese individuals typically exhibit hyperleptinemia, however, in obesity the appetitive and metabolic effects of leptin are lost due to central leptin resistance or insensitivity [97]. One suggestion for leptin resistance is reduced blood brain barrier transit of leptin in obesity [98]. Other suggestions include suppression of leptin signalling pathways via inhibition of signal transducer and activator of transcription-3 by suppressor of cytokine signalling-3 [99].

Adiponectin is secreted from adipocytes as oligomers of varying molecular weights. Different from leptin, it is secreted inversely proportionate to adipose mass. [100]. Low molecular weight adiponectin is thought to have anti-inflammatory properties [101] whilst high molecular weight adiponectin is correlated with reduced risk of type-two diabetes [102]. There are reports suggesting adiponectin can influence food intake [103, 104], however, this is conflicting. There is evidence to suggest that adiponectin can increase food intake through inhibiting POMC neurons in the ARC [105]. Conversely, there is evidence that adiponectin can reduce food intake when intramuscularly administered in the periphery [104]. Exogenous administration of adiponectin in obese rats reduced body mass, however, this was due to increased lipolysis rather than reduced food intake [106].

Pancreatic β -cells co-secrete insulin and amylin in proportion to adipose mass [107] and there is evidence to suggest they influence food intake. Although insulin is associated with the control of blood glucose levels, similar to leptin, circulating insulin levels increase post-prandially and can inhibit NPY neurones in the ARC to reduce food intake [108]. Interestingly, this inhibitory effect is not observed in NPY neurones that co-express AgRP [109]. Given this, and that insulin interacts with leptin [96], it can be considered an energy store signal.

Circulating amylin levels also increase post-prandially [110] in response to carbohydrates [111], where it can reduce meal size [112]. Amylin crosses the blood brain barrier via facilitated diffusion [113]. It acts upon its receptors in POMC neurons in the ARC [114] via in the NTS [115] where it can induce satiety. In obesity circulating levels of both insulin and amylin are increased, however, the normal satiety effects are not observed suggesting an insensitivity to these peptides [116, 117].

1.2.2.1| Gastrointestinal signals

The gastrointestinal tract is vital for the intake, digestion and absorption of nutrients. It also plays an important role in relaying signals to the CNS on the arrival, amount, and chemical composition of a meal. As food is digested, nutrients are sensed and stimulate hormone secretion. Their secretion is also regulated by other inputs including mechanical neural stimuli. This information is processed, eventually leading to satiety and termination of a meal. Whilst there are a multitude of gastrointestinal hormones, the following sections will focus on a select few as their role in food intake is well established. A summary of these gastrointestinal hormones, regulation of their secretion, and food intake effects are located in table 1.1.

Macronutrients

The three main macronutrients, proteins, carbohydrates, and lipids, can influence food intake via the release of gastrointestinal hormones, vagal afferent pathways, or directly on the CNS. Traditionally there were three main theories regarding macronutrient regulation of food intake, however, recent theories suggest it is a combination.

Proteins are broken down into amino acids by gastric acid and peptidase enzymes. They are detected by nutrient sensors on enteroendocrine cells. These sensors include: taste receptor 1 member 1 (T1R1)/T1R3 [118], calcium sensors, G-protein coupled receptor 93 (GPCR93), and GPCR93 [119]. Amino acids can trigger the production and secretion of satiety hormones such as CCK [120], the latter of which is mediated by the GPCR93 nutrient sensor [121].

Glucose, fructose and sucrose are the most commonly ingested simple carbohydrates. Complex carbohydrates such as oligosaccharides are broken down into these simple

carbohydrates. Sugars are detected by nutrient sensors on enteroendocrine cells such as T1R2/T1R3 and sodium-glucose transporters (SGLTs) [122]. SGLTs can induce the release of gastrointestinal hormones such glucagon like-peptide-1 (GLP-1). The potency of carbohydrates to induce hormone release is significantly higher when combined with fibre [123]. Whilst the reason for this is not known, fibre can slow the absorption of nutrients, allowing a prolonged sensing of nutrients and gastrointestinal hormone secretion [124].

Lipids are broken down by lipases to produce free fatty acids (FFAs) and monoglycerides. Similar to proteins and carbohydrates, FFAs are detected by nutrients sensors such as GPCR40, GPCR41, GPCR43, GPCR84, and GPCR120 [120] located on enteroendocrine cells. GPCR41 and GPCR43 generally sense short-chain FFAs [125] whereas GPCR40, GPCR84 and GPCR120 sense medium and long-chain FFAs [126]. Further, short-chain FFAs stimulate the release of PYY [125] whilst medium and long chain FFAs stimulate secretion of GLP-1 [126].

Macronutrients can also indirectly activate vagal afferent neurones via hormone release, particularly in the small intestine, to induce satiety [127]. A vagotomy can prevent the nutrient induced effects on food intake [128]. For example, satiety induced by carbohydrates is completely abolished by a vagotomy, whereas satiety induced by amino acids is only reduced by a vagotomy [128]. Macronutrients also act directly on the CNS. For example, amino acids can be sensed by ARC neurons and can increase the levels of α -MSH and decrease the levels of NPY [127]. Carbohydrates can induce satiety by reducing NPY levels in the LHA [129], however, over consumption of carbohydrates, especially simple ones, can increase NPY expression and food intake [130]. Lastly, FFAs inhibit expression of NPY in the ARC to reduce food intake [131].

Micronutrients

Micronutrients may also play a role in the regulation food intake. Although it is difficult to isolate the effects of a single micronutrient, reports have suggested calcium can influence food intake [132]. Studies have shown that dietary supplementation of calcium, or even a general multivitamin [133], in obese individuals led to a reduction in food intake and increased weight loss [134]. In the case of calcium, this may be due to the ability of calcium to stimulate PYY release [135]. However, this requires further investigation.

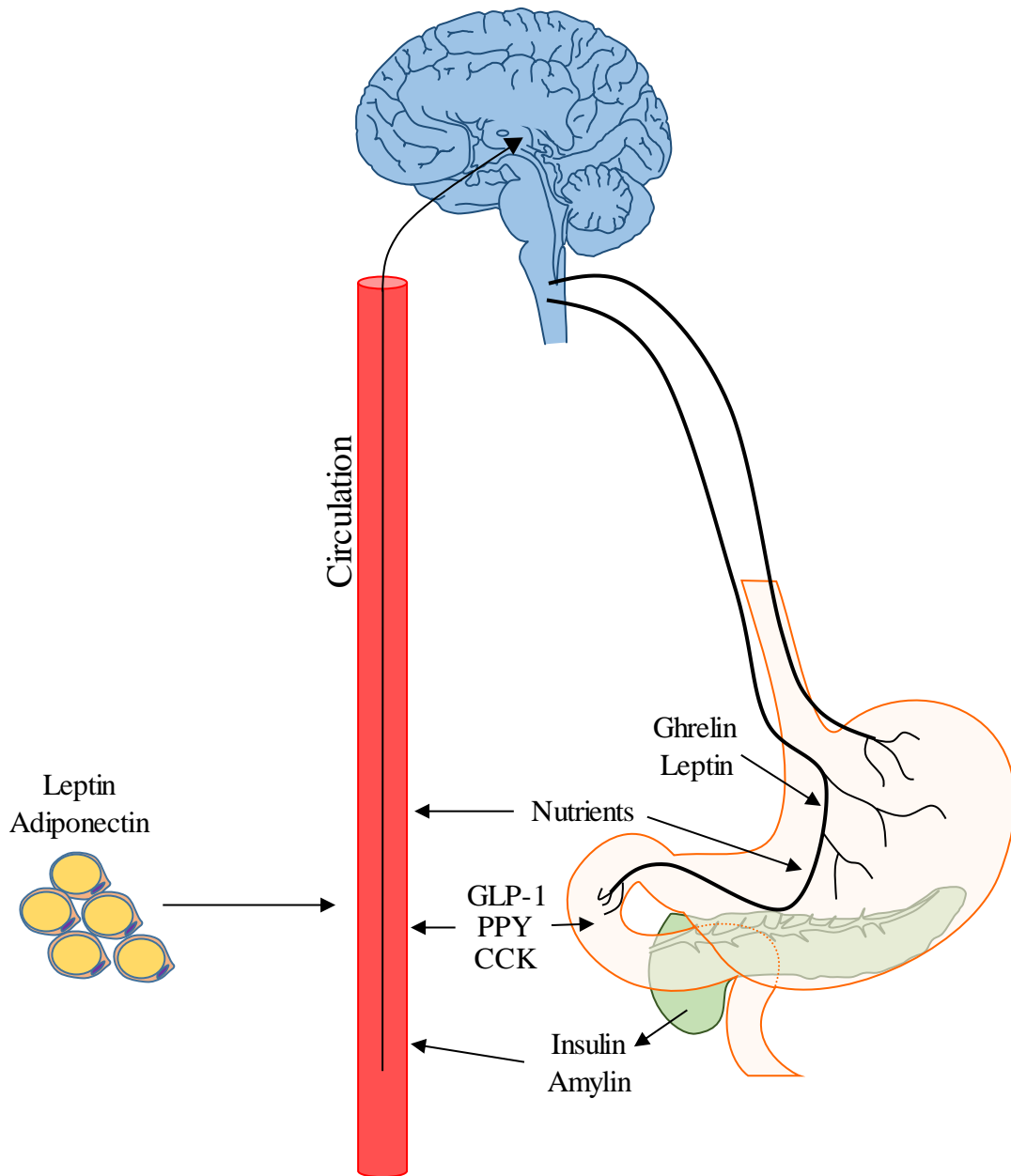


Figure 1.3 Peripheral regulation of appetite.

Signals from adipose tissue (e.g. leptin and adiponectin) and the pancreas (e.g. insulin and amylin) can enter the blood stream and act as indicators of energy storage to regulate appetite at the level of the hypothalamus. Ghrelin and leptin produced in the stomach can regulate appetite via action at the peripheral vagal afferent endings or via the circulation. Nutrients in the stomach can also regulate appetite in vagal afferent mediated manners. In the small intestines, glucagon-like peptide 1 (GLP-1), peptide tyrosine tyrosine (PYY),

and cholecystokinin (CKK) can regulate appetite either via vagal afferents or by entering the bloodstream.

PYY

PYY is a 36 amino acid peptide synthesised and secreted by L-cells in the proximal small intestine [136]. Following secretion it is cleaved and forms two isoforms, PYY (1-36) and PYY (3-36). PYY (1-36) is slightly more prevalent in the circulation compared to PYY (3-36) [137]. PYY can regulate gastrointestinal function by reducing gastric emptying [138] and gastric acid secretion [139]. Further, both isoforms of PYY can cross the hypothalamic blood brain barrier [140]. PYY (1-36) can bind to Y1 and Y5 receptors to stimulate food intake in the ARC [137]. Conversely, PYY (3-36) specifically binds to Y2 receptors in the ARC to decrease NPY signalling and food intake [141]. The effects of PYY (3-36) on food intake are more potent than PYY (1-36) [137].

Levels of PYY rise post-prandially to aid in the cessation of food intake [142]. In obesity, circulating levels of PYY are unchanged, although, postprandial levels are lower compared to lean individuals [143]. Further, the anorexigenic effects of PYY persist in obesity with PYY supplementation aiding in weight loss [144].

GLP-1

GLP-1 is produced from proglucagon in intestinal L-cells, and to a lesser extent from brainstem neurons. It is secreted in two isoforms, GLP-1 (7-36) and GLP-1 (7-37) [145], with the former being more prevalent [146]. Levels of GLP-1 rise rapidly (~15minutes [147]) following food intake and before intestinal exposure to food. The post-prandial

secretion of GLP-1 may be partly mediated via vagal efferent pathways with reports that a subdiaphragmatic vagotomy reduces lipid induced GLP-1 secretion [148].

GLP-1 can inhibit gastrointestinal motility and gastric emptying [149, 150], and reduce food intake [151]. This satiety effect is likely due to the peripheral effects of GLP-1 on vagal afferent nerves [152], however, the presence of GLP-1 receptors within the hypothalamus indicate a possible central effect [153]. Further, circulating GLP-1 is reduced in obesity, although, whilst the hypophagic effects are still present, there is a blunted post-prandial effect [154].

CCK

CCK was the first gastrointestinal hormone discovered to regulate food intake. It is postprandially secreted from intestinal I-cells [155] with concentrations peaking at 15 minutes after the initiation of food intake and before intestinal exposure to food. CCK has a relatively short half-life of approximately 3 minutes [156]. The release of CCK can also be mediated by vagal efferent neurons with stimulation of the vagal nerve alone for 10 minutes inducing CCK release [157]. CCK acts via vagal afferent neurones to inhibit gastrointestinal motility and gastric emptying, and reduce meal size [158]. Single acute doses of CCK reduce food intake [159] whereas chronic continuous doses have no effect [160], suggesting a role in the short term, but not long term, inhibition of food intake. Further, amylin can induce or enhance the satiety causes by CCK

In obesity, circulating levels of CCK are increased, and the satiety effects are maintained, suggesting it does not contribute to the hyperphagia observed in obesity [161].

Leptin

Whilst traditionally an adipokine, leptin is also produced and secreted by gastric chief cells and P-cells [162]. Leptin is secreted into the lumen of the stomach attached to its receptor [163] where it can regulate nutrient absorption and gastrointestinal motility.

The effect of leptin on nutrient absorption depends on the nutritional state. For example, in the fasting state leptin decreases the absorption of carbohydrates by reducing the activity of SGLTs [164]. Conversely, in the fed state leptin increases carbohydrate, protein, and FFA absorption by upregulating glucose transporters 2 and 5, tripeptide transporter 1, and fatty acid binding proteins (FABPs) respectively [165].

Leptin regulates gastrointestinal motility in conjunction with CCK by delaying gastric emptying [166]. It is plausible that the delayed gastric emptying may contribute to the satiety effects of leptin. However, the leptin receptor is also expressed in vagal afferent neurones suggesting another possible pathway [167], although this is controversial, and will be discussed in a later section.

Circulating leptin levels are generally in proportion to adipose mass to regulate long term energy balance, however, levels of leptin increase post-prandially to regulate short term energy balance [168]. In obesity leptin levels are elevated, however, its normal effects are lost due to leptin resistance [169].

Ghrelin

The orexigenic hormone ghrelin is an endogenous ligand for the growth hormone secretagogue receptor (GHSR). It is mainly produced and secreted by gastric X/A-like cells, however, it also produced in small amounts in the hypothalamus [170]. Structurally,

the active form of ghrelin, acyl-ghrelin, contains an octanyl group which is necessary for GHSR binding. The unacylated form is known desacyl-ghrelin [171]. Functionally, within the gastrointestinal tract ghrelin can increase motility [172] and gastric acid secretion [173], and may play a role in food intake.

Circulating levels increase pre-prandially and decline post-prandially [174] suggesting a role in food intake initiation. GHSR is expressed in the hypothalamus and vagal afferents [175], and therefore ghrelin can act on the CNS either via the weak hypothalamic blood brain barrier, or via vagal afferent endings in the stomach [175].

Circulating levels of ghrelin are reduced in obesity, however, the expression of GHSR in obesity is conflicting. Some reports indicate decreased GHSR expression in the hypothalamus and vagal nerve [176], whilst others report an increase [177]. Further, post-prandial circulating levels of ghrelin persist in obesity with no significant decline [178].

Similar to leptin, resistance to ghrelin is also present in obesity. It has been suggested that resistance to ghrelin protects against the establishment of a much higher set body weight point during obesity [179]. Further, obese mice with a ghrelin deletion exhibit reduced body weight regain following weight loss compared to wild-type mice [180].

Given this, it is possible that ghrelin resistance may also protect against weight rebound following weight loss. Ghrelin transit through the blood brain barrier, and the ability of ghrelin to stimulate NPY/AgRP neurons is reduced in obese mice [181] which may contribute to ghrelin resistance.

Table 1.2: Gastrointestinal hormone functions and their regulation by nutrients.

Hormone	Secretion	Nutrient Stimulation	Gastrointestinal Functions	Food Intake	Obesity Levels	Obesity Sensitivity
PPY (3-36)	Intestinal L-cells	Lipids	↓Gastric emptying [182] ↓Gastric acid [139]	↓ [141]	↔ [142]	↔ [143]
GLP-1	Intestinal L-cells	Carbohydrates Lipids	↓Gastric emptying [149] ↓Motility [150] ↓Gastric acid [183]	↓ [153]	↓ [154]	↔ [154]
CCK	Intestinal I-cells	Proteins Lipids	↓Gastric emptying [184] ↓Motility [185]	↓ [158]	↑ [185]	↔ [186]
Leptin	Gastric Chief cells and P-cells		Immune [187] Cell proliferation [188]	↓ [91]	↑ [169]	↓ [169]
Ghrelin	Gastric X/A cells	Proteins Lipids	↑Motility [189] ↑Gastric acid [173]	↑ [174]	↓ [172]	↓ [190]

1.3| Vagal Nerve

Cranial nerve ten, the paired vagal nerves, are involved in the parasympathetic control of the thoracic and visceral organs. Approximately 10% of the vagal fibres are efferent for motor functions, and 90% are afferent for sensory functions [191]. In the gastrointestinal tract the vagal nerve is involved in many functions including gastrointestinal motility, gastric emptying, and satiety signalling [191].

The vagal nerves exit the brainstem at the level of the medulla between the medullary olives and inferior cerebellar peduncles before exiting the skull through the jugular foramen [192]. Within the jugular foramen is the superior ganglia of the vagal nerve, which contains the pseudounipolar neuronal cell bodies of central vagal nerve fibres. The gastrointestinal projections of the superior ganglia primarily innervate the oesophagus.

Immediately inferior to the jugular foramen is the inferior ganglia of the vagal nerve, also known as the nodose ganglia, which contains the pseudounipolar neuronal cell bodies of peripheral vagal nerve fibres. The projections from the nodose ganglia innervate the rest of the gastrointestinal tract.[193].

In the neck the vagal nerves travel inferiorly in the sheath of the common carotid artery and the internal jugular vein before entering the thoracic chamber. The right vagal nerve travels posterior to the right lung descending to the posterior surface of the oesophagus where it becomes the posterior vagal trunk [194]. The left vagal nerve travels across the aortic arch and posterior to the left lung descending to the anterior side of the oesophagus where it becomes the anterior vagal trunk. Both the anterior and posterior vagal trunks enter the abdominal cavity via the oesophageal opening in the diaphragm [195].

The posterior trunk of the vagal nerve innervates the posterior stomach before branching into the large celiac branch to innervate the duodenum, liver, kidneys, small intestine, and the large intestine up to the distal colon. The anterior trunk of the vagal nerve innervates the anterior stomach, liver, proximal duodenum, and the pancreas [196].

1.3.1| Gastrointestinal Vagal Afferents

Gastrointestinal vagal afferents are involved in sensing mechanical, chemical, and hormonal stimuli. These signals are relayed to the CNS and integrated to regulate gastrointestinal homeostasis and satiety. It is important to note that intestinal vagal afferents are located in the crypts and villi, and are mainly chemosensitive [197]. Conversely, gastric vagal afferents (GVAs) are located in the gastric glands and are mainly mechanosensitive.

Within the gastrointestinal tract, there are three morphologically distinct types of vagal afferent endings, intraganglionic laminar endings (IGLEs), intramuscular arrays (IMAs), and mucosal vagal afferents.

IGLEs are flattened nerve branches present in the myenteric plexus of the gastrointestinal tract between the longitudinal and circular muscles (Figure 1.4). They are located in nearly all regions of the gastrointestinal tract including the oesophagus, stomach, small intestines, and large intestines, with their prevalence decreasing orally to aborally [198]. Given their location and high number of mitochondria [199], IGLEs likely have a mechanosensitive function to detect movement between the muscular layers such as stretch or distension. Distortion of the tissue surrounding the IGLEs causes stretch activated ion channels to open leading to an action potential [200]. Further, there is speculation that IGLEs may also have a paracrine chemosensitive role [198, 201].

IMAs form parallel fibres bundles within the circular and longitudinal muscular layers of the gastrointestinal tract [202] (Figure 1.4). They also bifurcate and progress in close proximity to interstitial cells of Cajal which are involved in smooth muscle function [203]. Given this, it is likely that IMAs also play a role in sensing stretch of the gastrointestinal wall [202].

Mucosal vagal afferent endings are present in the lamina propria of the gastrointestinal tract, most concentrated within the duodenum. [204]. They are located close to enteroendocrine cells that secrete appetite regulating hormones, suggesting a chemosensitive role [198]. Although, mucosal vagal afferents are also mechanosensitive to light contact but not stretch. It is likely that this mechanosensitive role is involved in

the detection of food particle size. A previous study indicated that denervation of the gastric mucosa increased the size of intestinal food particles [205].

Small Intestinal Vagal Afferents and Satiety

Intestinal vagal afferents are most concentrated in the duodenum, decreasing in prevalence distally to the ileum [198]. These vagal afferents play a role in gastrointestinal satiety signalling. Denervation of small intestinal vagal afferents reduces the carbohydrate and lipid induced inhibition of food intake [206]. Further, small intestinal vagal afferent endings express receptors for gastrointestinal hormones such as CCK [207], and GLP-1 [208]. CCK and GLP-1 excite small intestinal vagal afferents to inhibit food intake [209, 210], an effect blocked by vagotomy [211, 212]. This suggests that small intestinal vagal afferents mainly serve a chemosensitive role, however, they also respond to mechanical distension. A recent study indicated that duodenal, but not gastric, vagal afferents are necessary to generate satiety signals in response to stretch [213]. However, this study was performed in fasted mice where GVA mechanosensitivity is already reduced [167], and therefore, GVAs would not play a substantial role in producing satiety signals in this state.

Gastric Vagal Afferents

In addition to the accommodation and digestion of food, the stomach also plays a pivotal role in the peripheral control of food intake via GVAs which relay food related signals to the NTS and higher brain centres [214]. Within the gastric wall there are two distinct types of mechanosensitive GVAs, tension and mucosal sensitive GVAs.

Tension sensitive GVAs have a basal level of activity and become more active upon contact or distension of the gastric wall [215] (Figure 1.4). Current evidence suggests that

tension sensitive GVAs have a role in the initiation of gastric reflexes [196] and generating feelings of fullness and satiety [216].

Mucosal sensitive GVAs generally do not have a basal level of activity and become active upon contact with the gastric epithelia [215] (Figure 1.4). Current evidence suggests that mucosal sensitive GVAs have a role in nausea, vomiting [217], and detecting food particles, establishing negative feedback signals for gastric emptying [205].

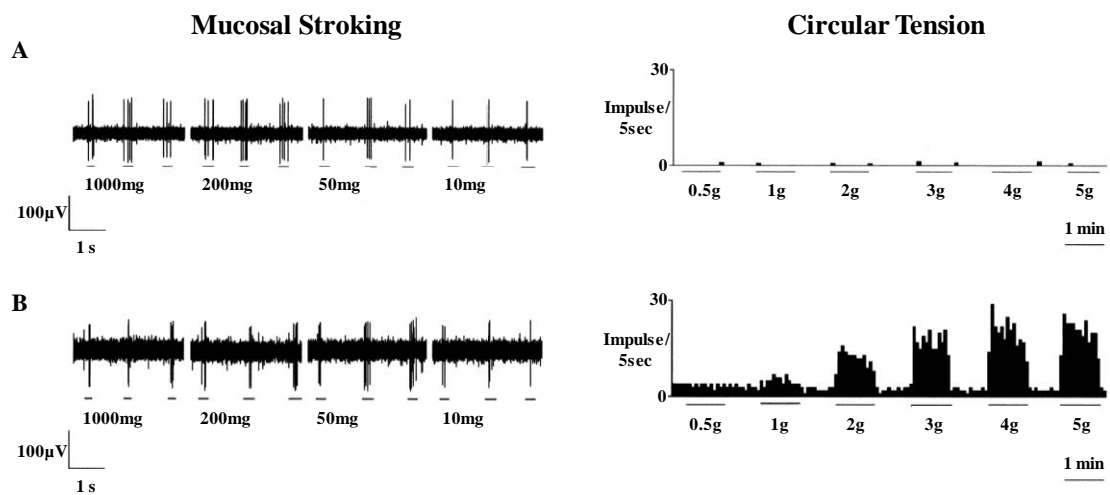


Figure 1.4: Typical response of mechanosensitive mucosal or tension gastric vagal afferent receptors to mucosal stroking or circular tension [215].

(A) Mucosal sensitive gastric vagal afferents (GVAs) produce a burst of action potentials upon contact with the gastric epithelia. This is a graded response with thicker von Frey hairs producing a higher response. Mucosal sensitive GVAs do not respond to circular tension applied to the gastric wall. (B) Tension sensitive GVAs respond to circular tension of the gastric wall with higher tensions producing a greater response. They also respond

to contact with the gastric epithelium, however, it is possible that this is due to slight stretching of the GVA upon von Frey hair stroking.

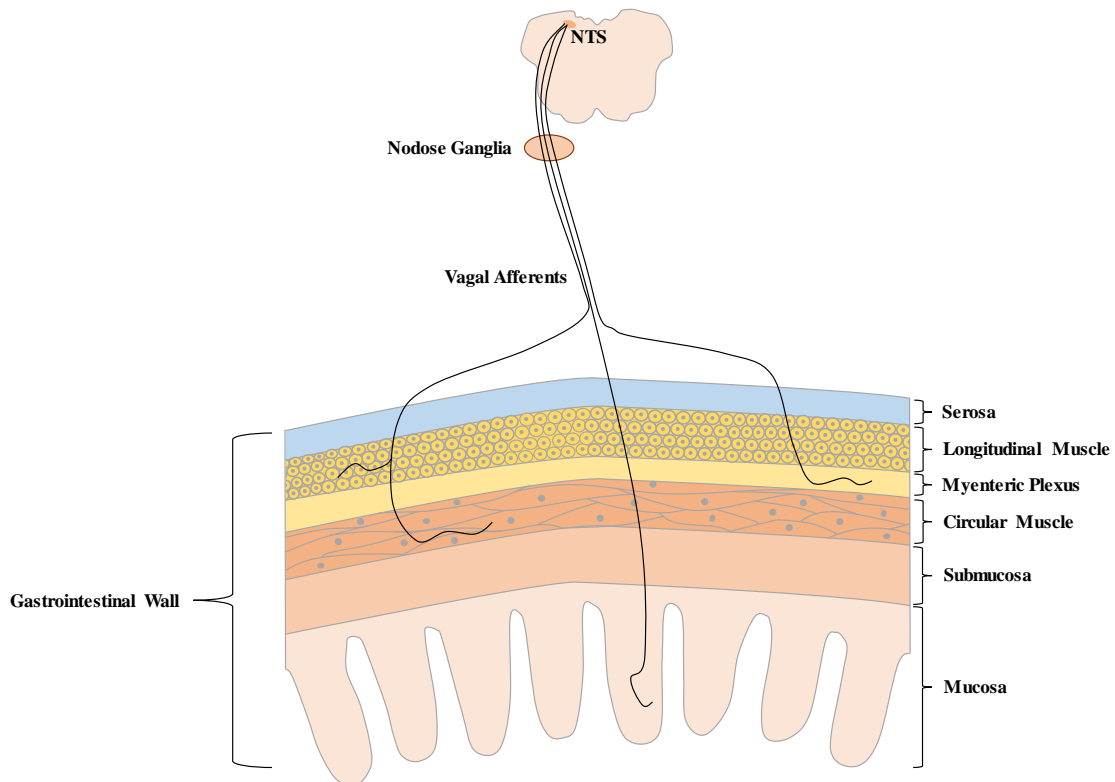


Figure 1.5: The structure and vagal afferent innervation of the gastrointestinal wall.

The gastrointestinal wall is composed of the mucosal layer for secretion of digestive acids, hormones, and nutrient absorption. This layer contains the mucosal vagal afferents. The submucosa contains blood vessels and nerves passing through. The circular and longitudinal muscular layers of the gastrointestinal wall aid in motility and are separated by the myenteric plexus. These three layers contains tension afferent innervation. The final outermost layer is the serosal layer which secretes fluid to minimise friction from muscle movement.

1.3.2| Modulation of gastric vagal afferents

The sensitivity of GVAs to mechanical stimuli can be regulated by gastrointestinal hormones and adipokines, time of day, stress, fasting, and diet-induced obesity.

Hormones and Adipokines

The gastric mucosa secretes hormones such as ghrelin and leptin which can regulate GVA mechanosensitivity. Ghrelin is associated with meal initiation and is secreted by gastric X/A-like cells [218] in close proximity to GVA endings [167]. Further, GHSR is expressed in GVA neurons [219]. Ghrelin reduced the mechanosensitivity of tension sensitive GVAs to stretch but did not affect GVA mucosal receptors [220]. Following a vagotomy, the stimulatory effects of ghrelin on food intake were lost [221] or dampened [175], supporting the notion that ghrelin's effects on food intake are partially mediated via vagal pathways.

Peripheral leptin is associated with meal termination and is secreted by gastric parietal and chief cells [166]. Further, leptin receptor is expressed in GVA neurons [222]. Leptin increases the mechanosensitivity of mucosal sensitive GVAs [223], an effect which may subsequently reduce gastric emptying [205]. The signalling pathway used by leptin on mucosal sensitive GVAs is dependent on phospholipase C (PLC) and transient receptor potential (TRP) canonical (TRPC) channels [223].

Circadian Rhythmicity

Circadian rhythms are necessary to help maintain an optimal and efficient environment by synchronising body systems with external cues. The sensitivity of GVAs to

mechanical stimuli exhibits a diurnal variation inversely proportional to food intake [224]. For example, murine GVA sensitivity peaks during the active or light phase when food intake is low, and nadirs during the dark or active phase when food intake is high [224]. These rhythms persist upon fasting or prolonged darkness (3 days) suggesting that, in the short term, they are not dependent on food intake or light/dark cycles. Although, in the long term, chronic high fat diet (HFD) feeding [225] or light cycle disruptions (e.g. shift work [226]) dampens GVA circadian rhythms.

Time of day can also influence the effects of leptin, but not ghrelin, on GVA mechanosensitivity. The potentiating effect on leptin on the mechanosensitivity of mucosal sensitive GVAs peaks during the light or resting phase in mice, and nadirs during the dark or resting phase [225]. It is plausible that this may partially contribute to the diurnal rhythms in food intake.

Stress

Stress can lead to undesirable gastrointestinal symptoms such as early satiety, and post-prandial pain [227-229]. Compared to non-stressed mice, chronically stressed mice exhibit hypersensitivity of mucosal and tension sensitive GVAs to mechanostimulation. This is associated with decreased food intake which is consistent with the function of tension sensitive GVAs [230]. The pathophysiology of the hypersensitive mucosal sensitive GVAs is not currently known as gastric emptying does not differ between stressed and non-stressed mice. Further the potentiating effects of leptin on mucosal sensitive GVAs is lost in stressed mice, suggesting stress also alters the interaction between hormones and GVAs [230].

Fasting

In the short term, fasting reduces the mechanosensitivity of tension sensitive GVAs, likely to accommodate food intake. Fasting also alters the effects of gastrointestinal hormones [167, 223]. The ghrelin receptor, GHSR, is increased in the nodose ganglia following an overnight fast, and, in addition to its inhibitory effect on tension sensitive GVAs, ghrelin acquires an inhibitory effect on mucosal sensitive GVAs [167]. Mucosal sensitive GVAs are associated with detecting food particle size and gastric emptying [205]. Gastric emptying is increased during fasting periods [231]. Therefore, the inhibitory effect of ghrelin on mucosal sensitive GVAs during fasting may contribute to the increased gastric emptying.

After an overnight fast, leptin receptor expression in nodose ganglia is unchanged, and, leptin loses its effect of the mechanosensitivity of mucosal sensitive GVAs, and acquires an inhibitory effect on tension sensitive GVAs [223]. This is likely to accommodate food intake. Further, the leptin signalling pathway in tension sensitive GVAs is mediated via phosphoinositide-3-kinase (PI3K) and large-conductance calcium-activated potassium channels (BKCa) [223].

1.3.3| Vagal Afferents and Diet-Induced Obesity

Obese individuals exhibit hyperphagic behaviour [177, 232] which could partly be due to impaired satiety signalling by gastrointestinal vagal afferents. In mice, chronic HFD feeding dampens the mechanosensitivity of oesophageal, gastric [167], and jejunal [233] vagal afferents to distension. In GVAs, this dampened response persists on return to a normal diet [234], suggesting diet-induced obesity has long term effects on vagal afferent responses to distension and subsequent satiety signalling.

Diet-induced obesity also alters the response of vagal afferents to gastrointestinal hormones. For example, in diet-induced obese mice, jejunal afferents exhibit dampened responses to the satiety hormone CCK [233]. Further, the effects of ghrelin and leptin on GVAs in diet-induced obese mice mimic that of fasting conditions [167, 223], subsequently promoting food intake.

Although it is not known what causes or contributes to the decreased mechanosensitivity of vagal afferents to distension in diet induced obesity, it is speculated that the TRP vanilloid 1 (TRPV1) channel may be involved [235]. The potentiating effects of the TRPV1 agonist N-oleoyldopamine (OLDA) on tension sensitive GVAs are lost in diet-induced obesity. Further, deletion of TRPV1 channels in lean mice causes dampened tension sensitive GVA responses to stretch. This effect is not exacerbated any further in TRPV1 null diet-induced obese mice [235]. Therefore it is plausible that dysregulation or dysfunction of the TRPV1 ion channel in GVAs may contribute to this. However, this is complicated by TRPV1 interactions with endocannabinoid and ghrelin systems.

1.4| Endocannabinoid System

The endocannabinoid system consists of a set of cannabinoid (CB) receptors, CB1 and CB2 receptors, and their lipid derived ligands, N-arachidonylethanolamine (also known as anandamide; AEA) and 2-arachidonoglycerol (2-AG) [236]. CB1 receptors are predominantly found in the nervous system and have a high affinity for AEA whilst CB2 receptors are predominantly found in the immune system and have a high affinity for 2-AG [237].

1.4.1| Cannabinoid Receptors

Expression

The CB1 receptor was first discovered in 1990 as a ligand for Δ^9 -tetrahydrocannabinol and the CB2 receptor was discovered in 1993 in leukaemia cells. Both receptors belong to a family of rhodopsin-like GPCRs [238]. Centrally, the CB1 receptor is highly expressed in the cerebellum [239], basal ganglia [240], hippocampus [241], and hypothalamus [242], whilst the CB2 receptor is highly expressed in microglia [41] with negligible expression in the brainstem [243]. In the periphery the CB1 receptor is highly expressed in the dorsal root ganglia [244] and vagal afferent nerves [245], whilst CB2 is expressed in immune tissues such as the spleen [246] and tonsils [247]. Further the CB1 receptor is also present in gastrointestinal mucosal cells such as enteroendocrine cells [248], where it is involved in hormone [249] and gastric acid secretion [250]. The CB2 receptor is also expressed in the gastrointestinal tract, however, here it is involved in intestinal inflammatory responses [251].

Structures

The CB1 receptor is composed of 472 amino acids (473 in murine species) whilst the CB2 receptor is composed of 330 amino acids [252]. Their structures are similar to most other GPCRs consisting of 7 transmembrane domains composed of α -helixes connected by extra- and intracellular loops, an extracellular N-terminal, and an intracellular amphipathic helix and C-terminal [253-256] (Figure 1.5).

In its inactive crystal form, the transmembrane domains of the CB1 and CB2 receptors form a cylindrical-like with a complex central orthosteric binding pocket [254, 255]. The orthosteric binding pockets are hydrophobic and largely negatively charged. This may

contribute to the selectivity of the receptors for lipid ligands and discourage interactions with negatively charged phospholipids [255, 256]. Further, the antagonist binding pocket of the CB1 receptor is large in comparison to the CB2 receptor antagonist binding pocket. However, the size of the CB2 receptor antagonist binding pocket is similar to the CB1 receptor agonist binding pocket [255]. This may partially explain why some CB2 receptor antagonists display partial agonist activity at the CB1 receptor.

The N-terminal of the CB1 receptor is approximately 110 amino acids long whilst the N-terminal of the CB2 receptor is only 33 amino acids long. The majority of the CB1 receptor N-terminal can be deleted without affecting ligand mediated G-protein activation [257-259]. However, the proximal region of the N-terminal may play a role in binding affinity and allosteric activation [260]. Further, the N-terminal also forms a lid over the orthosteric binding pocket when a ligand is bound, protecting it from extracellular degradation [256]. Conversely, the N-terminal of the CB2 receptor forms a short helix over the binding pocket but is not involved in ligand affinity.

Lastly, the C-terminal of the CB1 receptor consists of 73 amino acids whilst the C-terminal of the CB2 receptor consists of 59 amino acids. The main function of their C-terminals is G-protein coupling and activation [237]. However, there is evidence to suggest that the C-terminals of the CB1 and CB2 receptors may also interact with other secondary messengers [261] and mediate receptor desensitisation [262]. Further the C-terminal of the CB1 receptor can also regulate constitutive activity [263] and act as a membrane anchor [264].

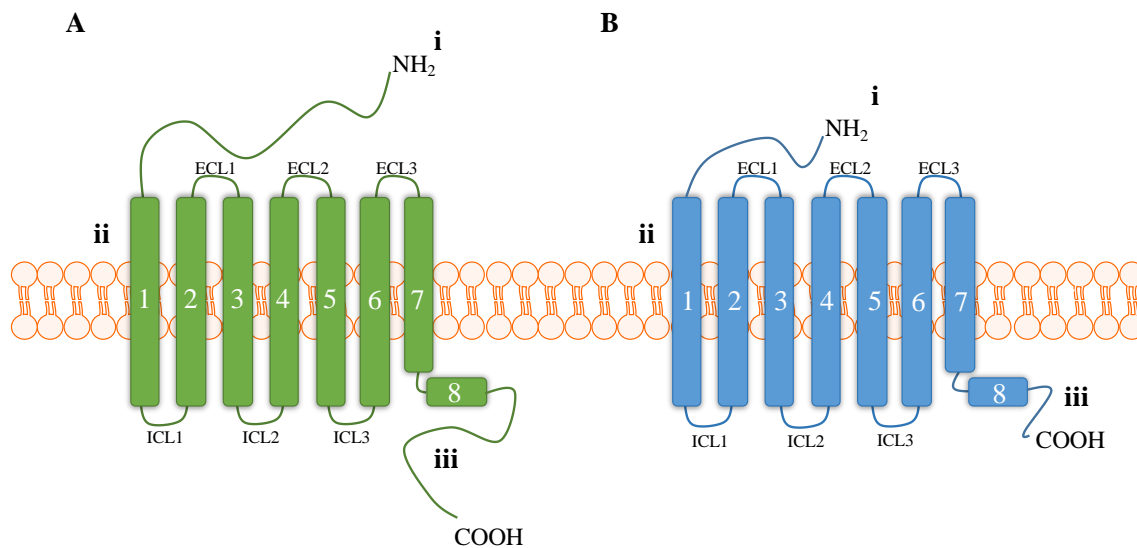


Figure 1.6: Generalised structure of the cannabinoid receptors.

(A) The cannabinoid 1 (CB1) receptor with (i) a long N-terminal involved in ligand affinity and orthosteric pocket covering, (ii) a transmembrane domain composed of 7 alpha helices and 1 amphipathic helix parallel to the membrane, and (iii) a long C-terminal. (B) The CB2 receptor with (i) a short N-terminal not involved in ligand affinity, (ii) a transmembrane domain composed of 7 alpha helices and 1 amphipathic helix parallel to the membrane, and (iii) a short C-terminal.

Localisation

Predominantly located on cell surface membranes, the CB1 and CB2 receptors can regulate intracellular calcium and cyclic adenosine monophosphate (cAMP) through secondary messenger pathways [265]. However, CB1 receptors are also present intracellularly on endosomes, lysosomes, and mitochondria (Figure 1.6). Endosomal CB1 receptors occur following internalisation from the cell surface membrane and their signalling is mediated via β -arrestins [266]. Lysosomal CB1 receptors increase intracellular calcium via release from the endoplasmic reticulum and the lysosome itself

[266]. Mitochondrial CB1 receptors act to decrease mitochondrial respiration and cAMP levels [267, 268]. Recently CB2 receptors have also been shown to have an intracellular presence where they can regulate calcium activated chloride channels, however, their exact intracellular localisation is not known [269].

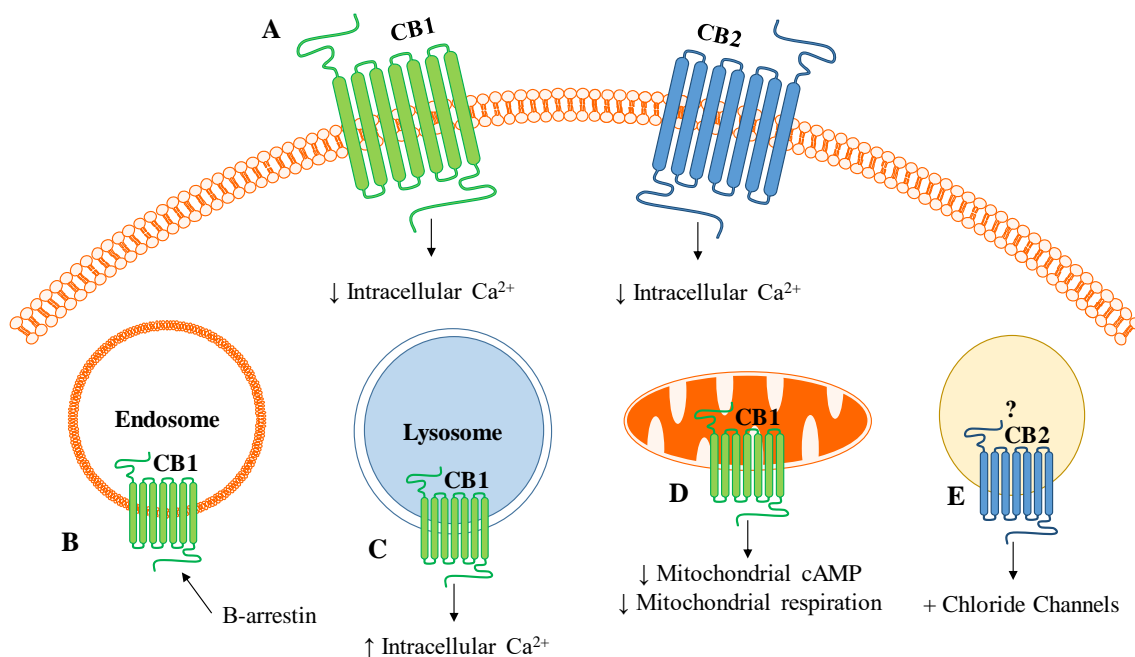


Figure 1.7: Cellular localisations of the cannabinoid receptors [252].

(A) Plasma membrane bound cannabinoid 1 (CB1) and CB2 receptors generally act to decrease intracellular calcium levels. (B) Endosome bound CB1 signalling following internalisation is mediated via β -arrestins. (C) Lysosome bound CB1 receptors act to increase intracellular calcium via endoplasmic reticulum. (D) Mitochondrial bound CB1 receptors act to decrease mitochondrial cyclic adenosine monophosphate (cAMP) levels and mitochondrial respiration. (E) Intracellular CB2 can act to activate calcium activated chloride channels.

Signalling

Both the CB1 and CB2 receptors are largely coupled to G-proteins with $G\alpha_{i/o}$ subunits [270]. However, there is evidence to suggest that they can also couple to G-proteins with $G\alpha_s$ and $G\alpha_q$ subunits (Figure 1.7). This differential coupling is tissue, ligand, and ligand concentration specific.

$G\alpha_{i/o}$ subunits can inhibit or activate various secondary messengers or ion channels. Predominantly, $G\alpha_{i/o}$ inhibits adenylyl cyclase (AC) to decrease cAMP production. This can lead to decreased protein kinase A (PKA) activity and stimulation of mitogen activated protein kinases (MAPKs) [271]. The $\beta\gamma$ subunits from the G-protein can inhibit calcium channels and activate G-protein coupled inward rectifying potassium channels [272]. Further, the $\beta\gamma$ subunit can also activate PI3K pathways to regulate various cellular and biological processes (Figure 1.7) [273].

$G\alpha_s$ subunits activate AC to increase cAMP levels leading to increased PKA activity [274] and phosphorylation of cAMP response element binding proteins (Figure 1.7) [275]. $G\alpha_s$ is generally activated when the dopamine 2 receptor is activated simultaneously [276] or when $G\alpha_{i/o}$ is unavailable due to sequestration or antagonism [277].

$G\alpha_q$ subunits increase intracellular calcium via membrane bound PLC [278]. PLC cleaves the phospholipid phosphatidylinositol-4,5-bisphosphate (PIP_2) to form diacylglycerol (DAG), and inositol-1,4,5-triphosphate (IP_3). DAG activates protein kinase C (PKC) subsequently affecting many cellular processes including calcium influx via voltage gated calcium ion channels [279]. IP_3 increases intracellular calcium stores via binding to IP_3

receptors on endoplasmic reticulum (Figure 1.7) [280]. This type of receptor signalling has been observed in rat hippocampus and may be ligand dependent [281].

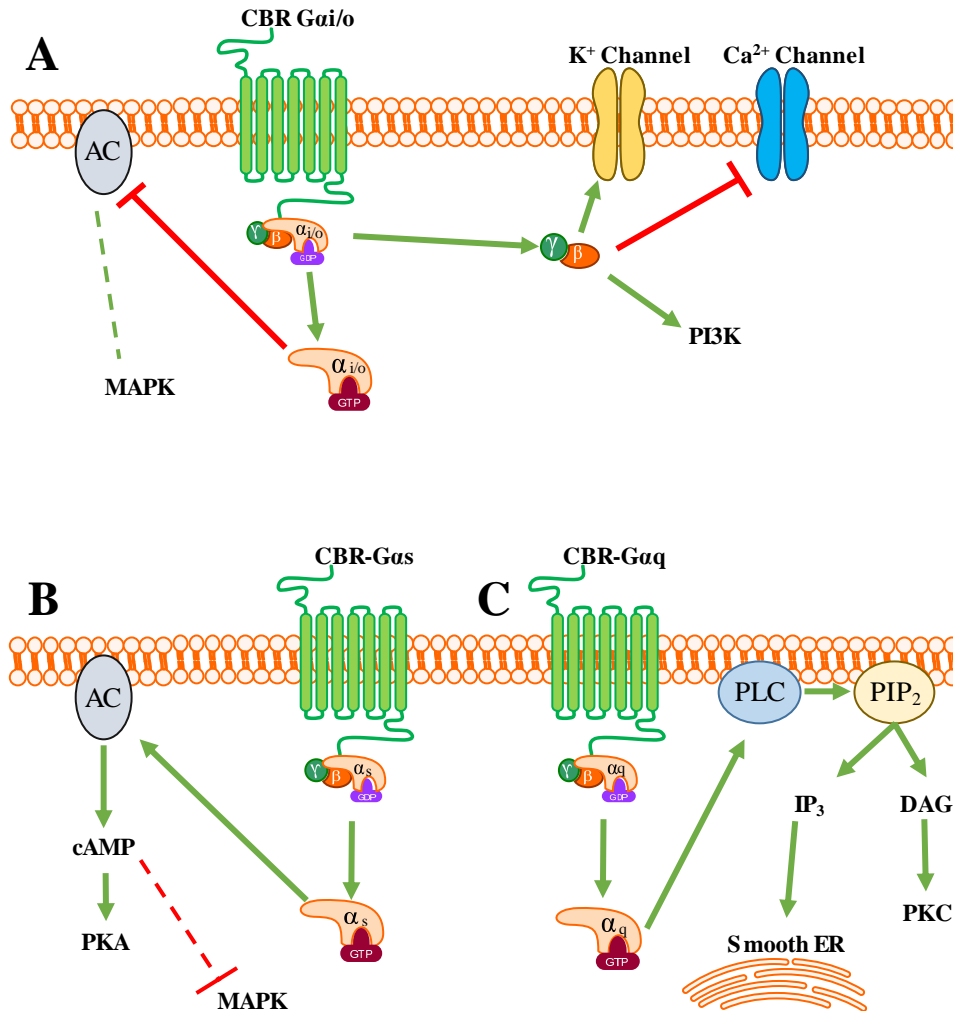


Figure 1.8: Different signalling pathways utilised by cannabinoid receptors.

(A) Cannabinoid receptor (CBR) coupled to Gai/o type G-protein can inhibit adenylyl cyclase (AC) to activate mitogen activated protein kinases (MAPKs). The $\beta\gamma$ subunit can activate potassium channels and phosphoinositide-3-kinase (PI3K) pathways, and inhibit calcium channels. (B) CBRs coupled to Gas type G-proteins can activate AC to increase cyclic adenosine monophosphate (cAMP) and subsequently increase protein kinase A (PKA) activity, and decrease MAPK activity. (C) CBRs coupled to Gaq type G-proteins

can activate phospholipase C (PLC) to cleave phosphatidylinositol-4,5-bisphosphate (PIP₂) into diacylglycerol (DAG), and inositol-1,4,5-triphosphate (IP₃). IP₃ releases calcium from smooth endoplasmic reticulum (ER) and DAG increases PKC activity. Green lines represent activation, red lines represent inhibition, dashed lines represent secondary effect.

Desensitisation

Desensitisation is common among GPCRs, preventing repeated G-protein signalling and indeed is also present to a degree with the CB1 and CB2 receptors [282]. However, the extent of desensitisation largely depends on the type and concentration of the agonist.

Following agonist binding and G-protein activation, a GPCR is phosphorylated by G-protein coupled receptor kinases. Generally, this allows the binding of an arrestin to prevent repeated signalling. However, it should be noted that it is not clear whether the phosphorylation alone or the arrestin prevents repeated signalling [282]. Further, whilst the initial signalling has been stopped by this process, the down-stream effects on targets such as ion channels can persist for an extended period [283].

In the case of the CB1 receptor this desensitisation process is dependent on ligand type and concentration. Some agonists such as desacetyllevonantradol can totally desensitise the CB1 receptor in as little as 30 minutes [284], whilst other agonists, such as Δ^9 -tetrahydrocannabinol (Δ^9 -THC), can take significantly longer and do not desensitise the CB1 receptor completely [285]. Further, the concentrations of CB1 agonists such as WIN55.21-2 also influence the extent of desensitisation with low concentrations only partially desensitising and high concentrations completely desensitising [286].

In contrast, data on CB2 receptor desensitisation is limited. Whilst there is evidence to suggest the CB2 receptor can be desensitised, it appears that endocannabinoids do not completely desensitise the CB2 receptor to stimuli [272, 287].

Internalisation

Following agonist stimulation the CB1 and CB2 receptors can undergo internalisation followed by either recycling or degradation [288, 289]. However, the mechanisms and extent to which this happens is unclear.

Internalisation of the CB1 receptor is mediated by clathrin or caveolae depending on the tissue [288, 290], and appears to be dependent on two factors. First, it is likely that not all agonists are capable of inducing CB1 receptor internalisation, suggesting an agonist dependent mechanisms [291]. Second, high expression of the CB1 receptor prevents internalisation. This is due to the saturation of intracellularly located CB1 receptors, which prevents further internalisation [292]. Further, in the current data the fate of the CB1 receptors following internalisation is conflicting. Some reports suggest that the CB1 receptors are recycled and returned to the cell surface [288, 289] whilst other reports indicate they are rapidly degraded requiring the synthesis and delivery of new CB1 receptors to the cell surface [293, 294].

Data on the internalisation and fate of the CB2 receptor is limited. It has been shown that the CB2 receptor is internalised in response to 2-AG [295]. Further, it has also been shown the CB2 receptors undergo recycling with repeated phosphorylation and dephosphorylation following agonist stimulation [296].

1.4.2| Endocannabinoids

1.4.2.1| Anandamide

AEA was first isolated in 1992 and is classified as a fatty acid neurotransmitter [297]. It is involved in a diverse range of biological processes including development, memory, reward related motivation and food intake. In development, AEA is important for uterine blastocyst implantation [298], and in memory it is involved in decreasing working memory retention [299]. Further, in reward related motivation it increases the pleasure derived from consuming sucrose products [300], and it also promotes food intake through an increase in appetite [301].

Synthesis

AEA is an N-acyl ethanolamine (NAE) and is synthesised on demand and degraded via cellular uptake and enzymatic hydrolysis. The traditional synthesis pathway of AEA and other NAEs utilises a transacylation-phosphodiesterase pathway (Figure 1.8) [302].

The transacylation phase is catalysed by either the enzyme N-acyltransferase (NAT) or the family of phospholipase A-acyltransferases (PLA-ATs). NAT is calcium dependent [303] whereas PLA-ATs are not, however, both transfer an acyl group from the sn-1 position of donor substrates (e.g. phosphatidylcholine and 1-acyl-lyso-phosphatidylcholine) to a phosphatidylethanolamine (PtdEtn) phospholipid to produce N-acylphosphatidyl-ethanolamines (NAPEs) (Figure 1.8) [304, 305]. The type of NAPE produced depends on the type of PtdEt phospholipid used. For example, the diacyl type PtdEtn produces NAPE, and the alkenylacyl type produces plasmen-NAPE [306].

The phosphodiesterase phase is characterised by the hydrolysis of NAPEs to produce AEA and other NAEs. This step is predominantly catalysed by membrane bound NAPE-

hydrolysing phospholipase D (NAPE-PLD) [307]. Further, there is evidence to suggest that PLC may also be involved in NAPE hydrolysis and NAE production, however this is mostly present in macrophages [308].

Overall, in the transacylation-phosphodiesterase pathways, acyl chains containing arachidonoyl have higher prevalence sn-2 rather than sn-1 positions of the donor substrates [306]. Since arachidonoyl is required on the sn-1 position of donor substrates for AEA synthesis, of the NAEs produced, AEA makes up only a small portion [302].

Degradation

There are two predominant enzymes involved in the degradation of AEA and other NAEs to ethanolamine and FFAs (Figure 1.8) [309]. The first is fatty acid amide hydrolase (FAAH) with FAAH-1 located on the endoplasmic reticulum and FAAH-2 located on lipid rafts, however the latter isoform is not present in rodents [310]. The second enzyme is N-acyl ethanolamine-hydrolysing acid amidase (NAAA) which is only active in acidic conditions [311]. Further, NAAA has a higher preference for other NAEs over AEA compared to FAAH, and it is mainly located in lysosomes of lung associated macrophages [312].

There are other pathways for AEA degradation that involve oxygenation processes. These include lipoxygenases [313] and cyclooxygenase-2 [314], however, their significance in AEA degradation is not clear.

1.4.2.2| 2-Arachidonoylglycerol

2-AG was first isolated in 1995 from the gastrointestinal tract of canines and is classified as a monoacylglycerol (MAG) [315]. Its main role is modulating immune and inflammatory responses, however, there is also evidence to suggest that it may mediate visceral pain responses via enteric neurons in the gastrointestinal tract [248].

Synthesis

The main synthesis pathway of 2-AG is largely dependent upon PLC β and DAG lipase (DAGL; Figure 1.8) [316]. First, a 2-arachidonoyl-phosphatidylinositol (PtdIn) phospholipid is hydrolysed to an arachidonic-containing DAG by PLC β [317]. Second, DAG is hydrolysed to form 2-AG and other MAGs by DAGL [318]. The type of MAG produced depends on the type of PtdIn hydrolysed, with the most abundant type being a 1-steroyl-2-arachidonoyl-PtdIn [306]. This type is what eventually forms 2-AG over other MAGs.

A second pathway for the synthesis of 2-AG involves PLA. First PLA hydrolyses a PtdIn to a lyso-PtdIn. Second, a lyso-specific-PtdIn PLC hydrolyses lyso-PtdIn to form 2-AG [306].

Degradation

The main pathway for the degradation of 2-AG is catalysed by MAG lipase (MAGL; Figure 1.8). MAGL is membrane bound and hydrolyses 2-AG to form arachidonic acid and glycerol [319]. However, a small portion of 2-AG degradation can also be catalysed by FAAH [320]. Further, like AEA, 2-AG can also be degraded by oxygenation via lipoxygenases and cyclooxygenase-2 [313, 314], but also like AEA, their significance in 2-AG degradation is not clear.

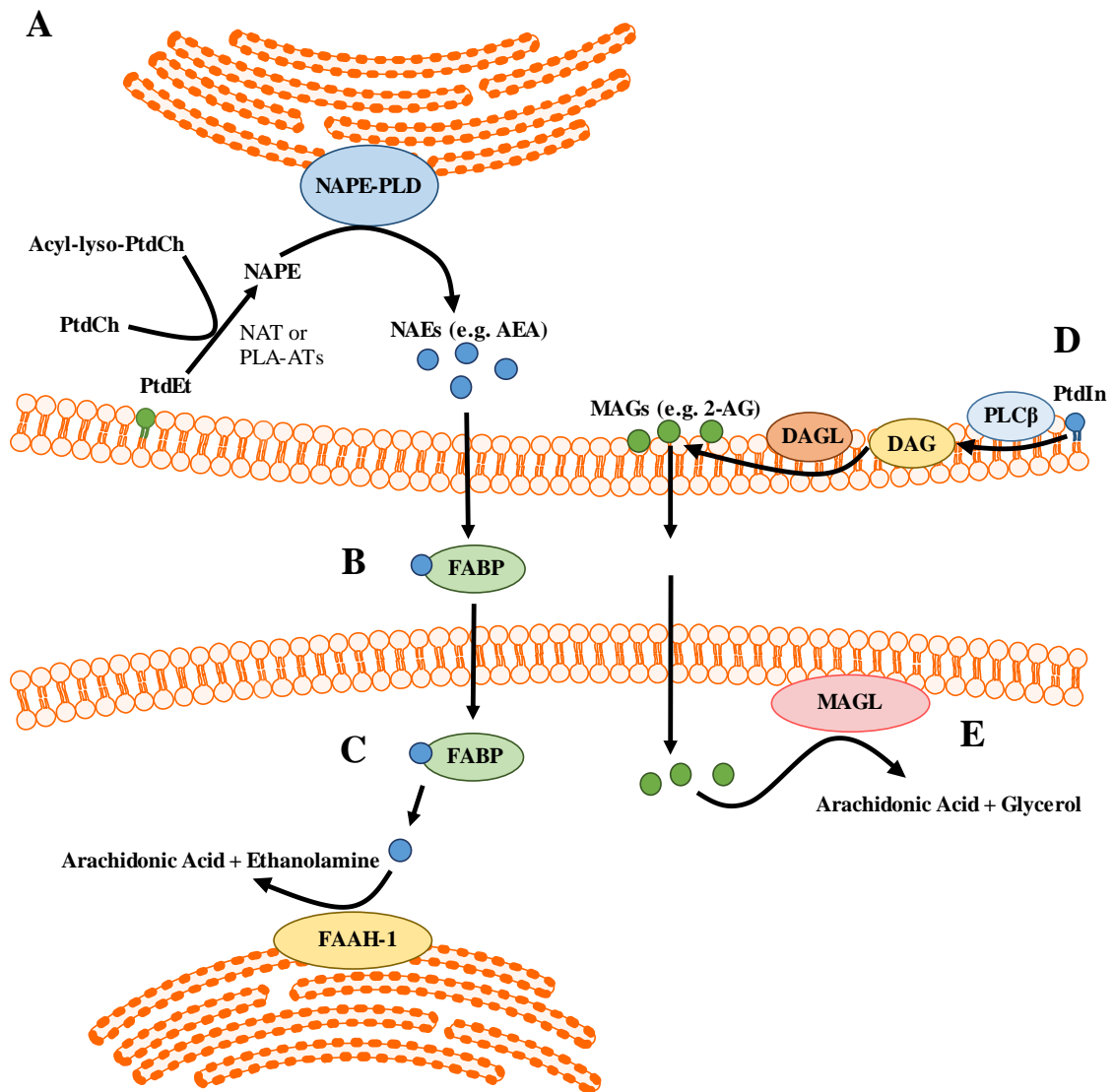


Figure 1.9: Synthesis and degradation of endocannabinoids.

(A) Phosphatidylethanolamine (PtdEt) phospholipid receives a donor acyl group from Ptd-Choline (PtdCh) catalysed by N-acyltransferase (NAT) or phospholipase A-acytransferase (PLA-AT) to produce N-acyl-phosphatidylethanolamine (NAPE). NAPE-hydrolysing phospholipase D (NAPE-PLD) then hydrolyses NAPE to N-acylethanolamines (NAEs) such as anandamide (AEA). (B) AEA is transported across cell membranes via fatty acid binding protein (FABP). (C) AEA is hydrolysed to arachidonic acid and ethanolamine by membrane bound fatty acid hydrolase 1 (FAAH-

1). **(D)** Phosphatidyl inositols (PtdIn) are hydrolysed by phospholipase C β (PLC β) to produce diacylglycerols which are then hydrolysed to monoacylglycerols (MAGs) such as 2-arachidonoylglycerol (2-AG) by DAG-lipase (DAGL). **(E)** 2-AG is hydrolysed by membrane bound MAG-lipase (MAGL) to produce arachidonic acid and glycerol.

1.4.2.3| Endocannabinoid Transport

Currently there is controversy surrounding the transport of endocannabinoids across membranes and the presence of an endocannabinoid membrane transporter.

There is evidence to suggest that AEA can diffuse through membranes, a process dependent upon cholesterol [321]. NAEs, such as AEA can form complexes with cholesterol to cross membranes without the aid of transport proteins, however, this process is generally slow [322].

In contrast, there is also evidence to suggest the presence of an endocannabinoid transporter. In basophilic leukaemia cells, application of 100nM AEA results in a considerably fast accumulation of AEA metabolites intracellularly [323]. This fast accumulation suggests not only a fast metabolism of AEA, but also the presence of an endocannabinoid membrane transporter. Current ideas for an AEA membrane transporter include fatty acid binding proteins (FABPs). FABP-5 has been shown to increase AEA transport across membranes, an effect that is lost following FABP-5 knockout [324, 325]. This suggests that FABP-5 may be involved in AEA transport, however, other transporters cannot be ruled out.

In regards to 2-AG transport across cell membranes, little information is available. It is known that 2-AG can cross cell membranes and accumulate in cells in a time dependent

manner [326, 327], however, it not known if this occurs via diffusion or via transport proteins.

1.4.3| Endocannabinoids and Food Intake

Whilst there is some evidence to suggest that 2-AG can play a role in food intake, the remainder of this thesis will focus on AEA and the CB1 receptor as their role is well established and most relevant.

Central Effects

Early studies identified the role of centrally located CB1 receptors in appetite. Centrally administered low doses of Δ^9 -THC or AEA increased food consumption in both fed and fasted rodents [328-330]. Specifically, they decreased meal initiation time and increased meal number and size [331]. Further, AEA and Δ^9 -THC also promoted the consumption of sweet tasting foods suggesting a role in reward pathways [332]. CB1 receptor antagonists [329], but not CB2 receptor antagonists [333], attenuated these effects on food intake.

The central effects of AEA and the CB1 receptor on food intake are largely mediated by the hypothalamic and mesolimbic systems. Administration of AEA into either of these areas stimulates food intake in rodents [334-336]. In the hypothalamus the CB1 receptor co-localises with corticotrophin releasing hormone (CRH), MC4R, and the orexin-1 receptor [337]. In the PVN, stimulation of the CB1 receptor decreases the anorexigenic CRH signalling with antagonism causing the inverse [337, 338]. In the LHA, stimulation of the CB1 receptor inhibits the anorexigenic effects of MC4R [339], and in the ventral hypothalamic area it enhances the activity of orexin-1 receptor [340]. These effects may be responsible for the stimulatory effect of AEA on food intake. Further, in the

mesolimbic system AEA and the CB1 receptor increase the release of dopamine in the nucleus accumbens subsequently increasing food seeking behaviour [40, 341].

In the hypothalamus and mesolimbic systems levels of AEA are known to change according to food intake status. During fasting AEA levels increase and then fall sharply following food consumption, supporting the notion that AEA is involved in food intake initiation [335]. Further, hypothalamic AEA levels are increased by ghrelin but reduced by leptin [342]. Ghrelin's effect on AEA levels are partially mediated via the CB1 receptor, whilst leptin's effects are mediated by inducing the expression and activity of FAAH [343, 344].

Peripheral Effects

Low doses of peripheral AEA can induce food intake [328], an effect dependent on CB1 receptors expressed in vagal afferent neurons [345]. Further, AEA and the CB1 receptor also interact with gastrointestinal hormones and peptides including ghrelin [346] and CCK [347]. Gastric X/A-like cells exhibit increased immunoreactivity for ghrelin following administration of AEA [348], and gastric ghrelin secretion is reduced by antagonism of the CB1 receptor [249]. Lastly, agonism of the CB1 receptor attenuates whilst antagonism increases the satiety effects of CCK [349].

Aside from their role in food intake, AEA and the CB1 receptor also regulate gastrointestinal functions such as motility, gastric emptying, and gastric acid and hormone secretion. AEA and the CB1 receptor slow intestinal peristalsis [350] and delay gastric emptying [351]. Further, activation of the CB1 receptor inhibits gastric acid secretion [352] and increases gastric ghrelin secretion.

It has been demonstrated that the effects AEA on gastrointestinal motility may be TRPV1 dependent [353, 354]. TRPV1 and its interactions with the endocannabinoid system will be discussed in the following sections.

1.5| Growth Hormone Secretagogue Receptor

Functions

There are two isoforms of GHSR, GHSR1a and GHSR1b, with the former being the receptor for acyl-ghrelin [355] and therefore the focus of this section. GHSR1a has been implicated in the release of hormones such as growth hormone, cortisol, and prolactin, and in the regulation of bodily processes such as energy balance, gastrointestinal motility, and cell proliferation [356]. In energy balance, GHSR1a has been associated with increasing food intake and adiposity [357]. In gastrointestinal motility GHSR1a activation has been associated with increased gastric emptying and gastrointestinal transit [358]. Lastly, activation of GHSR1a has also been associated with increased cell proliferation [359].

The expression of GHSR1a can be regulated by a variety of factors including hormones. In the pituitary GHSR1a expression is upregulated by β -estradiol and triiodothyronine [360]. Conversely, in the pituitary and hypothalamus, ghrelin and growth hormone [361] reduce GHSR1a levels suggesting a negative feedback loop.

Structure

GHSR1a is a GPCR consisting of 366 amino acids with an N-terminal, a transmembrane domain, and a C-terminal. The N-terminal is extracellular and forms a hairpin-like structure. The transmembrane domain consists of seven hydrophobic α -helices linked by

three intra- and three extracellular loops [362]. Overall, the transmembrane domain forms a calyx structure with domains two, six, and seven being the sites for ghrelin binding [363]. Lastly, the C-terminal is intracellular and is involved in the binding of G-proteins (predominantly $G_{\alpha i/o}$ and $G_{\alpha q}$) and β -arrestins [364].

Signalling

GHSR α has a high level of constitutive activity, and is predominantly coupled to $G_{\alpha q}$ proteins to elicit a rise in Ca^{2+} signalling. However, similar to the CB1 receptor, GHSR also couples to $G_{\alpha s}$ and $G_{\alpha i/o}$ proteins.

There is evidence to suggest that GHSR1 α can signal via $G_{\alpha s}$ proteins since antagonism of cAMP or PKA in the ARC [365] and aortic smooth muscle [366] prevents a ghrelin mediated rise in Ca^{2+} signalling. At the same time there is conflicting evidence suggesting that GHSR1 α stimulation by ghrelin alone has no effects on intracellular cAMP levels, but does in the presence of another GPCR, growth hormone releasing hormone (GHRH) [367]. Although this study doesn't specify the tissue type used, it is plausible that heterodimerising with other GPCRs such as GHRH may influence G-protein preference.

In the hippocampus [368] and pancreatic β -cells [369] GHSR1 α predominantly couples to $G_{\alpha i/o}$ proteins to reduce PKA activity. Given this, it is likely that preference of G-protein coupling by GHSR1 α is tissue specific, however, as mentioned previously, it cannot be ruled out that interaction with other GPCRs may also affect G-protein preference.

Desensitisation

Desensitisation of GPCRs is a common occurrence to prevent over stimulation and over signalling. Overall, this occurs via receptor/ligand de-coupling, and internalisation of the receptor.

Previous studies indicate that desensitisation of GHSR1a occurs 20-25 minutes following repeated stimulation, where it is internalised and then transported back to the cell membrane [370]. This process of internalisation of recycling largely depends on phosphorylation of the C-terminal. In tissues where the basal activity of GHSR1a is low, the subsequent phosphorylation of the C-terminal and internalisation is also low, and is determined by recruitment of β -arrestins [371].

Cell membrane composition also influences GHSR1a desensitisation. Cell membranes that contain high amounts of fatty acids such as oleic acid reduces internalisation of GHSR1a and increases its sensitivity to ghrelin [372]. This suggest that higher membrane levels of fatty acids may suppress GHSR1a desensitisation.

Interactions with G-Protein Coupled Receptors

Like other GPCRs, GHSR1a is notorious for dimerising with other receptors. Homodimers of GHSR1a have been detected in both the cellular and endoplasmic reticulum membranes [373]. Conversely, heterodimers of GHSR1a and GHSR1b have been detected only in the endoplasmic reticulum [373] which may be a process to reduce the expression of GHSR1a at the cell surface.

In the hypothalamus GHSR1a can heterodimerise with MC3R, interfering with each other's signalling. For example, activation of GHSR1a in the heterodimer boosts MC3R signalling, whilst activation of MC3R in the heterodimer inhibits GHSR1a signalling

[374]. It is likely that this mutually opposing heterodimer contributes to the control of food intake at the hypothalamic level.

Co-immunoprecipitation studies have indicated that GHSR1a forms functional heterodimer with the dopamine 1 receptor (D1R) [375]. Stimulation of this heterodimer by ghrelin alone results in activation of a G α q pathway, whilst stimulation by dopamine alone results in activation of a G α s pathway. However, concurrent stimulation of the GHSR1a and D1R heterodimer causes a switch to the activation of G α i/o pathway, reducing cAMP accumulation [375].

There is also evidence that GHSR1a can interact with the D2R to regulate food intake [376]. In the lateral hypothalamus dopamine inhibits food intake via D2R. This anorexic effect is lost upon GHSR1a knockout or antagonism, suggesting either an indirect functional interaction or dimerisation [376].

Lastly there is also speculation that GHSR1a dimerises with the CB1 receptor. In hypothalamus, deletion of the CB1 receptor attenuates the effects of ghrelin and vice versa [377, 378]. This suggests a possible dimerisation between GHSR1a and CB1, however, can also indicate a functional dependency mediated via secondary messenger pathways.

1.6| Transient receptor potential channels

TRP channels are a superfamily of approximately 30 structurally similar osmo- and mechanosensitive [379] ion channels. They were first discovered from an electroretinogram of a *Drosophila* fly that exhibited a short increase in retinal potential [380], thus the name 'transient receptor potential' [381]. They are involved in a wide

array of functions. For example TRP ankyrin 1 is involved in pain and inflammation [382], and TRPV1 is involved in pain, temperature [383], and more recently discovered, appetite control.

1.6.1| Transient receptor potential vanilloid 1

Expression

TRPV1 is a non-selective cation channel located in plasma membranes and is highly permeable to calcium ions. In the CNS, TRPV1 is expressed in the hypothalamus, limbic system, brain stem, and mid brain [384]. Peripherally it is expressed in various systems including the PNS (vagal and spinal sensory nerves [385, 386]), gastrointestinal system [387], and adipose tissue. TRPV1 expression can be influenced by development and pathologies such as inflammation. For example, in cardiomyocytes of neonatal rats TRPV1 is highly expressed whereas in cardiomyocytes of adult rats TRPV1 is undetectable [388]. Further, inflammation of the gastrointestinal tract increases TRPV1 expression on sensory fibres [389, 390], which may contribute to gastric oesophageal reflux disease [391].

TRPV1 exists in three known variants, TRPV1, TRPV1 '5 [392], or TRPV1 1b [393]. These variants are a results of alternate splicing during mRNA processing. TRPV1 is the most common variant, and TRPV1 '5 and 1b are expressed in rodents only. However, TRPV1 5' and 1b are insensitive to capsaicin and protons, but highly sensitive to heat [393]. Further, TRPV1 5' is expressed on sensory neurons, however, at a negligible level [394].

Structure

Structurally, TRPV1 is mainly present in homomers of four subunits, however, can also be present in heteromers. Each TRPV1 subunit consists of an N-terminal, a transmembrane domain, and a C-terminal (Figure 1.9) [395, 396]. The N-terminal contains six α - helices formed by ankyrin subunits and connected by finger loops [396]. Protein kinases are capable of phosphorylating several sites on the N-terminal with an S116 site being one of functional significance [397]. A linker and pre-helical section connects the N-terminal to the transmembrane region, and also acts as a connector for adjacent TRPV1 subunits [395-398].

The transmembrane domain of a TRPV1 subunit is comprised of 6 helical segments (S1-S6). The voltage sensing domain is formed by S1-S4, and the pore-forming domain is formed by S5-S6 [396]. These two sections are connected by a linking segment which contributes to the opening and activation of TRPV1. Further, the transmembrane domain also has binding sites for ligands. For example, vanilloids (e.g. capsaicin) bind to S3 and S4, and protons (H^+) bind to S5 and the linker segment [395].

The C-terminal of TRPV1 contains a TRP domain which forms a structural role by connecting with pre-S1 [396]. Further, the C-terminal also contains phosphorylation sites for protein kinase A and PKC, and binding sites for calmodulin and phosphatidylinositol-4,5-bisphosphate (PIP₂) [395, 396].

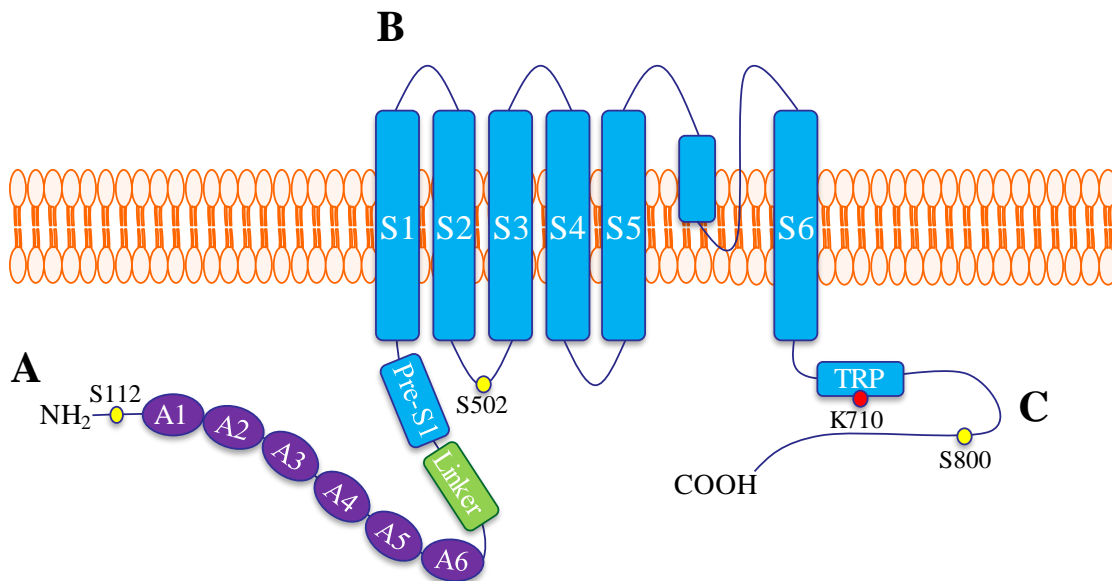


Figure 1.10: Structural components of a TRPV1 subunit [399].

A) N-terminal with 6 ankyrin subunits (A1-A6) and a linking region comprised of a Pre-S1 helix and linker segment. B) Transmembrane domain comprised of 6 helical segments (S1-S6). C) C-terminal with a TRP domain and binding sites for protein kinases and calmodulin.

Activation

Activation of TRPV1 generally results in an influx of cations to affect cellular processes. In neural tissue this generally causes depolarisation. TRPV1 is activated by many exogenous stimuli including capsaicin the pungent compound of chillies [400], garlic derived allicin and diallyl sulphides [401, 402], peperine from black pepper [403], and toxins derived from spider and jellyfish venom [404, 405].

TRPV1 is also intracellularly activated [406, 407] by many endogenous stimuli including NAEs [408], N-acyl-dopamines [409], and the inflammatory mediator leukotriene B4

[410]. Endogenous agonists such as these are collectively referred to as endovanilloids. Endovanilloids are generally present in sufficient concentrations to activate TRPV1 by direct binding. Further, they also have a short half-life to prevent TRPV1 desensitisation. This requires their synthesis and degradation to be in close proximity to TRPV1. However, endovanilloids can also be produced at a site distant to TRPV1 provided they have a way to be transported into the TRPV1 containing cell [411].

Intracellular secondary messengers can also regulate TRPV1 activity. For example, PKC sensitises TRPV1 to stimuli through phosphorylation of S502 on the S2-S3 linker region and S800 on the C-terminal [412, 413], and PKA enhances or activates TRPV1 through the S116 and T730 phosphorylation sites on the N-terminal [406]. Further, PIP₂ inhibits TRPV1 through binding to the K710 site on the TRP domain [414].

Desensitisation

Prolonged or repeated activation of TRPV1 can lead to its desensitisation, a process that is calcium dependent. TRPV1 activation leads to an influx of calcium and subsequently activates the intracellular calcium sensor calmodulin [415]. Calmodulin can compete with adenosine triphosphate at the ankyrin repeating domains on the N-terminal to desensitise TRPV1 to stimuli [416]. Further, calmodulin may also bind to the C-terminal to desensitise TRPV1. It is likely that TRPV1 desensitisation is largely mediated by the C-terminal since its deletion completely attenuates capsaicin induced desensitisation [415, 417].

There is also evidence to implicate calcineurin and PLC in TRPV1 desensitisation. Inhibition of calcineurin prevents capsaicin induced TRPV1 desensitisation [418]. PLC

is calcium dependent and can hydrolyse PIP₂ bound to TRPV1. Although a TRPV1 antagonist, depletion of PIP₂ prevents recovery from desensitisation [419].

Desensitisation of TRPV1 is dependent on the agonist and agonist concentration. Low doses (100nM) of capsaicin only partially desensitise TRPV1 whereas high doses (1µM) completely and rapidly (~ 20 minutes) desensitise TRPV1 [420]. Conversely, AEA does not significantly desensitise TRPV1 and is therefore considered to have a low-efficacy for TRPV1 desensitisation [421]. Further, there is some evidence to suggest that internalisation and degradation of TRPV1 by lysosomes may contribute to desensitisation, however, current data is limited [420].

1.6.2| TRPV1 and Food Intake

The effect of capsaicin on food intake are detailed in Table 1.2. Whilst conflicting, there is evidence to suggest that TRPV1 can regulate food intake and satiety signalling. In human studies, dietary supplementation of capsaicin, or the less spicy capsiate, can cause a short term decrease in food intake and increase or prolong satiety [422-426]. Further, consumption of capsaicin in conjunction with caffeine can potentiate these effects [427]. Conversely, in other human [423, 424] and animal studies [428-432], dietary supplementation of capsaicin had no effect on food intake or satiety.

The disparity between these studies may be due to different doses and frequency of exposure to capsaicin. Low intake of capsaicin can reduce food intake compared to high doses. It is plausible that this may be due to TRPV1 desensitisation with low doses either having a low efficacy, or a quick rebound from desensitisation [420]. Further, in regular consumers of capsaicin [433], or in obesity [434], capsaicin appears to lose its effect on food intake and satiety.

There is evidence to suggest that ingestion of capsaicin can also alter nutrient preference, however, it is conflicting. Supplementation of capsaicin can increase the preference for carbohydrates and decrease the preference for fatty foods [423, 435, 436]. Conversely, other studies have demonstrated that capsaicin reduces carbohydrate preference [424, 435] and increases salt preference [423, 437]. The mechanisms that influence these preferences are not known.

1.6.3| TRPV1 and Appetite Hormones

There is data to suggest that TRPV1 can interact with appetite regulating hormones such as leptin, GLP-1, and ghrelin; however the complete mechanisms are unknown.

TRPV1 activation regulates the levels and appetite effects of leptin. The normal appetite suppressing effects of exogenous leptin are lost and plasma leptin levels are increased in TRPV1 null mice [438]. It is plausible that the latter is due to the ability of TRPV1 to attenuate the development of mature adipocytes and increase lipolytic activity [428, 439].

TRPV1 activation enhances the post-prandial rise in plasma GLP-1, suggesting TRPV1 may be involved in GLP-1 secretion [440]. The mechanisms for this are unclear, however, since the postprandial rise of GLP-1 is partly vagal nerve mediated [156], it is plausible that TRPV1 on vagal fibres may be involved.

TRPV1 may also interact with and regulate ghrelin levels. Dietary supplementation of capsaicin reduces plasma ghrelin levels presumably via TRPV1 activation [440]. This may partially contribute to the ability of capsaicin to induce satiety. Further, in supraoptic magnocellular neurons, ghrelin interacts TRPV1 [441], however, here it is a potentiating effect and the exact mechanisms of interaction are unclear

Table 1.3: Human studies of capsaicin supplementation on food intake.

Dosage	Treatment Time	Appetite Effects	Nutrient Preference	Hormones	Reference
Capsaicin (7.68mg/day)	36 hours	↓ Energy intake* ↑ Satiety	-	-	[422]
Chilli (1.03g/meal)	24 hours	↑ Satiety	-	-	[426]
Capsaicin (7.68mg/meal)	24 hours	No Effects	-	-	[442]
Chilli (1g/meal)	1 meal	↓ Energy intake ↑ Satiety*	-	-	[423]
Chilli (0.3g/meal)	5 meals	No Effects	-	-	[443]
Chilli (1.03g/meal)	1 meal	-	-	↑ Plasma GLP-1 ↓ Plasma Ghrelin*	[440]
Capsaicin + green tea	3 weeks	↓ Energy intake ↑ Satiety	-	-	[427]
Chilli 3g + caffeine 200mg	24 hours	↓ Energy intake	↓ Fat intake	-	[444]
Chilli 0.9g/meal	2 days	↓ Energy intake ↑ Satiety	-	-	[435]
Chilli with meal	1 meal	↓ Energy intake*	↓ Fat intake	-	[436]
Capsaicin 135mg/day	3 months	-	-	↓ Plasma Leptin (likely due to weight loss)	[445]
Chilli 6g in appetiser	1 meal	↓ Energy intake	↓ Carbohydrate intake	-	[437]
Chilli 10g/meal	1 meal	↓ Energy intake*	↓ Protein and fat intake	-	[437]

* Indicates trend but not significant

1.7| TRPV1 and the Endocannabinoid System

Extensive evidence suggests that the endocannabinoid system and TRPV1 share a functional interaction, which may be biphasic in nature (Figure 1.10).

AEA is an endogenous ligand for TRPV1, acting intracellularly to activate or increase TRPV1 activity. Whilst AEA and capsaicin have a similar affinity for TRPV1, AEA is less potent and thus requires a generally high concentration (1-10 μ M) to elicit an excitatory response TRPV1 in some systems [408]. It is known that this can occur in vagal afferent neurons and independent of the CB1 receptor [446], however, there is evidence to suggest that activation of the CB1 receptor may also inhibit or potentiate TRPV1 via secondary messenger pathways [447].

In dorsal root ganglia, there are reports to suggest that AEA and the CB1 receptor can reduce or inhibit TRPV1 activity (Figure 1.10). Activation of CB1 is known to inhibit the AC and cAMP pathway causing reduced activity of the cAMP dependent PKA. PKA can activate or sensitise TRPV1 to stimuli [406, 447] and, therefore, reducing its activity would reduce the activity of TRPV1. This is likely mediated by the G α i/o protein. Further, the $\beta\gamma$ subunit associated with G α i/o proteins can inhibit calcium channels and activate inward rectifying potassium channels [272, 273], which may contribute to the ability of AEA and the CB1 receptor to reduce cell excitability.

As previously mentioned, the CB1 receptor is capable of activating or inhibiting various secondary messenger pathways depending on the associated G-protein. Reports in dorsal root ganglia have demonstrated that the CB1 receptor can activate a PLC pathway to increase DAG production and subsequent PKC activation [447]. PKC sensitises TRPV1 to stimuli and increases the chance of the TRPV1 channel opening in response to direct

AEA activation (Figure 1.10) [397, 412, 413]. Given that the CB1 receptor is able to activate PLC, it is likely that a G α q protein is involved, however there is also evidence to suggest that the $\beta\gamma$ subunit of a Gai/o protein is also able to activate PLC [448, 449].

It is likely that the change in these signalling pathways used by AEA is concentration dependent. Low concentrations of AEA typically reduce TRPV1 activity [450] whereas high concentrations stimulate TRPV1 activity [412]. However, the CB1 receptor can interact with other signalling molecules and GPCRs which may influence pathway preference. For example, the CB1 receptor interacting protein 1a has been shown to attenuate Gai/o mediated signalling [451, 452]. Further, the CB1 receptor is known to heterodimerise with the dopamine 2 receptor, causing a switch in G-protein preference from Gai/o to G α s [276, 453]. There is also speculation of a direct interaction with GHSR, however there is no current evidence to substantiate this [454]. Therefore, interactions with other signalling molecules and GPCRs to influence signalling pathways cannot be ruled out.

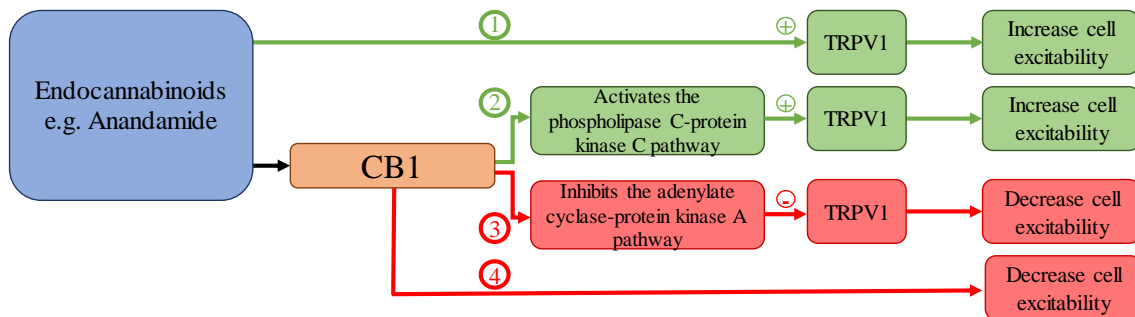


Figure 1.11: Interactions between endocannabinoids and TRPV1.

(1) The endocannabinoid anandamide can intracellularly activate transient receptor potential vanilloid 1 (TRPV1) channel to increase cell excitability. (2) Anandamide can also bind the cannabinoid 1 (CB1) receptor to activate a phospholipase C-protein kinase C pathway to subsequently sensitise TRPV1 and increase cell excitability. (3) CB1 activation by anandamide can also inhibit the adenylate cyclase-protein kinase A pathway to reduce TRPV1 activity and subsequent cell excitability. (4) Given the ability of CB1 to interact with many other receptors and proteins, another possible inhibitory pathway cannot be ruled out.

1.8| Aims

Tightly controlling food intake is necessary to maintain a healthy metabolic state. This is partly mediated by gastrointestinal hormones postprandially inducing satiety via vagal afferent signalling. In certain pathological conditions such as obesity, the secretion and signalling of gastrointestinal hormones via the vagus nerve are altered which may contribute to hyperphagia. Therefore it is important to investigate these changes in order to develop preventative measures or treatments to reduce the prevalence of obesity.

The mechanosensitivity of tension sensitive GVAs to stretch is dampened in diet-induced obesity. Whilst the cause for this is not currently known, it is plausible that the ion channel TRPV1 may be involved. TRPV1 gene deletions reduce the mechanosensitivity of tension sensitive GVAs. This effect is not exacerbated further in diet-induced obese mice with a TRPV1 knockout. This suggests that decreased TRPV1 channel activity may contribute to the dampened GVA responses to stretch.

In other systems TRPV1 interacts with a multitude of appetite regulating hormones including the ghrelin and endocannabinoid systems. It is plausible that these interactions may exist in GVAs to regulate satiety signalling. Therefore, the studies in this thesis aim to determine the following in mice:

1. The presence and co-localisation of TRPV1, CB1, GHSR, and FAAH in GVA cell bodies.
2. The role of methanandamide (mAEA; stable analogue of AEA) on the modulation of GVAs, and if this is mediated via TRPV1, CB1, and/or GHSR.
3. Any changes in mAEA signalling between lean and diet-induced obese mice.

4. The effect of mAEA and ghrelin on the mRNA content of TRPV1, CB1, GHSR, and FAAH in cultured nodose ganglia.

1.9| Thesis Outline

This thesis contains three studies divided into three chapters. Using an *in vitro* electrophysiology preparation, the first study (Chapter 3) confirmed that TRPV1 activity in tension sensitive gastric vagal afferents can be biphasically regulated by interactions with the ghrelin and endocannabinoid systems. Further, it also confirms the presence of TRPV1, CB1, and GHSR in individual tension sensitive gastric vagal afferent cell bodies, and demonstrates that they are co-expressed to a high degree.

The second study (Chapter 4) further confirmed that the ghrelin and endocannabinoid systems can biphasically regulate TRPV1 activity in tension sensitive gastric vagal afferents. This study also demonstrated that in diet-induced obesity, the biphasic regulation of TRPV1 in tension sensitive gastric vagal afferents is replaced with a single inhibitory effect. Further, this study demonstrated that the co-expression of TRPV1, CB1, and GHSR is increased in individual cell bodies of tension sensitive gastric vagal afferents from diet-induced obese mice.

The final study (Chapter 5) used a cell culture method to demonstrate that ghrelin and the endocannabinoid AEA are capable of regulating the mRNA expression of TRPV1, CB1, GHSR, and FAAH. Further, this study also demonstrated that this regulation is altered in diet-induced obesity.

Chapter 2 : Materials and Methods

2.1| Animal Studies

All studies were approved by the animal ethics committee of the South Australian Health and Medical Research Institute and carried out in accordance to the Australian code for the care and use of animals for scientific purposes 8th Edition.

All animals used in this study were C57BL/6 male mice housed in a 12hr/12hr light/dark cycle at constant temperature (22°C) with *ad libitum* access to a standard laboratory diet (SLD; 13kJ/g; 18% energy from fat, 24% energy from protein, 58% energy from carbohydrates; 2018SX, Specialty Feeds, Australia) and water, unless otherwise specified.

2.1.1| High Fat Diet Induced Obesity Studies

Eight week old male mice were housed in littermates of 3 to 4 with *ad libitum* access to either a SLD or a high fat diet (HFD; 21.79kJ/g; 60% energy from fat, 20% energy from protein, 20% energy from carbohydrates; adapted from Research Diets Inc. (D12492)) for 12 weeks. The mice were weighed weekly.

2.2| Retrograde Tracing Studies

A retrograde tracing procedure was performed as follows to target tension sensitive GVA cell bodies in nodose ganglia. Mice were fasted for two hours before being anaesthetised via inhalation of 3% isoflurane in 1-1.5% oxygen. A midline abdominal laparotomy was performed and the stomach was exteriorised using a sterile swab soaked in saline. Using a 30-gauge Hamilton syringe (Hamilton, USA), multiple equally spaced injections (10 x 1µL) of Alexa Fluor® 555 conjugate of cholera toxin β-subunit (C22841; Life Technologies, Australia) were administered under the serosal layer of the gastric wall. This was performed on the ventral and dorsal sides of the stomach ensuring maximum exposure to the tracer. The injections sites were then dried and the laparotomy was closed

via suture and staples (AutoClip® System; 12020-09; Fine Science Tools, USA), and sterilised with 70% ethanol. Mice were given a subcutaneous injection of antibiotics (baytril; 10mg/50µL and analgesia (buprenorphine; 0.1mg/kg) immediately following surgery. 8 hours post-surgery mice were given another subcutaneous injection of buprenorphine to aid in recovery. Cages were kept on a warming pad to also aid in recovery.

The tracer travelled from the stomach to the nodose ganglia cell bodies over the following two days [455]. Then the mice were humanely killed via CO₂ inhalation (fill rate of 30%; Quietek™ CO₂ induction system, Next Advance, USA) and decapitated. The nodose ganglia were bilaterally removed and processed for single cell RT-PCR or immunohistochemistry. An example of retrogradely traced nodose ganglia cells are illustrated in Figure 2.1.

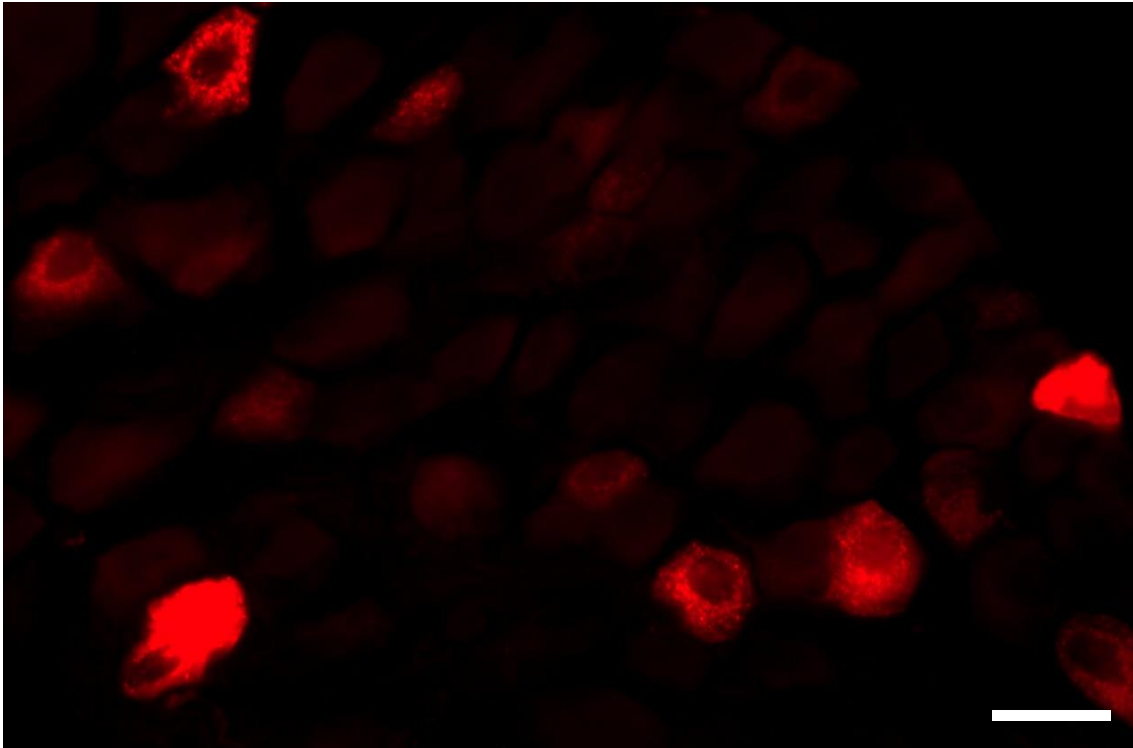


Figure 2.1: Retrogradely traced tension sensitive gastric vagal afferent cell bodies in mouse nodose ganglia.

Example of retrogradely traced tension sensitive gastric vagal afferent cell bodies in nodose ganglia. Scale bar represents 20 μ m.

2.3| Nodose Ganglia Single Cell RT-PCR

2.3.1| Cell Culture

Immediately following bilateral dissection, the retrogradely traced and normal non-traced nodose ganglia were placed in ice-cold F12 solution (11765-054; ThermoFisher, Australia). The F12 solution was then removed leaving the nodose ganglia undisturbed. Nodose ganglia were then incubated at 37°C for 30 minutes in a 3mL solution of collagenase and dispase (4mg/mL) in Hank's Balanced Salt Solution (HBSS; 14170-112;

ThermoFisher), followed by incubation at 37°C for 10 minutes in a 3mL solution of collagenase (4mg/mL) in HBSS. Nodose ganglia were gently agitated every 5 minutes during both incubation periods to aid in digestion of the extracellular matrix.

Most of the solution was removed leaving approximately 150µL containing the nodose ganglia clumped together, which were then mechanically sheared into single cells using decreasing sizes of fire polished glass pipettes. This was performed carefully to prevent air bubbles and until the solution was cloudy. The cells were then washed in ice cold HBSS and pelleted. This was performed twice before being resuspended and diluted to approximately 1 cell/µL in HBSS.

1µL of the cell suspension was pipetted onto a thin piece of 4mm by 8mm glass and examined under an epifluorescence microscope (BX-51, Olympus, Australia) equipped with filters for Alexa Fluor® 568. Where a single fluoresced cell was identified, the slide was then re-examined under bright field (BX-51, Olympus) to ensure no non-fluoresced cells were present. To lyse the cell the glass piece was immediately placed into a 50µL capacity RNA safe tube containing a 10µL solution of 9µL of Single Cell Lysis and 1µL of DNase-1 provided in a Single Cell-CT™ Kit (4458237; Life Technologies) and incubated at room temperature for 5 minutes. A stop solution (1µL; Life Technologies) was then added and incubated for 2 minutes to stop the lysis reaction. Samples were then stored at -20°C until required.

2.3.2| Single Cell RT-PCR

Stored lysed single cell samples were thawed to room temperature. Reverse transcription, pre-amplification, and RT-PCR were performed using a Single Cell-CT™ Kit following manufacturer's instructions. However, in the RT-PCR step, samples were diluted 1:10

instead of 1:20. The RT-PCR step was performed in a 7500 Fast Real-time PCR system (ThermoFisher) with the following steps: 50°C for 2 minutes, 95°C for 10 minutes, 40 cycles of 95°C for 5 seconds and 60°C for 1 minute.

Pre-designed Taqman gene expression assays (Life Technologies) were used to determine the mRNA expression and co-expression of CB1 (mm01212171_s1), TRPV1 (mm01246300_m1), GHSR (mm00616415_m1), and FAAH (mm00515684_m1) in untraced and retrogradely traced tension GVA neurons of both SLD- and HFD-mice. Beta-2-microglobulin (B2M) and beta-actin (ActB) were used as housekeeping genes. They were chosen based on stability across diets (stability value of B2M and ActB = 0.102) using NormFinder software (Department of Molecular Medicine (MOMA), Aarhus University Hospital, Denmark). An overview of all housekeeping genes tested in nodose ganglia can be observed in Table 2.1. Nuclease free water (Ambion; ThermoFisher) was substituted for amplified RNA as a control. RNA levels were calculated relative to the housekeeping genes using the $2^{\Delta\text{CT}}$ method [456].

Table 2.1: Details of housekeeping genes tested in single nodose neurons

Gene	Stability Value	Catalogue #
Class 3 β -Tubulin (Tubb-3)	0.306	mm00727586_m1
β -actin (ActB)	0.068	mm00437762_m1
β -2-microglobulin (B2M)	0.091	mm00437762_m1
Hypoxanthine-phosphoribosyltransferase (HPRT)	0.523	mm03024075_m1
Peptidylprolyl Isomerase A (PPIA)	0.208	mm00620857_s1

2.4| Immunohistochemistry

2.4.1| Fixation

Following bilateral dissection retrogradely traced nodose ganglia were fixed in 4% paraformaldehyde solution. Samples were incubated for 4 hours at room temperature with gentle agitation. The nodose ganglia were then removed from the paraformaldehyde solution and placed in a 30% sucrose solution in 1x phosphate buffered saline (PBS; 70012-032; Life Technologies). Samples were incubated for 18 hours at 4°C. The nodose ganglia were then removed from the sucrose solution and frozen in optimal cutting temperature (OCT) mounting medium (IA018; ProSciTech, Australia), followed by cryosectioning at 10µM thickness. Slides were coated with gelatin (1005612; Marienfeld, Germany) to promote adhesion and avoid tissue loss during immunostaining. Consecutive sections were placed on different slides for single and dual labelling. Slides were stored at -20°C for a maximum of 5 days before immunofluorescent staining.

2.4.2| Immunofluorescent Staining

Immunoreactivity for CB1, TRPV1, and GHSR was determined using the following primary antibodies: rabbit polyclonal antibody to CB1 (20754; Santa-Cruz, USA; 1:200 dilution), goat polyclonal antibody to TRPV1 (GT15129; Neuromics, USA; 1:400 dilution), and rabbit polyclonal antibody to GHSR (10359; Santa-Cruz; 1:200 dilution). The primary antibodies have been validated previously using knockout mice [358, 457, 458].

Visualisation of the primary antibodies was determined using the following secondary antibodies (Sigma): CB1, Alexa Fluor® 488 (A21206) or 350 (A10039) donkey anti-rabbit secondary antibody, TPRV1, Alexa Fluor® 350 donkey anti-goat secondary

antibody (A21081), GHSR, Alexa Fluor® 488 donkey anti-rabbit secondary antibody. All antibodies were diluted to 1:200 in PBS-Triton X100 (PBS-TX; X100-500mL; Sigma). CB1 and TRPV1 were dual labelled, and GHSR was single labelled on consecutive sections as CB1 and GHSR shared a common host antibody.

Slides were air dried for 40 minutes at room temperature. The sections were then washed 3 times for 5 minutes with PBS-triton X100 allowing the penetration of antibodies. The sections were then blocked with 10% donkey sera in PBS-TX for 40 minutes at room temperature. The primary antibody (diluted in PBS-TX) for either CB1 or GHSR (200µL) was then added to the sections and incubated for 20 hours at room temperature. To prevent evaporation of the primary antibody the slide box was covered in a water soaked pad. After 20 hours the sections were rinsed 3 times for 5 minutes with PBS-TX to remove any unbound primary antibodies. The secondary antibody for either CB1 or GHSR (200µL) was then added and incubated at room temperature for 1 hour. The sections were then rinsed 3 times for 5 minutes with PBS-TX to remove unbound secondary antibody. For single labelling the ProLong antifade (P36934; ThermoFisher) was added to the sections and a coverslip applied. For dual labelling the primary antibody for TRPV1 was added to the sections and the same immunostaining procedure was performed.

2.4.3| Visualisation

The sections were imaged using an epifluorescence microscope (BX-51, Olympus) equipped with filters for Alex Fluor® 350 (blue), 488 (green), and 568 (red). Images were captured using cellSens dimension software (Olympus) and overlaid using Image J software (University of Wisconsin, USA). Images of sections were analysed for the immunoreactivity of CB1, TRPV1, and GHSR in traced and un-traced cells.

Immunolabelled cells were counted manually on 15 sections per mouse from both the left and right nodose ganglia. The average of the 15 sections was used for analysis.

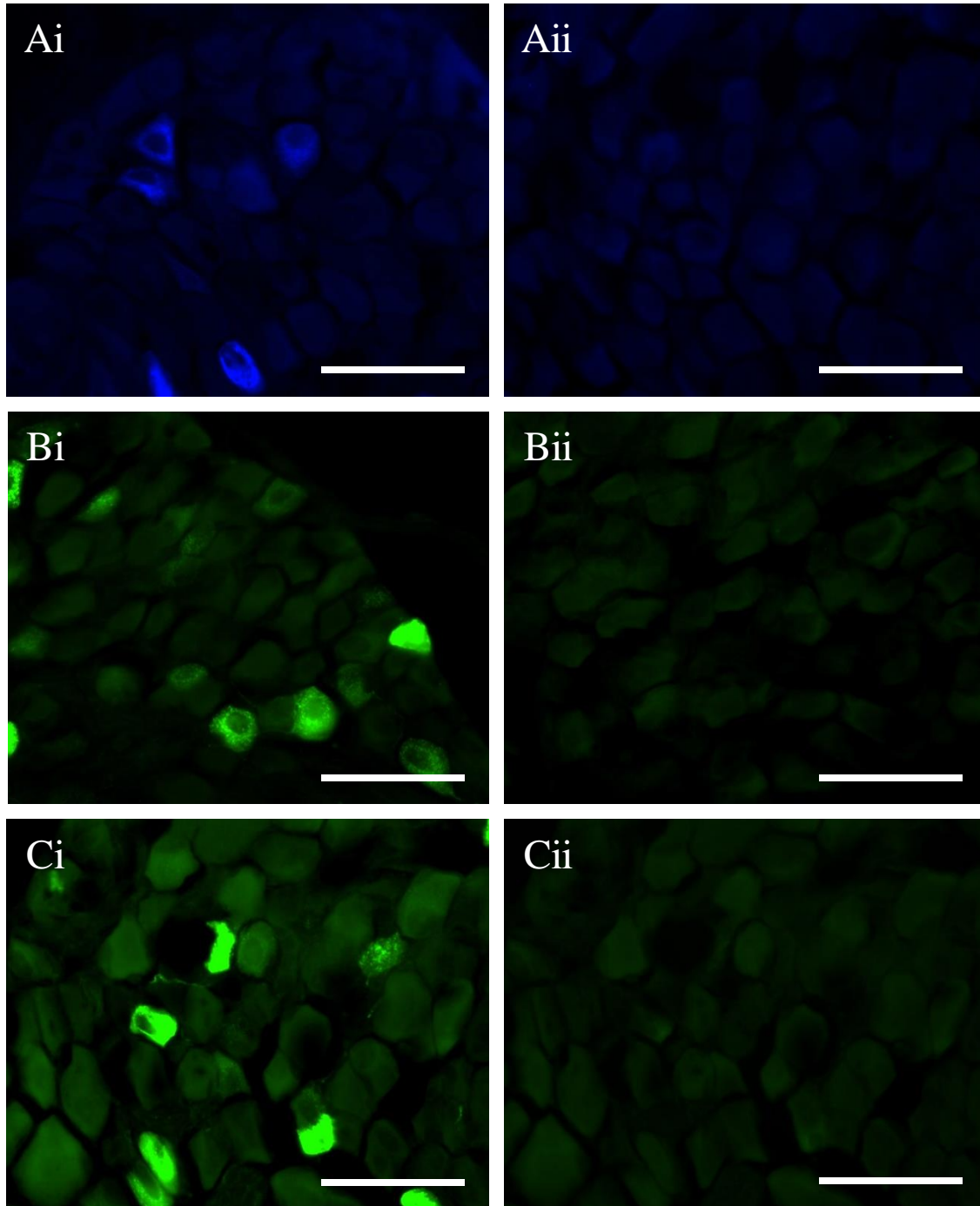


Figure 2.2: Immunolabelling of TRPV1, CB1, and GHSR in nodose ganglia cell bodies.

Immunolabelling of TRPV1 (Ai), CB1 (Bi), and GHSR (Ci) in nodose ganglia cell bodies. Negative controls of TRPV1 (Aii), CB1 (Bii), and GHSR (Cii) without the primary antibody. Scale bars represent 20µm.

2.5| Single Fibre Recording of Gastric Vagal Afferents

2.5.1| *in Vitro* gastric vagal afferent preparation

Mice were humanely killed via 5% isoflurane, exsanguinated via the abdominal aorta using a 23g needle, and decapitated. All mice were culled between 0700hr and 0730hr to minimise the influence of circadian variation.

A midline laparotomy was performed to expose the thoracic and abdominal cavities. The stomach, oesophagus, vagal nerves, heart, and lungs were dissected out together and pinned in a modified Krebs solution consisting of (in mM/L): 118.1 NaCl, 4.7 KCl, 25.1 NaHCO₃, 1.3 NaH₂PO₄, 1.2 MgSO₄•7H₂O, 1.5 CaCl₂, 1.0 citric acid, 11.1 glucose, 0.001 nifedipine and bubble with 95% O₂ – 5% CO₂. Nifedipine (N7634-10g; Sigma, Australia) was used to prevent smooth muscle contraction and does not affect the mechanosensitivity of vagal afferents [459]. During dissection the Krebs solution was kept at 4°C to prevent tissue degradation and metabolic breakdown.

After removal of excess tissue and isolation of the vagal nerves, the oesophagus and stomach were cut open longitudinally and along the greater curvature of the stomach respectively, and pinned mucosal side up in an organ bath containing a continuous flow of warmed (34°C) Krebs solution (Figure 2.3). To fit in the organ bath without unnecessary distortion of tissue only the ventral half of the stomach was used. The vagal nerves were threaded through a removable divider onto a glass plate in a liquid paraffin

filled chamber. The vagal nerves were then desheathed to expose the nerve trunk and split into smaller bundles (10-15) using fine forceps. Each individual bundle was placed one by one onto a platinum recording electrode for recording. A reference electrode rested on the glass plate in close proximity.

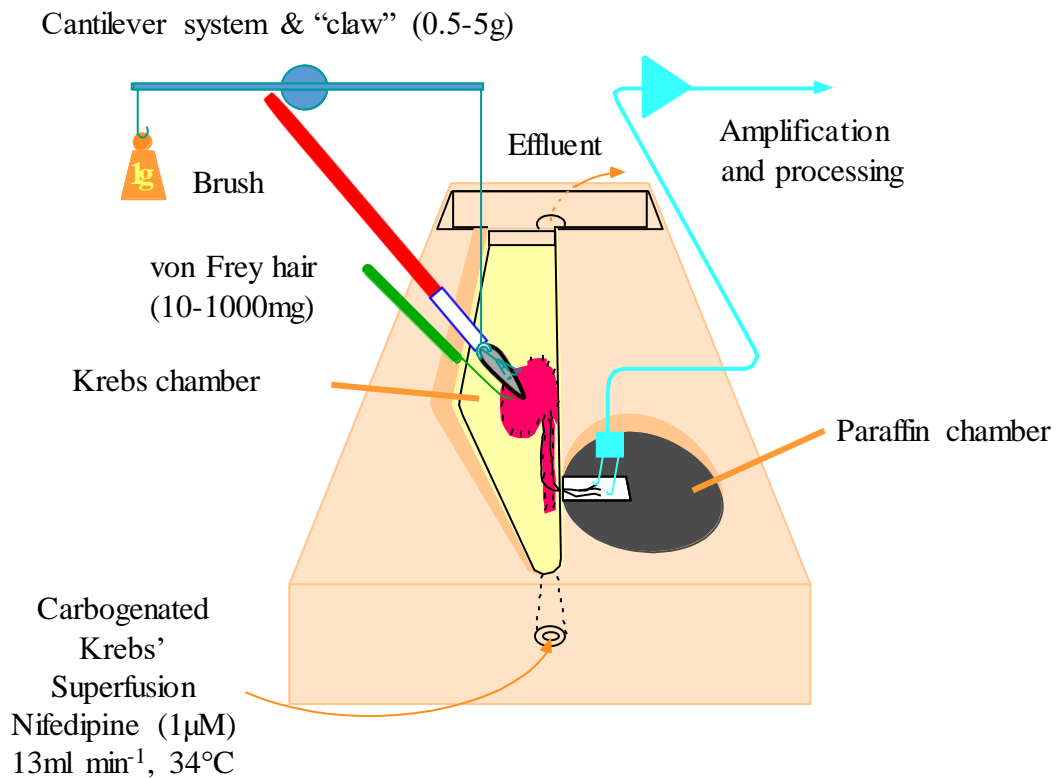


Figure 2.3: *In vitro* gastric vagal afferent preparation [215].

An organ bath containing a continuous flow of Krebs solution over the pinned out oesophagus and ventral stomach. The vagal nerves are placed on a glass platform in a liquid paraffin chamber, which was separated from the organ bath by a divider with a small hole. Small bundles of the vagal nerve were placed individually onto a platinum recording electrode. Mucosal stroking was performed with calibrated von Frey hairs (10mg-1000mg). Circular tension was performed by underpinning a hook adjacent to the

receptive field and attaching it to a cantilever. Weights are applied to the cantilever (1g, 3g, and 5g).

2.5.2| Characterisation of Gastric Vagal Afferent Properties

As previously reported [460], two types of mechanosensitive gastric vagal afferents were located, mucosal receptors and tension receptors. Mucosal sensitive receptors responded to mucosal stroking but not circular tension, and tension sensitive receptors responded to both mucosal stroking circular tension.

Receptive fields on the stomach were first determined broadly by the light stroking of the mucosal surface with a brush and then specifically using a calibrated 1000mg von Frey hair. The response of the GVAs receptive field to mechanosensation was then determined according to its subtype as outlined below.

The sensitivity of mucosal GVAs were determined using calibrated von Frey hairs. Initially the response was determined by the light stroking of a von Frey hair across the receptive field at a rate of 5mm/s. This was repeated 10 times with 1 second intervals between each stroke, and the middle 8 strokes were used for analysis. This was performed using von Frey hairs of increasing intensities (10mg, 50mg, 200mg, and 1000mg).

The sensitivity of tension GVAs to stretch was determined using a fine string attached to a claw that was underpinned adjacent to the receptive field using a hook. The other end of the string was attached to a cantilever system where various weights (1, 3, and 5g) were applied. Each weight was applied for 1 minute with a 1 minute rest period before the next weight was added. They were added with increasing weights. The response was

determined using the mean impulses per second over the 1 minute period. Only the response to 3g was used before and after superfusion with drugs. This was due to the fact that 3g provided a midpoint response to tension and thus provided opportunity for drugs to excite or inhibit mechanosensitivity. In contrast, 1g tension did not always elicit a response and 5g often elicited a maximum response therefore preventing inhibitory or excitatory effects respectively.

2.5.3| Effect of methanandamide on mechanosensitivity of gastric vagal afferents

Following the establishment of baseline mechanosensitivity of either mucosal or tension sensitive GVAs, 0.1nM of methanandamide (mAEA; a stable analogue of AEA; M186, Sigma) was added to the Krebs superfusion and was allowed to equilibrate for 20 minutes to allow penetration of the gastric layers. After 20 minutes the mechanosensitivity of the GVA was then re-determined. This was repeated for increasing concentrations of mAEA (0.3nM, 1nM, 3nM, 10nM, 30nM 100nM, and 300nM). Experiments were split into low mAEA (0.1, 0.3, 1, and 3nM) and high mAEA (10, 30, 100, 300 nM) concentrations on a single GVA unit. To ensure time had no effect on the mechanosensitivity of GVAs, control experiments were performed to measure GVA response to mucosal stroking or circular tension every 20 minutes over 2 hours in the absence of any drugs. Time had no significant effects on the mechanosensitivity of GVAs (Figure 2.4).

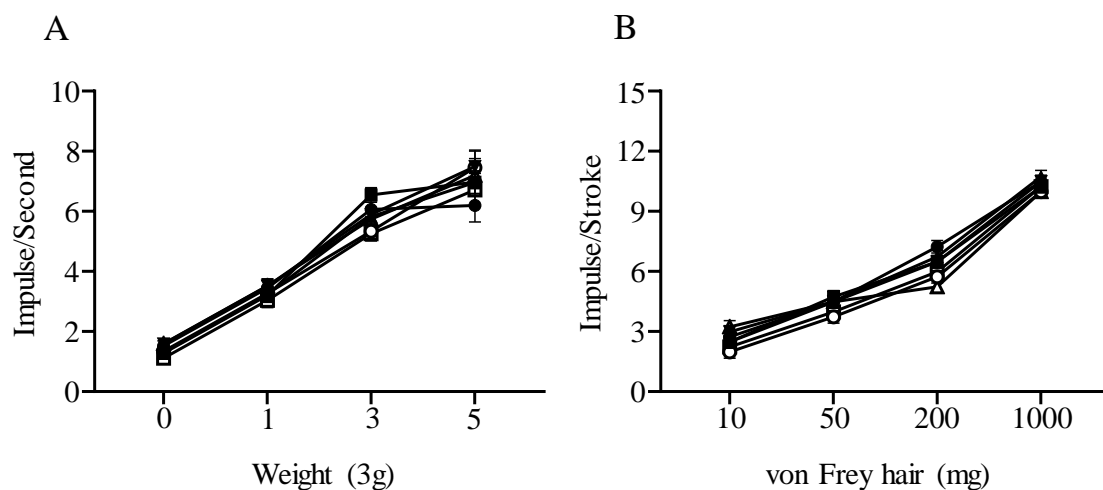


Figure 2.4: Mechanosensitivity of tension and mucosal gastric vagal afferents over time.

The response of tension (A) and mucosal (B) sensitive gastric vagal afferents before (•) and after 20 (■), 40 (▲), 60 (▼), 80 (○), 100 (□), 120 (△) minutes (N=5). There was no significant effect of time on the mechanosensitivity of tension or mucosal receptors.

2.5.4| Secondary messenger pathways used by anandamide

In a separate set of experiments, to study the secondary messenger pathways used by AEA to modulate GVA mechanosensitivity, antagonists of CB1 (rimonabant hydrochloride 300nM), TRPV1 (AMG9810), GHSR (YIL-781), $G\alpha_{i/o}$ (NF023 300nM), $G\alpha_q$ (YM-254980 100nM), PKA (PKA inhibitor fragment (6-22) amide (PKA-IFA) 5nM, and PKC (bisindolylmaleimide II (BIS-II) 10nM) were used. The details of the antagonists are illustrated in table 2.2 and the effects of the antagonists alone on tension GVA mechanosensitivity is illustrated in figure 2.5.

Firstly the effects of mAEA (1, 10, and 100nM) on GVA mechanosensitivity were determined, followed by a 20 minute washout period. Then the antagonist alone was added for 20 minutes and GVA mechanosensitivity was re-determined. Then the antagonist was combined with 1nM of mAEA and GVA mechanosensitivity was re-determined. This was repeated with increasing concentrations of mAEA (10, and 100nM) followed by a final washout.

2.5.5| Drugs

Stock solutions mAEA, rimonabant (1mM), AMG9810 (300µM) and BIS-II (100µM) were made using absolute ethanol. Control experiments were performed to measure the effect of ethanol on the mechanosensitivity tension sensitive GVAs. No significant effects were found at the concentrations measured (Figure 2.6). Stock solutions of NF023 (1mM), Ym-254980 (1mM), and YIL-781 (1mM) were made using Krebs solution. All drugs were stored at -20°C, and diluted to final concentrations in Krebs on the day of experiments. mAEA (M186), rimonabant hydrochloride (SML0800), AMG9810 (A2731), BIS-II (B3056), and PKA-IFA (P6062) were obtained from Sigma Aldrich. NF023 (1240) was obtained from In Vitro Technologies and YM-254980 (AG-CN2-0509-M001) was obtained from Sapphire Biosciences.

Table 2.2: Details of the antagonists used in electrophysiology studies

Drug	Target	Concentration	Ki/IC₅₀	Other interactions	Reference
Rimonabant	CB1	300nM	Ki 1.6nM		[450]
AMG9810	TRPV1	30nM	IC ₅₀ 17nM		[461]
Yil-781	GHSR	100nM	Ki 17nM		[462]
NF023	Gai/o	300nM	IC ₅₀ 300nM	P2X >50μM	[463]
YM-254890	Gαy	100nM	Ki 100nM		[464]
PKA-IFA	PKA	5nM	Ki 2.5nM		[465]
BIS-II	PKC	10nM	IC ₅₀ 10nM	PKA>2μM	[466]

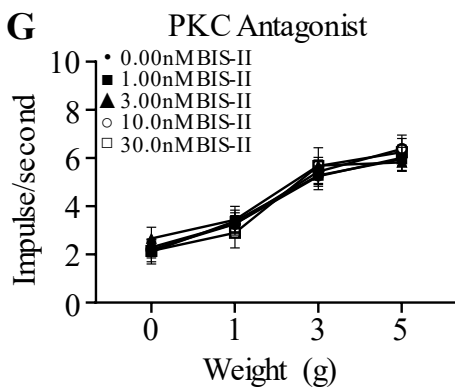
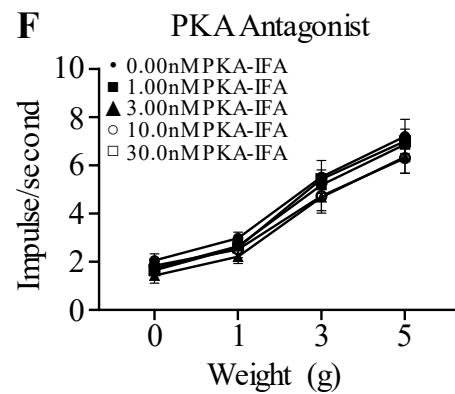
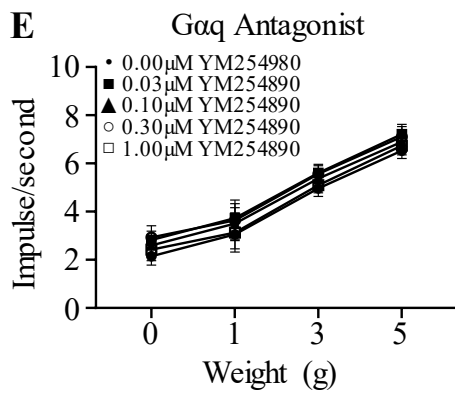
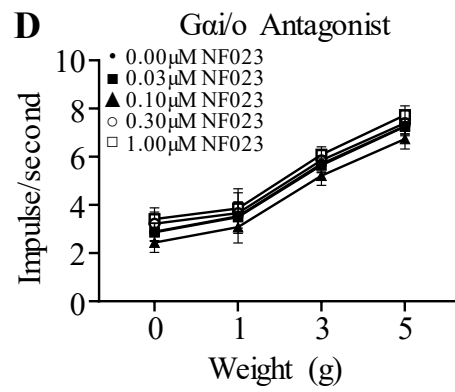
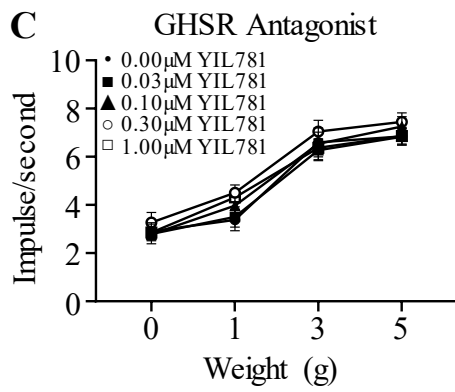
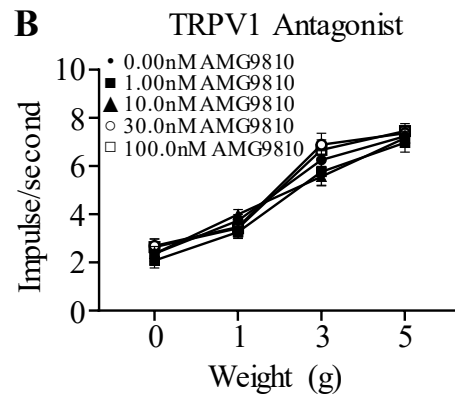
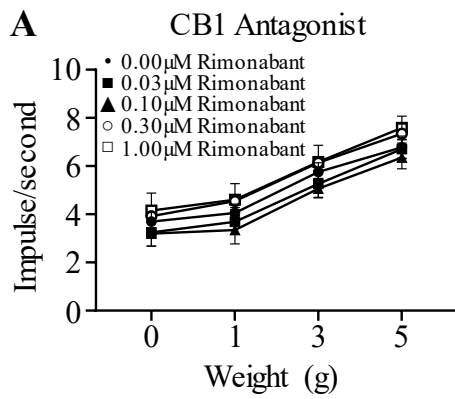


Figure 2.5: Response of tension sensitive gastric vagal afferents to antagonists.

The response of tension sensitive GVAs to stretch in the absence or presence of the CB1 antagonist rimonabant hydrochloride (A), TRPV1 antagonist AMG9810 (B), GHSR antagonist YIL-781 (C), G α i/o antagonist NF023 (D), G α q antagonist YM-254890 (E), PKA antagonist (PKA-IFA) (F), or PKC antagonist BIS-II (G). No significant effects of any antagonist on the mechanosensitivity of tension GVAs was found.

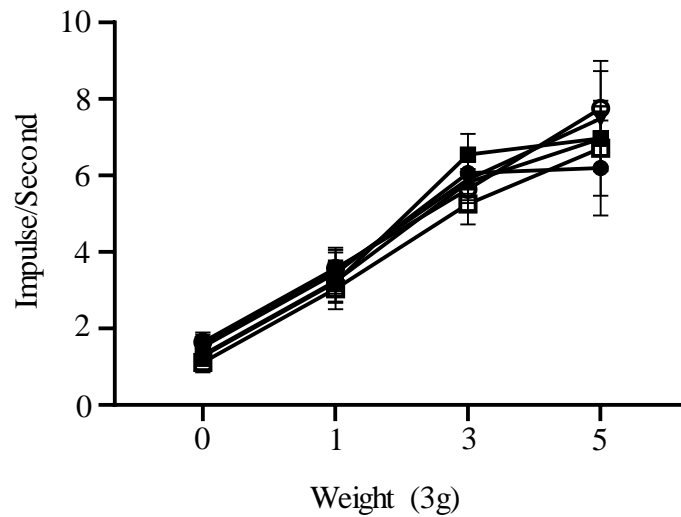


Figure 2.6: Response of tension sensitive gastric vagal afferents to ethanol.

The response of sensitive gastric vagal afferents before (●) and after 0.01% (■), 0.03% (▲), 0.1% (▼), 0.3% (○), and 1% (□), ethanol (N=5). There was no significant effect of ethanol on the mechanosensitivity of tension receptors.

2.5.6| Gastric Vagal Afferent Recording

Electrical nerve signals were amplified using a DAM50 biological amplifier (World Precision Instruments, USA) and a JRAK scaling amplifier (JRAK, Australia). Signals were then filtered with a band-pass filter-932 (CWE, USA) and recorded with a DL1200A oscilloscope (Yokogawa, Japan). Spike II software (Cambridge Electronic Design, UK) was used to determine single nerve units based on amplitude, duration and shape of the action potential. Electrophysiological data is presented as the mean \pm the SEM with n being the number of animals with at least 2 GVAs of each subtype recorded per animal.

2.6| Gastric Mucosal Analysis

Gastric mucosal scrapings were obtained from the dorsal half of the stomach during the vagal afferent preparation using a fine scalpel blade, snap frozen in liquid nitrogen, and stored at -80°C until required.

2.6.1| Total RNA extraction

Gastric mucosal scrapings were rapidly lysed and homogenised and RNA was extracted using a Purelink RNA minikit (Invitrogen, ThermoFisher Scientific) following the company's instruction for 50mg of tissue. The level of RNA and quality was determined with a NanoDrop LITE spectrophotometer at 260nm/280nm absorbance (A260/280). An A260/280 of 1.9 to 2.1 were considered acceptable for PCR analysis.

2.6.2| qRT-PCR

qRT-PCR analysis on RNA from stomach scrapings of SLD- and HFD-mice was performed using an Express One-Step Superscript qRT-PCR Universal kit (ThermoFisher Scientific) and a 7500 Fast Real-time PCR system (ThermoFisher) with the following

steps: 50°C for 15 minutes, 95°C for 20 seconds, 40 cycles of 95°C for 3 seconds, and 60°C for 30 seconds.

Pre-designed Taqman gene expression assays obtained from Life Technologies (Australia) were chosen to measure mRNA expression of FAAH (mm00515684_m1), N-acyl phosphatidylethanolamine-specific phospholipase D (NAPE-PLD; mm00724596_m1), CB1 (mm01212171_s1), and ghrelin O acyl transferase (GOAT; mm01200389_m1) in gastric cells. The average of peptidylprolyl Isomerase A (PPIA; mm00620857_s1), Hypoxanthine-phosphoribosyltransferase (*HPRT*; mm03024075_m1), and beta-actin (mm00437762_m1) were chosen as reference based on stability across all samples determined from NormFinder software (stability value = 0.098) (MOMA). Details of all the housekeeping genes tested are illustrated in Table 2.3. RNA levels relative to the housekeeping genes were calculated using the $2^{\Delta CT}$ method [456].

Table 2.3: Details of housekeeping genes tested in gastric mucosa scrapings

Gene	Stability Value	Catalogue #
β -actin (ActB)	0.468	mm00437762_m1
β -2-microglobulin (B2M)	0.110	mm00437762_m1
Hypoxanthine-phosphoribosyltransferase (HPRT)	0.180	mm03024075_m1
Peptidylprolyl Isomerase A (PPIA)	0.052	mm00620857_s1
Average of B2M, HPRT & PPIA*	0.098	-

* This is the average from the raw data obtained during analysis

2.6.3| Enzyme Linked Immunosorbance Assays

Anandamide and fatty acid amide hydrolase

Gastric AEA and FAAH levels were determined using Enzyme-linked immunosorbent assay (ELISA) kits for AEA (Clone-Cloud) and FAAH (Abbexa) and quantified via calorimetry at 450nm using a VersaMax ELISA microplate reader (Molecular Devices). The AEA ELISA kit had a detection range from 0.8ng to 200ng of AEA. The FAAH had detection range of 0.7ng to 5ng of FAAH. The standard curves for each ELISA kit are illustrated in figure 2.7.

Ghrelin

Ghrelin was extracted by boiling gastric mucosal scrapings for 10 minutes followed by homogenisation in a 3:9 ratio of protease inhibitors (MP Biomedicals) and 6% acetic acid (Sigma). The samples were then centrifuged and the supernatant was collected and diluted (1 in 500).

Active gastric ghrelin levels were determined using an ELISA kit for ghrelin (EMD Millipore) and quantified via calorimetry at 450nm and 590nm using a VersaMax ELISA microplate reader (Molecular Devices). The standard curve for the ghrelin ELISA kit is illustrated in figure 2.7.

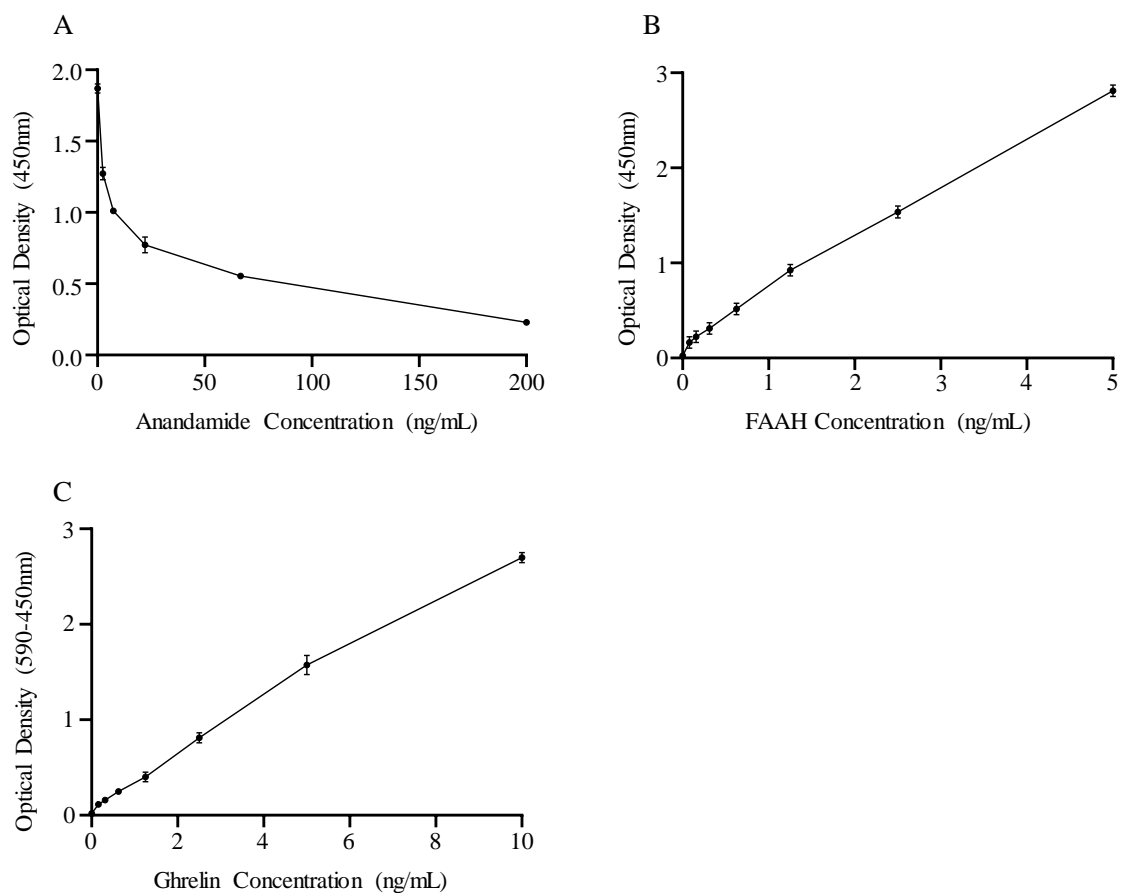


Figure 2.7: Standard curve of ELISA kits.

A. Standard curve obtained from AEA ELISA kit. B. Standard curve obtained from FAAH ELISA kit. C. Standard curve obtained from ghrelin ELISA kit. Whilst standard curves were performed in duplicates, some error bars are too small to be shown.

2.7| Nodose Ganglia Cell Culture Expression Analysis

2.7.1| Plate Coating

The day before experiments a Nunclon™ Delta Surface 48 well plate (150687; ThermoFisher) was coated with a poly-d-lysine (PDL; A3890401; ThermoFisher) and laminin (23017-015; ThermoFisher) solution (60uL per well). The plate was stored at 4°C for at least 18 hours prior to use. Immediately prior to use the PDL/laminin solution was removed completely and the wells were rinsed as excess PDL can be toxic to neuronal cells.

2.7.2| Cell Culture

Mice were killed via CO₂ inhalation and decapitated. Nodose ganglia were bilaterally removed and placed immediately in 10mL of ice cold F12 solution. Up to 4 nodose ganglia pairs were added to one tube. The nodose ganglia were cultured as outlined in section 2.4.1. However, following the final pelleting step, the HBSS was removed and 300uL of ice cold neural basal A (NBA; A35829-01; ThermoFisher) medium supplemented with B-27 (17504-44; ThermoFisher), penicillin/streptomycin (15140-122; ThermoFisher), and glutaMAX (35050061; ThermoFisher) was added.

5uL of the cell suspension was used to count cell numbers via trypan blue exclusion (T10282, Invitrogen, ThermoFisher). 10uL of the cell suspension (approximately 500-600 cells) was then added to the middle of the wells in the PDL/laminin coated 48 well plate. The plate was placed in an incubator for 2 hours at 37°C.

After incubation the cells were checked for adhesion and 500uL of NBA medium was added to each well. Control wells contained only NBA medium, whilst experimental wells contained either mAEA (1 or 100nM; Sigma) or ghrelin (1 or 3nM; G8903; Sigma).

The cells were then incubated for 14 hours at 37°C, a period shown to be sufficient to observe changes in mRNA expression [467].

After 14 hours the medium from the wells was carefully aspirated as to not disturb the cells. 50uL of ice cold PBS was then added to each well twice followed by careful aspiration as to not disturb the cells. 50uL of a lysis solution contained DNase 1 (provided in Cells-CT kit (A35374; ThermoFisher)) was then added to the wells, mixed via gentle pipetting and incubated at room temperature for 5 minutes. 5uL of a Stop Solution (provided in Cells-CT kit (ThermoFisher)) was then added and incubated at room temperature for 2 minutes. The lysed cells were then stored at -20°C for a maximum of 2 days before processing for qRT-PCR.

2.7.3| Cultured cells qRT-PCR

Cell culture samples were thawed to room temperature. Reverse transcription and qRT-PCR were performed using a Cells-CT Kit (Thermofisher) following manufacturer's instructions. The qRT-PCR step was performed in a 7500 Fast Real-time PCR system (ThermoFisher) with the following steps: 50°C for 2 minutes, 95°C for 10 minutes, and 40 cycles of 95°C for 15 seconds and 60°C for 1 minute.

Pre-designed Taqman gene expression assays (Life Technologies) were used to determine the mRNA expression and co-expression of CB1 (mm01212171_s1), TRPV1 (mm01246300_m1), GHSR (mm00616415_m1), and FAAH (mm00515684_m1) in nodose ganglia cell cultures of SLD- and HFD-mice. Beta-2-microglobulin (B2M) and beta-actin (ActB) were used as housekeeping genes. They were chosen based on stability across diets (stability value of B2M and ActB = 0.082) using NormFinder software (Department of Molecular Medicine (MOMA), Aarhus University Hospital, Denmark).

Other housekeeping genes tested are illustrated in Table 2.4. Nuclease free water was substituted for amplified RNA as a negative control. RNA levels were calculated relative to the housekeeping genes using the $2^{\Delta CT}$ method [456].

Table 2.4: Details of housekeeping genes tested in cultured nodose neurons

Gene	Stability Value	Catalogue #
Class 3 β -Tubulin (Tubb-3)	0.506	mm00727586_m1
β -actin (ActB)	0.071	mm00437762_m1
β -2-microglobulin (B2M)	0.089	mm00437762_m1
Hypoxanthine-phosphoribosyltransferase (HPRT)	0.420	mm03024075_m1
Peptidylprolyl Isomerase A (PPIA)	0.184	mm00620857_s1

2.8| Statistical Analysis

A one-way ANOVA with Tukey's *post hoc* test was used to determine significant effects of mAEA on GVA mechanosensitivity. A two-ANOVA with Sidak's *post hoc* was used to determine the differences between mAEA alone and in combination with an antagonist, mice body weight parameters, mRNA expression, and gastric content.

All data was analysed using GraphPad Prism 7. $P < 0.05$ were deemed significant.

2.9| Solutions

Collagenase

Collagenase Type II 12mg

HBBS (Mg²⁺/Ca²⁺ free) 3mL

Collagenase/Dispase

Collagenase Type II 12mg

Dispase 14mg

HBBS (Mg²⁺/Ca²⁺ free) 3mL

Gelatin Slides

Gelatin 5g

Chrome Alum 0.5g

dH₂O 1L

Krebs

NaCl 69g

NaHCO₃ 21g

Glucose 20g

KCl	3.5g
MgSO ₄ 7H ₂ O	2.95g
Citric acid	2.0g
NaH ₂ PO ₄	1.6g
Nifedipine (1μM)	1mL
dH ₂ O	10L

NBA Complete Medium

NBA	25mL
B-27	0.5mL
MEM/Glutamax	0.25mL
Penicillin/streptomycin	0.25mL

Paraformaldehyde 4%

0.2M Na ₂ HPO ₄	405mL
0.2M NaH ₂ PO ₄	95mL
Paraformaldehyde	40g
dH ₂ O	Diluted to 1L

PBS-TX

1x PBS 200mL

TritonX-100 400uL

PDL Stock

PDL 100μL

HBSS (Mg²⁺/Ca²⁺ free) 3.3mL

PDL/Laminin

PDL Stock 2.2mL

Laminin (filtered) 240uL

Chapter 3 : Biphasic effects of methanandamide on murine gastric vagal afferent mechanosensitivity

Christie. S¹, O'Reilly. R¹, Li. H^{1,2}, Wittert. G.A^{1,2}, Page. A.J^{1,2}

¹ Vagal Afferent Research Group, Centre for Nutrition and Gastrointestinal Disease, Adelaide Medical School, University of Adelaide, Adelaide, SA 5005, Australia

² Lifelong Health, South Australian Health and Medical Research Institute, Adelaide, SA 5000, Australia

Published in: Journal of Physiology, DOI: 10.1113/JP278696

Statement of Authorship

Title of Paper	Biphasic effects of methanandamide on murine gastric vagal afferent sensitivity
Publication Status	<input checked="" type="checkbox"/> Published <input type="checkbox"/> Accepted for Publication <input type="checkbox"/> Submitted for Publication <input type="checkbox"/> Unpublished and Unsubmitted work written in manuscript style
Publication Details	Published in Journal of Physiology DOI: 10.1113/JP278696

Principal Author

Name of Principal Author (Candidate)	Stewart Christie
Contribution to the Paper	Performed experiments and wrote the paper
Overall percentage (%)	80%
Certification:	This paper reports on original research I conducted during the period of my Higher Degree by Research candidature and is not subject to any obligations or contractual agreements with a third party that would constrain its inclusion in this thesis. I am the primary author of this paper.
Signature	Date 14/11/2019

Co-Author Contributions

By signing the Statement of Authorship, each author certifies that:

- i. the candidate's stated contribution to the publication is accurate (as detailed above);
- ii. permission is granted for the candidate to include the publication in the thesis; and
- iii. the sum of all co-author contributions is equal to 100% less the candidate's stated contribution.

Name of Co-Author	Rebecca O'Reilly
Contribution to the Paper	Helped perform tracing studies
Signature	Date 14/11/2019

Name of Co-Author	Hui Li		
Contribution to the Paper	Helped perform tracing studies and edited the paper		
Signature		Date	14/11/2019

Name of Co-Author	Gary Wittert		
Contribution to the Paper	Planning of experiments and edited the paper		
Signature	✓ ✓	Date	20/11/2019

Name of Co-Author	Amanda J Page		
Contribution to the Paper	Planning of experiments and edited the paper		
Signature		Date	14/11/2019

Significance Statement (120 words)

- The fine control of food intake is important for the maintenance of a healthy metabolic state.
- GVAs are involved in the peripheral regulation of food intake via signalling the degree of distension of the stomach which ultimately leads to feelings of fullness and satiety.
- This study provides evidence that endocannabinoids, such as anandamide, are capable of regulating GVA sensitivity in a concentration-dependent biphasic manner.
- This biphasic effect is dependent upon CB1, TRPV1, and GHSR interactions.
- These data have important implications for the peripheral control of food intake.

Abstract

Introduction: Gastric vagal afferents (GVAs) signal to the hindbrain resulting in satiety. Endocannabinoids are endogenous ligands of cannabinoid 1 receptor (CB1) and transient receptor potential vanilloid-1 (TRPV1) channels. The endocannabinoid anandamide (AEA) is expressed in the stomach, and its receptor CB1 is expressed in ghrelin-positive gastric mucosal cells. Further, TRPV1, CB1 and growth hormone secretagogue receptor (ghrelin receptor, GHSR) are expressed in subpopulations of GVA neurons. This study aimed to determine the interaction between TRPV1, CB1, GHSR and endocannabinoids in the modulation of GVA signalling.

Methods: An *in vitro* electrophysiology preparation was used to assess GVA mechanosensitivity in male C57BL/6 mice. Effects of methanandamide (mAEA; 1-100nM), on GVA responses to stretch were determined in the absence and presence of a CB1, TRPV1, GHSR, protein kinase-A (PKA), protein kinase-C (PKC), Gai/o, or Gαq antagonist.

Results: Low doses (1-10nM) of mAEA reduced, whereas high doses (30-100nM) increased GVA responses to 3g stretch. The inhibitory and excitatory effects of mAEA (1nM&100nM) were reduced/lost in the presence of a CB1 and TRPV1 antagonist. PKA, Gai/o, or GHSR antagonists prevented the inhibitory effect of mAEA on GVA mechanosensitivity. Conversely, in the presence of a PKC or Gαq antagonist the excitatory effect of mAEA was reduced or lost respectively.

Conclusions: Activation of CB1, by mAEA, can activate or inhibit TRPV1 to increase or decrease GVA responses to stretch depending on the pathway activated. These interactions could play an important role in the fine control of food intake.

Introduction

Endocannabinoids such as anandamide (AEA) increase appetite via central activation of the cannabinoid 1 receptor (CB1) [468, 469]. It has also been demonstrated that peripheral activation of CB1 can also increase appetite [333, 470, 471] which is dependent on intact vagal afferent neurones [345, 472].

In the periphery, the gut-brain axis plays an important role in signalling the arrival, amount and nutrient composition of a meal [214]. In the stomach there are two distinct gastric vagal afferent (GVA) receptors that respond to these stimuli, mucosal and tension receptors [460]. Mucosal receptors respond to gentle contact of food particles with the gastric epithelia and are thought to be involved in nausea, vomiting [217], and gastric emptying [205]. Tension receptors respond to stretch or distension of the gastric wall and are thought to be involved in the generation of fullness and satiety sensations [204]. The mechanosensitivity of GVAs are modulated by factors including: dietary status [167], time of day [224], hormones [220], and adipokines [223]. For example, activation of the transient receptor potential vanilloid 1 (TRPV1) ion channel with oleoylethanolamide increases the mechanosensitivity of GVAs [235] and ghrelin reduces the mechanosensitivity of tension sensitive GVAs through action at the growth hormone secretagogue receptor (GHSR) [220].

TRPV1 is a non-selective cation channel that is highly permeable to calcium [395]. Ingestion of capsaicin, a pungent component of chilli and an agonist of TRPV1, can decrease food intake [422, 434, 473]. This is complicated by TRPV1 interactions with CB1 receptors. In dorsal root ganglia, activation of CB1 by AEA can result in either an inhibitory or excitatory effect on TRPV1 depending on the secondary messenger

pathways activated [447]. Low concentrations of AEA (3-30nM) reduce TRPV1 activity via inhibition of the adenylyl cyclase and protein kinase A (PKA) pathway [406, 447, 474]. Conversely, high concentrations of AEA (1-10 μ M) can sensitise TRPV1 via activation of phospholipase C (PLC) and protein kinase C (PKC) pathways [397, 413]. It is unknown whether these biphasic effects occur in GVAs.

CB1 receptors are also expressed in ghrelin-positive gastric mucosal cells [249]. Activation of these CB1 receptors increases gastric ghrelin secretion [249]. It is known that ghrelin reduces the mechanosensitivity of GVAs [220]. Whether endocannabinoids in the stomach can regulate GVA function through the release of ghrelin is unclear.

It is known that AEA is produced in the stomach and that CB1 receptors are expressed on ghrelin positive cells and GVAs. Further, it is also known that GVAs express CB1, TRPV1 and GHSR. Therefore using an *in vitro* electrophysiology preparation this study aimed to determine the role of CB1, GHSR, and TRPV1 in the regulation of GVA satiety signals by methanandamide (mAEA), the stable analogue of AEA.

Methods

Ethical Approval

This study was approved by the animal ethics committee of the South Australian Health and Medical Research Institute (SAHMRI), and carried out in accordance with the Australian code for the care and use of animals for scientific purposes, 8th edition 2013 and the ARRIVE guidelines [475].

Mice

Seven-week-old C57BL/6 male mice (N=76; 27.69±0.11g; Bioresources Facility, SAHMRI, Adelaide, Australia) were group housed in littermates of 4 or 5 for one week. All mice were housed under a 12:12hr light: dark cycle at a constant temperature (22°C) with *ad libitum* access to a standard laboratory diet (SLD; 12% energy from fat, 65% energy from carbohydrates, 23% energy from protein) and water, unless otherwise stated.

Retrograde tracing studies

This procedure has been described in detail previously [223]. Briefly, mice were anaesthetised with 3% isoflurane in 1-1.5% oxygen and a midline abdominal laparotomy was performed. The stomach was exteriorised and Alexa Fluor® 555 conjugate of cholera toxin β -subunit (C22843; Life Sciences, Australia) was injected under the serosal layer with 10 equally spaced injections (10 μ L total). The laparotomy was sutured, and mice were given a subcutaneous injection of antibiotic (baytril; 10mg/50 μ L) and analgesic (buprenorphine; 0.1mg/kg) to aid recovery.

Two days post procedure mice were humanely killed via CO₂ inhalation and nodose ganglia were bilaterally dissected and prepared for either single cell RT-PCR or immunohistochemistry.

Cell Culture

This method has been described in detail previously [455]. Briefly, nodose ganglia were incubated in collagenase and dispase (4mg/mL) in Hank's Balanced Salt Solution (HBSS; 14170112; Thermo Fisher Scientific, Australia) at 37°C for 30 minutes and then a collagenase (4mg/mL) solution in HBSS at 37°C for 10 minutes. Nodose ganglia were then mechanically sheared into single cells using a fire polished pipette, washed in ice-cold HBSS and then diluted to approximately 1 cell/ μ L.

1 μ L of cell suspension was placed onto a piece of thin glass (approx. 4mm by 8mm) and examined for the presence of a single fluoresced cell under an epifluorescence microscope (BX-51, Olympus, Australia) equipped with filters for Alexa Fluor 568. The glass piece was then examined under bright field (BX-51, Olympus, Australia) to ensure non-fluoresced cells were not present, and then dropped into Single Cell Lysis/DNase 1 solution (10 μ L) provided in a Single Cell-CT™ Kit (4458235; Life Technologies, Australia) for 5 minutes incubation at room temperature. A stop solution (1 μ L; 4458235; Life Technologies, Australia) was added and incubated for 2 minutes, and then the samples were stored at -20°C until further processing for single cell RT-PCR.

Single Cell RT-PCR

Single cell qRT-PCR was performed on lysed single fluoresced cell using the Single Cell-CT™ Kit following the manufacturer's instructions. Pre-designed Taqman gene expression assays (Life Technologies, Australia) were used to measure the mRNA levels

and co-expression of TRPV1 (mm01246300_m1) and CB1 (mm01212171_s1) in traced tension GVA neurons and untraced nodose neurons. Beta-2-microglobulin (B2M; mm00437762_m1) and beta-actin (ActB; mm02619580_g1) were used as housekeeping genes and were chosen based on stability across all samples determined from NormFinder software (stability value of B2M and ActB = 0.102; Department of Molecular Medicine (MOMA), Aarhus University Hospital, Denmark). Relative mRNA levels were calculated using the $2^{\Delta\text{CT}}$ method [456].

Immunohistochemistry

Following dissection nodose ganglia were immediately placed in a 4% paraformaldehyde solution at room temperature for 4 hours with gentle agitation, and then placed in a 30% sucrose solution for a minimum of 18 hours at 4°C. nodose ganglia were then removed from the sucrose solution, frozen in Tissue-Tek mounting medium (IA018; ProSciTech), and cryosectioned at 10µM thickness.

Immunoreactivity for TRPV1, CB1, and GHSR in retrogradely traced nodose ganglia sections was determined using a rabbit polyclonal antibody to CB1 (diluted 1:200 in phosphate buffered saline + 0.2% Triton X-100 (PBS-TX; Sigma Aldrich), a goat polyclonal antibody to TRPV1 (diluted 1:400 in PBS-TX; GT15128; Neuromics-Life Research), and a rabbit polyclonal antibody to GHSR (diluted to 1:200 in PBSTX). The primary antibody for CB1 was visualised using donkey anti-rabbit secondary antibody coupled to Alexa Fluor 488 or 350 (diluted 1:200 in PBS-TX). The primary antibody for TRPV1 was visualised using donkey anti-goat secondary antibody coupled to Alexa Fluor 350 (diluted 1:200 in PBS-TX). The primary antibody for GHSR was visualised using donkey anti-rabbit secondary antibody coupled to Alexa Fluor 488 (diluted 1:200 in PBS-

TX). CB1 and TRPV1 were dual labelled on the same sections. As GHSR and CB1 share a host antibody, these were labelled on consecutive sections.

The sections were air dried at room temperature on gelatine-coated slides for 40 minutes then rinsed with PBSTX 3 times. The sections were then blocked with 10% donkey sera for 40 minutes and rinsed 3 times for 5 minutes with PBSTX. The sections were then incubated with primary antibodies for CB1 or GHSR at room temperature for 20 hours and then washed three times with PBS-TX to remove unbound antibody. Sections were then incubated for 1 hour at room temperature with the secondary antibody and washed in PBS-TX to remove unbound antibody. This process was repeated for the TRPV1 antibody after which sections were given final PBSTX washes and mounted with ProLong antifade.

Slides were imaged with an epifluorescence microscope (BX-51, Olympus, Australia) equipped with filters for Alexa Fluor® 350, 488, and 568. Images were overlaid using Image J software (University of Wisconsin, USA) and analysed for percentage of co-expression of CB1, TRPV1, and GHSR in traced and untraced cells. This was performed using 15 non-consecutive sections per animal.

In vitro gastric vagal afferent preparation

This preparation has been described in detail previously [460]. Briefly, mice were humanely killed via 5% isofluorane and decapitation between 0700 and 0730hr to minimise the influence of circadian variation. A midline laparotomy was performed, the oesophagus and stomach with attached vagal nerves were dissected out, opened longitudinally and pinned mucosal side up in a modified Krebs solution. The Krebs solution consisted of (in mM): 118.1 NaCl, 4.7 KCl, 25.1 NaHCO₃, 1.3 NaH₂PO₄, 1.2

MgSO₄·7H₂O, 1.5 CaCl₂, 1.0 citric acid, 11.1 glucose and 0.001 nifedipine, bubbled with 95% O₂- 5% CO₂. Whilst nifedipine is an L-type calcium channel blocker, previously it has been shown that it has no significant effects on GVA mechanosensitivity [459].

The vagal nerves were then threaded through a divider into a paraffin oil filled chamber. The nerves were then desheathed and split into smaller nerve bundles (10-16) which were subsequently placed onto a platinum electrode for recording.

Gastric vagal afferent subtypes

Consistent with previous reports [460], two types of murine mechanosensitive GVAs were recorded, mucosal and tension sensitive GVAs. Mucosal sensitive GVAs respond to mucosal stroking but not to circular tension, and tension sensitive GVAs respond to both mucosal stroking and circular tension. Responses of mucosal sensitive GVAs were determined using a calibrated von Frey hair (50mg). The von Frey hair was stroked across the receptive field at a rate of 5mm s⁻¹ 10 times with 1 second intervals. The middle 8 strokes were used for analysis.

Responses of tension sensitive GVAs were determined by underpinning a hook and thread to an area adjacent to the receptive field. The thread was then attached to a cantilever system. A standard weight (1g) was attached to the opposite end of the cantilever for a period of one minute followed by a one minute rest period. This was repeated with increasing weights (3g and 5g). The mean number of nerve impulses during the weight period were used for analysis. Only the response to 3g was obtained before and after superfusion with drugs. This was due to the fact that 3g provided a midpoint response to tension and thus provided opportunity for drugs to excite or inhibit mechanosensitivity. In contrast, 1g tension did not always elicit a response and 5g often elicited a maximum response therefore preventing inhibitory or excitatory effects respectively.

Effect of methanandamide on mechanosensitivity of gastric vagal afferents

Following the establishment of baseline GVA sensitivity, 0.1nM of mAEA, a stable analogue of AEA, was added to the Krebs superfusion and allowed to equilibrate for 20 minutes to allow penetration of the gastric wall. The mechanosensitivity of the GVAs was then re-determined. This process was repeated for increasing concentrations of mAEA. To avoid time dependent effects no more than 4 concentrations of mAEA were examined on individual GVAs. Therefore, the experiments were split into low (0.1, 0.3, 1, and 3nM) and high (10, 30, and 100nM) concentrations. Time controlled experiments were performed with no significant change in mechanosensitivity of mucosal and tension sensitive GVAs over a comparable duration.

In a separate set of experiments, to determine the receptors and secondary messenger pathways used by mAEA to modulate GVA mechanosensitivity, antagonists of CB1 (rimonabant 300nM [450]), GHSR (YIL-781 300nM [462]), TRPV1 (AMG9810 30nM [461]), $G\alpha_{i/o}$ (NF023 300nM [463]), $G\alpha_q$ (YM-254890 100nM [464]), PKA (PKA inhibitor fragment (6-22) amide (PKA-IFA 5nM [465]), and PKC (bisindolylmaleimide-II (BIS-II) 10nM [466]) were used. Firstly the baseline effect of mAEA on GVA mechanosensitivity was determined, then the mAEA was washed out, followed by the effect of the antagonist alone, and then the effect of mAEA in combination with the antagonist.

Drugs

Stock solutions of mAEA, rimonabant (1mM), AMG9810 (300 μ M) and BIS-II (100 μ M) were made using absolute ethanol. Stock solutions of NF023 (1mM), YM-254890 (1mM), and YIL-781 (1mM) were made using Krebs solution. All drugs were stored at -

20°C and diluted to final concentrations in Krebs the day prior to experiments. Ethanol control studies were performed to measure ethanol's effects on GVA mechanosensitivity. No significant effects were found at the concentrations used. mAEA (M186), rimonabant hydrochloride (SML0800), AMG9810 (A2731), YIL-781 (SML1148), BIS-II (B3056), and PKA-IFA (P6062) were obtained from Sigma Aldrich (Australia). NF 023 (1240/10) was obtained from In Vitro Technologies (Australia). YM-254980 (AG-CN2-0509-M001) was obtained from Sapphire Biosciences (Australia).

Data Analysis

All data in graphs is presented as the mean \pm SEM and was analysed using GraphPad Prism software. Data relating to the effect of mAEA alone on GVAs was analysed using a one-way ANOVA with a Tukey *post hoc* test. Data relating to the effect of mAEA on GVAs in combination with antagonists was analysed using a two-way ANOVA with a Sidak *post hoc* test. P-values less than or equal to 0.05 were deemed significant.

Results

CB1, GHSR and TRPV1 co-localise in tension sensitive gastric vagal afferent cell bodies

Co-localisation of CB1, GHSR, and TRPV1 mRNA are illustrated in Figure 1. TRPV1, CB1, and GHSR were expressed in individual retrogradely traced tension sensitive GVA cell bodies (relative expression: TRPV1 1.69 ± 0.25 ; CB1 0.70 ± 0.05 ; GHSR 0.19 ± 0.03 ; Figure 1Ai). The traced cell bodies expressed either TRPV1 alone (2% of traced cells), CB1 and GHSR (8% of traced cells) or TRPV1, CB1 and GHSR (90% of traced cells). In contrast, in untraced cell bodies 34% expressed neither TRPV1, CB1 nor GHSR, 22% expressed only TRPV1, 16% expressed CB1 and GHSR, and 28% expressed TRPV1, CB1 and GHSR (Figure 1Aii). No cells expressed only CB1 or GHSR.

By using immunohistochemistry, TRPV1, CB1, and GHSR protein were co-localised and present in retrogradely traced tension sensitive GVA cell bodies (Figure 1Bi, 1Bii, and 1Biii). All traced cell bodies were reactive for TRPV1, CB1, GHSR, or all, whilst 46% of untraced cell bodies were reactive for neither. TRPV1, CB1, and GHSR were co-localised in 85% of traced and 20% of untraced cell bodies. TRPV1 alone was reactive in 4% of traced and 20% of untraced cell bodies. CB1 and GHSR were reactive in 11% of traced and 14% of untraced cell bodies. No cell bodies expressed only CB1 or GHSR (Figure 1Biv).

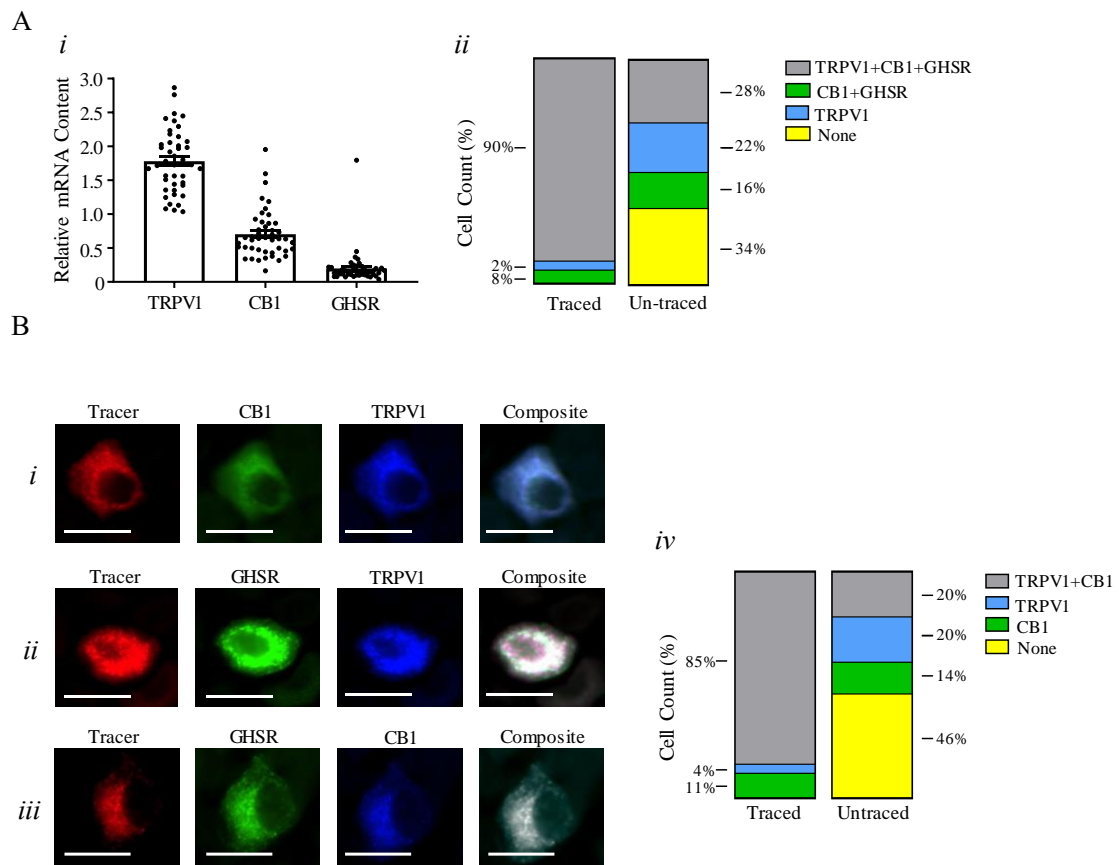


Figure 3.1: CB1, TRPV1, and GHSR are co-expressed in tension sensitive gastric vagal afferent neurons.

Single cell RT-PCR with (*Ai*) relative mRNA expression of TRPV1, CB1, and GHSR from traced tension sensitive gastric vagal afferent (GVA) neurons, and (*Aii*) cell counts for mRNA expression of TRPV1, CB1, and GHSR from traced tension sensitive GVA neurons and randomly acquired neurons from untraced nodose ganglia. Immunohistochemistry with (*Bi*) co-localisation of TRPV1 and CB1, (*Bii*) GHSR and TRPV1, and (*Biii*) GHSR and CB1 in traced tension sensitive GVA neurons, and (*Biv*) cell counts for expression of TRPV1 and/or CB1 from traced tension sensitive GVA neurons and untraced nodose ganglia. Cells were imaged at 40X magnification. White scale bar represents 10 μ m.

Methanandamide has dual effects on tension sensitive gastric vagal afferents

The effects of mAEA on the mechanosensitivity of mucosal and tension sensitive GVAs are illustrated in Figure 2. At all concentrations, mAEA had no effect on the mechanosensitivity of mucosal GVAs to mucosal stroking (Figure 2A).

At 0.1nM, mAEA had no significant effect on the response of tension sensitive GVAs to circular stretch. At 0.3nM, 1nM, and 3nM, mAEA significantly reduced the response of tension sensitive GVAs to circular stretch (Figure 2B), with the highest reduction at 1nM which was significantly greater than 0.3nM ($P=0.041$) (Figure 2C) (0.3nM $-46.2 \pm 0.02\%$, $P=0.011$; 1nM $-73.2 \pm 0.03\%$, $P \leq 0.048$; 3nM $-37.2 \pm 0.03\%$; $F=2.996(7, 46)$; mAEA effect). At 10nM, mAEA had no significant effect on the response of tension sensitive GVAs. At 30nM and 100nM mAEA significantly enhanced the response of tension sensitive GVAs to stretch (Figure 2B) with the highest excitation at 100nM; however this was not significantly different to 30nM (Figure 2D) (30nM $+43.9\%$, $P=0.023$; 100nM $+61.6\%$, $P=0.0003$; $F(7,46)=2.996$).

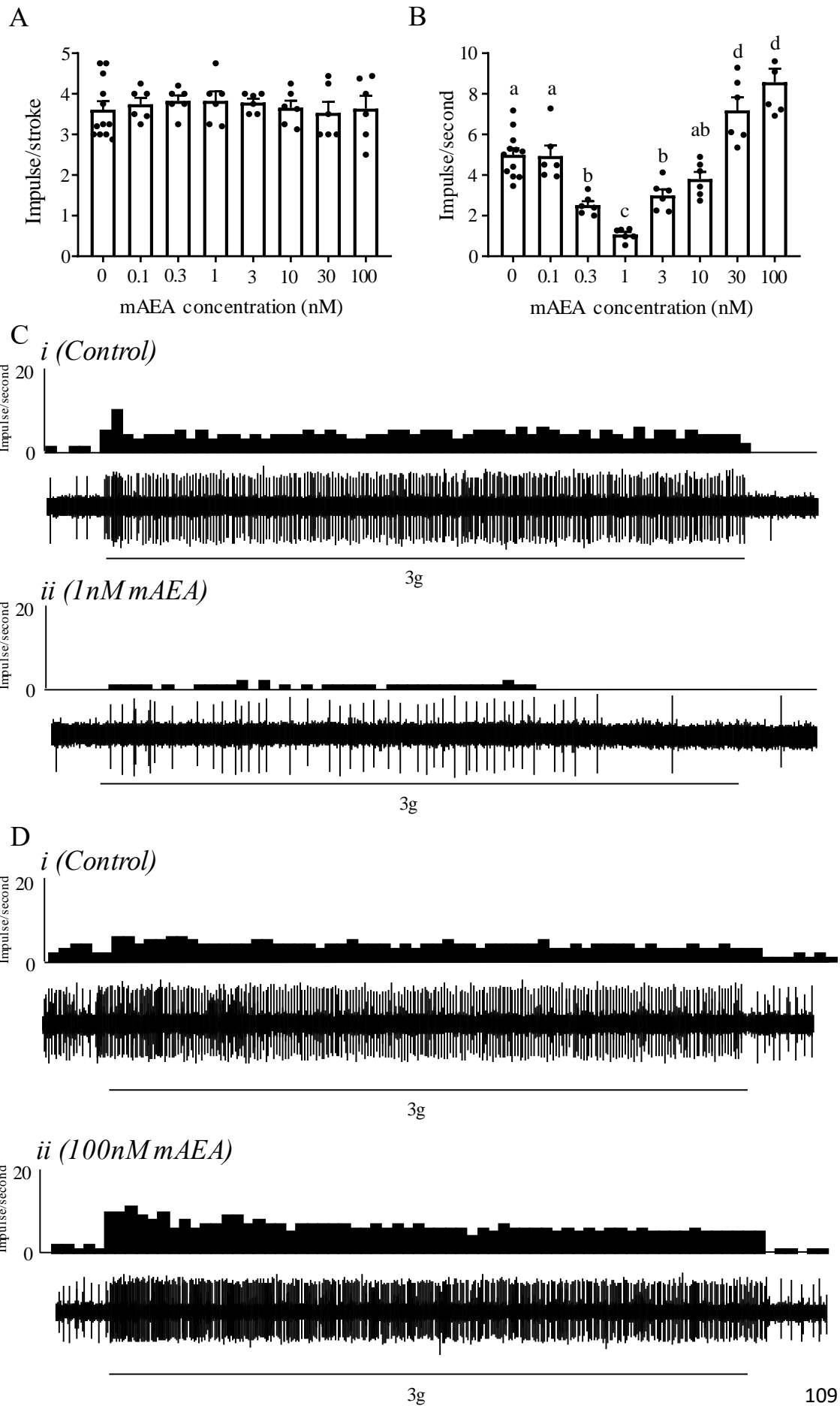


Figure 3.2: Methanandamide has dose-dependent biphasic effects on tension sensitive but not mucosal gastric vagal afferents.

(A) Mucosal gastric vagal afferent (GVA) responses to stroking over the receptive field with a 50mg von Frey hair and (B) tension sensitive GVA responses to 1 minutes of 3g circumferential stretch before and after addition of methanandamide (mAEA) (0.1-100nM). N=6 mice per concentration. Data are expressed as the mean \pm SEM. Concentrations with different letters denotes significance ($P < 0.05$; One way ANOVA, Tukey *post hoc* test). (C & D) Original recording of a tension sensitive GVA response to 3g stretch before (Ci, Di) and after application of 1nM (Cii) and 100nM (Dii) mAEA.

The biphasic effects of methanandamide are mediated via CB1 and TRPV1

The effects of mAEA alone or in combination with either the CB1 antagonist rimonabant or the TRPV1 antagonist AMG9810 are illustrated in Figure 3.

Rimonabant, alone (300nM) had no effect on the response of tension sensitive GVAs to circular stretch (Figure 3A). When combined with rimonabant, the inhibitory effect of 1nM mAEA was lost ($P < 0.0001$), and the excitatory effect of 100nM mAEA was reduced ($P < 0.05$) (Figure 3A; mAEA effect ($P < 0.0001$, $F(3,40)=58.92$), drug type effect ($P < 0.0001$, $F(3,40)=14.29$), and an interaction ($P=0.0005$, $F(1,40)=14.29$).

AMG9810 alone (30nM) had no effect on the response of tension GVAs to circular stretch (Figure 3B). When combined with AMG9810 the inhibitory and excitatory effects of 1nM and 100nM mAEA respectively were lost ($P < 0.0001$) (Figure 3B; mAEA effect ($P < 0.0001$, $F(3,40)=39.26$), and an interaction ($P < 0.0001$, $F(3,40)=34.93$).

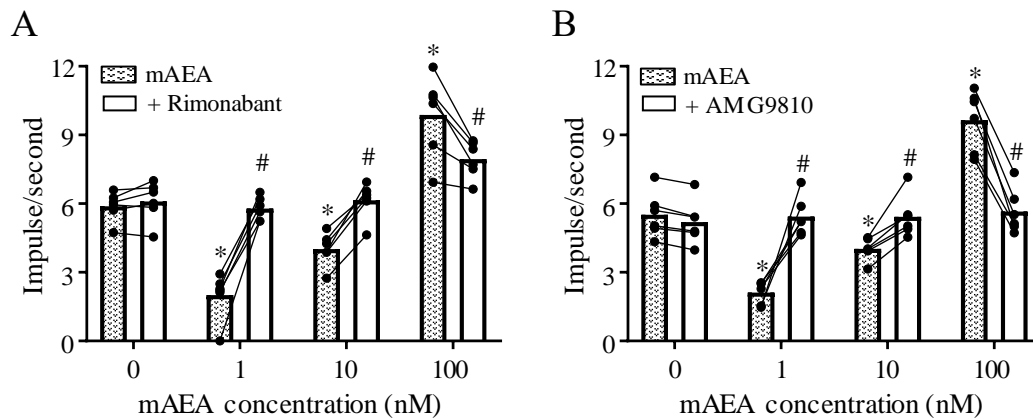


Figure 3.3: The inhibitory and excitatory effects of methanandamide on gastric vagal afferent mechanosensitivity, are mediated by CB1 and TRPV1.

Tension sensitive gastric vagal afferent (GVA) responses to 1 minute of 3g circumferential stretch in the presence of methanandamide (mAEA) alone (0-100nM) or in combination with (A) a CB1 antagonist (rimonabant hydrochloride; 300nM) or (B) a TRPV1 antagonist (AMG9810; 30nM). N=6 mice. Data are expressed as the mean \pm SEM. P<0.05 vs * mAEA at 0nM or # mAEA alone at the same mAEA concentration (Two way ANOVA, Sidak's *post hoc* test).

The inhibitory effect of methanandamide is mediated by $G\alpha_{i/o}$, PKA, and GHSR pathways

The effects of mAEA alone or in combination with either $G\alpha_{i/o}$ antagonist NF023, PKA antagonist PKA-IFA, or GHSR antagonist YIL-781 are illustrated in Figure 4.

NF023 alone (300nM) had no effect on the response of tension sensitive GVAs to circular stretch (Figure 4A). When combined with NF023 the inhibitory effect of 1nM mAEA was lost (P<0.0001), and the excitatory effect of 100nM mAEA remained (Figure 4A;

mAEA effect ($P < 0.0001$, $F(3,40) = 308.3$), drug type effect ($P < 0.0001$, $F(1,40) = 55.68$), and an interaction ($P < 0.0001$, $F(3,40) = 8.93$).

PKA-IFA alone (5nM) had no significant effect on the response of tension sensitive GVAs to circular stretch (Figure 4B). When combined with PKA-IFA, the inhibitory effect of 1nM mAEA was lost ($P < 0.0001$), and the excitatory effect of 100nM mAEA remained (Figure 4C; mAEA effect ($P < 0.0001$, $F(3,40) = 86.75$), drug type effect ($P = 0.034$, $F(1,40) = 4.79$) and no interaction).

YIL-781 alone (100nM) had no significant effect on the response of tension sensitive GVAs to circular stretch (Figure 4C). When combined with YIL-781 the inhibitory effect of 1nM mAEA was lost ($P < 0.0001$), and the excitatory effect of 100nM mAEA remained (Figure 4C; mAEA effect ($P < 0.0001$, $F(3,40) = 77.42$), drug type effect ($P = 0.0014$, $F(1,40) = 11.84$), and an interaction ($P < 0.0001$, $F(3,40) = 9.926$)).

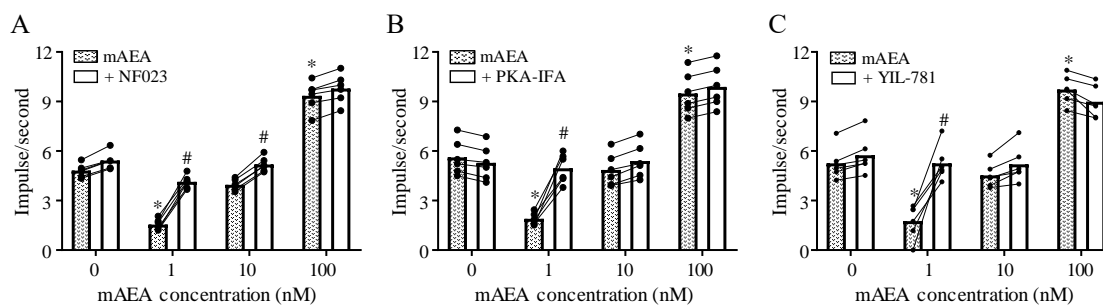


Figure 3.4: The inhibitory effect of methanandamide on gastric vagal afferent mechanosensitivity is mediated by $G\alpha_{i/o}$ – PKA, and GHSR pathways.

Tension sensitive gastric vagal afferent (GVA) responses to 1 minute of 3g circumferential stretch in the presence of methanandamide (mAEA) alone (0-100nM) or in combination with (A) a $G\alpha_{i/o}$ antagonist (NF023; 300nM), (B) a protein kinase-A (PKA) antagonist (PKA inhibitor fragment (6-22) amide (PKA-IFA) 5nM), or a GHSR antagonist (YIL-781; 300nM). N=6 mice per antagonist. Data are expressed as the mean \pm SEM. $P < 0.05$ vs * mAEA at 0nM or # mAEA alone at same mAEA concentration (Two way ANOVA, Sidak's *post hoc* test).

The excitatory effect of methanandamide is mediated by $G\alpha_q$ and PKC

The effects of mAEA alone or in combination with either $G\alpha_q$ antagonist YM-254980 or PKC antagonist BIS-II are illustrated in Figure 5.

YM-254980 alone (100nM) had no significant effect on the response of tension sensitive GVAs to circular stretch (Figure 5A). When combined with YM-254890 the inhibitory effect of 1nM mAEA remained and the excitatory effect of 100nM mAEA was reduced ($P < 0.05$) (Figure 5A; mAEA effect ($P < 0.0001$, $F(3,40)=117$) and an interaction ($P=0.0005$, $F(3,40)=7.29$)).

BIS-II alone (10nM) had no significant effect on the response of tension sensitive GVAs to circular stretch (Figure 5B). When combined with BIS-II the inhibitory effect of 1nM mAEA remained and the excitatory of 100nM mAEA was reduced ($P<0.001$) (Figure 5B; mAEA effect ($P<0.0001$, $F(3,40)=204.3$) and drug type effect ($P=0.014$, $F(1,40)=6.65$)).

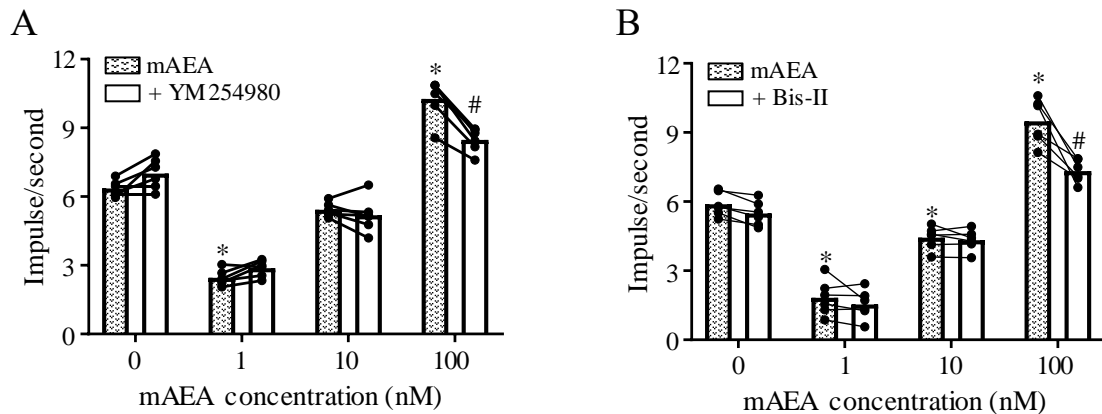


Figure 3.5: The excitatory effect of methanandamide is mediated by $G\alpha_q$ and PKC pathways.

Tension sensitive gastric vagal afferent (GVA) responses to 1 minute of 3g circumferential stretch in the presence of methanandamide (mAEA) alone (0-100nM) or in combination with (A) a $G\alpha_q$ antagonist (YM-254980; 100nM) or (B) a PKC antagonist (BIS-II; 10nM). N=6 mice. Data are expressed as the mean \pm SEM. $P<0.05$ vs * mAEA at 0nM or # mAEA alone at same mAEA concentration (Two way ANOVA, Sidak's *post hoc* test).

Discussion

The current study demonstrates that CB1, TRPV1, and GHSR are co-expressed in tension sensitive GVAs, and that mAEA has concentration dependent biphasic effects on the mechanosensitivity of tension sensitive GVAs. Further, this study demonstrates that these effects may be mediated by regulation of TRPV1 ion channels by CB1 and GHSR-dependent mechanisms.

CB1, GHSR, and TRPV1 are co-expressed in nodose ganglia

CB1, TRPV1, and GHSR were expressed in individual cells bodies of tension sensitive GVAs. Further, their co-expression was higher in GVA neurons than non-GVA neurons from the general nodose ganglia population, suggesting a possible selective role in this sub-group of vagal afferents. This also emphasises the importance of studying identified populations of neurones for specificity of action. A previous study [476] indicated that co-expression and immunoreactivity of CB1, TRPV1, and GHSR was much higher in the general nodose ganglia population compared to the current study. However this study was performed on rats that had been fasted for 48 hours [476] and fasting is known to alter the expression of GHSR and CB1 [477, 478]. We found that CB1 and GHSR mRNA were always co-expressed both in tension sensitive GVA neurons and nodose neurons from the general population. CB1 and GHSR have been demonstrated to be highly co-expressed in other tissues such as liver [479] and hypothalamus [480], and demonstrate co-dependency for functionality [336, 479]. Further, both CB1 and GHSR interact with TRPV1 in the dorsal root ganglia and the hypothalamus [441, 447]. Therefore, it is possible that TRPV1, CB1 and GHSR co-localised in the same cells could interact to modulate satiety signalling.

Methanandamide biphasically regulates tension sensitive gastric vagal afferent responses to stretch

The stable analogue of AEA, mAEA, biphasically modulated the response of tension sensitive GVAs to stretch, with inhibitory effects at low concentrations and excitatory effects at high concentrations. Tension sensitive GVAs are important for the regulation of food intake, signalling the degree of gastric distension to the hindbrain eventually leading to feelings of fullness and satiety [204]. Therefore, the reduced response to stretch at low mAEA concentrations may act to increase food intake. Conversely, at higher concentrations, mAEA increased the response of tension sensitive GVAs to stretch which may act to reduce food intake, suggesting a concentration dependent biphasic modulation [447].

The biphasic effects of methanandamide are mediated by CB1 and TRPV1 through activation of different second messenger pathways

The inhibitory and excitatory effects of mAEA were dependent on both CB1 and TRPV1. It has been shown that activation of CB1 can enhance or inhibit TRPV1 depending on the second messenger pathway utilised [447].

Antagonism of either $G\alpha_q$ or PKC reduced the excitatory effect of mAEA at high concentrations. $G\alpha_q$ leads to PLC activation and eventually PKC activation [447]. Further, PKC has been shown to sensitise TRPV1, to TRPV1 analogues [397, 413], suggesting this is a possible secondary messenger pathway for mAEA, at high concentrations, in tension sensitive GVAs (Figure 6A). Following CB1 antagonism there was a residual mAEA excitatory effect present. AEA is known to intracellularly activate TRPV1; an effect prevalent at high AEA concentrations [408, 447]. Therefore, the

residual effect is likely due to direct mAEA interactions with TRPV1. However, it is unknown whether the concentration of the CB1 antagonist was sufficient to completely block the CB1 receptors or whether other pathways are involved and, therefore, this requires further investigation.

The inhibitory effect, of mAEA on tension sensitive GVAs, at low concentrations was abolished in the presence of a $G\alpha_{i/o}$ or PKA antagonist. $G\alpha_{i/o}$ is known to inhibit adenylyl cyclase and reduce cellular cAMP and subsequently PKA activity [447]. Further, activation of CB1 can inhibit PKA to desensitise TRPV1 [447]. It has been demonstrated, including in sensory neurones of the dorsal root ganglia, that PKA enhances TRPV1 activity sensitising it to TRPV1 stimuli [406, 474, 481]. Therefore, it appears that mAEA activates CB1- $G\alpha_{i/o}$ to inhibit PKA and thus reduce TRPV1 activity. However, antagonism of PKA alone had no effect on tension sensitive GVA activity [474]. If the antagonist was inhibiting the excitatory effect of PKA, similar to CB1 activation, then the antagonist alone should reduce TRPV1 activity and thus GVA mechanosensitivity. Therefore, although there is evidence that PKA plays a role in the inhibitory effect of mAEA on tension sensitive GVAs, further investigation is required to determine the exact role. Nonetheless, this data raises the possibility that another pathway is involved.

In the current study, the inhibitory effect, of mAEA on tension sensitive GVAs, was also abolished in the presence of the GHSR antagonist YIL-781. It is known that CB1 can promote ghrelin release via modulation of the mammalian target of rapamycin (mTOR) pathway [249]. Activation of CB1 inhibits mTOR activity, presumably via $G\alpha_{i/o}$ [482], subsequently increasing ghrelin release from gastric cells. Further, endogenous ghrelin, acting at GHSR [220], has been shown to reduce the mechanosensitivity of tension sensitive GVAs [220]. Therefore, it is likely that the inhibitory effect of mAEA, at low

concentrations, is through CB1 mediated ghrelin release, from gastric X/A-like cells [483], which subsequently acts on tension sensitive GVA endings to reduce mechanosensitivity [220] (Figure 6B). This possibly involves an interaction between GHSR and TRPV1, however, this is highly speculative and requires further investigation. GHSR has been shown to interact with TRPV1 in magnocellular neurons [441], albeit, in these neurons activation of GHSR leads to activation of TRPV1 [441], not inhibition as observed in the current study. This may be due to tissue specific differences in the action of ghrelin and GHSR [484]. Further, GHSR has very high constitutive activity [485], therefore, although it is likely that CB1 mediated ghrelin release from gastric mucosal cells is acting on GHSR on GVA endings, blocking GHSR may impact on the CB1 response independent of ghrelin release.

GHSR predominantly couples to $G\alpha_q$ in most tissues, however, the current study suggests that in GVA endings it may couple to $G\alpha_i/o$. This is supported by previous evidence indicating that GHSR signals via $G\alpha_i/o$ in vagal afferent cell bodies [486]. However, it should be noted that this study was performed in whole nodose ganglia, and not specific subpopulations and, therefore, the role of $G\alpha_i/o$ in GHSR signalling in GVAs requires further investigation.

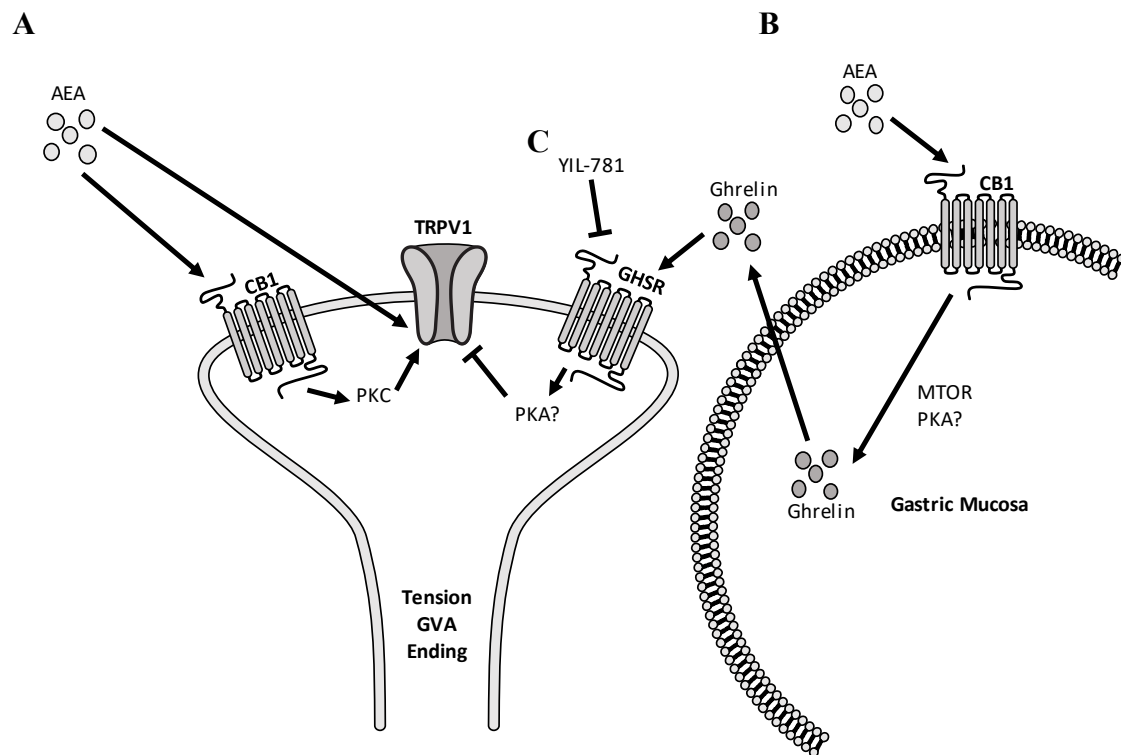


Figure 3.6: Schematic of the possible pathways for the inhibitory and excitatory effects of methanandamide on gastric vagal afferent mechanosensitivity.

(A) The excitatory effect of methanandamide (mAEA) on the mechanosensitivity of gastric vagal afferents (GVAs) is likely due to both the direct intracellular activation of TRPV1 and indirect activation of the CB1 mediated PKC-TRPV1 secondary messenger pathway. (B) The inhibitory effect is likely a result of mAEA activating CB1 mediated gastric ghrelin release, with subsequent ghrelin action upon GHSR on tension sensitive gastric vagal afferent (GVA) endings. (C) It cannot be ruled out that blocking GHSR without direct ghrelin activation may also alter secondary messenger pathways.

The biased agonism observed may be facilitated by different mechanisms. Ghrelin levels typically decrease post prandially [487]. Therefore the absence of ghrelin in these

conditions could result in a TRPV1 mediated increase in vagal afferent activity and a subsequent decrease in food intake. In addition, CB1 is known to interact with other G-protein coupled receptors and regulatory proteins. For example, CB1 is known to form a heterodimer with the dopamine 2 receptor causing a shift in G-protein signalling, even in the absence of dopamine [453, 465]. Further, regulators of CB1 such as the CB1 interacting protein 1a are known to attenuate *Gai/o* signalling [451, 452]. Therefore it is conceivable that these interactions may influence bias agonism by CB1. This requires further investigation. In addition, GVAs display circadian rhythmicity to finely control food intake to energy demand [224]. It is possible that biased CB1 signalling could play a role in the regulation of these circadian rhythms. However, this is highly speculative and requires further investigation.

The antagonists used in the current study were either potent or selective to the molecular targets intended. However, the possibility of the antagonists acting on other molecules cannot be ruled out. Further, it is not possible to determine whether the molecular targets have been completely blocked by the concentrations used. These possibilities need to be considered when evaluating potential mechanisms. In addition, future experiments should include single cell calcium imaging or patch clamp experiments to tease out the mechanisms at the cellular level.

In conclusion, the current study demonstrates that there is an interaction between CB1, TRPV1 and GHSR to mediate the biphasic effects of mAEA on tension sensitive GVAs. The dose-dependent effects of mAEA is either via direct action on GVAs or via CB1 receptors on gastric ghrelin cells. Further, investigation is required to understand how these interactions are altered by nutritional status, such as in high fat diet-induced obesity.

Chapter 4 : Modulatory effect of methanandamide on gastric vagal afferents depends on nutritional status

Stewart Christie¹, Rebecca O'Reilly¹, Hui Li^{1,2}, Maria Nunez¹, Gary Wittert^{1,2}, Amanda Page^{1,2}

¹ Vagal Afferent Research Group, Centre for Nutrition and Gastrointestinal Disease, Adelaide Medical School, University of Adelaide, Adelaide, SA 5005, Australia

² Diabetes, Nutrition and Gut Health, Lifelong Health Theme, South Australian Health and Medical Research Institute, Adelaide, SA 5000, Australia

Published in: Journal of Physiology

Statement of Authorship

Title of Paper	Modulatory effect of methanandamide on gastric vagal afferents depends on nutritional status
Publication Status	<input checked="" type="checkbox"/> Published <input type="checkbox"/> Accepted for Publication <input type="checkbox"/> Submitted for Publication <input type="checkbox"/> Unpublished and Unsubmitted work written in manuscript style
Publication Details	Published in the Journal of Physiology, DOI: 10.1113/JP279449

Principal Author

Name of Principal Author (Candidate)	Stewart Christie			
Contribution to the Paper	Performed experiments and wrote the paper			
Overall percentage (%)	80%			
Certification:	This paper reports on original research I conducted during the period of my Higher Degree by Research candidature and is not subject to any obligations or contractual agreements with a third party that would constrain its inclusion in this thesis. I am the primary author of this paper.			
Signature	<table border="1" style="width: 100%;"> <tr> <td style="width: 80%;"></td> <td style="width: 20%;">Date</td> <td>14/11/2019</td> </tr> </table>		Date	14/11/2019
	Date	14/11/2019		

Co-Author Contributions

By signing the Statement of Authorship, each author certifies that:

- i. the candidate's stated contribution to the publication is accurate (as detailed above);
- ii. permission is granted for the candidate to include the publication in the thesis; and
- iii. the sum of all co-author contributions is equal to 100% less the candidate's stated contribution.

Name of Co-Author	Rebecca O'Reilly			
Contribution to the Paper	Helped perform tracing studies			
Signature	<table border="1" style="width: 100%;"> <tr> <td style="width: 80%;"></td> <td style="width: 20%;">Date</td> <td>14/11/2019</td> </tr> </table>		Date	14/11/2019
	Date	14/11/2019		

Name of Co-Author	Hui Li		
Contribution to the Paper	Helped perform tracing studies and edited the paper		
Signature		Date	14/11/2019

Name of Co-Author	Maria Nunez		
Contribution to the Paper	Helped with high fat diet animals		
Signature		Date	14/11/2019

Name of Co-Author	Gary Wittert		
Contribution to the Paper	Planning of experiments and edited the paper		
Signature		Date	20/11/2019

Name of Co-Author	Amanda J Page		
Contribution to the Paper	Planning of experiments and edited the paper		
Signature		Date	14/11/2019

Significance Statement

- Gastric vagal afferent responses to tension are dampened in high fat diet-induced obesity.
- Endocannabinoids are known to dose dependently inhibit and excite gastric vagal afferents but their effect on gastric vagal afferents in diet-induced obesity is not known.
- In individual gastric vagal afferent neurons of diet-induced obese mice the co-expression of CB1, GHSR, TRPV1, and FAAH was increased compared to lean mice.
- In diet-diet induced obese mice methanandamide only inhibited gastric vagal afferent responses to tension, possibly due to the observed change in balance of receptors, hormones, and breakdown enzymes in this system.
- Collectively, these data suggest that endocannabinoid signalling by gastric vagal afferents is altered in diet-induced obesity which may impact satiety and gastrointestinal function.

Abstract

Gastric vagal afferents (GVAs) play a role in appetite regulation. The endocannabinoid anandamide (AEA) dose dependently inhibits and excites tension sensitive GVAs. However, it is also known that high fat diet (HFD) feeding alters GVA responses to stretch. The aim of this study was to determine the role of AEA in GVA signalling in lean and HFD-induced obese mice.

Male C57BL/6 mice were fed (12wks) a standard laboratory diet (SLD) or HFD. Protein and mRNA expression of components of the cannabinoid system was determined in individual GVA cell bodies and the gastric mucosa. An *in vitro* GVA preparation was used to assess the effect of methanandamide (mAEA) on tension sensitive GVAs and the second messenger pathways involved.

In individual GVA cell bodies, cannabinoid 1 (CB1) and ghrelin (GHSR) receptor mRNA was higher in HFD- compared to SLD-mice. Conversely, gastric mucosal AEA and ghrelin protein levels were lower in HFD- compared to SLD-mice. In SLD-mice, mAEA exerted dose-dependent inhibitory and excitatory effects on tension sensitive GVAs. Only an inhibitory effect of mAEA was observed in HFD-mice. The excitatory effect of mAEA was dependent on CB1, transient receptor potential vanilloid 1 (TRPV1) and protein kinase C. Conversely, the inhibitory effect was dependent on CB1, GHSR, TRPV1, and protein kinase A.

Endocannabinoids, acting through CB1 and TRPV1, have a pivotal role in modulating GVA satiety signals depending on the second messenger pathway utilised. In HFD-mice only an inhibitory effect was observed. These changes may contribute to the development and/or maintenance of obesity.

Introduction

Obesity generally occurs due to energy intake exceeding energy expenditure. Globally it is a major health issue with rates almost tripling since 1980 and continuing to rise [488]. Although there are pharmacological interventions many have unwanted side effects [88, 489]. In order to minimise these side effects attention has focused on the peripheral control of appetite.

Gastrointestinal vagal afferents are important for relaying peripheral signals generated by food related stimuli to the hindbrain [204] where they are processed eventually leading to meal termination. In the stomach there are two types of gastric vagal afferents (GVAs), mucosal and tension receptors [460]. Mucosal receptors respond to contact with the gastric epithelia and are thought to be involved in nausea [217] and gastric emptying [205]. Tension receptors respond to stretch or distension of the gastric wall and are involved in the generation of satiety signals which ultimately terminate a meal [204]. In obesity the response of tension sensitive GVAs to stretch is reduced [223], which may contribute to the development or maintenance of obesity through dampened satiety signalling. The reduced sensitivity of tension receptors may be due to transient receptor potential vanilloid 1 (TRPV1) ion channels which are present in GVAs [235].

TRPV1 is a non-selective cation channel and its activation is associated with a reduction in food intake [434, 473], an effect lost in obese conditions [434]. This is complicated by TRPV1 interactions with appetite regulating substances such as the endocannabinoid anandamide (AEA) and ghrelin. AEA and its receptor, cannabinoid 1 (CB1) receptor, can inhibit or excite TRPV1 depending on the secondary messenger pathways activated [447],

Further, the ghrelin receptor, growth hormone secretagogue receptor (GHSR), can interact with TRPV1 [441], although the mechanisms are unclear.

TRPV1, CB1, and GHSR are expressed on vagal afferents [177, 235], and AEA and ghrelin are produced in the stomach [351, 484]. In GVAs, the stable analogue of AEA, methanandamide (mAEA) has concentration dependent inhibitory and excitatory effects on the mechanosensitivity of tension receptors [490]. These effects are dependent upon CB1, TRPV1, and GHSR. At low concentrations, mAEA binds to CB1 expressed in gastric ghrelin cells to increase ghrelin secretion [249]. Ghrelin then binds GHSR on GVA endings to decrease tension receptor mechanosensitivity via a TRPV1 dependent mechanism [490]. Conversely, at higher concentrations, mAEA increases the mechanosensitivity of tension sensitive GVAs either by direct intracellular binding and activation of TRPV1, or activating TRPV1 via a CB1-dependent protein kinase C (PKC) pathway [490]. The impact of high fat diet (HFD)-induced obesity on these inhibitory and excitatory effects of mAEA is not known.

Using an *in vitro* electrophysiology preparation this study aimed to determine the role of CB1, GHSR, and TRPV1 in the regulation of GVA satiety signals by mAEA in lean and HFD-induced obese mice. It is hypothesised that in HFD-induced obesity the inhibitory effect of mAEA on tension sensitive GVA mechanosensitivity will become dominant.

Ethical Approval

This study was approved by the animal ethics committee of the South Australian Health and Medical Research Institute (SAHMRI), and carried out in accordance with the Australian code for the care and use of animals for scientific purposes, 8th edition 2013 and the ARRIVE guidelines [475].

Animals

Seven week old C56BL/6 male mice (N=104) were housed in littermates of 3-4. After one week acclimatisation, mice were randomly assigned to either a standard laboratory diet (SLD; 12% energy from fat; N=53) or HFD (60% energy from fat; N=51) for twelve weeks. All mice were housed under a 12:12hr light:dark cycle with *ad libitum* access to their respective diet and water unless otherwise stated.

Retrograde tracing studies

This procedure has been described in detail previously [223]. In short, mice were fasted for two hours before being anaesthetised with 3% isoflurane in 1-1.5% oxygen prior to a midline abdominal laparotomy. The stomach was exteriorised and multiple (x10) equally spaced injections (1 μ L) of Alexa Fluor® 555 conjugate of cholera toxin β -subunit (C22843; ThermoFisher Scientific, Australia) were made under the serosal layer. The laparotomy was closed and mice were given analgesia (buprenorphine, 0.1mg/kg) and antibiotics (baytril, 10mg/kg).

Two days after the procedure mice were humanely killed via CO₂ inhalation (fill rate of 30%; QuietekTM CO₂ induction system, Next Advance, USA) and nodose ganglia were bilaterally dissected and prepared for single cell PCR.

Cell culture

This procedure has been described in detail previously [455]. In short, retrogradely traced nodose ganglia were bilaterally dissected and placed immediately in ice cold F12 solution. The nodose were then incubated for 30 minutes at 37°C with 12mg collagenase/14mg dispase in 3mL Hanks Balance Salt Solution (HBSS; 14170112; ThermoFisher Scientific, Australia) and then incubated for 10 minutes at 37°C with 12mg collagenase in HBSS. Nodose ganglia were then mechanically sheared using a fire polished glass pipette, washed in ice cold HBSS and then diluted to approximately 1 cell per 1µL.

1µL of cell suspension was then pipetted onto a thin piece of glass (approx. 5mm²) and examined for the presence of a single fluoresced cell under an epifluorescence microscope (BX-51, Olympus, Australia) equipped with a filter for Alexa Fluor 568. The glass was then examined under a brightfield (BX-51, Olympus, Australia) to confirm no non-fluoresced cells were present, and then placed in a Single Cell Lysis/Dnase 1 solution (10µL) (provided in Single Cell-CT™ Kit; 4458235; Life Technologies, Australia) for 5 minutes at room temperature. A stop solution (1µL) (provided in Single Cell-CT™ Kit; 4458235; Life Technologies, Australia) was added for 2 minutes and then the samples were stored at -20°C until required.

Single Cell PCR of gastric traced vagal afferent cell bodies

Using a Single Cell-CT™ Kit (4458235; Life Technologies, Australia), single cell qRT-PCR was performed on lysed retrogradely traced single nodose cells as per manufacturers protocol. Pre-designed Taqman gene expression assays obtained from Life Technologies (Australia) were chosen to measure the mRNA expression and co-expression of TRPV1

(mm01246300_m1), CB1 (mm01212171_s1), GHSR (mm00616415_m1), and fatty acid amide hydrolase (FAAH; enzyme for AEA breakdown; mm00515684_m1) in traced tension sensitive GVA cell bodies of SLD and HFD mice. Class 3 beta-tubulin (Tubb3; mm00727586_m1), Peptidylprolyl Isomerase A (PPIA; mm00620857_s1), *Hypoxanthine-phosphoribosyltransferase* (HPRT; mm03024075_m1), beta-2-microglobulin (B2M; mm00437762_m1) and beta-actin (ActB; mm02619580_g1) were tested as potential housekeeping genes. B2M and ActB were chosen based on stability across all samples determined from NormFinder software (stability value of B2M and ActB = 0.102). Relative mRNA levels were calculated using the $2^{\Delta CT}$ method [456].

qRT-PCR of the gastric mucosal layer

Stomach scrapings were obtained from half of the stomach during dissection for the vagal afferent electrophysiology preparation, snap frozen in liquid nitrogen and stored at -80°C. RNA was extracted using a Purelink RNA minikit (12183018A; Invitrogen, ThermoFisher Scientific) following a standard protocol for 50 mg of tissue. RNA levels were determined with a NanoDrop LITE spectrophotometer (ThermoFisher Scientific), and quality was at 260nm/280nm absorbance (A260/A280).

qRT-PCR was performed using an Express One-Step Superscript qRT-PCR Universal kit (11781200; Invitrogen, ThermoFisher Scientific) and 7500 Fast Real-Time PCR system (Applied Biosystems, ThermoFisher Scientific). Pre-designed Taqman gene expression assays obtained from Life Technologies (Australia) were chosen to measure mRNA expression of FAAH (mm00515684_m1), N-acyl phosphatidylethanolamine phospholipase D (NAPE-PLD; enzyme for AEA synthesis; mm00724596_m1), CB1 (mm01212171_s1), and ghrelin O-acyltransferase (GOAT; mm01200389_m1) in gastric

cells. PPIA, *HPRT*, ActB, B2M were tested as potential housekeeping genes. PPIA, HRPT, and ActB were chosen based on stability across all samples determined from NormFinder software (stability value = 0.098) (Department of Molecular Medicine (MOMA), Aarhus University Hospital, Denmark). Relative mRNA levels were calculated using the $2^{\Delta\text{CT}}$ method [456].

Gastric protein levels of AEA, FAAH, and ghrelin

Stomach scrapings were obtained from half of the stomach during dissection for the vagal afferent electrophysiology preparation, snap frozen in liquid nitrogen and stored at -80°C . Gastric AEA and FAAH levels were determined using Enzyme-linked immunosorbent assay (ELISA) kit for anandamide (CEO440Ge; Cloud-Clone Corp., USA) and FAAH (abx389255; Abnova Ltd. UK), and quantified via colorimetry at 450nm using a VersaMax ELISA microplate reader (Molecular Devices).

Total gastric ghrelin was extracted by boiling the stomach scrapings for 10 minutes, followed by rapid homogenisation in a solution of protease inhibitors (5892791001; Merck Millipore) and 6% acetic acid [491]. Total gastric levels were then determined using an ELISA kit for ghrelin (EZRGRA-90K; Merck Millipore, USA) and quantified via colorimetry at 450nm and 590nm using a VersaMax ELISA microplate reader (Molecular Devices).

***In vitro* gastric vagal afferent preparation**

This preparation has been described in detail previously [215]. In brief, mice were anaesthetised with 5% isoflurane, exsanguinated, and decapitated. The oesophagus, stomach, and attached vagal nerves were removed, opened longitudinally, and placed mucosal side up in an organ bath containing a modified Krebs solution (in mM: 118.1

NaCl, 4.7 KCl, 25.1 NaHCO₃, 1.3 NaH₂PO₄, 1.2 MgSO₄·7H₂O, 1.5 CaCl₂, 1.0 citric acid, 11.1 glucose and 0.001 nifedipine, bubbled with 95% O₂- 5% CO₂) at 34°C.

The vagal nerves were threaded through a barrier into a liquid paraffin chamber for electrical isolation. They were then desheathed and split into smaller nerve bundles (10-15 bundles). The nerve bundles were then placed individually on a platinum electrode for recording.

Gastric vagal afferent subtypes

Whilst there are two types of mechanosensitive GVAs, mucosal and tension [460], the focus of the current study was on tension sensitive GVAs as they are known to be modulated by mAEA whereas mucosal receptors were unresponsive [490].

The location of a tension sensitive GVA was first determined broadly by brushing the stomach, then specifically using a 200mg calibrated von Frey hair. The response of tension sensitive GVAs to stretch was determined using a cantilever system. A hook and thread was underpinned in close proximity to the receptive area, and attached to a cantilever with weights on the opposite end. A standard weight (3g) was attached to the cantilever for 1 minute with the mean number of nerve impulses per second being used for analysis.

Effect of methanandamide on mechanosensitivity of gastric vagal afferents

After measuring the baseline sensitivity of a tension sensitive GVA, 1nM of mAEA was added to the Krebs super infusion and allowed to equilibrate for 20 minutes to allow full penetration of the tissue. The mechanosensitivity of the tension sensitive GVA was then re-determined. This process was repeated with increasing concentrations of mAEA (10, 100, and 300nM).

To determine the secondary messenger pathways used by mAEA, and changes in these pathways between diets, antagonists of CB1 (rimonabant 300nM [450]), GHSR (YIL-781 300nM [462]) TRPV1 (AMG9810 30nM [461]), $G\alpha_{i/o}$ (NF023 300nM [463]), $G\alpha_q$ (YM-254890 100nM [464]), PKA (PKA inhibitor fragment (6-22) amide (PKA-IFA 5nM [465]), and PKC (bisindolylmaleimide-II (BIS-II) 10nM [466]) were used.

First the baseline effect of mAEA on GVA mechanosensitivity was determined, followed by a 20 minute washout and antagonist equilibration. GVA mechanosensitivity was then re-determined and then the antagonist in combination with 1nM mAEA was added for 20 minutes and GVA mechanosensitivity was re-determined. This was repeated with increasing concentrations of mAEA (10, and 100nM) followed by a final washout.

Drugs

Stock solutions of mAEA, rimonabant (1 μ M), AMG9810 (300nM) and BIS-II (100nM) were made using absolute ethanol. Stock solutions of NF023 (1 μ M), YM-254890 (1 μ M), and YIL-781 (1 μ M) were made using Krebs solution. All drugs were stored at -20°C and diluted to final concentrations in Krebs the day prior to experiments. mAEA (M186), rimonabant hydrochloride (SML0800), AMG9810 (A2731), BIS-II (B3056), and PKA-IFA (P6062) were obtained from Sigma Aldrich (Australia). NF 023 (1240/10) was obtained from In Vitro Technologies (Australia). YM-254980 (AG-CN2-0509-M001) was obtained from Sapphire Biosciences (Australia).

Data analysis

All data is presented as the mean \pm the standard deviation (SD) and was analysed using GraphPad Prism software (version 8). Data relating to gonadal fat, PCR, and gastric peptides were analysed using an unpaired *t*-test. Data relating to weight gain and

electrophysiology was analysed using a two-way ANOVA with a Tukey *post hoc* test. P-values less than or equal to 0.05 were deemed significant.

Results

HFD mice gained more weight than SLD mice

Weight gain and gonadal fat pad mass are illustrated in figure 1. Mice fed a HFD gained significantly more weight than mice fed a SLD (Figure 1A; SLD 9.27 ± 2.72 g, HFD 21.45 ± 3.18 g, $P < 0.0001$, diet effect $F(1, 1326) = 2087$). Gonadal fat pad mass was significantly increased in HFD-mice compared to SLD-mice (Figure 1B; SLD $2.43 \pm 0.41\%$ of body weight, HFD $6.36 \pm 1.03\%$ of body weight; $P < 0.0001$, $t = 22.15$, $df = 99$).

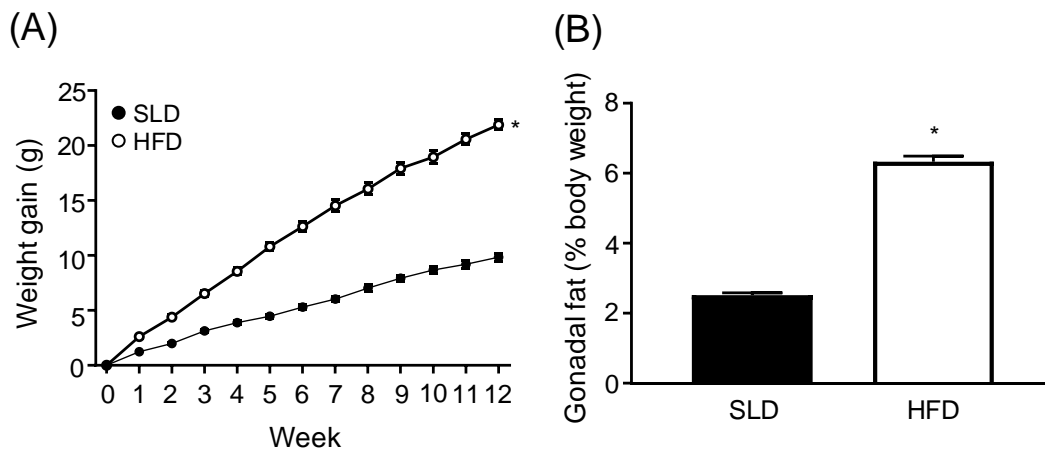


Figure 1: High fat diet fed mice gained more weight and adiposity than standard laboratory diet fed mice. (A) Weekly weight gain of mice fed either a standard laboratory diet (SLD; N=53) or high fat diet (HFD; N=51). (B) Gonadal fat as percentage of body weight in SLD- and HFD-mice after 12 weeks on their respective diet. Data are expressed as the mean \pm SEM. * $P < 0.0001$ vs SLD-mice (A: Two way ANOVA, Sidak's *post hoc* test; B: Unpaired t-test).

Tension sensitive GVA cell bodies express TRPV1, CB1, GHSR, and the enzyme responsible for breakdown of AEA, fatty acid amide hydrolase (FAAH) mRNA

Retrograde tracing studies were performed to identify tension sensitive GVA cell bodies in nodose ganglia for single-cell QT-RT PCR. The relative expression of TRPV1, CB1, GHSR, and FAAH mRNA in individual GVA cell bodies is illustrated in figure 2. TRPV1, CB1, GHSR, and FAAH were expressed in traced tension sensitive GVA cell bodies of SLD-mice. In HFD-mice the expression of CB1 ($P < 0.0001$, $t = 5.344$, $df = 94$), GHSR ($P < 0.0001$, $t = 5.730$, $df = 94$), and FAAH ($P < 0.0001$, $t = 5.838$, $df = 94$) were significantly increased compared to SLD-mice (Figure 2A).

In SLD-mice all traced cell bodies expressed either: TRPV1 and FAAH (10% of traced cells), CB1, GHSR, and FAAH (6% of traced cells), or TRPV1, CB1, GHSR, and FAAH (84% of traced cells). In contrast, in HFD-mice all traced cell bodies expressed TRPV1, CB1, GHSR, and FAAH (100% of traced cells; Figure 2B).

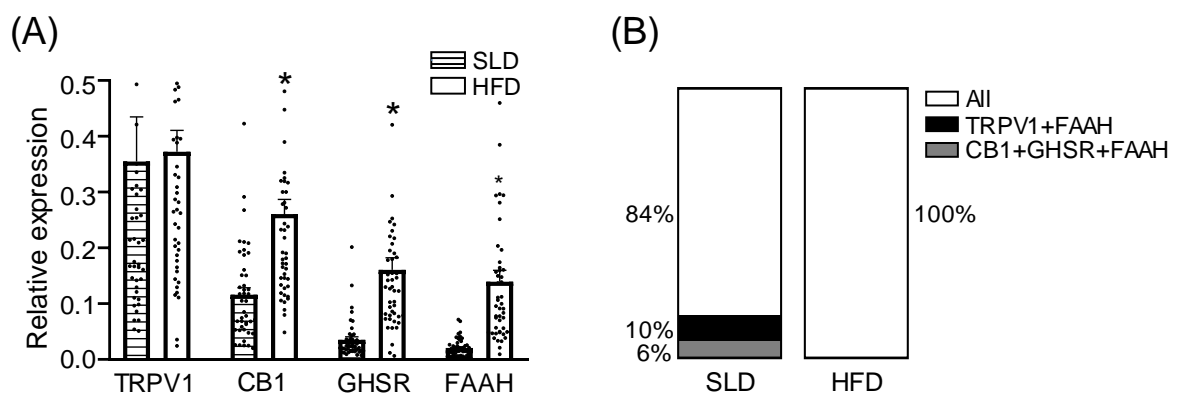


Figure 2: The expression of CB1, GHSR, and FAAH are increased in retrogradely traced gastric vagal afferent neurons of high fat diet fed mice. (A) The mRNA expression of transient receptor potential vanilloid 1 (TRPV1), cannabinoid receptor 1

(CB1), growth hormone secretagogue receptor (GHSR), and fatty acid amide hydrolase (FAAH) in retrogradely traced tension sensitive gastric vagal afferent (GVA) cell bodies of standard laboratory diet (SLD) and high fat diet (HFD) fed mice. (B) The co-expression of TRPV1, CB1, GHSR, and FAAH mRNA in single retrogradely traced tension sensitive GVA cell bodies of SLD- and HFD-mice. N = 5 mice per diet, 10 random GVA cell bodies per mouse. Data are expressed as the mean \pm SEM. * $P < 0.0001$ vs SLD-mice (Unpaired t-test).

Gastric mucosal anandamide and ghrelin levels are decreased and FAAH levels increased in HFD-induced obese mice

Gastric mucosal scrapings were used to determine the expression of AEA and ghrelin related mRNA and protein.

Gastric mucosal levels of FAAH, CB1, N-acyl phosphatidylethanolamine phospholipase D (NAPE-PLD; enzyme for AEA synthesis) and ghrelin O-acyltransferase (GOAT; enzyme for ghrelin activation) mRNA, and AEA, FAAH, and ghrelin protein are illustrated in figure 3. FAAH, CB1, NAPE-PLD, and GOAT mRNA were expressed in the gastric mucosa from SLD-mice. Gastric mRNA content of NAPE-PLD and GOAT was similar between SLD- and HFD-mice, however FAAH and CB1 mRNA content was significantly increased in HFD-mice compared to SLD-mice (FAAH; $P = 0.0001$, $t = 6.118$, $df = 10$), CB1; $P = 0.0006$, $t = 4.923$, $df = 10$) (Figure 3A).

Gastric mucosal AEA protein content was significantly reduced ($P < 0.0001$; $t = 12.43$, $df = 10$), whilst FAAH protein content was significantly increased ($P < 0.0001$; $t = 14.48$, $df = 10$) in HFD-mice compared to SLD-mice. Total gastric ghrelin protein was significantly

decreased in HFD-mice compared to SLD-mice (Figure 3B) ($P < 0.0001$; $t = 8.026$, $df = 10$).

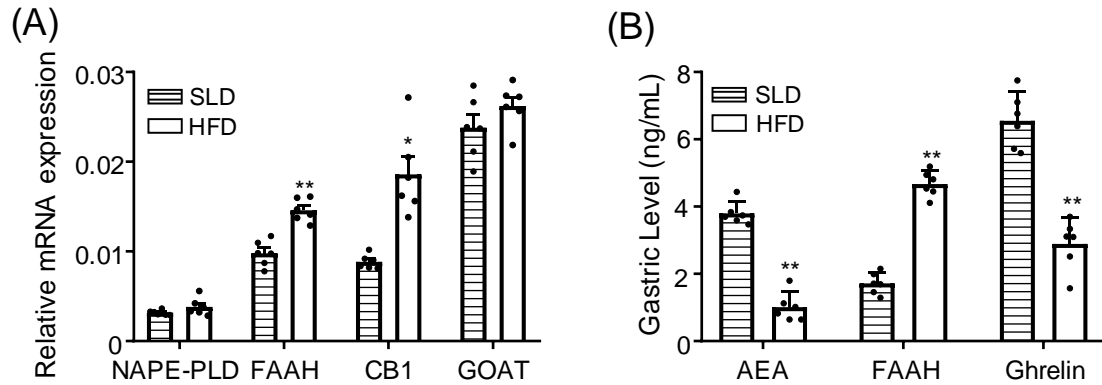


Figure 3: The mRNA expression of FAAH and CB1 is increased whilst the expression of AEA and ghrelin peptide is decreased in the gastric mucosa of high fat diet-induced obese mice. (A) The mRNA expression of N-acyl phosphatidylethanolamine specific phospholipase D (NAPE-PLD), fatty acid amide hydrolase (FAAH), cannabinoid receptor 1 (CB1), and ghrelin O acyl transferase (GOAT) in stomach scrapings of standard laboratory diet (SLD) and high fat diet (HFD) fed mice. (B) Gastric content of anandamide (AEA), FAAH, and ghrelin from stomach scrapings of SLD- and HFD-mice. N = 6 mice per diet. Data are expressed as the mean \pm SEM. * $P < 0.001$, ** $P < 0.0001$ vs SLD-mice (Unpaired t-test).

Sensitising effect of methanandamide is lost in HFD mice

During electrophysiology mAEA was super infused to determine its effects on the mechanosensitivity of tension sensitive GVAs in SLD- and HFD-mice (Figure 4).

The mechanosensitivity of tension GVAs to stretch in the absence of mAEA was significantly reduced in HFD-mice compared to SLD-mice ($P < 0.0001$) (Figure 4A, B, Ci and D). After exposure to 1nM mAEA the mechanosensitivity of tension sensitive GVAs to stretch was significantly reduced to a similar degree in both SLD- ($P < 0.0001$) and HFD-mice ($P = 0.0035$; Figure 4A, B, Cii & Dii). 10nM mAEA had no significant effect on tension sensitive GVA mechanosensitivity in SLD-mice but significantly reduced mechanosensitivity in HFD-mice ($P = 0.044$). In the presence of 100nM mAEA the mechanosensitivity of tension sensitive GVAs to stretch was significantly increased in SLD-mice ($P < 0.0001$) but significantly reduced in HFD-mice ($P = 0.008$) (Figure 4A, B, Ciii and Diii) (mAEA effect ($P < 0.0001$ $F = (4, 60) 29.98$, diet effect ($P < 0.0001$ $F(1, 60) = 198.2$, and an interaction ($P < 0.0001$ $F(4, 60) = 29.46$). Infusion of 300nM mAEA had no significant effect on tension sensitive GVA mechanosensitivity in either SLD- or HFD-mice (Figure 4A and B).

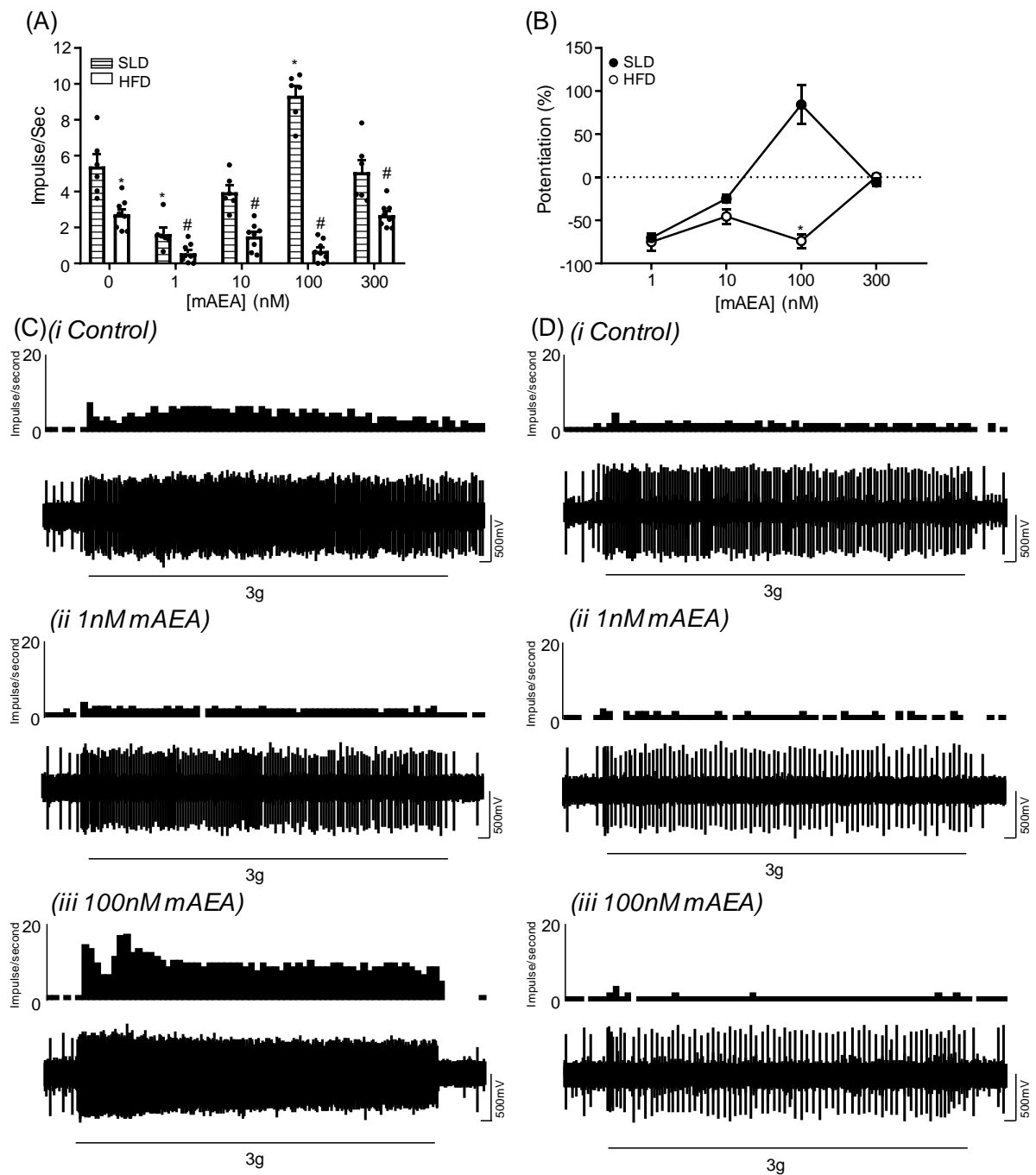


Figure 4: The excitatory effect of methanandamide on gastric vagal afferents is lost in high fat diet fed mice. (A) The response of tension sensitive gastric vagal afferents (GVAs) to circumferential stretch (3g) before and after the addition of methanandamide (mAEA) in standard laboratory diet (SLD) and high fat diet (HFD) fed mice. N = 6-8 mice per concentration. Data are expressed as the mean \pm SEM. *P<0.0001 vs SLD

control, [#]P<0.05 vs HFD control (Two way ANOVA, Sidak's *post hoc* test). (B) Percentage change of tension sensitive GVAs in response to circumferential stretch (3g) when exposed to mAEA compared to the control of SLD- or HFD-mice. Data are expressed as the mean ± SEM. * P<0.0001 vs SLD at the same concentration of mAEA (Two way ANOVA, Sidak's *post hoc* test). (C) Original recording of a tension sensitive GVA response to circumferential stretch (3g) from a SLD fed mouse (*i*) before and after the addition of (*ii*) 1nM or (*ii*) 100nM mAEA. (D) Original recording of a tension sensitive GVA response to circumferential stretch (3g) from a HFD fed mouse (*i*) before and after the addition of (*ii*) 1nM or (*ii*) 100nM mAEA.

The effects of mAEA are mediated by CB1 and TRPV1

To investigate the CB1 and TRPV1 dependent effects of mAEA signalling mAEA was used alone or in combination with a CB1 (rimonabant) or TRPV1 (AMG9810) antagonist (Figure 5).

Rimonabant alone (300nM) had no significant effect on the mechanosensitivity of tension sensitive GVAs in either SLD- or HFD-mice (Figure 5Ai and Bi). In SLD-mice, the inhibitory effect of 1nM mAEA was lost (P<0.0001) and the excitatory effect of 100nM mAEA was reduced in the presence of rimonabant (300nM) (Figure 5Ai; mAEA effect (P<0.0001 F(3, 40)=43.21), antagonist effect (P=0.015 F(1, 40)=6.465), and an interaction (P<0.0001 F(3, 40)=17.56)). In HFD-mice, the inhibitory effect of mAEA at 1nM (P<0.0001), 10nM (P<0.0001), and 100nM (P<0.0001) mAEA was lost in the presence of rimonabant (300nM; Figure 5Bi; mAEA effect (P<0.0001 F(3, 56)=11.24),

antagonist effect ($P < 0.0001$ $F(1, 56) = 182.4$), and an interaction ($P < 0.0001$ $F(3, 56) = 17.95$)).

AMG9810 (30nM) alone had no significant effect on the mechanosensitivity of tension sensitive GVAs in either SLD- or HFD-mice (Figure 5Aii and Bii). In SLD-mice the inhibitory effect of 1nM mAEA ($P = 0.0002$) and the excitatory effect of 100nM mAEA ($P < 0.0001$) were lost in the presence of AMG9810 (30nM; Figure 5Bi; mAEA effect ($P < 0.0001$ $F(3, 40) = 19.17$), antagonist effect ($P < 0.001$ $F(1, 40) = 8.024$), and an interaction ($P < 0.0001$ $F(3, 40) = 19.01$)). In HFD-mice the inhibitory effects of 1nM ($P < 0.0001$), 10nM ($P = 0.0003$), and 100nM ($P < 0.0001$) mAEA were lost in the presence of AMG9810 (30nM; Figure 5Bii; mAEA effect ($P < 0.0001$ $F(3, 56) = 17.53$), antagonist effect ($P < 0.0001$ $F(1, 56) = 102.9$), and an interaction ($P < 0.0001$ $F(3, 56) = 14.24$)).

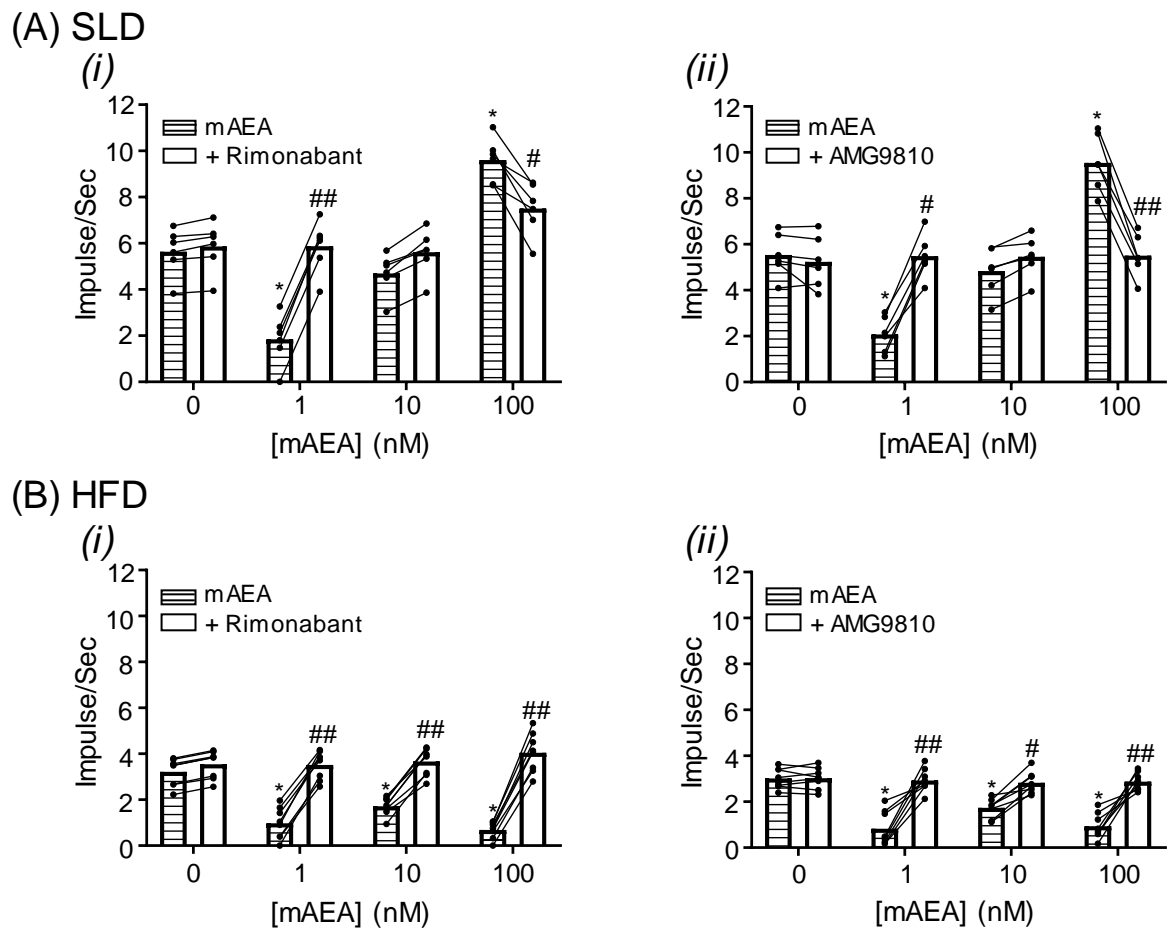


Figure 5: The response of gastric vagal afferents to methanandamide are mediated by CB1 and TRPV1. The response of tension sensitive gastric vagal afferents (GVAs) to 3g circumferential stretch in (A) standard laboratory diet (SLD) or (B) high fat diet (HFD) fed mice in the absence and presence of methanandamide (mAEA) alone or in combination with (i) a CB1 antagonist (rimonabant hydrochloride; 300nM) or (ii) a TRPV1 antagonist (AMG9810; 30nM). N = 6-8 mice per antagonist. Data are expressed as the mean \pm SEM. *P<0.0001 vs mAEA (0nM), #P<0.001, ##P<0.0001 vs mAEA alone at same concentration (Two way ANOVA, Sidak's *post hoc* test).

The inhibitory effects of mAEA is mediated by $G\alpha_{i/o}$, PKA, and GHSR pathways

To investigate the $G\alpha_{i/o}$, PKA, and GHSR dependent effects of mAEA signalling mAEA was used alone or in combination with either a $G\alpha_{i/o}$ (NF023), PKA (PKA-IFA), or GHSR (YIL-781) antagonist (Figure 6).

Infusion of NF023 (300nM) alone had no significant effect on the mechanosensitivity of tension sensitive GVAs in either SLD- or HFD-mice (Figure 6Ai and Bi). In SLD-mice, the inhibitory effect of 1nM mAEA was lost ($P<0.0001$) whilst the excitatory effect of 100nM mAEA remained in the presence of NF023 (300nM; Figure 6Ai; mAEA effect ($P<0.0001$, $F(3, 40)=147.1$), antagonist effect ($P=0.0002$, $F(1, 40)=17.81$), and an interaction ($P<0.0001$, $F(3, 40)=9.913$)). In HFD-mice, the inhibitory effect of mAEA (1-100nM) was lost in the presence of NF023 (300nM; Figure 6Bi; mAEA effect ($P<0.0001$, $F(3, 56)=10.46$), antagonist effect ($P<0.0001$, $F(1, 56)=35.05$), and an interaction ($P=0.007$, $F(3, 56)=4.385$)).

PKA-IFA (5nM) alone had no significant effect on the mechanosensitivity of tension sensitive GVAs in either SLD- or HFD-mice (Figures 6Aii and Bii). In SLD-mice, the inhibitory effect of 1nM mAEA was lost ($P=0.0032$) whilst the excitatory effect of 100nM mAEA remained in the presence of PKA-IFA (5nM; Figure 6Aii; mAEA effect ($P<0.0001$, $F(3, 40)=37.34$), antagonist effect ($P=0.011$, $F(1, 40)=7.292$), and an interaction ($P=0.0075$, $F(3, 40)=4.758$)). In HFD-mice, the inhibitory effects of mAEA (1-100nM) were lost in the presence of PKA-IFA (5nM; Figure 6Bii; mAEA effect ($P<0.0001$, $F(3, 56)=11.45$), antagonist effect ($P<0.0001$, $F(1, 56)=138.5$), and an interaction ($P<0.0001$, $F(3, 56)=16.6$)).

YIL-781 (300nM) alone had no significant effect on the mechanosensitivity of tension sensitive GVAs in either SLD- or HFD-mice (Figures 6Aii and Bii). In SLD-mice, the inhibitory effect of 1nM mAEA was lost ($P=0.0188$) whilst the excitatory effect of 100nM mAEA remained in the presence of YIL-781 (300nM; Figure 6Aii; mAEA effect ($P<0.0001$, $F(3, 40)=45.16$), and antagonist effect ($P=0.0103$, $F(1, 40)=7.442$)). In HFD-mice, the inhibitory effects of mAEA (1-100nM) were lost in the presence of YIL-781 (300nM; Figure 6Bii; antagonist effect ($P<0.0001$, $F(1, 40)=32.25$)).

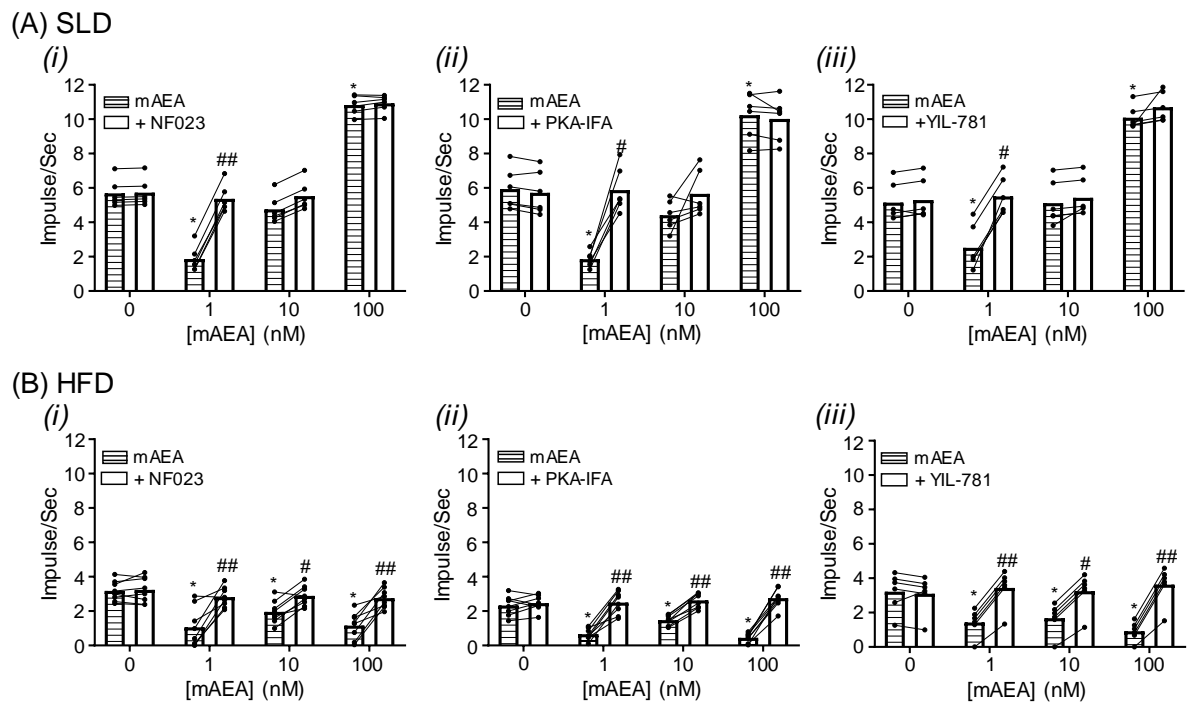


Figure 6: The inhibitory effects of methanandamide on gastric vagal afferent mechanosensitivity in SLD and HFD mice are mediated by *Gai/o* – PKA – GHSR pathways. The response of tension sensitive gastric vagal afferents (GVAs) to 3g circumferential stretch in (A) standard laboratory diet (SLD) or high fat diet (HFD) fed mice in the absence and presence of methanandamide (mAEA) alone or in combination

with (i) a *Gai/o* antagonist (NF023; 300nM) or A (ii) protein kinase A (PKA) antagonist (PKA-inhibitory fragment (6-22) amide; PKA-IFA; 5nM) or A (iii) growth hormone secretagogue (GHSR) antagonist (YIL-781; 300nM). N = 6-8 mice per antagonist. Data are expressed as the mean \pm SEM. *P<0.0001 vs mAEA (0nM), #P<0.05, ##P<0.0001 vs mAEA alone at same concentration (Two way ANOVA, Sidak's *post hoc* test).

The excitatory effect of mAEA is mediated by $G\alpha_q$ and PKC

To investigate the $G\alpha_q$, and PKC dependent effects of mAEA signalling mAEA was used alone or in combination with either a $G\alpha_q$ (YM-254980) or PKC (BIS-II) antagonists (Figure 7).

YM-254890 (100nM) alone had no significant effect on the mechanosensitivity of tension sensitive GVAs in SLD-mice (Figure 7A). This antagonist was not used in HFD-mice as there was no excitatory effect of mAEA present. In SLD-mice, the inhibitory effect of 1nM mAEA remained whilst the excitatory effect of 100nM mAEA was reduced in the presence of YM-254980 (100nM; Figure 7A; mAEA effect (P<0.0001, F(3, 40)=140.3), antagonist effect (P=0.0134, F(1, 40)=6.701), and an interaction (P=0.0037, F(3, 40)=5.271)).

BIS-II (10nM) alone had no significant effect on the mechanosensitivity of tension sensitive GVAs in SLD-mice (Figure 7B). This antagonist was not used in HFD-mice as there was no excitatory effect of mAEA present. In SLD-mice, the inhibitory effect of 1nM mAEA remained whilst the excitatory effect of 100nM mAEA was reduced in the presence of BIS-II (10nM; Figure 7B; mAEA effect (P<0.0001, F(3, 40)=14.6),

antagonist effect ($P=0.0005$, $F(1, 40)=14.6$), and an interaction ($P<0.0001$, $F(3, 40)=9.739$)).

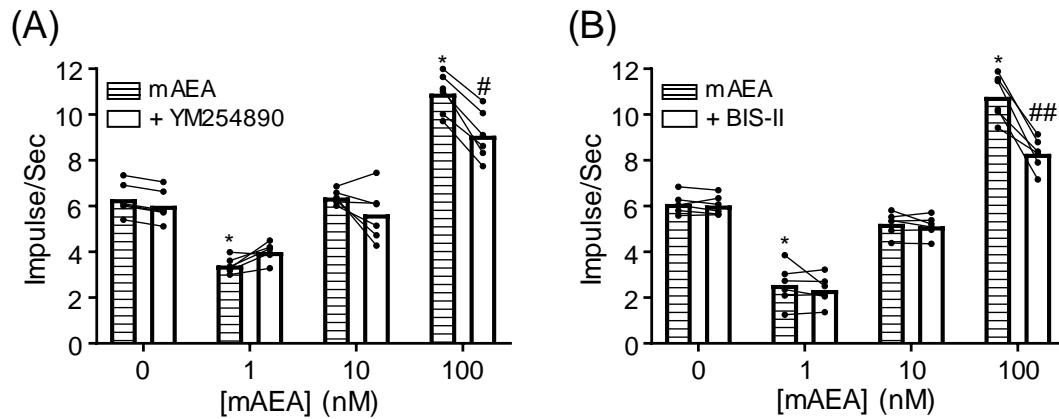


Figure 7: The excitatory effects of methanandamide on gastric vagal afferent mechanosensitivity in SLD mice is mediated by a $G\alpha_q$ – PKC pathway. The response of tension sensitive gastric vagal afferents to 3g circumferential stretch in the absence and presence of methanandamide (mAEA) alone or in combination with (A) a $G\alpha_q$ antagonist (YM254890; 100nM) or (B) a protein kinase C (PKC) antagonist (BIS-II; 10nM). N=6-8 SLD- mice per antagonist. Data are expressed as the mean \pm SEM. * $P<0.0001$ vs mAEA (0nM), # $P<0.001$, ## $P<0.0001$ vs mAEA alone at same concentration (Two way ANOVA, Sidak's *post hoc* test).

Discussion

The current study demonstrates that expression and co-expression of CB1, GHSR, TRPV1, and FAAH in tension sensitive GVAs are increased in HFD-induced obese mice. Further, this study also demonstrates that the dual inhibitory and excitatory effect of mAEA on tension sensitive GVA mechanosensitivity in SLD-mice is lost in HFD-induced obese mice where only inhibitory effects are observed.

The co-expression of CB1, TRPV1, GHSR, and FAAH in GVAs is increased in HFD-induced obesity

CB1, TRPV1, GHSR, and FAAH were co-expressed in individual cell bodies of tension sensitive GVAs. Further, the expression of CB1, GHSR, and FAAH, and the co-expression of CB1, TRPV1, GHSR, and FAAH were higher in tension sensitive GVA neurons of HFD-mice compared to SLD-mice. The increased expression is consistent with a previous study [177] demonstrating that the expression of CB1, GHSR, and FAAH are increased in the whole nodose of diet-induced obese rats. It is plausible that the increased expression and interaction of these orexigenic factors may contribute to the increased meals sizes observed in obesity [232, 492], however, this is highly speculative and requires further clarification.

The presence of FAAH in GVA cell bodies suggest a neural level of endocannabinoid regulation. AEA can enter a cell via a transport protein [493], or attached to a CB1 receptor [288], where it is rapidly degraded by FAAH. In other sensory ganglia, such as the dorsal root ganglia, FAAH controls AEA levels [494], however, it is not known if this occurs in nodose ganglia. Therefore, further investigation is required.

Gastric FAAH is increased while anandamide is decreased in HFD-induced obesity

Gastric mucosal AEA levels were reduced in HFD-induced obese mice consistent with a previous study which demonstrated decreased gastric AEA levels in diet-induced obese rats [351]. In contrast, FAAH levels were increased in the gastric mucosa of HFD-mice compared to SLD-mice. FAAH rapidly hydrolyses AEA upon entry into the cell [310] and its levels are negatively correlated with AEA levels [309]. Therefore, as expression of NAPE-PLD, an enzyme involved in biosynthesis of AEA [307], was similar between lean SLD-mice and HFD-induced obese mice, it is likely that the increased FAAH is responsible for the decreased gastric AEA levels in the HFD-induced obese mice. The mechanisms that drive the increased levels of FAAH in obesity are unknown. It has been demonstrated that the adipokine leptin activates the FAAH promoter in human T lymphocytes [344]. Circulating leptin levels are known to be increased in obesity [97] and, therefore, it could contribute to the increased FAAH levels observed in the gastric mucosa. However, this requires further investigation as it is highly speculative and does not take into account leptin resistance observed in obesity [495].

Consistent with a previous study [351] gastric concentrations of AEA were in the low nanomolar range. However, this is a mean concentration obtained from homogenised gastric mucosa and, therefore, the concentration of AEA at the gastric vagal afferent ending could be much higher and requires further investigation.

Excitatory effect of methanandamide on gastric vagal afferent sensitivity is lost in diet induced obesity

In lean SLD-mice mAEA elicited concentration-dependent inhibitory and excitatory effects on the mechanosensitivity of tension sensitive GVAs. This is consistent with a

previous study in younger male mice [490], suggesting a consistency regardless of age. However, the mice in the current study were still relatively young (20 weeks old) and therefore studies in aged mice are required to confirm this. The dual inhibitory and excitatory effect of mAEA was replaced with a single inhibitory effect in HFD-induced obese mice regardless of the concentration of mAEA. Tension sensitive GVAs respond to stretch of the gastric wall [460] which eventually produce feelings of fullness and satiety [214]. Concentrations of AEA are dependent on the type of tissue and the time of day. For example, hippocampal AEA is increased during the active phase and decreased during resting phases [496], whilst hypothalamic AEA is decreased during the active phase and increased during the inactive phase [497]. It is plausible that in lean SLD-mice the inhibitory effect of mAEA at low concentrations and excitatory effect of mAEA at high concentrations may contribute to the diurnal patterns in tension sensitive GVA mechanosensitivity and food intake previously reported [224]. Further, in diet-induced obesity diurnal rhythms in GVA mechanosensitivity and food intake are lost [225]. It is plausible that this is due to the loss in excitatory effect of mAEA observed in HFD-induced obese mice. However, it is currently not clear whether gastric endocannabinoids are regulated by or if they themselves can regulate circadian rhythms [315] or whether this is altered in HFD-induced obesity and, therefore, this requires further investigation.

The effects of methanandamide are dependent on CB1 and TRPV1

The inhibitory and excitatory effects of mAEA, in SLD-mice, were dependent on CB1 and TRPV1. Further, consistent to a previous report [490], antagonism of Gαq or PKC reduced the excitatory effect of mAEA at high concentrations, whilst antagonism of Gαi/o, PKA or GHSR abolished the inhibitory effect of mAEA.

The excitatory effect of mAEA in SLD-mice was blocked by a CB1, TRPV1, or PKC antagonist, and was absent in HFD-mice. The loss of the excitatory effect of mAEA in HFD-mice could be due to the concentration-response curve for mAEA being shifted to the right. However, this is unlikely given that gastric AEA levels were reduced in the HFD-mice and, therefore, presumably there was less competition for the receptor reducing the probability of a right shift in the concentration-response curve

In HFD-mice, CB1 receptor expression was increased in GVA cell bodies. In theory, if the inhibitory effect is mediated through CB1 receptors on gastric ghrelin cells, there should have been an increase in CB1 signalling at the GVA ending with a subsequent increase in the excitatory response to mAEA. However, this was not observed in the current study. In addition to the increased CB1 expression in GVAs, there was an increase in CB1 expression in the gastric mucosa and GHSR expression in GVA cell bodies, therefore, it is possible that this inhibitory pathway dominates over the excitatory pathway. It has been shown that CB1 and GHSR are co-dependent for functionality [336, 479]. Therefore, the increased CB1 expression in HFD-mice may contribute to the increased GHSR expression in GVA cell bodies contributing to the dominant inhibitory pathway.

PKC sensitises TRPV1 [397, 413] which may contribute to the increased mechanosensitivity observed in the presence of high concentrations of mAEA. Knockout of PKC in proopiomelanocortin neurons has been shown to predispose mice to obesity [498]. Mice with total PKC knockouts also exhibit hyperphagic behaviour, consuming 20% more food compared to wild-type mice [499]. Further, in skeletal muscle tissue of diet-induced obese mice, the stimulatory effects of insulin on PKC activity was about half of what was observed in lean mice [500]. In contrast, in adipose tissue of diet-induced

obese mice PKC activity is increased [501], suggesting the effects of obesity on PKC activity may be tissue specific. Therefore, further investigation is required to determine PKC activity in vagal afferents and how this may relate to the observed change in mAEA signalling in vagal afferents of diet-induced obese mice.

In the current study, mAEA inhibited tension sensitive GVA mechanosensitivity in a CB1, TRPV1, and PKA-dependent manner in both lean SLD-mice and HFD-induced obese mice. In dorsal root ganglia neurons, CB1 can inhibit PKA to desensitise TRPV1 [447]. It is possible that the same occurs in vagal afferent neurones. However, theoretically antagonism of TRPV1 or PKA alone should reduce GVA sensitivity. This was not observed, suggesting other signalling molecules are involved. AMG9180 prevents the binding of ligands to TRPV1 without necessarily having any effect on TRPV1 activity when used alone [502]. When combined with AMG9810 the inhibitory effect of mAEA was lost possibly due to prevention of the inhibitory secondary messenger pathway. Inhibition of this inhibitory pathway would suggest possible constitutive activity. However, this is highly speculative and requires further investigation.

PKA signalling during obesity appears to be tissue specific with reports that myocardial PKA activity does not change [503], and that hypothalamic PKA activity decreases [504]. Therefore, further studies are required to determine PKAs exact involvement in mAEA's effects on GVA mechanosensitivity and how this changes in obesity.

The inhibitory effect of mAEA in SLD- and HFD-mice was blocked by a GHSR antagonist suggesting mAEA effects are mediated via ghrelin. Ghrelin secretion from gastric cells is partially mediated by AEA [249] and ghrelin can decrease tension sensitive

GVA mechanosensitivity to a similar degree in SLD- and HFD-mice [167, 220]. Gastric ghrelin secretion is typically reduced in HFD-induced obesity [505]. It has been demonstrated that inhibition of CB1 receptors decreased ghrelin production through activation of the mTOR pathway [249]. Therefore, the reduced AEA levels observed in HFD-induced obese mice could be driving the decreased gastric ghrelin levels observed in the current study. Nonetheless, GHSR expression on GVAs is increased [177], perhaps in an attempt to maintain or increase signalling during low gastric ghrelin concentrations. Therefore, increased gastric ghrelin production and secretion through endogenous application of mAEA may subsequently act on the elevated levels of GVA GHSRs to induce inhibition. However, a more detailed study on the role of ghrelin in mAEA signalling is required. Further, GHSR has very high constitutive activity [485], therefore, although it is likely that CB1 mediated ghrelin release from gastric mucosal cells is acting on GHSR on GVA endings, blocking GHSR may impact on the CB1 response independent of ghrelin release.

GHSR predominantly couples to $G\alpha_q$ in most tissues, however, the current study suggests that in GVA endings it may couple to $G\alpha_i/o$. This is supported by previous evidence indicating that GHSR signals via $G\alpha_i/o$ in vagal afferent cell bodies [486]. However, it should be noted that this study was performed in whole nodose ganglia, and not specific subpopulations and, therefore, the role of $G\alpha_i/o$ in GHSR signalling in GVAs requires further investigation.

In conclusion, the current study demonstrates that the dual effects of mAEA on the mechanosensitivity of tension sensitive GVAs in lean SLD-mice is lost in HFD-induced obesity. Further investigation is required to understand how this may relate to food intake.

Author contributions

S.C., R.O., M.N-S., H.L.: acquisition or analysis or interpretation of data for the work, drafting the work or revising it critically for important intellectual content. G.A.W. and A.J.P.: conception or design of the work, acquisition or analysis or interpretation of the data for the work, drafting the work or revising it critically for important intellectual content.

Funding

Department of Health, Australian Government National Health and Medical Research Council (NHMRC) APP1159744 (A.J.P).

Chapter 5 : A high fat diet alters endocannabinoid and ghrelin mediated regulation of endocannabinoid pathway expression in nodose ganglia

Stewart Christie¹, Rebecca O'Reilly¹, Hui Li^{1,2}, Gary Wittert^{1,2}, Amanda Page^{1,2}

¹ Vagal Afferent Research Group, Centre for Nutrition and Gastrointestinal Disease, Adelaide Medical School, University of Adelaide, Adelaide, SA 5005, Australia

² Nutrition and Metabolism, South Australian Health and Medical Research Institute, Adelaide, SA 5000, Australia

Statement of Authorship

Title of Paper	A high fat diet alters endocannabinoid and ghrelin mediated regulation of orexigenic receptor expression in nodose ganglia
Publication Status	<input type="checkbox"/> Published <input type="checkbox"/> Accepted for Publication <input checked="" type="checkbox"/> Submitted for Publication <input type="checkbox"/> Unpublished and Unsubmitted work written in manuscript style
Publication Details	Submitted to Peptides

Principal Author

Name of Principal Author (Candidate)	Stewart Christie				
Contribution to the Paper	Performed experiments and wrote the paper				
Overall percentage (%)	80%				
Certification:	This paper reports on original research I conducted during the period of my Higher Degree by Research candidature and is not subject to any obligations or contractual agreements with a third party that would constrain its inclusion in this thesis. I am the primary author of this paper.				
Signature	<table border="1" style="width: 100%;"> <tr> <td style="width: 80%;"></td> <td style="width: 20%;">Date</td> </tr> <tr> <td></td> <td>14/11/2019</td> </tr> </table>		Date		14/11/2019
	Date				
	14/11/2019				

Co-Author Contributions

By signing the Statement of Authorship, each author certifies that:

- i. the candidate's stated contribution to the publication is accurate (as detailed above);
- ii. permission is granted for the candidate to include the publication in the thesis; and
- iii. the sum of all co-author contributions is equal to 100% less the candidate's stated contribution.

Name of Co-Author	Rebecca O'Reilly				
Contribution to the Paper	Helped prepare cell cultures				
Signature	<table border="1" style="width: 100%;"> <tr> <td style="width: 80%;"></td> <td style="width: 20%;">Date</td> </tr> <tr> <td></td> <td>14/11/2019</td> </tr> </table>		Date		14/11/2019
	Date				
	14/11/2019				

Name of Co-Author	Hui Li		
Contribution to the Paper	Planning and edited paper		
Signature		Date	14/11/2019

Name of Co-Author	Gary Wittert		
Contribution to the Paper	Intellectual input		
Signature		Date	20/11/2019

Name of Co-Author	Amanda J Page		
Contribution to the Paper	Planning of experiments and edited the paper		
Signature		Date	14/11/2019

Abstract

Background: Ghrelin and anandamide (AEA) can regulate the sensitivity of gastric vagal afferents (GVAs) to stretch, an effect mediated via the transient receptor potential vanilloid 1 (TRPV1) channel. High fat diet (HFD)-induced obesity alters the modulatory effects of ghrelin and AEA on GVA sensitivity. This may be a result of altered gastric levels of these hormones and subsequent changes in the expression of their receptors. Therefore, the current study aimed to determine the effects of ghrelin and AEA on vagal afferent cell body mRNA content of cannabinoid 1 receptor (CB1), ghrelin receptor (GHSR), TRPV1, and the enzyme responsible for the breakdown of AEA, fatty acid amide hydrolase (FAAH).

Methods: Mice were fed a standard laboratory diet (SLD) or HFD for 12wks. Nodose ganglia were removed and cultured for 14hrs in the absence or presence of ghrelin or methAEA (mAEA; stable analogue of AEA). Relative mRNA content of CB1, GHSR, TRPV1, and FAAH were measured.

Results: In nodose cells from SLD-mice, mAEA increased TRPV1 and FAAH mRNA content, and decreased CB1 and GHSR mRNA content. Ghrelin decreased TRPV1, CB1, and GHSR mRNA content.

In nodose cells from HFD-mice, mAEA had no effect on TRPV1 mRNA content, and increased CB1, GHSR, and FAAH mRNA content. Ghrelin decreased TRPV1 mRNA content and increased CB1 and GHSR mRNA content.

Conclusions: AEA and ghrelin modulate receptors and breakdown enzymes involved in the mAEA gastric vagal afferent satiety signalling pathways. This was disrupted in HFD-mice, which may contribute to the altered vagal afferent signalling in obesity.

Key words: Endocannabinoids, ghrelin, TRPV1, CB1, vagal afferents

Abbreviations: AEA, anandamide; CB1, cannabinoid 1 receptor; FAAH, fatty acid amide hydrolase; GHSR, growth hormone secretagogue receptor; GVA, gastric vagal afferent; HBSS, Hank's balance salt solution; HFD, high fat diet; mAEA, methanandamide; NBA, neurobasal A medium; PBS, phosphate buffered saline; SLD, standard laboratory diet; TRPV1, transient receptor potential vanilloid 1.

1. Introduction

Vagal afferent nerves innervating the gastrointestinal tract play an important role in the short-term regulation of food intake [88]. These nerves respond to both mechanical and chemical food related stimuli [214, 460], sending signals to the Nucleus Tractus Solitarius which relays information to other regions of the brain such as the Arcuate Nucleus and Paraventricular Nucleus, involved in the regulation of food intake [79]. In the stomach vagal afferents predominantly respond to mechanical stimuli, such as distension of the stomach wall.[204]. The mechanosensitivity of these gastric vagal afferents (GVAs) can be modulated by locally released peptides such as leptin [223] and ghrelin [220], secreted by gastric endocrine or epithelial cells [170].

Recently, it has been demonstrated that meth-anandamide (mAEA), the stable analogue of anandamide (AEA), can biphasically modulate the sensitivity of GVAs to stretch with inhibition at low and excitation at high concentrations [490]. The inhibitory effect is dependent in cannabinoid 1 (CB1) receptors in the gastric mucosa, and ghrelin receptors (growth hormone secretagogue receptor; GHSR) and transient receptor potential vanilloid 1 (TRPV1) ion channels in GVA cell bodies. Conversely, the excitatory effect of mAEA is only dependent CB1 receptors and TRPV1 ion channels in GVA cell bodies [490].

The sensitivity of GVAs to stretch is reduced in diet-induced obesity [234] and may contribute to the increased food intake observed in obese individuals [506]. Furthermore, in diet-induced obese mice, the inhibitory effect of ghrelin on the mechanosensitivity of GVAs to stretch is enhanced [167], and the normal excitatory effect of N-oleoyldopamine (TRPV1 agonist) is abolished [235].

The mRNA content of CB1 and GHSR, but not TRPV1 [235], in nodose ganglia can be influenced by nutritional status. Fasting increases GHSR [167], but not CB1 [471, 507], mRNA content whilst diet-induced obesity increases the mRNA content of GHSR and CB1 in nodose ganglia [177]. Gastric AEA [351] and circulating ghrelin protein [172] are reduced in diet-induced obesity, the former of which is due to increased fatty acid amide hydrolase (FAAH) protein, the enzyme involved in AEA degradation [309]. Further, ghrelin decreases and increases the mRNA content of GHSR in nodose ganglia from lean and diet-induced obese mice respectively [467]. However, it is not known if AEA and ghrelin can alter the mRNA content receptors for the endocannabinoid system in vagal afferent neurons.

The current study aimed to determine the effects of mAEA and ghrelin on the mRNA content of GHSR, CB1, TPRV1, and FAAH in the nodose ganglia of lean and high fat diet (HFD)-induced obese mice.

2. Methods

2.1. Ethics

This study was approved by the animal ethics committee of the South Australian Health and Medical Research Institute, and carried out in accordance with the Australian code for the care and use of animals for scientific purposes, 8th edition 2013, and the ARRIVE guidelines [475].

2.2. Animals

Seven week-old male C57BL/6 mice (N=24) were housed in littermates of 3 for 1 week acclimatisation. The mice were then randomly assigned to either a standard laboratory diet (SLD: 12% energy from fat, 65% energy from carbohydrates, 23% energy from protein; N=12) or HFD (60% energy from fat, 20% energy from protein, 20% energy from carbohydrates; N=12) for 12 weeks. During this time all mice were housed in a 12:12hour light:dark cycle at constant temperature (22°C) with *ad libitum* access to their respective diet and water.

2.3. Cell Culture

This method has been described in detail previously [467]. Briefly, after 12 weeks mice were humanely culled via CO₂ inhalation followed by decapitation. All mice were culled between 1200 and 1230hr to minimise circadian variation. The left and right nodose ganglia were then immediately removed and placed in ice cold F12 medium containing penicillin and streptomycin. The nodose ganglia were then dissociated at 37°C for 30 minutes in Hanks balanced salt solution (HBSS) containing 3mg/ml collagenase and dispase, followed by incubation for 37°C for 15 minutes in HBSS containing 3mg/ml collagenase. The cells were then rinsed with ice cold HBSS and F12 followed by further

dissociation with a fire polished pipette. Cells were then pelleted and resuspended in Neurobasal A (NBA) medium with B-27 supplement. A cell count was performed via trypan blue exclusion and cells were plated equally as 10 μ L dots (~500 cells) in the centre of wells coated with poly-D-lysine and laminin. Cells were then incubated at 37°C for 2 hours. After 2 hours wells were filled with warmed (37°C) NBA medium. Two wells were left with just NBA medium to act as controls. NBA/mAEA medium was added to other wells where the final concentration of mAEA was 1nM or 100nM. This was repeated for 1nM or 3nM of ghrelin.

The plate was then incubated for 14 hours at 37°C which is sufficient time for hormone induced changes in steady state mRNA content in nodose ganglia [467].

2.4. Quantitative RT-PCR

Following the 14 hours incubation the culture medium was removed, and the cells were washed with cold 1x phosphate buffered saline (PBS). Quantitative RT-PCR was then performed using a TaqMan® Gene Expression Cells-to-CT™ Kit (Invitrogen, ThermoFisher Scientific, Australia) as per manufacturer's protocol. Pre-designed Taqman® gene expression assays (Life Technologies, Australia) were used to measure mRNA levels of TRPV1 (mm01246300_m1), GHSR (mm00616415_m1), CB1 (mm01212171_s1), and FAAH (mm00515684_m1) in cultured nodose cell bodies from SLD and HFD fed mice. Beta-2-microglobulin (B2M; mm00437762_m1) and beta-actin (ACTB; mm02619580_g1) were used as housekeeping genes and were chosen based on stability across all samples determined from NormFinder software (stability value of B2M and ACTB = 0.102) (Department of Molecular Medicine (MOMA), Aarhus

University Hospital, Denmark). Relative mRNA content was calculated using the $2^{\Delta\text{CT}}$ method [456].

2.5. Data Analysis

All data is presented as the mean \pm the SEM and was analysed with GraphPad Prism. Data relating to gonadal fat mass was analysed using an unpaired t-test. Data relating to weight gain, and the effect of mAEA and ghrelin on mRNA content was analysed using a two-way ANOVA with a Tukey's *post hoc* test. P-values less than or equal to 0.05 were deemed significant.

3. Results

3.1. Effect of a high fat diet on body weight

Weight gain and gonadal fat pad mass are illustrated in Figure 1. Mice fed a HFD gained significantly more weight than mice fed a SLD ($P < 0.001$) (Figure 1A; SLD 8.91 ± 0.81 g; HFD 22.95 ± 0.83 g; diet effect ($P < 0.0001$, $F(1,286) = 500.7$), week effect ($P < 0.0001$, $F(12,286) = 109.6$), and an interaction ($P < 0.0001$, $F(12,286) = 24.31$). Gonadal fat pad mass as percentage body weight was significantly greater in mice fed a HFD compared to mice fed a SLD (Figure 1B; SLD $0.88 \pm 0.037\%$, HFD $3.30 \pm 0.09\%$; $P < 0.0001$; $t = 22.88$, $df = 22$).

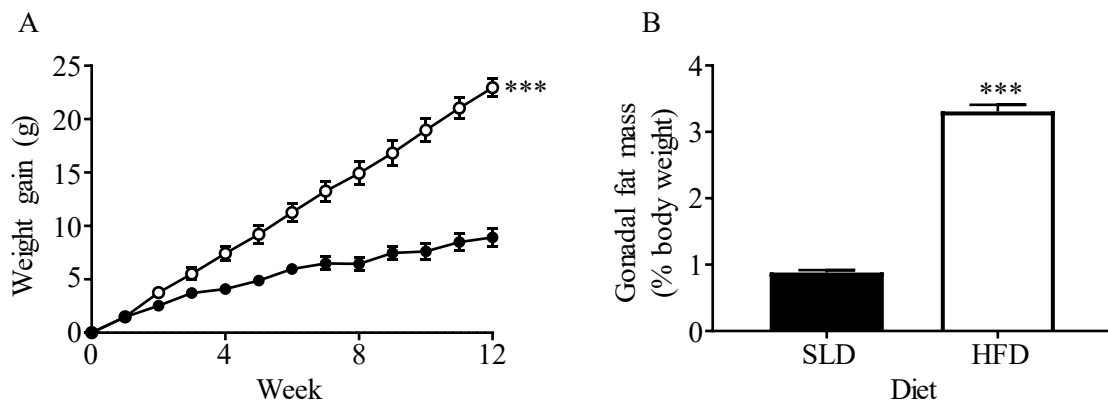


Figure 5.1: High fat diet fed mice gained more weight than standard laboratory diet fed mice.

(A) The weekly weight gain of mice fed either a high fat diet (HFD; \circ) or standard laboratory diet (SLD; \bullet) for 12 weeks. (B) Gonadal fat pad mass of SLD and HFD fed mice at the end of the 12 week diet period. Data are expressed as the mean \pm the SEM. $N = 6$ per diet. Weight gain was analysed using a two-way ANOVA. Gonadal fat pad mass was analysed using an unpaired t -test. *** $P < 0.0001$ vs SLD fed mice.

3.2. Effect of methanandamide on TRPV1, GHSR, CB1, and FAAH expression in nodose ganglia

TRPV1 mRNA content in nodose ganglia cell bodies was similar between SLD- and HFD-mice (Figure 2Ai). In SLD-mice, TRPV1 mRNA content was 1.52 fold higher in nodose neurons incubated with mAEA (100nM only) compared to no mAEA control neurons (Figure 2Ai; $P=0.0148$, $F(2, 15) = 7.903$). Conversely mAEA (1nM and 100nM) had no effect on TRPV1 mRNA content in nodose neurons from HFD-mice. Therefore a HFD abolished the effect of mAEA on TRPV1 mRNA content in nodose ganglia cell bodies (Figure 2Aii; diet effect ($P=0.0179$, $F(1, 20) = 5.25$)).

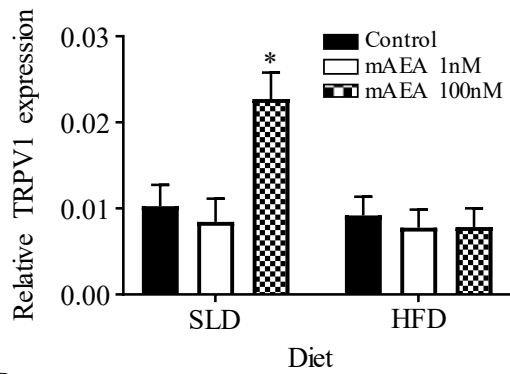
GHSR mRNA content in nodose ganglia cell bodies was similar between SLD- and HFD-mice. In SLD-mice, GHSR mRNA content was 0.80 fold lower in nodose neurons incubated with 100nM mAEA compared to no mAEA control neurons (Figure 2Bi; $P<0.0001$, $F(2, 15) = 33.41$). Conversely, in HFD-mice GHSR mRNA content was 1.84 fold higher in nodose neurons incubated with 100nM mAEA compared to no mAEA control neurons (Figure 2Bi; $P=0.0034$, $F(2, 15) = 8.522$). Therefore the effect of mAEA on nodose GHSR content switched from a decrease in SLD-mice to an increase in HFD-mice (Figure 2Bii; diet effect ($P<0.0001$, $F(1, 20) = 25.21$) and an interaction ($P=0.0255$, $F(1, 20) = 5.830$)).

In HFD-mice, CB1 mRNA content in nodose neurons was increased 1.70 fold compared to neurons from SLD-mice ($P=0.0056$; Figure 2Ci). In SLD-mice, CB1 mRNA content was 0.95 fold lower in nodose neurons incubated with mAEA (100nM only) compared to no mAEA control neurons (Figure 2Ci; $P=0.0003$, $F(2, 15) = 13.71$). Conversely, in HFD-mice, CB1 mRNA content was increased 0.71 fold in nodose neurons incubated with

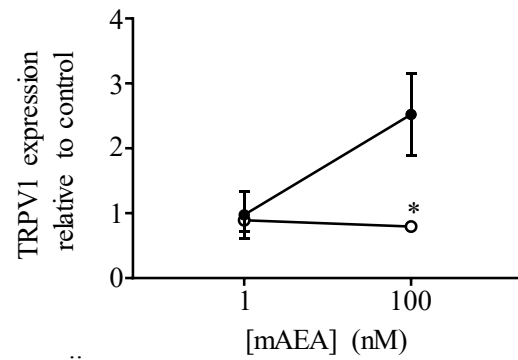
100nM mAEA compared to control neurons (Figure 2Ci; $P=0.0402$, $F(2, 15) = 4.013$). Therefore the effect of mAEA on nodose CB1 mRNA content switched from a decrease in SLD-mice to an increase in HFD-mice (Figure 2Cii; diet effect ($P<0.0001$, $F(1,20) = 65.68$) and an interaction ($P=0.0230$, $F(1,20) = 6.066$)).

In nodose neurons from HFD-mice FAAH mRNA content was 2.56 fold compared to neurons from SLD-mice ($P=0.46$; Figure 2Di). In SLD-mice, FAAH mRNA content was 3.44 fold higher in nodose neurons incubated with 100nM mAEA compared to no mAEA control neurons (Figure 2Di; $P=0.0007$, $F(2, 15) = 11.64$). Similarly, in HFD-mice FAAH content was 2.62 fold higher in nodose neurons incubated with 100nM mAEA compared to no mAEA control neurons (Figure 2Di; $P<0.0001$, $F(2, 15) = 22.81$). Therefore, a HFD had no effect on the regulation of mAEA on FAAH mRNA content in nodose neurons (Figure 2Dii; mAEA effect ($P=0.0011$, $F(1, 20) = 14.60$), no diet effect ($P=0.0879$, $F(1, 20) = 3.22$)).

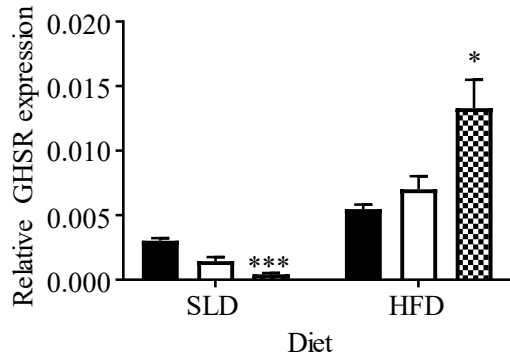
A *i*



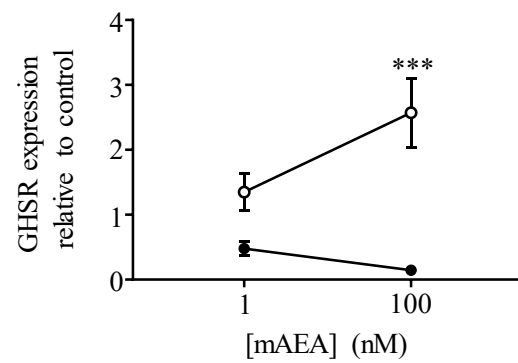
ii



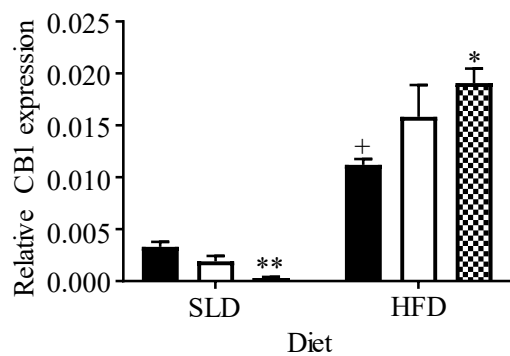
B *i*



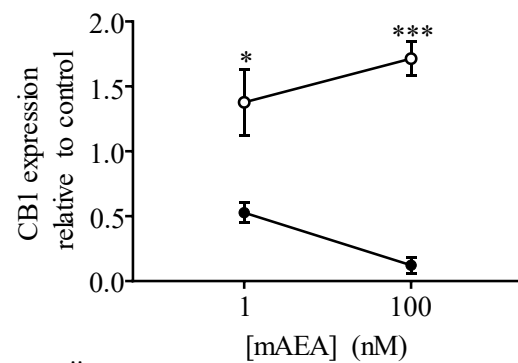
ii



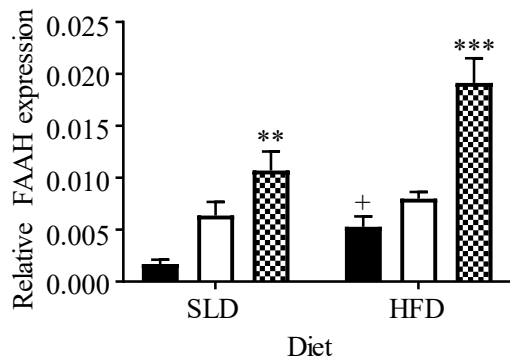
C *i*



ii



D *i*



ii

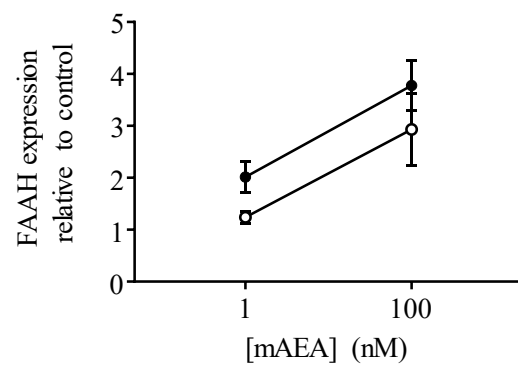


Figure 5.2: Methanandamide exposure alters TRPV1, GHSR, CB1, and FAAH expression.

Relative mRNA content of (Ai) TRPV1, (Bi) GHSR, (Ci) CB1, and (Di) FAAH in nodose ganglia cell bodies of standard laboratory diet (SLD) and high fat diet (HFD) mice before and after incubation with 1nM or 100nM of methanandamide (mAEA). Changes in the mRNA content of (Aii) TRPV1, (Bii) GHSR, (Cii) CB1, and (Dii) FAAH in nodose ganglia cell bodies of SLD (●) and HFD (○) mice incubated with 1nM or 100nM of mAEA relative to control. Data are expressed as the mean \pm SEM. N = 6 per diet. *P<0.05, **P<0.001, and ***P<0.0001 vs control in same diet, +P<0.05 vs SLD control (two-way ANOVA, Tukey's post hoc test).

3.3. Effect of ghrelin on TRPV1, GHSR, CB1, and FAAH expression in nodose ganglia

In SLD-mice, TRPV1 mRNA content was 0.85 and 0.97 fold lower in nodose neurons incubated with 1nM and 3nM of ghrelin, respectively, compared to no ghrelin control neurons (Figure 3Ai; P<0.0001, F(2, 15) = 32.44). Similarly, in HFD-mice TRPV1 mRNA content was 0.83 and 0.94 fold lower in nodose neurons incubated with 1nM and 3nM of ghrelin, respectively, compared to no ghrelin control neurons (Figure 3Ai; P<0.0001, F(2, 15) = 36.69). Therefore, a HFD had no effect on the regulation of TRPV1 mRNA content by ghrelin (Figure 3Aii; mAEA effect (P=0.0133, F(1, 20) = 7.378), no diet effect (P=0.616, F(1, 20) = 0.259)).

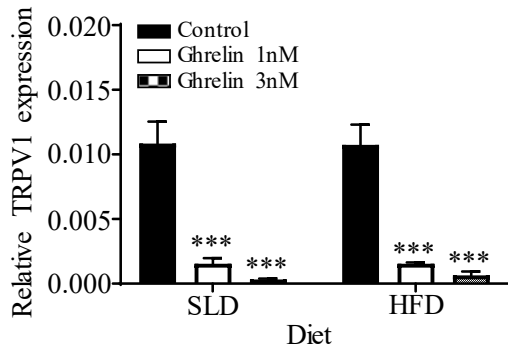
In SLD-mice, GHSR mRNA content was 0.42 fold lower in nodose neurones incubated with 3nM of ghrelin compared to no ghrelin control neurons (Figure 3Bi; P<0.0001, F(2, 15) = 40.43). In contrast, in HFD-mice GHSR mRNA content was 1.61 fold higher in

nodose neurons incubated with 3nM of ghrelin compared to no ghrelin control neurons (Figure 3Bi; $P=0.007$, $F(2, 5) = 6.849$). Therefore, a HFD caused a switch in the effect of ghrelin on nodose GHSR mRNA content from a decrease in SLD-mice to an increase in HFD-mice (Figure 3Bii; diet effect ($P<0.0001$, $F(1,20) = 23.68$)).

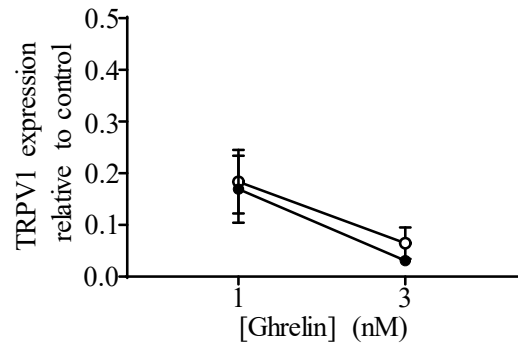
In SLD-mice, CB1 mRNA content was 0.47 fold lower in nodose neurons incubated with 3nM of ghrelin compared to no ghrelin control neurons (Figure 3Ci; $P=0.001$, $F(2, 15) = 11.11$). Conversely, in HFD-mice, CB1 mRNA content was 0.77 fold higher in nodose neurons incubated with 3nM of ghrelin compared to no ghrelin control neurons (Figure 3Ci; $P=0.019$, $F(2, 15) = 5.212$). Therefore, a HFD switched the effect of ghrelin on CB1 mRNA content in nodose neurons (Figure 3Cii; diet effect ($P<0.0001$, $F(1,20) = 23.48$)).

Incubation of nodose neurons from both SLD-mice and HFD-mice with 1nM or 3nM of ghrelin had no effect on FAAH mRNA content ($P=0.98$; Figure 3Di and 3Dii).

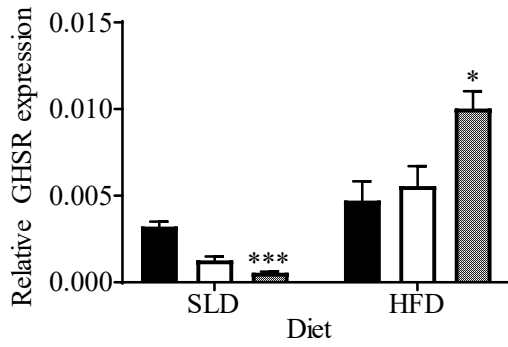
A *i*



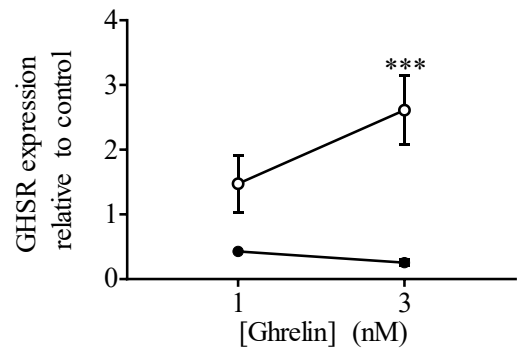
ii



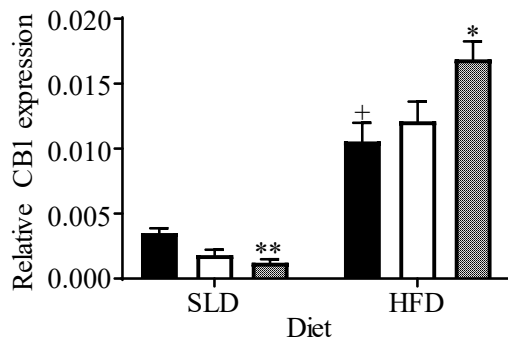
B *i*



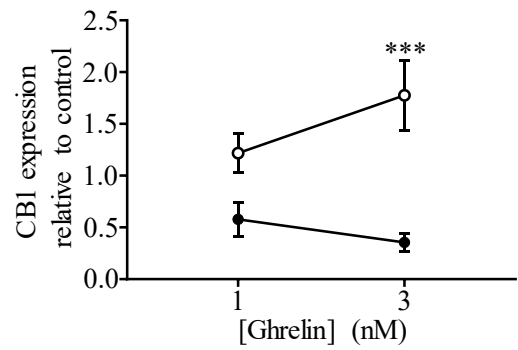
ii



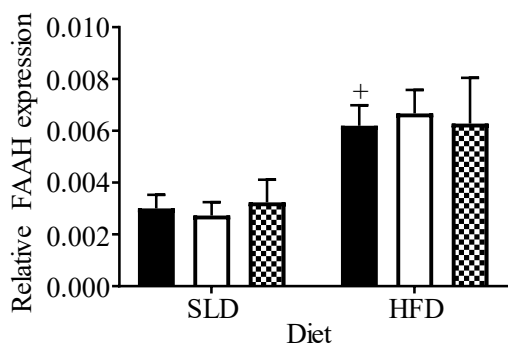
C *i*



ii



D *i*



ii

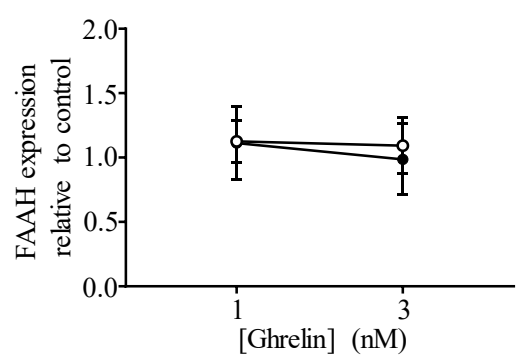


Figure 5.3: Ghrelin exposure alters TRPV1, GHSR, CB1, and FAAH expression.

Relative mRNA content of (Ai) TRPV1, (Bi) GHSR, (Ci) CB1, and (Di) FAAH in nodose ganglia cell bodies of standard laboratory diet (SLD) and high fat diet (HFD) mice before and after incubation with 1nM or 3nM of ghrelin. Changes in the mRNA content of (Aii) TRPV1, (Bii) GHSR, (Cii) CB1, and (Dii) FAAH in nodose ganglia cell bodies of SLD (●) and HFD (○) mice incubated with 1nM or 3nM of ghrelin relative to control. Data are expressed as the mean \pm SEM. N = 6 per diet. *P<0.05, **P<0.001, ***P<0.0001 vs control in same diet, +P<0.05 vs SLD control (two-way ANOVA, Tukey's post hoc test).

4. Discussion

The current study demonstrates that mAEA and ghrelin can regulate TRPV1, GHSR, CB1, and FAAH mRNA content in primary cultured nodose neurons. Further, these regulatory effects are altered in HFD-induced obese mice which could impact on vagal afferent signalling and appetite regulation.

Compared to SLD-mice, in HFD-mice there was an increase in relative CB1 and FAAH mRNA content, but no difference in relative GHSR or TRPV1 mRNA content in nodose cells. Consistent with this study it has been demonstrated that GHSR and TRPV1 mRNA levels in the nodose ganglia were not altered in HFD-induced obese mice [235, 467]. However, it has been shown that CB1, GHSR, and FAAH mRNA content was increased in nodose ganglia from HFD-induced obese rats compared to lean rats [177]. This suggests the effect of HFD-induced obesity on GHSR, but not CB1 or FAAH, mRNA content in nodose ganglia is species specific. Further, peripheral CB1 receptors have been implicated in the control of food intake and gastrointestinal motility [336, 508]. In lean conditions, the CB1 receptor was shown to be involved in the biphasic regulation of tension sensitive GVA mechanosensitivity [490]. Conversely, in HFD-induced obese conditions, the biphasic effect is replaced with a single inhibitory effect which may promote food intake [509]. Therefore, the increased mRNA content of CB1 in the nodose ganglia of HFD-mice may contribute to the hyperphagia typically observed in obesity [177, 492], however, this requires further investigation. Whilst protein levels were not measured in the current study, there is generally an acceptable degree of similarity between mRNA and protein levels for CB1 and GHSR [245, 476, 510].

Ghrelin and mAEA reduced the relative mRNA content of GHSR and CB1, respectively, in nodose cells from SLD-mice. G-coupled protein receptor mediated pathways, such as CB1 and GHSR, often have negative feedback loops to prevent over activation [511]. It is possible this negative feedback is reducing receptor mRNA expression in vagal afferent neurons in the current study. In HFD-mice, mAEA and ghrelin increased the relative mRNA content of both CB1 and GHSR in culture vagal afferent neurons, suggesting a switch in effect. The mechanism for the switch in effect of mAEA and ghrelin on their respective receptor expression is unknown, but may be a result of the reduced gastric AEA [351] and ghrelin [512] protein levels in HFD-induced obesity. This requires further investigation.

It is speculated that CB1 and GHSR are co-dependent for functionality [336, 479] which may explain the observation in the current study that mAEA and ghrelin can regulate the mRNA content of each other's receptors. Further, it should be noted that in 'normal' conditions, gastric concentrations of AEA and ghrelin protein are in the low nanomolar range (1-10nM), and are decreased in obese conditions [351, 505]. However, in the case of ghrelin, GVA endings have been shown to be located close to ghrelin positive cells [167]. Therefore, the concentration of ghrelin released directly onto vagal afferent endings may be considerably higher than the average content throughout the tissue. The location of gastric AEA stores, and their proximity to vagal afferent endings, is currently unknown [513] and requires further investigation.

Ghrelin decreased the relative mRNA content of TRPV1 in nodose neurons from both SLD- and HFD-mice. Consistent with this, in other tissues such as the intestinal mucosa [514] and trigeminal ganglia [515], ghrelin treatment decreased TRPV1 mRNA content. However, in these tissues ghrelin only decreased TRPV1 mRNA content in pathological

conditions such as hyperalgesia, and not 'normal' conditions. In 'normal' conditions, TRPV1 on gastrointestinal vagal afferent neurons is associated with increased gastrointestinal motility and satiety [516]. Conversely, ghrelin is associated with decreased gastrointestinal motility and satiety [517]. Therefore, the reduced TRPV1 mRNA content mediated by ghrelin, in theory, should reduce gastrointestinal motility. This requires further investigation.

Relative TRPV1 mRNA content was increased by mAEA exposure in nodose neurons from SLD-mice; an effect lost in nodose neurons from HFD-mice. AEA is a full agonist for TRPV1 [408], and can influence TRPV1 mRNA content. For example, in bronchial epithelial cells AEA increased TRPV1 mRNA content [518], albeit, at a substantially higher concentration compared to the current study. In GVAs from lean mice, high concentrations of mAEA increased the mechanosensitive of tension receptors to stretch, an effect mediated via TRPV1 [490]. This effect is replaced with an inhibitory effect in HFD-induced obese mice [509]. Therefore, the loss of effect of mAEA on TRPV1 mRNA content may contribute to this. The mechanisms by which this occurs is not currently known, and, therefore this requires further investigation.

Exposure to mAEA, but not ghrelin, increased the relative mRNA content of FAAH in cells from both SLD- and HFD-mice. FAAH is involved in the degradation of AEA upon entry into the cell [309] and its concentration is typically negatively correlated with the concentration of AEA [519, 520]. It should be noted that although AEA is secreted from gastric epithelial cells [351], the presence of FAAH mRNA in the nodose ganglia may impact endocannabinoid effects in vagal afferents and ultimately vagal afferent signalling. Further, whilst the relative mRNA content of TRPV1 in nodose ganglia from HFD-mice treated with 100nM mAEA was significantly higher than SLD-mice, the fold

increase was similar. This suggests that the effects of AEA are preserved between diets. Therefore, the fact that gastric AEA levels are reduced in obesity would suggest that the increased TRPV1 mRNA content is being driven by an alternate pathway. However, this requires further investigation.

In conclusion, the current study demonstrates that HFD-induced obesity can alter the effect of mAEA and/or ghrelin on the expression of CB1, GHSR, and TRPV1 mRNA in nodose neurons, which may impact signalling from the gastrointestinal tract and appetite regulation. The cell cultures used in this study were from fed mice at a single time point and therefore do not take into account any possible fasting or circadian variations that may be present. Further, AEA and ghrelin represent only a small portion of a multitude of appetite modulating gut hormones, and, as such, the current study does not take into account the complex interactions that may exist *in vivo* to regulate mRNA expression in nodose ganglia, and the physiological effects they may cause.

Chapter 6 : General Conclusions

This thesis provides evidence that the endocannabinoid AEA biphasically modulates tension sensitive GVA signalling in a diet-dependent manner. These effects are dependent on CB1, TRPV1, and GHSR interactions which are co-expressed in individual tension sensitive GVA neurons. Tension sensitive GVAs may play a role in satiety signalling and therefore AEA, which is synthesised in the stomach, may play a role in regulating these signals.

Expression in the stomach and vagal afferents

The CB1 receptor is expressed on gastric epithelial cells, and in vagal afferent neurons. On gastric epithelial cells it regulates the secretion of gastric acid [352] and ghrelin [249]. In vagal afferent neurons the CB1 receptor is synthesised in the cell body and then transported to the axon terminals in the gastrointestinal tract [521]. Consistent with this, the studies in this thesis demonstrate that CB1 mRNA is expressed in both the gastric mucosa and in GVA cell bodies. This suggests that mAEA does not have to act directly on tension sensitive GVA endings but can induce the release of gastrointestinal hormones such as ghrelin which can act on these afferents.

CB1 receptor mRNA was also expressed in individual tension sensitive GVA cell bodies, and co-expressed to a high degree with TRPV1 and GHSR mRNA. Studying identified subpopulations of neurons is important for specificity of action. The co-expression of CB1, GHSR, and TRPV1 mRNA in individual tension GVA neurons was different from the general nodose ganglia population. This suggests they have a specific function to influence satiety signalling. Likewise, the increased GHSR and CB1 receptor mRNA

expression in individual tension sensitive GVA neurons of diet-induced obese mice could act to increase or maintain signalling of their corresponding ligands which were reduced in the gastric mucosa. Further, the research in this thesis demonstrates that mAEA and ghrelin can regulate each other's receptor expression. This reinforces previous reports in other tissues suggesting that the the endocannabinoid and ghrelin systems are co-dependent for functionality [479, 522]. This potentially provides information that can lead to targeting of these receptors to modulate appetite since if you are targeting one, you are likely to be influencing the other. This is important regarding potential side effects of pharmacological therapy as it is necessary to take in to account both the endocannabinoid and ghrelin systems.

Immunohistochemistry was performed to confirm the presence of TRPV1, CB1, and GHSR protein in vagal afferent neurons. Whilst their presence was confirmed, immunohistochemistry is typically a semi-quantitative method [523] and therefore their levels were not directly measured. It is well known that mRNA levels do not always correlate well with protein levels [524]. However, for the CB1 receptor and GHSR there is generally a degree of similarity between mRNA and protein levels in human and murine nodose ganglia [245, 476, 510]. Nonetheless, further studies are required to determine protein levels in vagal afferent neurones, although this may prove difficult in single cells.

Modulatory effects of methanandamide on gastric vagal afferents

Electrophysiology studies in this thesis revealed that, in lean mice, mAEA exhibited biphasic effects on the mechanosensitivity of tension sensitive GVAs to stretch. Consumption of food causes stretch or distension of the stomach wall leading to feelings

of fullness. Generally, distension of the stomach wall alone is sufficient as non-nutrient liquids can also generate feelings of fullness [525]. Therefore, the excitatory effect of mAEA on tension sensitive GVAs at high concentrations may act to increase satiety signalling in response to stomach distension, presumably reducing food intake. Conversely, the inhibitory effect of mAEA on tension sensitive GVAs at low concentrations could act to delay satiety signalling and increase food intake. Whilst exogenous AEA experiments may confirm this hypothesis, the experimental design may prove difficult. AEA also regulates mood and memory, and can centrally regulate food intake via the circulation [301, 526]. Therefore, it would be necessary to restrict AEA administration peripherally to the stomach.

It should be noted that endocannabinoids such as AEA can interact with other gastrointestinal hormones. Whilst it has been established that there is a possible ghrelin interaction in the inhibitory pathway of mAEA, isolated *in vitro* studies generally do not take into account the multitude of other interactions that may exist *in vivo*. Studies have shown that CCK downregulates CB1 receptor mRNA expression in vagal afferents [510], and counteracts the effects of AEA [527]. Additionally, leptin increases AEA degradation via increasing FAAH protein activity [343]. These hormones may influence AEA signalling *in vivo* by partly regulating AEA effects and levels, making it necessary to include these two gastrointestinal hormones in future studies.

The biphasic signalling of mAEA in lean mice is complicated further by other factors including nutritional status and circadian rhythms. AEA levels in the gastrointestinal tract are increased by fasting [335]. Generally, during fasting it would be favourable to increase signals that promote food intake. Given this, it would seem counterintuitive that high levels of mAEA increase the mechanosensitivity of tension sensitive GVAs. However,

after fasting, control mechanisms may occur to prevent over eating. This has been observed in rats where initial food intake following a fast is decreased [528]. Nonetheless, given that the excitatory effect of mAEA is lost in diet-induced obese mice, mAEA signalling via tension sensitive GVAs may also change in fasted mice. This has previously been reported for other gastrointestinal hormones such as leptin which gains an inhibitory effect on tension sensitive GVAs in fasted mice [223].

The studies in this thesis were only performed at one time point to minimise circadian variation. AEA protein exhibits tissue specific diurnal variation in both rodents and humans [315]. Specifically, hypothalamic AEA protein is increased during the inactive phase and decreased during the active phase of rats [497]. GVA mechanosensitivity also displays diurnal variation in mice, with highest sensitivity during the inactive phase, and lowest sensitivity during the active phase [224]. This raises the possibility that the effect of mAEA on the mechanosensitivity of tension sensitive GVAs may also differ depending on the time of day. Further, it is also possible that the biphasic effects of AEA signalling on GVAs is driving the diurnal rhythms in GVA mechanosensitivity. This requires detailed circadian studies to confirm.

Methanandamide signalling in diet-induced obesity

In diet-induced obese mice the biphasic effect of mAEA on the mechanosensitivity of tension sensitive GVAs was replaced with a single inhibitory effect. An increase in food intake can contribute to the development and maintenance of obesity. This can be achieved through a dampening of anorexigenic signals, or dominance of orexigenic signals [529]. Previously it has been reported that the mechanosensitivity of tension

sensitive GVAs to stretch is reduced in diet-induced obesity [167]. Given the possible role of tension sensitive GVAs in satiety this would suggest a reduced response to gastric distension and likely a delay in satiety signalling. In the current thesis, electrophysiology studies revealed that in diet-induced obese mice mAEA reduced the mechanosensitivity of tension sensitive GVAs even further. Previously in diet-induced obese rats it has been demonstrated that the pattern of food intake is altered with an increase in meal size [530]. Additionally, HFD-induced obese mice exhibit a lack of GVA diurnal variation with a loss of peak response to mechanical stimuli [225]. Therefore, the inhibitory effect of mAEA on tension sensitive GVAs in diet-induced obese mice may contribute to the dampened response and loss of circadian variation in GVA mechanosensitivity, and subsequent increase in meal size. Further, the reduced mechanosensitivity of tension sensitive GVAs observed in diet-induced obesity persists even after return to SLD conditions [234] which may compromise the ability to sustain weight loss. Further studies are required to determine if the effects of mAEA on the mechanosensitivity of tension sensitive GVAs also return to 'normal' after return to SLD conditions.

The inhibitory effect of mAEA in diet-induced obese mice, similar to SLD-mice, is mediated through GHSR. In the current studies, gastric ghrelin protein levels were reduced, whereas ghrelin receptor mRNA expression in individual tension sensitive GVA neurons was increased in HFD-induced obesity. Further, in the cell culture studies in this thesis, ghrelin increased GHSR mRNA expression in vagal afferent neurons from diet-induced obese mice. Therefore, the increased GHSR mRNA expression in diet-induced obesity may be driven by ghrelin itself. However, ghrelin protein levels are reduced in the gastric mucosa and therefore this require further investigation.

It is worth noting that in obesity the phenomenon of ghrelin resistance can occur as described earlier. However, it should also be noted that the inhibitory effect of ghrelin on tension sensitive GVAs in lean mice persists in diet-induced obese mice [167]. This suggests that ghrelin resistance is not present in GVAs.

Exogenous administration of ghrelin causes a greater increase in food intake in obese compared to lean individuals [190], which may partly be mediated via vagal afferents [167]. However, ghrelin and AEA are also involved in central signalling in the hypothalamus and reward pathways [531, 532]. Further, in obesity central endocannabinoid systems are overactive [342, 533]. Therefore, the involvement of these systems in hyperphagia cannot be ruled out. Overall, the effect of mAEA on the mechanosensitivity of tension sensitive GVAs in diet-induced obese mice may cause a latency in satiety signalling and a subsequent increase in meal size, consistent with meal patterns in obese rodents [530].

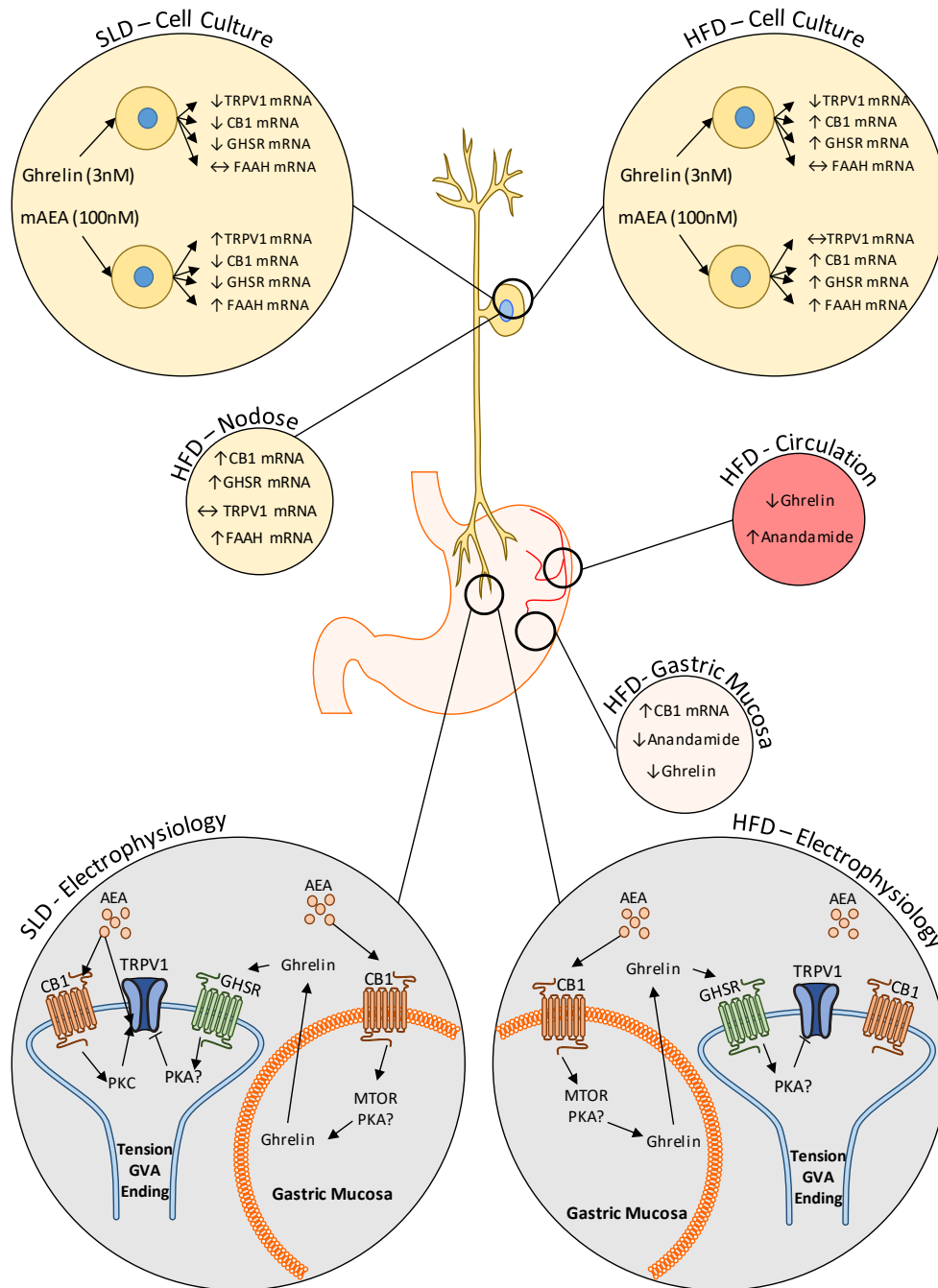


Figure 6.1: Overall schematic of the peripheral vagal afferent system linking together the studies in this thesis.

In the nodose ganglia ghrelin and methanandamide (mAEA) diet dependently alter the expression of TRPV1, CB1, and GHSR mRNA. Levels of ghrelin and anandamide are decreased in gastric mucosal tissue whilst CB1 mRNA is increased. In the circulation levels of ghrelin are decreased whilst levels of anandamide are increased. Lastly, at

tension sensitive GVA endings, mAEA diet dependently regulates the sensitivity of GVAs to stretch via CB1, GHSR, and TRPV1.

Targeting of the endocannabinoid system for pharmacotherapy of pathologies continues to be an area of research interest. Notably, rimonabant, a CB1 receptor antagonist, was approved as an anorectic drug for obesity in 2006, however, was quickly withdrawn two years later due to psychological side effects [534]. Recent advancements have turned towards targeting FAAH to regulate AEA levels; however one test drug has resulted in neurological complications and a death [535, 536]. In the current study, the inhibitory effect of mAEA was dominant in diet-induced obese mice regardless of mAEA concentration. This suggests that regulating gastric AEA levels using a FAAH inhibitor to increase satiety signalling may not be viable.

There has been interest in TRPV1 as a potential target for pain therapy. The studies in this thesis suggest that it may be feasible to target TRPV1 for appetite regulation. There is a lack of knowledge regarding agonistic targeting of TRPV1, however, antagonistic targeting of specific TRPV1 domains can block some of its functions without affecting the others. For example, some antagonists block activation by capsaicin without blocking activation by low pH [537]. This suggests it is plausible to specifically target TRPV1 with an agonist to affect only one function. However, there is a general lack of knowledge regarding the role of TRPV1 on food intake. Therefore, whilst it may seem a viable target, there is the need for more research.

It is well established that GVA neurons are involved in the control of food intake and gastrointestinal functions such as gastric emptying and motility [216, 538]. Whilst it is

speculated, there is no definitive proof on the exact physiological roles of subpopulations of GVAs. Mucosal sensitive GVAs are speculated to be involved in gastric emptying, with their activation causing a delay. Larger food particle sizes elicit a greater response from mucosal sensitive GVAs causing a delayed gastric emptying. This allows further breakdown of the larger food particles before intestinal transit to aid in digestion [205]. AEA, through the CB1 receptor, but not TRPV1, delays gastric emptying [351]. Therefore, it could be hypothesised that mAEA modulates the mechanosensitivity of mucosal GVAs. However, mAEA had no effect on the mechanosensitivity of mucosal sensitive GVAs, and, therefore AEA is likely to mediate gastric emptying via other mechanisms.

Tension sensitive GVAs are speculated to play a role in satiety signalling, however, they may also play a role in the generation of gastrointestinal reflexes such as motility. Recently, it has been suggested that GVAs are not necessary to produce satiety signals in response to stretch, and that duodenal vagal afferents are more important [213]. However, this study was performed in fasted mice where the mechanosensitivity of GVAs to stretch is reduced compared to fed mice [167]. Therefore, GVA satiety signalling in the fasted state is not dominant. Nonetheless, AEA, CB1, TRPV1, and ghrelin have all been implicated in both food intake and gastrointestinal motility [472, 539, 540]. Whilst this thesis suggests it is likely AEA may act to control food intake, it cannot be excluded that tension sensitive GVAs also influence gastrointestinal reflexes. Therefore, future studies must determine the physiological and behavioural effects of biphasic AEA signalling in tension sensitive GVA neurons.

Summary

In summary, the studies in this thesis provide evidence that mAEA biphasically modulates the mechanosensitivity of tension sensitive GVAs to stretch, an effect dependent on nutritional status. Further, the inhibitory effect of mAEA on tension sensitive GVAs is dominant in diet-induced obese mice which may contribute to increased food intake, however behavioural studies are required to confirm this hypothesis. In the gastrointestinal tract AEA, CB1, and TRPV1 are also involved in other processes such as gastric acid secretion and motility, and thus should also be considered for future studies. Nonetheless, the evidence presented in this thesis may provide potential mechanisms that favour the maintenance of obesity, and thus highlights potential targets that can be explored and developed further.

Chapter 7 : References

1. Jensen, M.D., et al., *2013 AHA/ACC/TOS guideline for the management of overweight and obesity in adults: a report of the American College of Cardiology/American Heart Association Task Force on Practice Guidelines and The Obesity Society*. J Am Coll Cardiol, 2014. **63**(25 Pt B): p. 2985-3023.
2. Sahoo, K., et al., *Childhood obesity: causes and consequences*. J Family Med Prim Care, 2015. **4**(2): p. 187-92.
3. Collaborators, G.B.D.O., et al., *Health Effects of Overweight and Obesity in 195 Countries over 25 Years*. N Engl J Med, 2017. **377**(1): p. 13-27.
4. Valery, P.C., et al., *Diet, physical activity, and obesity in school-aged indigenous youths in northern australia*. J Obes, 2012. **2012**: p. 893508.
5. Prospective Studies, C., et al., *Body-mass index and cause-specific mortality in 900 000 adults: collaborative analyses of 57 prospective studies*. Lancet, 2009. **373**(9669): p. 1083-96.
6. Kitahara, C.M., et al., *Association between class III obesity (BMI of 40-59 kg/m²) and mortality: a pooled analysis of 20 prospective studies*. PLoS Med, 2014. **11**(7): p. e1001673.
7. Sturm, R., *The effects of obesity, smoking, and drinking on medical problems and costs*. Health Aff (Millwood), 2002. **21**(2): p. 245-53.
8. Lee, C.M.Y., et al., *The cost of diabetes and obesity in Australia*. J Med Econ, 2018. **21**(10): p. 1001-1005.
9. Janda, M., et al., *An instrument to measure adherence to weight loss programs: the compliance praxis survey-diet (COMPASS-Diet)*. Nutrients, 2013. **5**(10): p. 3828-38.

10. Filozof, C.M., et al., *Low plasma leptin concentration and low rates of fat oxidation in weight-stable post-obese subjects*. *Obes Res*, 2000. **8**(3): p. 205-10.
11. Brand-Miller, J.C. and A.W. Barclay, *Declining consumption of added sugars and sugar-sweetened beverages in Australia: a challenge for obesity prevention*. *Am J Clin Nutr*, 2017. **105**(4): p. 854-863.
12. Pescud, M., et al., *How does whole of government action address inequities in obesity? A case study from Australia*. *Int J Equity Health*, 2019. **18**(1): p. 8.
13. An, H., H. Sohn, and S. Chung, *Phentermine, sibutramine and affective disorders*. *Clin Psychopharmacol Neurosci*, 2013. **11**(1): p. 7-12.
14. Glazer, G., *Long-term pharmacotherapy of obesity 2000: a review of efficacy and safety*. *Arch Intern Med*, 2001. **161**(15): p. 1814-24.
15. Haslam, D., *Weight management in obesity - past and present*. *Int J Clin Pract*, 2016. **70**(3): p. 206-17.
16. Zhi, J., et al., *Review of limited systemic absorption of orlistat, a lipase inhibitor, in healthy human volunteers*. *J Clin Pharmacol*, 1995. **35**(11): p. 1103-8.
17. Pace, D.G., S. Blotner, and R. Guerciolini, *Short-term orlistat treatment does not affect mineral balance and bone turnover in obese men*. *J Nutr*, 2001. **131**(6): p. 1694-9.
18. Weir, M.A., et al., *Orlistat and acute kidney injury: an analysis of 953 patients*. *Arch Intern Med*, 2011. **171**(7): p. 703-4.
19. Singh, S., et al., *Glucagonlike peptide 1-based therapies and risk of hospitalization for acute pancreatitis in type 2 diabetes mellitus: a population-based matched case-control study*. *JAMA Intern Med*, 2013. **173**(7): p. 534-9.

20. Barak, L.S., et al., *Pharmacological characterization of membrane-expressed human trace amine-associated receptor 1 (TAAR1) by a bioluminescence resonance energy transfer cAMP biosensor*. *Mol Pharmacol*, 2008. **74**(3): p. 585-594.
21. Rothman, R.B. and E.J. Hendricks, *Phentermine cardiovascular safety. In response to Yosefy C, Berman M, Beeri R. Cusp tear in bicuspid aortic valve possibly caused by phentermine. International journal of cardiology 2006;106:262-3*. *Int J Cardiol*, 2010. **144**(2): p. 241-2; author reply 242-3.
22. Kim, K.K., et al., *Effects on weight reduction and safety of short-term phentermine administration in Korean obese people*. *Yonsei Med J*, 2006. **47**(5): p. 614-25.
23. Rueda-Clausen, C.F., R.S. Padwal, and A.M. Sharma, *New pharmacological approaches for obesity management*. *Nat Rev Endocrinol*, 2013. **9**(8): p. 467-78.
24. Castells, X., et al., *Efficacy of central nervous system stimulant treatment for cocaine dependence: a systematic review and meta-analysis of randomized controlled clinical trials*. *Addiction*, 2007. **102**(12): p. 1871-87.
25. Saka, C., *Analytical Strategies for the Determination of Norepinephrine Reuptake Inhibitors in Pharmaceutical Formulations and Biological Fluids*. *Crit Rev Anal Chem*, 2016. **46**(1): p. 40-66.
26. Rothman, R.B., et al., *(+)-Fenfluramine and its major metabolite, (+)-norfenfluramine, are potent substrates for norepinephrine transporters*. *J Pharmacol Exp Ther*, 2003. **305**(3): p. 1191-9.
27. Connolly, H.M., et al., *Valvular heart disease associated with fenfluramine-phentermine*. *N Engl J Med*, 1997. **337**(9): p. 581-8.

28. Dahl, C.F., et al., *Valvular regurgitation and surgery associated with fenfluramine use: an analysis of 5743 individuals*. BMC Med, 2008. **6**: p. 34.
29. Hofmaier, T., et al., *Aminorex, a metabolite of the cocaine adulterant levamisole, exerts amphetamine like actions at monoamine transporters*. Neurochem Int, 2014. **73**: p. 32-41.
30. Gaine, S.P., et al., *Recreational use of aminorex and pulmonary hypertension*. Chest, 2000. **118**(5): p. 1496-7.
31. Weigle, D.S., *Pharmacological therapy of obesity: past, present, and future*. J Clin Endocrinol Metab, 2003. **88**(6): p. 2462-9.
32. McNeely, W. and K.L. Goa, *Sibutramine. A review of its contribution to the management of obesity*. Drugs, 1998. **56**(6): p. 1093-124.
33. Siebenhofer, A., et al., *Long-term effects of weight-reducing drugs in people with hypertension*. Cochrane Database Syst Rev, 2016. **3**: p. CD007654.
34. Andersson, C., et al., *Acute effect of weight loss on levels of total bilirubin in obese, cardiovascular high-risk patients: an analysis from the lead-in period of the Sibutramine Cardiovascular Outcome trial*. Metabolism, 2009. **58**(8): p. 1109-15.
35. Johansson, K., et al., *Discontinuation due to adverse events in randomized trials of orlistat, sibutramine and rimonabant: a meta-analysis*. Obes Rev, 2009. **10**(5): p. 564-75.
36. Curran, M.P. and L.J. Scott, *Orlistat: a review of its use in the management of patients with obesity*. Drugs, 2004. **64**(24): p. 2845-64.

37. Ahnen, D.J., et al., *Effect of orlistat on fecal fat, fecal biliary acids, and colonic cell proliferation in obese subjects*. Clin Gastroenterol Hepatol, 2007. **5**(11): p. 1291-9.
38. Cavaliere, H., I. Floriano, and G. Medeiros-Neto, *Gastrointestinal side effects of orlistat may be prevented by concomitant prescription of natural fibers (psyllium mucilloid)*. Int J Obes Relat Metab Disord, 2001. **25**(7): p. 1095-9.
39. Bansal, A.B. and Y. Al Khalili, *Orlistat*, in *StatPearls*. 2019: Treasure Island (FL).
40. Duarte, C., et al., *Blockade by the cannabinoid CB1 receptor antagonist, rimonabant (SR141716), of the potentiation by quinolorane of food-primed reinstatement of food-seeking behavior*. Neuropsychopharmacology, 2004. **29**(5): p. 911-20.
41. Stella, N., *Cannabinoid and cannabinoid-like receptors in microglia, astrocytes, and astrocytomas*. Glia, 2010. **58**(9): p. 1017-30.
42. Soyka, M., *Rimonabant and depression*. Pharmacopsychiatry, 2008. **41**(5): p. 204-5.
43. Backhouse, K., et al., *Fatty acid flux and oxidation are increased by rimonabant in obese women*. Metabolism, 2012. **61**(9): p. 1220-3.
44. Boekholdt, S.M. and R.J. Peters, *Rimonabant: obituary for a wonder drug*. Lancet, 2010. **376**(9740): p. 489-90.
45. Greenway, F.L., et al., *Rational design of a combination medication for the treatment of obesity*. Obesity (Silver Spring), 2009. **17**(1): p. 30-9.
46. Smith, S.R., *Naltrexone-bupropion causes weight loss in overweight and obese adults*. Evid Based Med, 2011. **16**(2): p. 53-4.

47. Nau, J.Y., [*Mysimba, an American appetite suppressant and the logic of the single European market*]. Rev Med Suisse, 2015. **11**(470): p. 890-1.
48. Redman, L.M. and E. Ravussin, *Lorcaserin for the treatment of obesity*. Drugs Today (Barc), 2010. **46**(12): p. 901-10.
49. DiNicolantonio, J.J., et al., *Lorcaserin for the treatment of obesity? A closer look at its side effects*. Open Heart, 2014. **1**(1): p. e000173.
50. Brashier, D.B., et al., *Lorcaserin: A novel antiobesity drug*. J Pharmacol Pharmacother, 2014. **5**(2): p. 175-8.
51. Christou, G.A., N. Katsiki, and D.N. Kiortsis, *The Current Role of Liraglutide in the Pharmacotherapy of Obesity*. Curr Vasc Pharmacol, 2016. **14**(2): p. 201-7.
52. Tronieri, J.S., et al., *Effects of liraglutide plus phentermine in adults with obesity following 1year of treatment by liraglutide alone: A randomized placebo-controlled pilot trial*. Metabolism, 2019. **96**: p. 83-91.
53. Khoraki, J., et al., *Long-term outcomes of laparoscopic adjustable gastric banding*. Am J Surg, 2018. **215**(1): p. 97-103.
54. Pollard, S., *The current status of bariatric surgery*. Frontline Gastroenterol, 2011. **2**(2): p. 90-95.
55. Hayes, K. and G. Eid, *Laparoscopic Sleeve Gastrectomy: Surgical Technique and Perioperative Care*. Surg Clin North Am, 2016. **96**(4): p. 763-71.
56. Puzziferri, N. and J.P. Almandoz, *Sleeve Gastrectomy for Weight Loss*. JAMA, 2018. **319**(3): p. 316.
57. van Rutte, P.W., et al., *Nutrient deficiencies before and after sleeve gastrectomy*. Obes Surg, 2014. **24**(10): p. 1639-46.

58. van Rutte, P.W., et al., *To Sleeve or NOT to Sleeve in Bariatric Surgery?* ISRN Surg, 2012. **2012**: p. 674042.
59. Brocks, D.R., et al., *The effects of gastric bypass surgery on drug absorption and pharmacokinetics.* Expert Opin Drug Metab Toxicol, 2012. **8**(12): p. 1505-19.
60. Hedberg, J., J. Sundstrom, and M. Sundbom, *Duodenal switch versus Roux-en-Y gastric bypass for morbid obesity: systematic review and meta-analysis of weight results, diabetes resolution and early complications in single-centre comparisons.* Obes Rev, 2014. **15**(7): p. 555-63.
61. Beaulac, J. and D. Sandre, *Critical review of bariatric surgery, medically supervised diets, and behavioural interventions for weight management in adults.* Perspect Public Health, 2017. **137**(3): p. 162-172.
62. Gautron, L., J.F. Zechner, and V. Aguirre, *Vagal innervation patterns following Roux-en-Y gastric bypass in the mouse.* Int J Obes (Lond), 2013. **37**(12): p. 1603-7.
63. Foschi, D., et al., *Different effects of vertical banded gastroplasty and Roux-en-Y gastric bypass on meal inhibition of ghrelin secretion in morbidly obese patients.* J Invest Surg, 2008. **21**(2): p. 77-81.
64. Karamanakos, S.N., et al., *Weight loss, appetite suppression, and changes in fasting and postprandial ghrelin and peptide-YY levels after Roux-en-Y gastric bypass and sleeve gastrectomy: a prospective, double blind study.* Ann Surg, 2008. **247**(3): p. 401-7.
65. Rodieux, F., et al., *Effects of gastric bypass and gastric banding on glucose kinetics and gut hormone release.* Obesity (Silver Spring), 2008. **16**(2): p. 298-305.

66. Berthoud, H.R., *Multiple neural systems controlling food intake and body weight.* Neurosci Biobehav Rev, 2002. **26**(4): p. 393-428.
67. Joseph, S.A., W.H. Pilcher, and K.M. Knigge, *Anatomy of the corticotropin-releasing factor and opiomelanocortin systems of the brain.* Fed Proc, 1985. **44**(1 Pt 1): p. 100-7.
68. Kristensen, P., et al., *Hypothalamic CART is a new anorectic peptide regulated by leptin.* Nature, 1998. **393**(6680): p. 72-6.
69. Broberger, C., et al., *The neuropeptide Y/agouti gene-related protein (AGRP) brain circuitry in normal, anorectic, and monosodium glutamate-treated mice.* Proc Natl Acad Sci U S A, 1998. **95**(25): p. 15043-8.
70. Wang, Q., et al., *Arcuate AgRP neurons mediate orexigenic and glucoregulatory actions of ghrelin.* Mol Metab, 2014. **3**(1): p. 64-72.
71. Poggioli, R., A.V. Vergoni, and A. Bertolini, *ACTH-(1-24) and alpha-MSH antagonize feeding behavior stimulated by kappa opiate agonists.* Peptides, 1986. **7**(5): p. 843-8.
72. Butler, A.A., et al., *A unique metabolic syndrome causes obesity in the melanocortin-3 receptor-deficient mouse.* Endocrinology, 2000. **141**(9): p. 3518-21.
73. Butler, A.A., et al., *Melanocortin-4 receptor is required for acute homeostatic responses to increased dietary fat.* Nat Neurosci, 2001. **4**(6): p. 605-11.
74. Larsen, P.J., et al., *Chronic intracerebroventricular administration of recombinant CART(42-89) peptide inhibits and causes weight loss in lean and obese Zucker (fa/fa) rats.* Obes Res, 2000. **8**(8): p. 590-6.

75. Rossi, M., et al., *A C-terminal fragment of Agouti-related protein increases feeding and antagonizes the effect of alpha-melanocyte stimulating hormone in vivo*. *Endocrinology*, 1998. **139**(10): p. 4428-31.
76. Stanley, B.G. and S.F. Leibowitz, *Neuropeptide Y injected in the paraventricular hypothalamus: a powerful stimulant of feeding behavior*. *Proc Natl Acad Sci U S A*, 1985. **82**(11): p. 3940-3.
77. Hahn, T.M., et al., *Coexpression of Agrp and NPY in fasting-activated hypothalamic neurons*. *Nat Neurosci*, 1998. **1**(4): p. 271-2.
78. Hu, Y., et al., *Identification of a novel hypothalamic neuropeptide Y receptor associated with feeding behavior*. *J Biol Chem*, 1996. **271**(42): p. 26315-9.
79. Broberger, C., *Brain regulation of food intake and appetite: molecules and networks*. *J Intern Med*, 2005. **258**(4): p. 301-27.
80. Sims, J.S. and J.F. Lorden, *Effect of paraventricular nucleus lesions on body weight, food intake and insulin levels*. *Behav Brain Res*, 1986. **22**(3): p. 265-81.
81. Gray, T.S., M.E. Carney, and D.J. Magnuson, *Direct projections from the central amygdaloid nucleus to the hypothalamic paraventricular nucleus: possible role in stress-induced adrenocorticotropin release*. *Neuroendocrinology*, 1989. **50**(4): p. 433-46.
82. Bittencourt, J.C. and C.F. Elias, *Melanin-concentrating hormone and neuropeptide EI projections from the lateral hypothalamic area and zona incerta to the medial septal nucleus and spinal cord: a study using multiple neuronal tracers*. *Brain Res*, 1998. **805**(1-2): p. 1-19.

83. Sakurai, T., et al., *Orexins and orexin receptors: a family of hypothalamic neuropeptides and G protein-coupled receptors that regulate feeding behavior*. Cell, 1998. **92**(5): p. 1 page following 696.
84. Mogenson, G.J., L.W. Swanson, and M. Wu, *Neural projections from nucleus accumbens to globus pallidus, substantia innominata, and lateral preoptic-lateral hypothalamic area: an anatomical and electrophysiological investigation in the rat*. J Neurosci, 1983. **3**(1): p. 189-202.
85. Jean, A., [*The nucleus tractus solitarius: neuroanatomic, neurochemical and functional aspects*]. Arch Int Physiol Biochim Biophys, 1991. **99**(5): p. A3-52.
86. Wang, D., et al., *Whole-brain mapping of the direct inputs and axonal projections of POMC and AgRP neurons*. Front Neuroanat, 2015. **9**: p. 40.
87. Travagli, R.A., et al., *Brainstem circuits regulating gastric function*. Annu Rev Physiol, 2006. **68**: p. 279-305.
88. Cummings, D.E. and J. Overduin, *Gastrointestinal regulation of food intake*. J Clin Invest, 2007. **117**(1): p. 13-23.
89. Zhang, Y., et al., *Positional cloning of the mouse obese gene and its human homologue*. Nature, 1994. **372**(6505): p. 425-32.
90. Banks, W.A., et al., *Leptin enters the brain by a saturable system independent of insulin*. Peptides, 1996. **17**(2): p. 305-11.
91. Elias, C.F., et al., *Chemical characterization of leptin-activated neurons in the rat brain*. J Comp Neurol, 2000. **423**(2): p. 261-81.
92. Doring, H., et al., *Leptin selectively increases energy expenditure of food-restricted lean mice*. Int J Obes Relat Metab Disord, 1998. **22**(2): p. 83-8.

93. Scarpace, P.J., et al., *Leptin increases uncoupling protein expression and energy expenditure*. Am J Physiol, 1997. **273**(1 Pt 1): p. E226-30.
94. Chen, H., et al., *Evidence that the diabetes gene encodes the leptin receptor: identification of a mutation in the leptin receptor gene in db/db mice*. Cell, 1996. **84**(3): p. 491-5.
95. Lee, G.H., et al., *Abnormal splicing of the leptin receptor in diabetic mice*. Nature, 1996. **379**(6566): p. 632-5.
96. Varela, L. and T.L. Horvath, *Leptin and insulin pathways in POMC and AgRP neurons that modulate energy balance and glucose homeostasis*. EMBO Rep, 2012. **13**(12): p. 1079-86.
97. Myers, M.G., Jr., et al., *Obesity and leptin resistance: distinguishing cause from effect*. Trends Endocrinol Metab, 2010. **21**(11): p. 643-51.
98. Adam, C.L. and P.A. Findlay, *Decreased blood-brain leptin transfer in an ovine model of obesity and weight loss: resolving the cause of leptin resistance*. Int J Obes (Lond), 2010. **34**(6): p. 980-8.
99. Lubis, A.R., et al., *The role of SOCS-3 protein in leptin resistance and obesity*. Acta Med Indones, 2008. **40**(2): p. 89-95.
100. Reinehr, T., et al., *Adiponectin before and after weight loss in obese children*. J Clin Endocrinol Metab, 2004. **89**(8): p. 3790-4.
101. Schober, F., et al., *Low molecular weight adiponectin negatively correlates with the waist circumference and monocytic IL-6 release*. Biochem Biophys Res Commun, 2007. **361**(4): p. 968-73.
102. Zhu, N., et al., *High-molecular-weight adiponectin and the risk of type 2 diabetes in the ARIC study*. J Clin Endocrinol Metab, 2010. **95**(11): p. 5097-104.

103. Kubota, N., et al., *Adiponectin stimulates AMP-activated protein kinase in the hypothalamus and increases food intake*. Cell Metab, 2007. **6**(1): p. 55-68.
104. Shklyayev, S., et al., *Sustained peripheral expression of transgene adiponectin offsets the development of diet-induced obesity in rats*. Proc Natl Acad Sci U S A, 2003. **100**(24): p. 14217-22.
105. Suyama, S., et al., *Adiponectin at physiological level glucose-independently enhances inhibitory postsynaptic current onto NPY neurons in the hypothalamic arcuate nucleus*. Neuropeptides, 2017. **65**: p. 1-9.
106. Masaki, T., et al., *Peripheral, but not central, administration of adiponectin reduces visceral adiposity and upregulates the expression of uncoupling protein in agouti yellow (Ay/a) obese mice*. Diabetes, 2003. **52**(9): p. 2266-73.
107. Bagdade, J.D., E.L. Bierman, and D. Porte, Jr., *The significance of basal insulin levels in the evaluation of the insulin response to glucose in diabetic and nondiabetic subjects*. J Clin Invest, 1967. **46**(10): p. 1549-57.
108. Woods, S.C., et al., *Pancreatic signals controlling food intake; insulin, glucagon and amylin*. Philos Trans R Soc Lond B Biol Sci, 2006. **361**(1471): p. 1219-35.
109. Loh, K., et al., *Insulin controls food intake and energy balance via NPY neurons*. Mol Metab, 2017. **6**(6): p. 574-584.
110. Butler, P.C., et al., *Effects of meal ingestion on plasma amylin concentration in NIDDM and nondiabetic humans*. Diabetes, 1990. **39**(6): p. 752-6.
111. Young, A. and M. Denaro, *Roles of amylin in diabetes and in regulation of nutrient load*. Nutrition, 1998. **14**(6): p. 524-7.
112. Lutz, T.A., et al., *Amylin decreases meal size in rats*. Physiol Behav, 1995. **58**(6): p. 1197-202.

113. Banks, W.A., et al., *Permeability of the blood-brain barrier to amylin*. Life Sci, 1995. **57**(22): p. 1993-2001.
114. Lutz, T.A., et al., *Amylin Selectively Signals Onto POMC Neurons in the Arcuate Nucleus of the Hypothalamus*. Diabetes, 2018. **67**(5): p. 805-817.
115. Lutz, T.A., et al., *Lesion of the area postrema/nucleus of the solitary tract (AP/NTS) attenuates the anorectic effects of amylin and calcitonin gene-related peptide (CGRP) in rats*. Peptides, 1998. **19**(2): p. 309-17.
116. Bray, N., *Obesity: Reversing resistance to leptin in obesity*. Nat Rev Drug Discov, 2015. **14**(7): p. 458-9.
117. Reda, T.K., A. Geliebter, and F.X. Pi-Sunyer, *Amylin, food intake, and obesity*. Obes Res, 2002. **10**(10): p. 1087-91.
118. Norton, M. and K.G. Murphy, *Targeting gastrointestinal nutrient sensing mechanisms to treat obesity*. Curr Opin Pharmacol, 2017. **37**: p. 16-23.
119. Miyamoto, T., G. Wright, and H. Amrein, *Nutrient sensors*. Curr Biol, 2013. **23**(9): p. R369-73.
120. Tremblay, A. and F. Bellisle, *Nutrients, satiety, and control of energy intake*. Appl Physiol Nutr Metab, 2015. **40**(10): p. 971-9.
121. Choi, S., et al., *GPR93 activation by protein hydrolysate induces CCK transcription and secretion in STC-1 cells*. Am J Physiol Gastrointest Liver Physiol, 2007. **292**(5): p. G1366-75.
122. Dyer, J., et al., *Glucose sensing in the intestinal epithelium*. Eur J Biochem, 2003. **270**(16): p. 3377-88.
123. Holt, S., et al., *Relationship of satiety to postprandial glycaemic, insulin and cholecystokinin responses*. Appetite, 1992. **18**(2): p. 129-41.

124. Karhunen, L.J., et al., *Effect of protein, fat, carbohydrate and fibre on gastrointestinal peptide release in humans*. Regul Pept, 2008. **149**(1-3): p. 70-8.
125. Miyauchi, S., et al., *New frontiers in gut nutrient sensor research: free fatty acid sensing in the gastrointestinal tract*. J Pharmacol Sci, 2010. **112**(1): p. 19-24.
126. Hirasawa, A., et al., *Free fatty acids regulate gut incretin glucagon-like peptide-1 secretion through GPR120*. Nat Med, 2005. **11**(1): p. 90-4.
127. Tome, D., et al., *Protein, amino acids, vagus nerve signaling, and the brain*. Am J Clin Nutr, 2009. **90**(3): p. 838S-843S.
128. Yox, D.P., H. Stokesberry, and R.C. Ritter, *Vagotomy attenuates suppression of sham feeding induced by intestinal nutrients*. Am J Physiol, 1991. **260**(3 Pt 2): p. R503-8.
129. Beck, B., et al., *Influence of diet composition on food intake and hypothalamic neuropeptide Y (NPY) in the rat*. Neuropeptides, 1990. **17**(4): p. 197-203.
130. Babaei, S., et al., *Effect of dietary macronutrients on the expression of cholecystinin, leptin, ghrelin and neuropeptide Y in gilthead sea bream (Sparus aurata)*. Gen Comp Endocrinol, 2017. **240**: p. 121-128.
131. Duca, F.A. and J.T. Yue, *Fatty acid sensing in the gut and the hypothalamus: in vivo and in vitro perspectives*. Mol Cell Endocrinol, 2014. **397**(1-2): p. 23-33.
132. Tordoff, M.G., *Calcium: taste, intake, and appetite*. Physiol Rev, 2001. **81**(4): p. 1567-97.
133. Major, G.C., et al., *Multivitamin and dietary supplements, body weight and appetite: results from a cross-sectional and a randomised double-blind placebo-controlled study*. Br J Nutr, 2008. **99**(5): p. 1157-67.

134. Major, G.C., et al., *Calcium plus vitamin D supplementation and fat mass loss in female very low-calcium consumers: potential link with a calcium-specific appetite control*. Br J Nutr, 2009. **101**(5): p. 659-63.
135. Jones, K.W., et al., *Effect of a dairy- and calcium-rich diet on weight loss and appetite during energy restriction in overweight and obese adults: a randomized trial*. Eur J Clin Nutr, 2013. **67**(4): p. 371-6.
136. Adrian, T.E., et al., *Human distribution and release of a putative new gut hormone, peptide YY*. Gastroenterology, 1985. **89**(5): p. 1070-7.
137. Ballantyne, G.H., *Peptide YY(1-36) and peptide YY(3-36): Part I. Distribution, release and actions*. Obes Surg, 2006. **16**(5): p. 651-8.
138. Savage, A.P., et al., *Effects of peptide YY (PYY) on mouth to caecum intestinal transit time and on the rate of gastric emptying in healthy volunteers*. Gut, 1987. **28**(2): p. 166-70.
139. Guo, Y.S., et al., *Inhibitory action of peptide YY on gastric acid secretion*. Am J Physiol, 1987. **253**(3 Pt 1): p. G298-302.
140. Hernandez, E.J., et al., *Saturable binding of circulating peptide YY in the dorsal vagal complex of rats*. Am J Physiol, 1994. **266**(3 Pt 1): p. G511-6.
141. Druce, M.R., C.J. Small, and S.R. Bloom, *Minireview: Gut peptides regulating satiety*. Endocrinology, 2004. **145**(6): p. 2660-5.
142. Viardot, A., et al., *Abnormal postprandial PYY response in insulin sensitive nondiabetic subjects with a strong family history of type 2 diabetes*. Int J Obes (Lond), 2008. **32**(6): p. 943-8.
143. le Roux, C.W., et al., *Attenuated peptide YY release in obese subjects is associated with reduced satiety*. Endocrinology, 2006. **147**(1): p. 3-8.

144. Batterham, R.L., et al., *Inhibition of food intake in obese subjects by peptide YY3-36*. N Engl J Med, 2003. **349**(10): p. 941-8.
145. Mojsov, S., et al., *Preproglucagon gene expression in pancreas and intestine diversifies at the level of post-translational processing*. J Biol Chem, 1986. **261**(25): p. 11880-9.
146. Orskov, C., et al., *Tissue and plasma concentrations of amidated and glycine-extended glucagon-like peptide I in humans*. Diabetes, 1994. **43**(4): p. 535-9.
147. Rask, E., et al., *Impaired incretin response after a mixed meal is associated with insulin resistance in nondiabetic men*. Diabetes Care, 2001. **24**(9): p. 1640-5.
148. Rocca, A.S. and P.L. Brubaker, *Role of the vagus nerve in mediating proximal nutrient-induced glucagon-like peptide-1 secretion*. Endocrinology, 1999. **140**(4): p. 1687-94.
149. Hellstrom, P.M., et al., *GLP-1 suppresses gastrointestinal motility and inhibits the migrating motor complex in healthy subjects and patients with irritable bowel syndrome*. Neurogastroenterol Motil, 2008. **20**(6): p. 649-59.
150. Schirra, J., et al., *Endogenous glucagon-like peptide 1 controls endocrine pancreatic secretion and antro-pyloro-duodenal motility in humans*. Gut, 2006. **55**(2): p. 243-51.
151. Williams, D.L., D.G. Baskin, and M.W. Schwartz, *Leptin regulation of the anorexic response to glucagon-like peptide-1 receptor stimulation*. Diabetes, 2006. **55**(12): p. 3387-93.
152. Abbott, C.R., et al., *The inhibitory effects of peripheral administration of peptide YY(3-36) and glucagon-like peptide-1 on food intake are attenuated by ablation*

- of the vagal-brainstem-hypothalamic pathway*. Brain Res, 2005. **1044**(1): p. 127-31.
153. Williams, D.L., *Minireview: finding the sweet spot: peripheral versus central glucagon-like peptide 1 action in feeding and glucose homeostasis*. Endocrinology, 2009. **150**(7): p. 2997-3001.
154. Anandhkrishnan, A. and M. Korbonits, *Glucagon-like peptide 1 in the pathophysiology and pharmacotherapy of clinical obesity*. World J Diabetes, 2016. **7**(20): p. 572-598.
155. Gibbs, J., R.C. Young, and G.P. Smith, *Cholecystokinin decreases food intake in rats*. J Comp Physiol Psychol, 1973. **84**(3): p. 488-95.
156. Liddle, R.A., et al., *Cholecystokinin bioactivity in human plasma. Molecular forms, responses to feeding, and relationship to gallbladder contraction*. J Clin Invest, 1985. **75**(4): p. 1144-52.
157. Cantor, P., et al., *The effect of vagal stimulation on the release of cholecystokinin in anaesthetized pigs*. Scand J Gastroenterol, 1986. **21**(9): p. 1069-72.
158. Moran, T.H., et al., *Vagal afferent and efferent contributions to the inhibition of food intake by cholecystokinin*. Am J Physiol, 1997. **272**(4 Pt 2): p. R1245-51.
159. West, D.B., D. Fey, and S.C. Woods, *Cholecystokinin persistently suppresses meal size but not food intake in free-feeding rats*. Am J Physiol, 1984. **246**(5 Pt 2): p. R776-87.
160. Crawley, J.N. and M.C. Beinfeld, *Rapid development of tolerance to the behavioural actions of cholecystokinin*. Nature, 1983. **302**(5910): p. 703-6.
161. Mollet, A., et al., *Endogenous amylin contributes to the anorectic effects of cholecystokinin and bombesin*. Peptides, 2003. **24**(1): p. 91-8.

162. Ahima, R.S. and J.S. Flier, *Leptin*. *Annu Rev Physiol*, 2000. **62**: p. 413-37.
163. Kaplan, L.M., *Leptin, obesity, and liver disease*. *Gastroenterology*, 1998. **115**(4): p. 997-1001.
164. Ducroc, R., et al., *Luminal leptin induces rapid inhibition of active intestinal absorption of glucose mediated by sodium-glucose cotransporter 1*. *Diabetes*, 2005. **54**(2): p. 348-54.
165. Yarandi, S.S., et al., *Diverse roles of leptin in the gastrointestinal tract: modulation of motility, absorption, growth, and inflammation*. *Nutrition*, 2011. **27**(3): p. 269-75.
166. Cammisotto, P. and M. Bendayan, *A review on gastric leptin: the exocrine secretion of a gastric hormone*. *Anat Cell Biol*, 2012. **45**(1): p. 1-16.
167. Kentish, S., et al., *Diet-induced adaptation of vagal afferent function*. *J Physiol*, 2012. **590**(1): p. 209-21.
168. Iraklianiou, S., et al., *Postprandial leptin responses after an oral fat tolerance test: differences in type 2 diabetes*. *Diabetes Care*, 2001. **24**(7): p. 1299-301.
169. Suzuki, K., et al., *The role of gut hormones and the hypothalamus in appetite regulation*. *Endocr J*, 2010. **57**(5): p. 359-72.
170. Kojima, M., et al., *Ghrelin is a growth-hormone-releasing acylated peptide from stomach*. *Nature*, 1999. **402**(6762): p. 656-60.
171. Muller, T.D., et al., *Ghrelin*. *Mol Metab*, 2015. **4**(6): p. 437-60.
172. Alvarez-Castro, P., L. Pena, and F. Cordido, *Ghrelin in obesity, physiological and pharmacological considerations*. *Mini Rev Med Chem*, 2013. **13**(4): p. 541-52.
173. Yakabi, K., J. Kawashima, and S. Kato, *Ghrelin and gastric acid secretion*. *World J Gastroenterol*, 2008. **14**(41): p. 6334-8.

174. Cummings, D.E., et al., *A preprandial rise in plasma ghrelin levels suggests a role in meal initiation in humans*. Diabetes, 2001. **50**(8): p. 1714-9.
175. Date, Y., et al., *The role of the gastric afferent vagal nerve in ghrelin-induced feeding and growth hormone secretion in rats*. Gastroenterology, 2002. **123**(4): p. 1120-8.
176. Naznin, F., et al., *Diet-induced obesity causes peripheral and central ghrelin resistance by promoting inflammation*. J Endocrinol, 2015. **226**(1): p. 81-92.
177. Paulino, G., et al., *Increased expression of receptors for orexigenic factors in nodose ganglion of diet-induced obese rats*. Am J Physiol Endocrinol Metab, 2009. **296**(4): p. E898-903.
178. Korek, E., et al., *Fasting and postprandial levels of ghrelin, leptin and insulin in lean, obese and anorexic subjects*. Prz Gastroenterol, 2013. **8**(6): p. 383-9.
179. Cui, H., M. Lopez, and K. Rahmouni, *The cellular and molecular bases of leptin and ghrelin resistance in obesity*. Nat Rev Endocrinol, 2017. **13**(6): p. 338-351.
180. Briggs, D.I., et al., *Calorie-restricted weight loss reverses high-fat diet-induced ghrelin resistance, which contributes to rebound weight gain in a ghrelin-dependent manner*. Endocrinology, 2013. **154**(2): p. 709-17.
181. Banks, W.A., B.O. Burney, and S.M. Robinson, *Effects of triglycerides, obesity, and starvation on ghrelin transport across the blood-brain barrier*. Peptides, 2008. **29**(11): p. 2061-5.
182. Allen, J.M., et al., *Effects of peptide YY and neuropeptide Y on gastric emptying in man*. Digestion, 1984. **30**(4): p. 255-62.

183. Wettergren, A., et al., *The inhibitory effect of glucagon-like peptide-1 (GLP-1) 7-36 amide on gastric acid secretion in humans depends on an intact vagal innervation*. Gut, 1997. **40**(5): p. 597-601.
184. Liddle, R.A., et al., *Regulation of gastric emptying in humans by cholecystokinin*. J Clin Invest, 1986. **77**(3): p. 992-6.
185. Schwizer, W., et al., *Role of cholecystokinin in the regulation of liquid gastric emptying and gastric motility in humans: studies with the CCK antagonist loxiglumide*. Gut, 1997. **41**(4): p. 500-4.
186. Lieveise, R.J., et al., *Role of cholecystokinin in the regulation of satiation and satiety in humans*. Ann N Y Acad Sci, 1994. **713**: p. 268-72.
187. Karmiris, K., I.E. Koutroubakis, and E.A. Kouroumalis, *Leptin, adiponectin, resistin, and ghrelin--implications for inflammatory bowel disease*. Mol Nutr Food Res, 2008. **52**(8): p. 855-66.
188. FitzGerald, A.J., N. Mandir, and R.A. Goodlad, *Leptin, cell proliferation and crypt fission in the gastrointestinal tract of intravenously fed rats*. Cell Prolif, 2005. **38**(1): p. 25-33.
189. Swartz, E.M., et al., *Ghrelin increases vagally mediated gastric activity by central sites of action*. Neurogastroenterol Motil, 2014. **26**(2): p. 272-82.
190. Druce, M.R., et al., *Ghrelin increases food intake in obese as well as lean subjects*. Int J Obes (Lond), 2005. **29**(9): p. 1130-6.
191. Berthoud, H.R. and W.L. Neuhuber, *Functional and chemical anatomy of the afferent vagal system*. Auton Neurosci, 2000. **85**(1-3): p. 1-17.
192. Ivanov, N.M., et al., *[Surgical anatomy of the vagus nerves in the vagotomy aspect]*. Vestn Khir Im I I Grek, 1988. **140**(5): p. 22-5.

193. Botar, J., et al., [*Nerve cells and ganglia of the vagal nerve*]. *Acta Anat (Basel)*, 1950. **10**(3): p. 284-314.
194. Rutecki, P., *Anatomical, physiological, and theoretical basis for the antiepileptic effect of vagus nerve stimulation*. *Epilepsia*, 1990. **31 Suppl 2**: p. S1-6.
195. Barratt, W., *On the Anatomical Structure of the Vagus Nerve*. *J Anat Physiol*, 1898. **32**(Pt 3): p. 422-7.
196. Grundy, D., *Vagal control of gastrointestinal function*. *Baillieres Clin Gastroenterol*, 1988. **2**(1): p. 23-43.
197. Kentish, S.J. and A.J. Page, *Plasticity of gastro-intestinal vagal afferent endings*. *Physiol Behav*, 2014. **136**: p. 170-8.
198. Berthoud, H.R., et al., *Distribution and structure of vagal afferent intraganglionic laminar endings (IGLEs) in the rat gastrointestinal tract*. *Anat Embryol (Berl)*, 1997. **195**(2): p. 183-91.
199. Neuhuber, W.L., *Sensory vagal innervation of the rat esophagus and cardia: a light and electron microscopic anterograde tracing study*. *J Auton Nerv Syst*, 1987. **20**(3): p. 243-55.
200. Hamill, O.P. and D.W. McBride, Jr., *The pharmacology of mechanogated membrane ion channels*. *Pharmacol Rev*, 1996. **48**(2): p. 231-52.
201. Grundy, D., *What activates visceral afferents?* *Gut*, 2004. **53 Suppl 2**: p. ii5-8.
202. Powley, T.L., et al., *Vagal Intramuscular Arrays: The Specialized Mechanoreceptor Arbors That Innervate the Smooth Muscle Layers of the Stomach Examined in the Rat*. *J Comp Neurol*, 2016. **524**(4): p. 713-37.

203. Powley, T.L. and R.J. Phillips, *Vagal intramuscular array afferents form complexes with interstitial cells of Cajal in gastrointestinal smooth muscle: analogues of muscle spindle organs?* Neuroscience, 2011. **186**: p. 188-200.
204. Berthoud, H.R., *The vagus nerve, food intake and obesity.* Regul Pept, 2008. **149**(1-3): p. 15-25.
205. Becker, J.M. and K.A. Kelly, *Antral control of canine gastric emptying of solids.* Am J Physiol, 1983. **245**(3): p. G334-8.
206. Yox, D.P. and R.C. Ritter, *Capsaicin attenuates suppression of sham feeding induced by intestinal nutrients.* Am J Physiol, 1988. **255**(4 Pt 2): p. R569-74.
207. Broberger, C., et al., *Cocaine- and amphetamine-regulated transcript in the rat vagus nerve: A putative mediator of cholecystinin-induced satiety.* Proc Natl Acad Sci U S A, 1999. **96**(23): p. 13506-11.
208. Nakagawa, A., et al., *Receptor gene expression of glucagon-like peptide-1, but not glucose-dependent insulinotropic polypeptide, in rat nodose ganglion cells.* Auton Neurosci, 2004. **110**(1): p. 36-43.
209. Bucinskaite, V., et al., *Receptor-mediated activation of gastric vagal afferents by glucagon-like peptide-1 in the rat.* Neurogastroenterol Motil, 2009. **21**(9): p. 978-e78.
210. Richards, W., et al., *Sensitivity of vagal mucosal afferents to cholecystinin and its role in afferent signal transduction in the rat.* J Physiol, 1996. **497** (Pt 2): p. 473-81.
211. Kanoski, S.E., et al., *Peripheral and central GLP-1 receptor populations mediate the anorectic effects of peripherally administered GLP-1 receptor agonists, liraglutide and exendin-4.* Endocrinology, 2011. **152**(8): p. 3103-12.

212. Smith, G.P., et al., *Abdominal vagotomy blocks the satiety effect of cholecystokinin in the rat*. *Science*, 1981. **213**(4511): p. 1036-7.
213. Bai, L., et al., *Genetic Identification of Vagal Sensory Neurons That Control Feeding*. *Cell*, 2019. **179**(5): p. 1129-1143 e23.
214. Page, A.J. and S.J. Kentish, *Plasticity of gastrointestinal vagal afferent satiety signals*. *Neurogastroenterol Motil*, 2017. **29**(5).
215. Page, A.J., C.M. Martin, and L.A. Blackshaw, *Vagal mechanoreceptors and chemoreceptors in mouse stomach and esophagus*. *J Neurophysiol*, 2002. **87**(4): p. 2095-103.
216. Owyang, C. and A. Heldsinger, *Vagal control of satiety and hormonal regulation of appetite*. *J Neurogastroenterol Motil*, 2011. **17**(4): p. 338-48.
217. Babic, T. and K.N. Browning, *The role of vagal neurocircuits in the regulation of nausea and vomiting*. *Eur J Pharmacol*, 2014. **722**: p. 38-47.
218. Murakami, N., et al., *Role for central ghrelin in food intake and secretion profile of stomach ghrelin in rats*. *J Endocrinol*, 2002. **174**(2): p. 283-8.
219. Egerod, K.L., T.W. Schwartz, and L. Gautron, *The Molecular Diversity of Vagal Afferents Revealed*. *Trends Neurosci*, 2019.
220. Page, A.J., et al., *Ghrelin selectively reduces mechanosensitivity of upper gastrointestinal vagal afferents*. *Am J Physiol Gastrointest Liver Physiol*, 2007. **292**(5): p. G1376-84.
221. le Roux, C.W., et al., *Ghrelin does not stimulate food intake in patients with surgical procedures involving vagotomy*. *J Clin Endocrinol Metab*, 2005. **90**(8): p. 4521-4.

222. Peiser, C., et al., *Leptin receptor expression in nodose ganglion cells projecting to the rat gastric fundus*. *Neurosci Lett*, 2002. **320**(1-2): p. 41-4.
223. Kentish, S.J., et al., *Gastric vagal afferent modulation by leptin is influenced by food intake status*. *J Physiol*, 2013. **591**(7): p. 1921-34.
224. Kentish, S.J., et al., *Circadian variation in gastric vagal afferent mechanosensitivity*. *J Neurosci*, 2013. **33**(49): p. 19238-42.
225. Kentish, S.J., et al., *High-Fat Diet-Induced Obesity Ablates Gastric Vagal Afferent Circadian Rhythms*. *J Neurosci*, 2016. **36**(11): p. 3199-207.
226. Kentish, S.J., et al., *Disruption of the light cycle ablates diurnal rhythms in gastric vagal afferent mechanosensitivity*. *Neurogastroenterol Motil*, 2019. **31**(12): p. e13711.
227. Tack, J., et al., *Symptoms associated with hypersensitivity to gastric distention in functional dyspepsia*. *Gastroenterology*, 2001. **121**(3): p. 526-35.
228. Talley, N.J. and A.C. Ford, *Functional Dyspepsia*. *N Engl J Med*, 2015. **373**(19): p. 1853-63.
229. Vanheel, H. and R. Farre, *Changes in gastrointestinal tract function and structure in functional dyspepsia*. *Nat Rev Gastroenterol Hepatol*, 2013. **10**(3): p. 142-9.
230. Li, H., et al., *Chronic stress induces hypersensitivity of murine gastric vagal afferents*. *Neurogastroenterol Motil*, 2019: p. e13669.
231. Falken, Y., et al., *Actions of prolonged ghrelin infusion on gastrointestinal transit and glucose homeostasis in humans*. *Neurogastroenterol Motil*, 2010. **22**(6): p. e192-200.
232. Paulino, G., et al., *Adaptation of lipid-induced satiation is not dependent on caloric density in rats*. *Physiol Behav*, 2008. **93**(4-5): p. 930-6.

233. Daly, D.M., et al., *Impaired intestinal afferent nerve satiety signalling and vagal afferent excitability in diet induced obesity in the mouse*. *J Physiol*, 2011. **589**(Pt 11): p. 2857-70.
234. Kentish, S.J., et al., *Altered gastric vagal mechanosensitivity in diet-induced obesity persists on return to normal chow and is accompanied by increased food intake*. *Int J Obes (Lond)*, 2014. **38**(5): p. 636-42.
235. Kentish, S.J., et al., *TRPV1 Channels and Gastric Vagal Afferent Signalling in Lean and High Fat Diet Induced Obese Mice*. *PLoS One*, 2015. **10**(8): p. e0135892.
236. Harrold, J.A. and G. Williams, *The cannabinoid system: a role in both the homeostatic and hedonic control of eating?* *Br J Nutr*, 2003. **90**(4): p. 729-34.
237. Howlett, A.C., *Pharmacology of cannabinoid receptors*. *Annu Rev Pharmacol Toxicol*, 1995. **35**: p. 607-34.
238. Pertwee, R.G., *Cannabinoid pharmacology: the first 66 years*. *Br J Pharmacol*, 2006. **147 Suppl 1**: p. S163-71.
239. Ibrahim, B.M. and A.A. Abdel-Rahman, *Cannabinoid receptor 1 signaling in cardiovascular regulating nuclei in the brainstem: A review*. *J Adv Res*, 2014. **5**(2): p. 137-45.
240. Romero, J., et al., *Cannabinoid receptor and WIN-55,212-2-stimulated [35S]GTP gamma S binding and cannabinoid receptor mRNA levels in the basal ganglia and the cerebellum of adult male rats chronically exposed to delta 9-tetrahydrocannabinol*. *J Mol Neurosci*, 1998. **11**(2): p. 109-19.

241. Zhao, X., et al., *Cannabinoid 1 receptor blockade in the dorsal hippocampus prevents the reinstatement but not acquisition of morphine-induced conditioned place preference in rats*. *Neuroreport*, 2017. **28**(10): p. 565-570.
242. Jelsing, J., P.J. Larsen, and N. Vrang, *Identification of cannabinoid type 1 receptor expressing cocaine amphetamine-regulated transcript neurons in the rat hypothalamus and brainstem using in situ hybridization and immunohistochemistry*. *Neuroscience*, 2008. **154**(2): p. 641-52.
243. Liu, Q.R., et al., *Species differences in cannabinoid receptor 2 (CNR2 gene): identification of novel human and rodent CB2 isoforms, differential tissue expression and regulation by cannabinoid receptor ligands*. *Genes Brain Behav*, 2009. **8**(5): p. 519-30.
244. Bridges, D., et al., *Localisation of cannabinoid receptor 1 in rat dorsal root ganglion using in situ hybridisation and immunohistochemistry*. *Neuroscience*, 2003. **119**(3): p. 803-12.
245. Burdyga, G., et al., *Expression of cannabinoid CB1 receptors by vagal afferent neurons: kinetics and role in influencing neurochemical phenotype*. *Am J Physiol Gastrointest Liver Physiol*, 2010. **299**(1): p. G63-9.
246. Simkins, T.J., et al., *Reduced Noradrenergic Signaling in the Spleen Capsule in the Absence of CB1 and CB2 Cannabinoid Receptors*. *J Neuroimmune Pharmacol*, 2016. **11**(4): p. 669-679.
247. Galiegue, S., et al., *Expression of central and peripheral cannabinoid receptors in human immune tissues and leukocyte subpopulations*. *Eur J Biochem*, 1995. **232**(1): p. 54-61.

248. Galiazzo, G., et al., *Localization of cannabinoid receptors CB1, CB2, GPR55, and PPARalpha in the canine gastrointestinal tract*. *Histochem Cell Biol*, 2018. **150**(2): p. 187-205.
249. Senin, L.L., et al., *The gastric CB1 receptor modulates ghrelin production through the mTOR pathway to regulate food intake*. *PLoS One*, 2013. **8**(11): p. e80339.
250. Adami, M., et al., *Gastric antisecretory role and immunohistochemical localization of cannabinoid receptors in the rat stomach*. *Br J Pharmacol*, 2002. **135**(7): p. 1598-606.
251. Wright, K.L., M. Duncan, and K.A. Sharkey, *Cannabinoid CB2 receptors in the gastrointestinal tract: a regulatory system in states of inflammation*. *Br J Pharmacol*, 2008. **153**(2): p. 263-70.
252. Zou, S. and U. Kumar, *Cannabinoid Receptors and the Endocannabinoid System: Signaling and Function in the Central Nervous System*. *Int J Mol Sci*, 2018. **19**(3).
253. Feng, Z., et al., *Modeling, molecular dynamics simulation, and mutation validation for structure of cannabinoid receptor 2 based on known crystal structures of GPCRs*. *J Chem Inf Model*, 2014. **54**(9): p. 2483-99.
254. Hua, T., et al., *Crystal Structure of the Human Cannabinoid Receptor CB1*. *Cell*, 2016. **167**(3): p. 750-762 e14.
255. Li, X., et al., *Crystal Structure of the Human Cannabinoid Receptor CB2*. *Cell*, 2019. **176**(3): p. 459-467 e13.
256. Shao, Z., et al., *High-resolution crystal structure of the human CB1 cannabinoid receptor*. *Nature*, 2016. **540**(7634): p. 602-606.

257. Andersson, H., et al., *Membrane assembly of the cannabinoid receptor 1: impact of a long N-terminal tail*. Mol Pharmacol, 2003. **64**(3): p. 570-7.
258. Fay, J.F. and D.L. Farrens, *A key agonist-induced conformational change in the cannabinoid receptor CB1 is blocked by the allosteric ligand Org 27569*. J Biol Chem, 2012. **287**(40): p. 33873-82.
259. Murphy, J.W. and D.A. Kendall, *Integrity of extracellular loop 1 of the human cannabinoid receptor 1 is critical for high-affinity binding of the ligand CP 55,940 but not SR 141716A*. Biochem Pharmacol, 2003. **65**(10): p. 1623-31.
260. Fay, J.F. and D.L. Farrens, *The membrane proximal region of the cannabinoid receptor CB1 N-terminus can allosterically modulate ligand affinity*. Biochemistry, 2013. **52**(46): p. 8286-94.
261. Stadel, R., K.H. Ahn, and D.A. Kendall, *The cannabinoid type-1 receptor carboxyl-terminus, more than just a tail*. J Neurochem, 2011. **117**(1): p. 1-18.
262. Jin, W., et al., *Distinct domains of the CB1 cannabinoid receptor mediate desensitization and internalization*. J Neurosci, 1999. **19**(10): p. 3773-80.
263. Vasquez, C. and D.L. Lewis, *The CB1 cannabinoid receptor can sequester G-proteins, making them unavailable to couple to other receptors*. J Neurosci, 1999. **19**(21): p. 9271-80.
264. Gurevich, V.V. and E.V. Gurevich, *The structural basis of arrestin-mediated regulation of G-protein-coupled receptors*. Pharmacol Ther, 2006. **110**(3): p. 465-502.
265. Howlett, A.C., et al., *International Union of Pharmacology. XXVII. Classification of cannabinoid receptors*. Pharmacol Rev, 2002. **54**(2): p. 161-202.

266. Brailoiu, G.C., et al., *Intracellular cannabinoid type 1 (CB1) receptors are activated by anandamide*. J Biol Chem, 2011. **286**(33): p. 29166-74.
267. Benard, G., et al., *Mitochondrial CB(1) receptors regulate neuronal energy metabolism*. Nat Neurosci, 2012. **15**(4): p. 558-64.
268. Martin, B.R., *Cellular effects of cannabinoids*. Pharmacol Rev, 1986. **38**(1): p. 45-74.
269. den Boon, F.S., et al., *Excitability of prefrontal cortical pyramidal neurons is modulated by activation of intracellular type-2 cannabinoid receptors*. Proc Natl Acad Sci U S A, 2012. **109**(9): p. 3534-9.
270. Felder, C.C., et al., *Comparison of the pharmacology and signal transduction of the human cannabinoid CB1 and CB2 receptors*. Mol Pharmacol, 1995. **48**(3): p. 443-50.
271. Rubovitch, V., M. Gafni, and Y. Sarne, *The involvement of VEGF receptors and MAPK in the cannabinoid potentiation of Ca²⁺ flux into N18TG2 neuroblastoma cells*. Brain Res Mol Brain Res, 2004. **120**(2): p. 138-44.
272. Soethoudt, M., et al., *Cannabinoid CB2 receptor ligand profiling reveals biased signalling and off-target activity*. Nat Commun, 2017. **8**: p. 13958.
273. Daigle, T.L., C.S. Kearns, and K. Mackie, *Rapid CB1 cannabinoid receptor desensitization defines the time course of ERK1/2 MAP kinase signaling*. Neuropharmacology, 2008. **54**(1): p. 36-44.
274. Bash, R., et al., *The stimulatory effect of cannabinoids on calcium uptake is mediated by Gs GTP-binding proteins and cAMP formation*. Neurosignals, 2003. **12**(1): p. 39-44.

275. Laprairie, R.B., et al., *Type 1 cannabinoid receptor ligands display functional selectivity in a cell culture model of striatal medium spiny projection neurons*. J Biol Chem, 2014. **289**(36): p. 24845-62.
276. Glass, M. and C.C. Felder, *Concurrent stimulation of cannabinoid CB1 and dopamine D2 receptors augments cAMP accumulation in striatal neurons: evidence for a Gs linkage to the CB1 receptor*. J Neurosci, 1997. **17**(14): p. 5327-33.
277. Gonzalez, B., et al., *Cannabinoid agonists stimulate [3H]GABA release in the globus pallidus of the rat when G(i) protein-receptor coupling is restricted: role of dopamine D2 receptors*. J Pharmacol Exp Ther, 2009. **328**(3): p. 822-8.
278. Kamato, D., et al., *Gaq proteins: molecular pharmacology and therapeutic potential*. Cell Mol Life Sci, 2017. **74**(8): p. 1379-1390.
279. Khan, S.M., J.Y. Sung, and T.E. Hebert, *Gbetagamma subunits-Different spaces, different faces*. Pharmacol Res, 2016. **111**: p. 434-441.
280. Neves, S.R., P.T. Ram, and R. Iyengar, *G protein pathways*. Science, 2002. **296**(5573): p. 1636-9.
281. Lauckner, J.E., B. Hille, and K. Mackie, *The cannabinoid agonist WIN55,212-2 increases intracellular calcium via CB1 receptor coupling to Gq/11 G proteins*. Proc Natl Acad Sci U S A, 2005. **102**(52): p. 19144-9.
282. Moore, C.A., S.K. Milano, and J.L. Benovic, *Regulation of receptor trafficking by GRKs and arrestins*. Annu Rev Physiol, 2007. **69**: p. 451-82.
283. Connor, M., P.B. Osborne, and M.J. Christie, *Mu-opioid receptor desensitization: is morphine different?* Br J Pharmacol, 2004. **143**(6): p. 685-96.

284. Howlett, A.C., et al., *The cannabinoid receptor: biochemical and cellular properties in neuroblastoma cells*. Pharmacol Biochem Behav, 1991. **40**(3): p. 565-9.
285. Rinaldi-Carmona, M., et al., *Modulation of CB1 cannabinoid receptor functions after a long-term exposure to agonist or inverse agonist in the Chinese hamster ovary cell expression system*. J Pharmacol Exp Ther, 1998. **287**(3): p. 1038-47.
286. Blair, R.E., et al., *Prolonged exposure to WIN55,212-2 causes downregulation of the CB1 receptor and the development of tolerance to its anticonvulsant effects in the hippocampal neuronal culture model of acquired epilepsy*. Neuropharmacology, 2009. **57**(3): p. 208-18.
287. McGuinness, D., et al., *Characterizing cannabinoid CB2 receptor ligands using DiscoverX PathHunter beta-arrestin assay*. J Biomol Screen, 2009. **14**(1): p. 49-58.
288. Hsieh, C., et al., *Internalization and recycling of the CB1 cannabinoid receptor*. J Neurochem, 1999. **73**(2): p. 493-501.
289. Leterrier, C., et al., *Constitutive endocytic cycle of the CB1 cannabinoid receptor*. J Biol Chem, 2004. **279**(34): p. 36013-21.
290. Keren, O. and Y. Sarne, *Multiple mechanisms of CB1 cannabinoid receptors regulation*. Brain Res, 2003. **980**(2): p. 197-205.
291. Raehal, K.M., et al., *Functional selectivity at the mu-opioid receptor: implications for understanding opioid analgesia and tolerance*. Pharmacol Rev, 2011. **63**(4): p. 1001-19.

292. Daigle, T.L., M.L. Kwok, and K. Mackie, *Regulation of CB1 cannabinoid receptor internalization by a promiscuous phosphorylation-dependent mechanism*. J Neurochem, 2008. **106**(1): p. 70-82.
293. Grimsey, N.L., et al., *Cannabinoid Receptor 1 trafficking and the role of the intracellular pool: implications for therapeutics*. Biochem Pharmacol, 2010. **80**(7): p. 1050-62.
294. Martini, L., et al., *Ligand-induced down-regulation of the cannabinoid 1 receptor is mediated by the G-protein-coupled receptor-associated sorting protein GASP1*. FASEB J, 2007. **21**(3): p. 802-11.
295. Carrier, E.J., et al., *Cultured rat microglial cells synthesize the endocannabinoid 2-arachidonylglycerol, which increases proliferation via a CB2 receptor-dependent mechanism*. Mol Pharmacol, 2004. **65**(4): p. 999-1007.
296. Bouaboula, M., et al., *Signaling pathway associated with stimulation of CB2 peripheral cannabinoid receptor. Involvement of both mitogen-activated protein kinase and induction of Krox-24 expression*. Eur J Biochem, 1996. **237**(3): p. 704-11.
297. Devane, W.A., et al., *Isolation and structure of a brain constituent that binds to the cannabinoid receptor*. Science, 1992. **258**(5090): p. 1946-9.
298. Piomelli, D., *THC: moderation during implantation*. Nat Med, 2004. **10**(1): p. 19-20.
299. Braida, D. and M. Sala, *Cannabinoid-induced working memory impairment is reversed by a second generation cholinesterase inhibitor in rats*. Neuroreport, 2000. **11**(9): p. 2025-9.

300. Mahler, S.V., K.S. Smith, and K.C. Berridge, *Endocannabinoid hedonic hotspot for sensory pleasure: anandamide in nucleus accumbens shell enhances 'liking' of a sweet reward*. *Neuropsychopharmacology*, 2007. **32**(11): p. 2267-78.
301. Cristino, L., T. Becker, and V. Di Marzo, *Endocannabinoids and energy homeostasis: an update*. *Biofactors*, 2014. **40**(4): p. 389-97.
302. Ueda, N., K. Tsuboi, and T. Uyama, *Enzymological studies on the biosynthesis of N-acylethanolamines*. *Biochim Biophys Acta*, 2010. **1801**(12): p. 1274-85.
303. Hansen, H.S., et al., *N-Acylethanolamines and precursor phospholipids - relation to cell injury*. *Chem Phys Lipids*, 2000. **108**(1-2): p. 135-50.
304. Jin, X.H., et al., *Discovery and characterization of a Ca²⁺-independent phosphatidylethanolamine N-acyltransferase generating the anandamide precursor and its congeners*. *J Biol Chem*, 2007. **282**(6): p. 3614-23.
305. Cadas, H., E. di Tomaso, and D. Piomelli, *Occurrence and biosynthesis of endogenous cannabinoid precursor, N-arachidonoyl phosphatidylethanolamine, in rat brain*. *J Neurosci*, 1997. **17**(4): p. 1226-42.
306. Ueda, N., K. Tsuboi, and T. Uyama, *Metabolism of endocannabinoids and related N-acylethanolamines: canonical and alternative pathways*. *FEBS J*, 2013. **280**(9): p. 1874-94.
307. Okamoto, Y., et al., *Biosynthetic pathways of the endocannabinoid anandamide*. *Chem Biodivers*, 2007. **4**(8): p. 1842-57.
308. Liu, J., et al., *A biosynthetic pathway for anandamide*. *Proc Natl Acad Sci U S A*, 2006. **103**(36): p. 13345-50.
309. Deutsch, D.G., N. Ueda, and S. Yamamoto, *The fatty acid amide hydrolase (FAAH)*. *Prostaglandins Leukot Essent Fatty Acids*, 2002. **66**(2-3): p. 201-10.

310. McKinney, M.K. and B.F. Cravatt, *Structure and function of fatty acid amide hydrolase*. *Annu Rev Biochem*, 2005. **74**: p. 411-32.
311. Ueda, N., et al., *An acid amidase hydrolyzing anandamide as an endogenous ligand for cannabinoid receptors*. *FEBS Lett*, 1999. **454**(3): p. 267-70.
312. Ueda, N., K. Yamanaka, and S. Yamamoto, *Purification and characterization of an acid amidase selective for N-palmitoylethanolamine, a putative endogenous anti-inflammatory substance*. *J Biol Chem*, 2001. **276**(38): p. 35552-7.
313. Ueda, N., et al., *Lipoxygenase-catalyzed oxygenation of arachidonylethanolamide, a cannabinoid receptor agonist*. *Biochim Biophys Acta*, 1995. **1254**(2): p. 127-34.
314. Yu, M., D. Ives, and C.S. Ramesha, *Synthesis of prostaglandin E2 ethanolamide from anandamide by cyclooxygenase-2*. *J Biol Chem*, 1997. **272**(34): p. 21181-6.
315. Vaughn, L.K., et al., *Endocannabinoid signalling: has it got rhythm?* *Br J Pharmacol*, 2010. **160**(3): p. 530-43.
316. Prescott, S.M. and P.W. Majerus, *Characterization of 1,2-diacylglycerol hydrolysis in human platelets. Demonstration of an arachidonoyl-monoacylglycerol intermediate*. *J Biol Chem*, 1983. **258**(2): p. 764-9.
317. Fukami, K., et al., *Phospholipase C is a key enzyme regulating intracellular calcium and modulating the phosphoinositide balance*. *Prog Lipid Res*, 2010. **49**(4): p. 429-37.
318. Suhara, Y., et al., *Synthesis and biological evaluation of several structural analogs of 2-arachidonoylglycerol, an endogenous cannabinoid receptor ligand*. *Bioorg Med Chem*, 2007. **15**(2): p. 854-67.

319. Fowler, C.J., P. Doherty, and S.P.H. Alexander, *Endocannabinoid Turnover*. Adv Pharmacol, 2017. **80**: p. 31-66.
320. Blankman, J.L., G.M. Simon, and B.F. Cravatt, *A comprehensive profile of brain enzymes that hydrolyze the endocannabinoid 2-arachidonoylglycerol*. Chem Biol, 2007. **14**(12): p. 1347-56.
321. Bari, M., et al., *Lipid rafts control signaling of type-1 cannabinoid receptors in neuronal cells. Implications for anandamide-induced apoptosis*. J Biol Chem, 2005. **280**(13): p. 12212-20.
322. Di Pasquale, E., et al., *The insertion and transport of anandamide in synthetic lipid membranes are both cholesterol-dependent*. PLoS One, 2009. **4**(3): p. e4989.
323. Kaczocha, M., et al., *Anandamide uptake is consistent with rate-limited diffusion and is regulated by the degree of its hydrolysis by fatty acid amide hydrolase*. J Biol Chem, 2006. **281**(14): p. 9066-75.
324. Kaczocha, M., S.T. Glaser, and D.G. Deutsch, *Identification of intracellular carriers for the endocannabinoid anandamide*. Proc Natl Acad Sci U S A, 2009. **106**(15): p. 6375-80.
325. Oddi, S., et al., *Molecular identification of albumin and Hsp70 as cytosolic anandamide-binding proteins*. Chem Biol, 2009. **16**(6): p. 624-32.
326. Chicca, A., et al., *Evidence for bidirectional endocannabinoid transport across cell membranes*. J Biol Chem, 2012. **287**(41): p. 34660-82.
327. Guzman, M., et al., *Oleylethanolamide stimulates lipolysis by activating the nuclear receptor peroxisome proliferator-activated receptor alpha (PPAR-alpha)*. J Biol Chem, 2004. **279**(27): p. 27849-54.

328. Hao, S., et al., *Low dose anandamide affects food intake, cognitive function, neurotransmitter and corticosterone levels in diet-restricted mice*. Eur J Pharmacol, 2000. **392**(3): p. 147-56.
329. Williams, C.M. and T.C. Kirkham, *Anandamide induces overeating: mediation by central cannabinoid (CB1) receptors*. Psychopharmacology (Berl), 1999. **143**(3): p. 315-7.
330. Williams, C.M., P.J. Rogers, and T.C. Kirkham, *Hyperphagia in pre-fed rats following oral delta9-THC*. Physiol Behav, 1998. **65**(2): p. 343-6.
331. Williams, C.M. and T.C. Kirkham, *Observational analysis of feeding induced by Delta9-THC and anandamide*. Physiol Behav, 2002. **76**(2): p. 241-50.
332. Simiand, J., et al., *SR 141716, a CB1 cannabinoid receptor antagonist, selectively reduces sweet food intake in marmoset*. Behav Pharmacol, 1998. **9**(2): p. 179-81.
333. Gomez, R., et al., *A peripheral mechanism for CB1 cannabinoid receptor-dependent modulation of feeding*. J Neurosci, 2002. **22**(21): p. 9612-7.
334. Jamshidi, N. and D.A. Taylor, *Anandamide administration into the ventromedial hypothalamus stimulates appetite in rats*. Br J Pharmacol, 2001. **134**(6): p. 1151-4.
335. Kirkham, T.C., et al., *Endocannabinoid levels in rat limbic forebrain and hypothalamus in relation to fasting, feeding and satiation: stimulation of eating by 2-arachidonoyl glycerol*. Br J Pharmacol, 2002. **136**(4): p. 550-7.
336. Tucci, S.A., et al., *The cannabinoid CB1 receptor antagonist SR141716 blocks the orexigenic effects of intrahypothalamic ghrelin*. Br J Pharmacol, 2004. **143**(5): p. 520-3.

337. Cota, D., et al., *The endogenous cannabinoid system affects energy balance via central orexigenic drive and peripheral lipogenesis*. J Clin Invest, 2003. **112**(3): p. 423-31.
338. Hillard, C.J., *Stress regulates endocannabinoid-CB1 receptor signaling*. Semin Immunol, 2014. **26**(5): p. 380-8.
339. Verty, A.N., et al., *Evidence for an interaction between CB1 cannabinoid and melanocortin MCR-4 receptors in regulating food intake*. Endocrinology, 2004. **145**(7): p. 3224-31.
340. Hilairt, S., et al., *Hypersensitization of the Orexin 1 receptor by the CB1 receptor: evidence for cross-talk blocked by the specific CB1 antagonist, SR141716*. J Biol Chem, 2003. **278**(26): p. 23731-7.
341. Verty, A.N., I.S. McGregor, and P.E. Mallet, *The dopamine receptor antagonist SCH 23390 attenuates feeding induced by Delta9-tetrahydrocannabinol*. Brain Res, 2004. **1020**(1-2): p. 188-95.
342. Di Marzo, V., et al., *Leptin-regulated endocannabinoids are involved in maintaining food intake*. Nature, 2001. **410**(6830): p. 822-5.
343. Balsevich, G., et al., *Role for fatty acid amide hydrolase (FAAH) in the leptin-mediated effects on feeding and energy balance*. Proc Natl Acad Sci U S A, 2018. **115**(29): p. 7605-7610.
344. Maccarrone, M., et al., *Leptin activates the anandamide hydrolase promoter in human T lymphocytes through STAT3*. J Biol Chem, 2003. **278**(15): p. 13318-24.
345. Capasso, R. and A.A. Izzo, *Gastrointestinal regulation of food intake: general aspects and focus on anandamide and oleoylethanolamide*. J Neuroendocrinol, 2008. **20 Suppl 1**: p. 39-46.

346. Alen, F., et al., *Ghrelin-induced orexigenic effect in rats depends on the metabolic status and is counteracted by peripheral CB1 receptor antagonism*. PLoS One, 2013. **8**(4): p. e60918.
347. Argueta, D.A., et al., *Cannabinoid CB1 Receptors Inhibit Gut-Brain Satiety Signaling in Diet-Induced Obesity*. Front Physiol, 2019. **10**: p. 704.
348. Zbucki, R.L., et al., *Cannabinoids enhance gastric X/A-like cells activity*. Folia Histochem Cytobiol, 2008. **46**(2): p. 219-24.
349. Orio, L., et al., *Additive effects of cannabinoid CB1 receptors blockade and cholecystinin on feeding inhibition*. Pharmacol Biochem Behav, 2011. **98**(2): p. 220-6.
350. Pertwee, R.G., *Cannabinoids and the gastrointestinal tract*. Gut, 2001. **48**(6): p. 859-67.
351. Di Marzo, V., et al., *The role of endocannabinoids in the regulation of gastric emptying: alterations in mice fed a high-fat diet*. Br J Pharmacol, 2008. **153**(6): p. 1272-80.
352. Borrelli, F., *Cannabinoid CB(1) receptor and gastric acid secretion*. Dig Dis Sci, 2007. **52**(11): p. 3102-3.
353. Capasso, R., et al., *Palmitoylethanolamide normalizes intestinal motility in a model of post-inflammatory accelerated transit: involvement of CB(1) receptors and TRPV1 channels*. Br J Pharmacol, 2014. **171**(17): p. 4026-37.
354. Hasenoehrl, C., et al., *The gastrointestinal tract - a central organ of cannabinoid signaling in health and disease*. Neurogastroenterol Motil, 2016. **28**(12): p. 1765-1780.

355. Cong, W.N., et al., *Ghrelin receptor signaling: a promising therapeutic target for metabolic syndrome and cognitive dysfunction*. *CNS Neurol Disord Drug Targets*, 2010. **9**(5): p. 557-63.
356. Yin, Y., Y. Li, and W. Zhang, *The growth hormone secretagogue receptor: its intracellular signaling and regulation*. *Int J Mol Sci*, 2014. **15**(3): p. 4837-55.
357. Lv, Y., et al., *Ghrelin, a gastrointestinal hormone, regulates energy balance and lipid metabolism*. *Biosci Rep*, 2018. **38**(5).
358. Yang, C.G., et al., *Gastric motility in ghrelin receptor knockout mice*. *Mol Med Rep*, 2013. **7**(1): p. 83-8.
359. Huang, H.J., et al., *The protective effects of Ghrelin/GHSR on hippocampal neurogenesis in CUMS mice*. *Neuropharmacology*, 2019. **155**: p. 31-43.
360. Petersenn, S., et al., *Genomic structure and transcriptional regulation of the human growth hormone secretagogue receptor*. *Endocrinology*, 2001. **142**(6): p. 2649-59.
361. Bennett, P.A., et al., *Hypothalamic growth hormone secretagogue-receptor (GHS-R) expression is regulated by growth hormone in the rat*. *Endocrinology*, 1997. **138**(11): p. 4552-7.
362. Pedretti, A., et al., *Construction of human ghrelin receptor (hGHS-R1a) model using a fragmental prediction approach and validation through docking analysis*. *J Med Chem*, 2006. **49**(11): p. 3077-85.
363. Holst, B., et al., *Ghrelin receptor inverse agonists: identification of an active peptide core and its interaction epitopes on the receptor*. *Mol Pharmacol*, 2006. **70**(3): p. 936-46.

364. Bouzo-Lorenzo, M., et al., *Distinct phosphorylation sites on the ghrelin receptor, GHSR1a, establish a code that determines the functions of ss-arrestins*. *Sci Rep*, 2016. **6**: p. 22495.
365. Kohno, D., et al., *Ghrelin directly interacts with neuropeptide-Y-containing neurons in the rat arcuate nucleus: Ca²⁺ signaling via protein kinase A and N-type channel-dependent mechanisms and cross-talk with leptin and orexin*. *Diabetes*, 2003. **52**(4): p. 948-56.
366. Rossi, F., et al., *Ghrelin inhibits contraction and proliferation of human aortic smooth muscle cells by cAMP/PKA pathway activation*. *Atherosclerosis*, 2009. **203**(1): p. 97-104.
367. Inoue, H., et al., *Identification and functional analysis of novel human growth hormone secretagogue receptor (GHSR) gene mutations in Japanese subjects with short stature*. *J Clin Endocrinol Metab*, 2011. **96**(2): p. E373-8.
368. Cavalier, M., et al., *Involvement of PKA and ERK pathways in ghrelin-induced long-lasting potentiation of excitatory synaptic transmission in the CA1 area of rat hippocampus*. *Eur J Neurosci*, 2015. **42**(8): p. 2568-76.
369. Kurashina, T., et al., *The beta-cell GHSR and downstream cAMP/TRPM2 signaling account for insulinostatic and glycemic effects of ghrelin*. *Sci Rep*, 2015. **5**: p. 14041.
370. Camina, J.P., et al., *Desensitization and endocytosis mechanisms of ghrelin-activated growth hormone secretagogue receptor 1a*. *Endocrinology*, 2004. **145**(2): p. 930-40.

371. Holliday, N.D., et al., *Importance of constitutive activity and arrestin-independent mechanisms for intracellular trafficking of the ghrelin receptor*. *Mol Endocrinol*, 2007. **21**(12): p. 3100-12.
372. Delhanty, P.J., et al., *Unsaturated fatty acids prevent desensitization of the human growth hormone secretagogue receptor by blocking its internalization*. *Am J Physiol Endocrinol Metab*, 2010. **299**(3): p. E497-505.
373. Chow, K.B., et al., *The truncated ghrelin receptor polypeptide (GHS-R1b) is localized in the endoplasmic reticulum where it forms heterodimers with ghrelin receptors (GHS-R1a) to attenuate their cell surface expression*. *Mol Cell Endocrinol*, 2012. **348**(1): p. 247-54.
374. Rediger, A., et al., *Mutually opposite signal modulation by hypothalamic heterodimerization of ghrelin and melanocortin-3 receptors*. *J Biol Chem*, 2011. **286**(45): p. 39623-31.
375. Jiang, H., L. Betancourt, and R.G. Smith, *Ghrelin amplifies dopamine signaling by cross talk involving formation of growth hormone secretagogue receptor/dopamine receptor subtype 1 heterodimers*. *Mol Endocrinol*, 2006. **20**(8): p. 1772-85.
376. Kern, A., et al., *Apo-ghrelin receptor forms heteromers with DRD2 in hypothalamic neurons and is essential for anorexigenic effects of DRD2 agonism*. *Neuron*, 2012. **73**(2): p. 317-32.
377. Kola, B., et al., *The orexigenic effect of ghrelin is mediated through central activation of the endogenous cannabinoid system*. *PLoS One*, 2008. **3**(3): p. e1797.

378. Kola, B., et al., *Cannabinoids and ghrelin have both central and peripheral metabolic and cardiac effects via AMP-activated protein kinase*. J Biol Chem, 2005. **280**(26): p. 25196-201.
379. Tracey, W.D., Jr., et al., *painless, a Drosophila gene essential for nociception*. Cell, 2003. **113**(2): p. 261-73.
380. Cosens, D.J. and A. Manning, *Abnormal electroretinogram from a Drosophila mutant*. Nature, 1969. **224**(5216): p. 285-7.
381. Montell, C. and G.M. Rubin, *Molecular characterization of the Drosophila trp locus: a putative integral membrane protein required for phototransduction*. Neuron, 1989. **2**(4): p. 1313-23.
382. Asgar, J., et al., *The role of TRPA1 in muscle pain and mechanical hypersensitivity under inflammatory conditions in rats*. Neuroscience, 2015. **310**: p. 206-15.
383. Cao, E., et al., *TRPV1 channels are intrinsically heat sensitive and negatively regulated by phosphoinositide lipids*. Neuron, 2013. **77**(4): p. 667-79.
384. Edwards, J.G., *TRPV1 in the central nervous system: synaptic plasticity, function, and pharmacological implications*. Prog Drug Res, 2014. **68**: p. 77-104.
385. Eid, S.R. and D.N. Cortright, *Transient receptor potential channels on sensory nerves*. Handb Exp Pharmacol, 2009(194): p. 261-81.
386. Zhang, L.L., et al., *Activation of transient receptor potential vanilloid type-1 channel prevents adipogenesis and obesity*. Circ Res, 2007. **100**(7): p. 1063-70.
387. Bielefeldt, K. and B.M. Davis, *Differential effects of ASIC3 and TRPV1 deletion on gastroesophageal sensation in mice*. Am J Physiol Gastrointest Liver Physiol, 2008. **294**(1): p. G130-8.

388. Dvorakova, M. and W. Kummer, *Transient expression of vanilloid receptor subtype 1 in rat cardiomyocytes during development*. *Histochem Cell Biol*, 2001. **116**(3): p. 223-5.
389. Matthews, P.J., et al., *Increased capsaicin receptor TRPV1 nerve fibres in the inflamed human oesophagus*. *Eur J Gastroenterol Hepatol*, 2004. **16**(9): p. 897-902.
390. Yiangou, Y., et al., *Vanilloid receptor 1 immunoreactivity in inflamed human bowel*. *Lancet*, 2001. **357**(9265): p. 1338-9.
391. Szallasi, A., *Vanilloid (capsaicin) receptors in health and disease*. *Am J Clin Pathol*, 2002. **118**(1): p. 110-21.
392. Schumacher, M.A., et al., *Molecular cloning of an N-terminal splice variant of the capsaicin receptor. Loss of N-terminal domain suggests functional divergence among capsaicin receptor subtypes*. *J Biol Chem*, 2000. **275**(4): p. 2756-62.
393. Wang, C., et al., *An alternative splicing product of the murine trpv1 gene dominant negatively modulates the activity of TRPV1 channels*. *J Biol Chem*, 2004. **279**(36): p. 37423-30.
394. Sanchez, J.F., J.E. Krause, and D.N. Cortright, *The distribution and regulation of vanilloid receptor VR1 and VR1 5' splice variant RNA expression in rat*. *Neuroscience*, 2001. **107**(3): p. 373-81.
395. Cao, E., et al., *TRPV1 structures in distinct conformations reveal activation mechanisms*. *Nature*, 2013. **504**(7478): p. 113-8.
396. Liao, M., et al., *Structure of the TRPV1 ion channel determined by electron cryo-microscopy*. *Nature*, 2013. **504**(7478): p. 107-12.

397. Bhawe, G., et al., *Protein kinase C phosphorylation sensitizes but does not activate the capsaicin receptor transient receptor potential vanilloid 1 (TRPV1)*. Proc Natl Acad Sci U S A, 2003. **100**(21): p. 12480-5.
398. Lishko, P.V., et al., *The ankyrin repeats of TRPV1 bind multiple ligands and modulate channel sensitivity*. Neuron, 2007. **54**(6): p. 905-18.
399. Christie, S., et al., *Involvement of TRPV1 Channels in Energy Homeostasis*. Front Endocrinol (Lausanne), 2018. **9**: p. 420.
400. Caterina, M.J., et al., *The capsaicin receptor: a heat-activated ion channel in the pain pathway*. Nature, 1997. **389**(6653): p. 816-24.
401. Koizumi, K., et al., *Diallyl sulfides in garlic activate both TRPA1 and TRPV1*. Biochem Biophys Res Commun, 2009. **382**(3): p. 545-8.
402. Salazar, H., et al., *A single N-terminal cysteine in TRPV1 determines activation by pungent compounds from onion and garlic*. Nat Neurosci, 2008. **11**(3): p. 255-61.
403. Okumura, Y., et al., *Activation of TRPV1 and TRPA1 by black pepper components*. Biosci Biotechnol Biochem, 2010. **74**(5): p. 1068-72.
404. Cromer, B.A. and P. McIntyre, *Painful toxins acting at TRPV1*. Toxicon, 2008. **51**(2): p. 163-73.
405. Siemens, J., et al., *Spider toxins activate the capsaicin receptor to produce inflammatory pain*. Nature, 2006. **444**(7116): p. 208-12.
406. De Petrocellis, L., et al., *The vanilloid receptor (VR1)-mediated effects of anandamide are potently enhanced by the cAMP-dependent protein kinase*. J Neurochem, 2001. **77**(6): p. 1660-3.

407. Jordt, S.E. and D. Julius, *Molecular basis for species-specific sensitivity to "hot" chili peppers*. Cell, 2002. **108**(3): p. 421-30.
408. Smart, D., et al., *The endogenous lipid anandamide is a full agonist at the human vanilloid receptor (hVR1)*. Br J Pharmacol, 2000. **129**(2): p. 227-30.
409. van der Stelt, M., et al., *Anandamide acts as an intracellular messenger amplifying Ca²⁺ influx via TRPV1 channels*. EMBO J, 2005. **24**(17): p. 3026-37.
410. Vigna, S.R., et al., *Leukotriene B₄ mediates inflammation via TRPV1 in duct obstruction-induced pancreatitis in rats*. Pancreas, 2011. **40**(5): p. 708-14.
411. Van Der Stelt, M. and V. Di Marzo, *Endovanilloids. Putative endogenous ligands of transient receptor potential vanilloid 1 channels*. Eur J Biochem, 2004. **271**(10): p. 1827-34.
412. Premkumar, L.S. and G.P. Ahern, *Induction of vanilloid receptor channel activity by protein kinase C*. Nature, 2000. **408**(6815): p. 985-90.
413. Vellani, V., et al., *Protein kinase C activation potentiates gating of the vanilloid receptor VR1 by capsaicin, protons, heat and anandamide*. J Physiol, 2001. **534**(Pt 3): p. 813-25.
414. Chuang, H.H., et al., *Bradykinin and nerve growth factor release the capsaicin receptor from PtdIns(4,5)P₂-mediated inhibition*. Nature, 2001. **411**(6840): p. 957-62.
415. Lau, S.Y., E. Procko, and R. Gaudet, *Distinct properties of Ca²⁺-calmodulin binding to N- and C-terminal regulatory regions of the TRPV1 channel*. J Gen Physiol, 2012. **140**(5): p. 541-55.

416. Liu, B., C. Zhang, and F. Qin, *Functional recovery from desensitization of vanilloid receptor TRPV1 requires resynthesis of phosphatidylinositol 4,5-bisphosphate*. J Neurosci, 2005. **25**(19): p. 4835-43.
417. Chaudhury, S., et al., *AKAP150-mediated TRPV1 sensitization is disrupted by calcium/calmodulin*. Mol Pain, 2011. **7**: p. 34.
418. Docherty, R.J., et al., *Inhibition of calcineurin inhibits the desensitization of capsaicin-evoked currents in cultured dorsal root ganglion neurones from adult rats*. Pflugers Arch, 1996. **431**(6): p. 828-37.
419. Planells-Cases, R., et al., *Complex regulation of TRPV1 and related thermo-TRPs: implications for therapeutic intervention*. Adv Exp Med Biol, 2011. **704**: p. 491-515.
420. Sanz-Salvador, L., et al., *Agonist- and Ca²⁺-dependent desensitization of TRPV1 channel targets the receptor to lysosomes for degradation*. J Biol Chem, 2012. **287**(23): p. 19462-71.
421. Wang, E.E., et al., *Induction of TRPV1 desensitization by a biased receptor agonist*. Channels (Austin), 2011. **5**(6): p. 464-7.
422. Janssens, P.L., R. Hursel, and M.S. Westerterp-Plantenga, *Capsaicin increases sensation of fullness in energy balance, and decreases desire to eat after dinner in negative energy balance*. Appetite, 2014. **77**: p. 44-9.
423. Ludy, M.J. and R.D. Mattes, *The effects of hedonically acceptable red pepper doses on thermogenesis and appetite*. Physiol Behav, 2011. **102**(3-4): p. 251-8.
424. Reinbach, H.C., T. Martinussen, and P. Moller, *Effects of hot spices on energy intake, appetite and sensory specific desires in humans*. Food Quality and Preference, 2010. **21**(6): p. 7.

425. Shin, K.O. and T. Moritani, *Alterations of autonomic nervous activity and energy metabolism by capsaicin ingestion during aerobic exercise in healthy men*. J Nutr Sci Vitaminol (Tokyo), 2007. **53**(2): p. 124-32.
426. Smeets, A.J., P.L. Janssens, and M.S. Westerterp-Plantenga, *Addition of capsaicin and exchange of carbohydrate with protein counteract energy intake restriction effects on fullness and energy expenditure*. J Nutr, 2013. **143**(4): p. 442-7.
427. Reinbach, H.C., et al., *Effects of capsaicin, green tea and CH-19 sweet pepper on appetite and energy intake in humans in negative and positive energy balance*. Clin Nutr, 2009. **28**(3): p. 260-5.
428. Baskaran, P., et al., *TRPV1 activation counters diet-induced obesity through sirtuin-1 activation and PRDM-16 deacetylation in brown adipose tissue*. Int J Obes (Lond), 2017. **41**(5): p. 739-749.
429. Baskaran, P., et al., *Capsaicin induces browning of white adipose tissue and counters obesity by activating TRPV1 channel-dependent mechanisms*. Br J Pharmacol, 2016. **173**(15): p. 2369-89.
430. Kang, J.H., et al., *Dietary capsaicin reduces obesity-induced insulin resistance and hepatic steatosis in obese mice fed a high-fat diet*. Obesity (Silver Spring), 2010. **18**(4): p. 780-7.
431. Lim, K., et al., *Dietary red pepper ingestion increases carbohydrate oxidation at rest and during exercise in runners*. Med Sci Sports Exerc, 1997. **29**(3): p. 355-61.
432. Ohnuki, K., et al., *Administration of capsiate, a non-pungent capsaicin analog, promotes energy metabolism and suppresses body fat accumulation in mice*. Biosci Biotechnol Biochem, 2001. **65**(12): p. 2735-40.

433. Shi, Z., et al., *Chilli consumption and the incidence of overweight and obesity in a Chinese adult population*. Int J Obes (Lond), 2017. **41**(7): p. 1074-1079.
434. Matsumoto, T., et al., *Effects of capsaicin-containing yellow curry sauce on sympathetic nervous system activity and diet-induced thermogenesis in lean and obese young women*. J Nutr Sci Vitaminol (Tokyo), 2000. **46**(6): p. 309-15.
435. Westerterp-Plantenga, M.S., A. Smeets, and M.P. Lejeune, *Sensory and gastrointestinal satiety effects of capsaicin on food intake*. Int J Obes (Lond), 2005. **29**(6): p. 682-8.
436. Yoshioka, M., et al., *Maximum tolerable dose of red pepper decreases fat intake independently of spicy sensation in the mouth*. Br J Nutr, 2004. **91**(6): p. 991-5.
437. Yoshioka, M., et al., *Effects of red pepper on appetite and energy intake*. Br J Nutr, 1999. **82**(2): p. 115-23.
438. Lee, E., et al., *Transient receptor potential vanilloid type-1 channel regulates diet-induced obesity, insulin resistance, and leptin resistance*. FASEB J, 2015. **29**(8): p. 3182-92.
439. Motter, A.L. and G.P. Ahern, *TRPV1-null mice are protected from diet-induced obesity*. FEBS Lett, 2008. **582**(15): p. 2257-62.
440. Smeets, A.J. and M.S. Westerterp-Plantenga, *The acute effects of a lunch containing capsaicin on energy and substrate utilisation, hormones, and satiety*. Eur J Nutr, 2009. **48**(4): p. 229-34.
441. Yokoyama, T., et al., *Ghrelin potentiates miniature excitatory postsynaptic currents in supraoptic magnocellular neurones*. J Neuroendocrinol, 2009. **21**(11): p. 910-20.

442. Janssens, P.L., et al., *Acute effects of capsaicin on energy expenditure and fat oxidation in negative energy balance*. PLoS One, 2013. **8**(7): p. e67786.
443. Reinbach, H.C., T. Martinussen, and P. Moller, *Effects of hot spices on energy intake, appetite and sensory specific desires in humans*. Food Quality and Preference, 2010. **21**: p. 655-661.
444. Yoshioka, M., et al., *Combined effects of red pepper and caffeine consumption on 24 h energy balance in subjects given free access to foods*. Br J Nutr, 2001. **85**(2): p. 203-11.
445. Lejeune, M.P., E.M. Kovacs, and M.S. Westerterp-Plantenga, *Effect of capsaicin on substrate oxidation and weight maintenance after modest body-weight loss in human subjects*. Br J Nutr, 2003. **90**(3): p. 651-59.
446. Storr, M.A. and K.A. Sharkey, *The endocannabinoid system and gut-brain signalling*. Curr Opin Pharmacol, 2007. **7**(6): p. 575-82.
447. Hermann, H., et al., *Dual effect of cannabinoid CB1 receptor stimulation on a vanilloid VR1 receptor-mediated response*. Cell Mol Life Sci, 2003. **60**(3): p. 607-16.
448. Ho, B.Y., et al., *Coupling of the expressed cannabinoid CB1 and CB2 receptors to phospholipase C and G protein-coupled inwardly rectifying K⁺ channels*. Receptors Channels, 1999. **6**(5): p. 363-74.
449. Netzeband, J.G., et al., *Cannabinoids enhance NMDA-elicited Ca²⁺ signals in cerebellar granule neurons in culture*. J Neurosci, 1999. **19**(20): p. 8765-77.
450. Mahmud, A., et al., *Cannabinoid 1 receptor activation inhibits transient receptor potential vanilloid type 1 receptor-mediated cationic influx into rat cultured primary sensory neurons*. Neuroscience, 2009. **162**(4): p. 1202-11.

451. Blume, L.C., et al., *Cannabinoid receptor interacting protein (CRIP1a) attenuates CB1R signaling in neuronal cells*. *Cell Signal*, 2015. **27**(3): p. 716-726.
452. Guggenhuber, S., et al., *Cannabinoid receptor-interacting protein Crip1a modulates CB1 receptor signaling in mouse hippocampus*. *Brain Struct Funct*, 2016. **221**(4): p. 2061-74.
453. Kearns, C.S., et al., *Concurrent stimulation of cannabinoid CB1 and dopamine D2 receptors enhances heterodimer formation: a mechanism for receptor cross-talk?* *Mol Pharmacol*, 2005. **67**(5): p. 1697-704.
454. Wellman, M. and A. Abizaid, *Growth Hormone Secretagogue Receptor Dimers: A New Pharmacological Target*. *eNeuro*, 2015. **2**(2).
455. Li, H., et al., *Apelin modulates murine gastric vagal afferent mechanosensitivity*. *Physiol Behav*, 2018. **194**: p. 466-473.
456. Rao, X., et al., *An improvement of the 2^{-delta delta CT} method for quantitative real-time polymerase chain reaction data analysis*. *Biostat Bioinforma Biomath*, 2013. **3**(3): p. 71-85.
457. Hegarty, D.M., et al., *Capsaicin-responsive corneal afferents do not contain TRPV1 at their central terminals in trigeminal nucleus caudalis in rats*. *J Chem Neuroanat*, 2014. **61-62**: p. 1-12.
458. Olah, T., et al., *Cannabinoid signalling inhibits sarcoplasmic Ca(2+) release and regulates excitation-contraction coupling in mammalian skeletal muscle*. *J Physiol*, 2016. **594**(24): p. 7381-7398.
459. Page, A.J., T.A. O'Donnell, and L.A. Blackshaw, *Inhibition of mechanosensitivity in visceral primary afferents by GABAB receptors involves calcium and potassium channels*. *Neuroscience*, 2006. **137**(2): p. 627-36.

460. Page, A.J. and L.A. Blackshaw, *An in vitro study of the properties of vagal afferent fibres innervating the ferret oesophagus and stomach*. J Physiol, 1998. **512 (Pt 3)**: p. 907-16.
461. Ambrus, L., et al., *Human podocytes express functional thermosensitive TRPV channels*. Br J Pharmacol, 2017. **174**(23): p. 4493-4507.
462. Evron, T., et al., *G Protein and beta-arrestin signaling bias at the ghrelin receptor*. J Biol Chem, 2014. **289**(48): p. 33442-55.
463. Freissmuth, M., et al., *Suramin analogues as subtype-selective G protein inhibitors*. Mol Pharmacol, 1996. **49**(4): p. 602-11.
464. Uemura, T., et al., *Effect of YM-254890, a specific Galphaq/11 inhibitor, on experimental peripheral arterial disease in rats*. Eur J Pharmacol, 2006. **536**(1-2): p. 154-61.
465. Glass, D.B., et al., *Protein kinase inhibitor-(6-22)-amide peptide analogs with standard and nonstandard amino acid substitutions for phenylalanine 10. Inhibition of cAMP-dependent protein kinase*. J Biol Chem, 1989. **264**(24): p. 14579-84.
466. Toullec, D., et al., *The bisindolylmaleimide GF 109203X is a potent and selective inhibitor of protein kinase C*. J Biol Chem, 1991. **266**(24): p. 15771-81.
467. Kentish, S.J., et al., *A chronic high fat diet alters the homologous and heterologous control of appetite regulating peptide receptor expression*. Peptides, 2013. **46**: p. 150-8.
468. Turu, G. and L. Hunyady, *Signal transduction of the CB1 cannabinoid receptor*. J Mol Endocrinol, 2010. **44**(2): p. 75-85.

469. Sharkey, K.A. and Q.J. Pittman, *Central and peripheral signaling mechanisms involved in endocannabinoid regulation of feeding: a perspective on the munchies*. Sci STKE, 2005. **2005**(277): p. pe15.
470. Argueta, D.A. and N.V. DiPatrizio, *Peripheral endocannabinoid signaling controls hyperphagia in western diet-induced obesity*. Physiol Behav, 2017. **171**: p. 32-39.
471. Cluny, N.L., et al., *A novel peripherally restricted cannabinoid receptor antagonist, AM6545, reduces food intake and body weight, but does not cause malaise, in rodents*. Br J Pharmacol, 2010. **161**(3): p. 629-42.
472. Izzo, A.A., et al., *Peripheral endocannabinoid dysregulation in obesity: relation to intestinal motility and energy processing induced by food deprivation and re-feeding*. Br J Pharmacol, 2009. **158**(2): p. 451-61.
473. Shen, W., et al., *Anti-obesity Effect of Capsaicin in Mice Fed with High-Fat Diet Is Associated with an Increase in Population of the Gut Bacterium Akkermansia muciniphila*. Front Microbiol, 2017. **8**: p. 272.
474. Schnizler, K., et al., *Protein kinase A anchoring via AKAP150 is essential for TRPV1 modulation by forskolin and prostaglandin E2 in mouse sensory neurons*. J Neurosci, 2008. **28**(19): p. 4904-17.
475. Kilkenny, C., et al., *Improving bioscience research reporting: The ARRIVE guidelines for reporting animal research*. J Pharmacol Pharmacother, 2010. **1**(2): p. 94-9.
476. Burdyga, G., et al., *Ghrelin receptors in rat and human nodose ganglia: putative role in regulating CB-1 and MCH receptor abundance*. Am J Physiol Gastrointest Liver Physiol, 2006. **290**(6): p. G1289-97.

477. Opazo, R., et al., *Fasting Upregulates npy, agrp, and ghsr Without Increasing Ghrelin Levels in Zebrafish (Danio rerio) Larvae*. *Front Physiol*, 2018. **9**: p. 1901.
478. Cottone, E., et al., *Goldfish CBI mRNA expression is affected by fasting and anandamide administration*. *Neuroreport*, 2009. **20**(6): p. 595-9.
479. Lim, C.T., et al., *Ghrelin and cannabinoids require the ghrelin receptor to affect cellular energy metabolism*. *Mol Cell Endocrinol*, 2013. **365**(2): p. 303-8.
480. Lee, J.H., et al., *Neuronal Deletion of Ghrelin Receptor Almost Completely Prevents Diet-Induced Obesity*. *Diabetes*, 2016. **65**(8): p. 2169-78.
481. Efendiev, R., et al., *Scaffolding by A-kinase anchoring protein enhances functional coupling between adenylyl cyclase and TRPV1 channel*. *J Biol Chem*, 2013. **288**(6): p. 3929-37.
482. Bermudez-Silva, F.J., et al., *The cannabinoid CBI receptor and mTORC1 signalling pathways interact to modulate glucose homeostasis in mice*. *Dis Model Mech*, 2016. **9**(1): p. 51-61.
483. Kojima, M., et al., *Ghrelin is a growth-hormone-releasing acylated peptide from stomach*. *Nature*, 1999. **402**: p. 656-660.
484. Sato, T., et al., *Structure, regulation and function of ghrelin*. *J Biochem*, 2012. **151**(2): p. 119-28.
485. Fernandez, G., et al., *Evidence Supporting a Role for Constitutive Ghrelin Receptor Signaling in Fasting-Induced Hyperphagia in Male Mice*. *Endocrinology*, 2018. **159**(2): p. 1021-1034.
486. Grabauskas, G., et al., *KATP channels in the nodose ganglia mediate the orexigenic actions of ghrelin*. *J Physiol*, 2015. **593**(17): p. 3973-89.

487. Callahan, H.S., et al., *Postprandial suppression of plasma ghrelin level is proportional to ingested caloric load but does not predict intermeal interval in humans*. J Clin Endocrinol Metab, 2004. **89**(3): p. 1319-24.
488. Hurt, R.T., et al., *The obesity epidemic: challenges, health initiatives, and implications for gastroenterologists*. Gastroenterol Hepatol (N Y), 2010. **6**(12): p. 780-92.
489. Hurt, R.T., et al., *Obesity epidemic: overview, pathophysiology, and the intensive care unit conundrum*. JPEN J Parenter Enteral Nutr, 2011. **35**(5 Suppl): p. 4S-13S.
490. Christie, S., et al., *Biphasic effects of methanandamide on murine gastric vagal afferent mechanosensitivity*. J Physiol, 2019.
491. Steensels, S., L. Vancleef, and I. Depoortere, *The Sweetener-Sensing Mechanisms of the Ghrelin Cell*. Nutrients, 2016. **8**(12).
492. Donovan, M.J., G. Paulino, and H.E. Raybould, *CCK(1) receptor is essential for normal meal patterning in mice fed high fat diet*. Physiol Behav, 2007. **92**(5): p. 969-74.
493. Fowler, C.J., *Transport of endocannabinoids across the plasma membrane and within the cell*. FEBS J, 2013. **280**(9): p. 1895-904.
494. Lever, I.J., et al., *Localization of the endocannabinoid-degrading enzyme fatty acid amide hydrolase in rat dorsal root ganglion cells and its regulation after peripheral nerve injury*. J Neurosci, 2009. **29**(12): p. 3766-80.
495. Frederich, R.C., et al., *Leptin levels reflect body lipid content in mice: evidence for diet-induced resistance to leptin action*. Nat Med, 1995. **1**(12): p. 1311-4.

496. Valenti, M., et al., *Differential diurnal variations of anandamide and 2-arachidonoyl-glycerol levels in rat brain*. Cell Mol Life Sci, 2004. **61**(7-8): p. 945-50.
497. Murillo-Rodriguez, E., F. Desarnaud, and O. Prospero-Garcia, *Diurnal variation of arachidonylethanolamine, palmitoylethanolamide and oleoylethanolamide in the brain of the rat*. Life Sci, 2006. **79**(1): p. 30-7.
498. Dorfman, M.D., et al., *Deletion of Protein Kinase C lambda in POMC Neurons Predisposes to Diet-Induced Obesity*. Diabetes, 2017. **66**(4): p. 920-934.
499. Bansode, R.R., et al., *Protein kinase C deficiency increases fatty acid oxidation and reduces fat storage*. J Biol Chem, 2008. **283**(1): p. 231-6.
500. Kim, Y.B., et al., *Insulin-stimulated protein kinase C lambda/zeta activity is reduced in skeletal muscle of humans with obesity and type 2 diabetes: reversal with weight reduction*. Diabetes, 2003. **52**(8): p. 1935-42.
501. Talior, I., et al., *Increased glucose uptake promotes oxidative stress and PKC-delta activation in adipocytes of obese, insulin-resistant mice*. Am J Physiol Endocrinol Metab, 2003. **285**(2): p. E295-302.
502. McVey, D.C., et al., *Endocannabinoids induce ileitis in rats via the capsaicin receptor (VR1)*. J Pharmacol Exp Ther, 2003. **304**(2): p. 713-22.
503. Vileigas, D.F., et al., *Saturated high-fat diet-induced obesity increases adenylate cyclase of myocardial beta-adrenergic system and does not compromise cardiac function*. Physiol Rep, 2016. **4**(17).
504. Vagena, E., et al., *A high-fat diet promotes depression-like behavior in mice by suppressing hypothalamic PKA signaling*. Transl Psychiatry, 2019. **9**(1): p. 141.

505. Zigman, J.M., S.G. Bouret, and Z.B. Andrews, *Obesity Impairs the Action of the Neuroendocrine Ghrelin System*. Trends Endocrinol Metab, 2016. **27**(1): p. 54-63.
506. Geliebter, A., *Gastric distension and gastric capacity in relation to food intake in humans*. Physiol Behav, 1988. **44**(4-5): p. 665-8.
507. Jelsing, J., P.J. Larsen, and N. Vrang, *The effect of leptin receptor deficiency and fasting on cannabinoid receptor 1 mRNA expression in the rat hypothalamus, brainstem and nodose ganglion*. Neurosci Lett, 2009. **463**(2): p. 125-9.
508. Corchero, J., et al., *Time-dependent differences of repeated administration with Delta9-tetrahydrocannabinol in proenkephalin and cannabinoid receptor gene expression and G-protein activation by mu-opioid and CB1-cannabinoid receptors in the caudate-putamen*. Brain Res Mol Brain Res, 1999. **67**(1): p. 148-57.
509. Christie, S., et al., *Modulatory effect of methanandamide on gastric vagal afferent satiety signals depends on nutritional status*. J Physiol, 2020. **In Press**.
510. Burdyga, G., et al., *Expression of cannabinoid CB1 receptors by vagal afferent neurons is inhibited by cholecystokinin*. J Neurosci, 2004. **24**(11): p. 2708-15.
511. Black, J.B., R.T. Premont, and Y. Daaka, *Feedback regulation of G protein-coupled receptor signaling by GRKs and arrestins*. Semin Cell Dev Biol, 2016. **50**: p. 95-104.
512. Moesgaard, S.G., et al., *Effects of high-fat feeding and fasting on ghrelin expression in the mouse stomach*. Regul Pept, 2004. **120**(1-3): p. 261-7.
513. Izzo, A.A. and K.A. Sharkey, *Cannabinoids and the gut: new developments and emerging concepts*. Pharmacol Ther, 2010. **126**(1): p. 21-38.

514. Mao, Y., et al., *Antinociceptive Effect of Ghrelin in a Rat Model of Irritable Bowel Syndrome Involves TRPV1/Opioid Systems*. *Cell Physiol Biochem*, 2017. **43**(2): p. 518-530.
515. Farajdokht, F., et al., *Ghrelin attenuated hyperalgesia induced by chronic nitroglycerin: CGRP and TRPV1 as targets for migraine management*. *Cephalalgia*, 2018. **38**(11): p. 1716-1730.
516. Geppetti, P. and M. Trevisani, *Activation and sensitisation of the vanilloid receptor: role in gastrointestinal inflammation and function*. *Br J Pharmacol*, 2004. **141**(8): p. 1313-20.
517. Kitazawa, T. and H. Kaiya, *Regulation of Gastrointestinal Motility by Motilin and Ghrelin in Vertebrates*. *Front Endocrinol (Lausanne)*, 2019. **10**: p. 278.
518. Thomas, K.C., et al., *Contributions of TRPV1, endovanilloids, and endoplasmic reticulum stress in lung cell death in vitro and lung injury*. *Am J Physiol Lung Cell Mol Physiol*, 2012. **302**(1): p. L111-9.
519. Cable, J.C., et al., *The effects of obesity, diabetes and metabolic syndrome on the hydrolytic enzymes of the endocannabinoid system in animal and human adipocytes*. *Lipids Health Dis*, 2014. **13**: p. 43.
520. Engeli, S., et al., *Activation of the peripheral endocannabinoid system in human obesity*. *Diabetes*, 2005. **54**(10): p. 2838-43.
521. Koda, S., et al., *The role of the vagal nerve in peripheral PYY3-36-induced feeding reduction in rats*. *Endocrinology*, 2005. **146**(5): p. 2369-75.
522. Kalafateli, A.L., et al., *A cannabinoid receptor antagonist attenuates ghrelin-induced activation of the mesolimbic dopamine system in mice*. *Physiol Behav*, 2018. **184**: p. 211-219.

523. Taylor, C.R. and R.M. Levenson, *Quantification of immunohistochemistry--issues concerning methods, utility and semiquantitative assessment II*. *Histopathology*, 2006. **49**(4): p. 411-24.
524. Greenbaum, D., et al., *Comparing protein abundance and mRNA expression levels on a genomic scale*. *Genome Biol*, 2003. **4**(9): p. 117.
525. Mathis, C., T.H. Moran, and G.J. Schwartz, *Load-sensitive rat gastric vagal afferents encode volume but not gastric nutrients*. *Am J Physiol*, 1998. **274**(2): p. R280-6.
526. Iannotti, F.A., V. Di Marzo, and S. Petrosino, *Endocannabinoids and endocannabinoid-related mediators: Targets, metabolism and role in neurological disorders*. *Prog Lipid Res*, 2016. **62**: p. 107-28.
527. Alen, F., et al., *Cannabinoid receptors and cholecystokinin in feeding inhibition*. *Vitam Horm*, 2013. **92**: p. 165-96.
528. Bjorntorp, P. and M.U. Yang, *Refeeding after fasting in the rat: effects on body composition and food efficiency*. *Am J Clin Nutr*, 1982. **36**(3): p. 444-9.
529. Duca, F.A., Y. Sakar, and M. Covasa, *The modulatory role of high fat feeding on gastrointestinal signals in obesity*. *J Nutr Biochem*, 2013. **24**(10): p. 1663-77.
530. Alingh Prins, A., et al., *Daily rhythms of feeding in the genetically obese and lean Zucker rats*. *Physiol Behav*, 1986. **38**(3): p. 423-6.
531. Oleson, E.B. and J.F. Cheer, *A brain on cannabinoids: the role of dopamine release in reward seeking*. *Cold Spring Harb Perspect Med*, 2012. **2**(8).
532. Perello, M. and S.L. Dickson, *Ghrelin signalling on food reward: a salient link between the gut and the mesolimbic system*. *J Neuroendocrinol*, 2015. **27**(6): p. 424-34.

533. Silvestri, C. and V. Di Marzo, *The endocannabinoid system in energy homeostasis and the etiopathology of metabolic disorders*. Cell Metab, 2013. **17**(4): p. 475-90.
534. Costa, B., *Rimonabant: more than an anti-obesity drug?* Br J Pharmacol, 2007. **150**(5): p. 535-7.
535. Ahn, K., D.S. Johnson, and B.F. Cravatt, *Fatty acid amide hydrolase as a potential therapeutic target for the treatment of pain and CNS disorders*. Expert Opin Drug Discov, 2009. **4**(7): p. 763-784.
536. Feldwisch-Drentrup, H., *New clues to why a French drug trial went horribly wrong*, in *Science*. 2017: Health, Scientific Community.
537. Gavva, N.R., et al., *Proton activation does not alter antagonist interaction with the capsaicin-binding pocket of TRPV1*. Mol Pharmacol, 2005. **68**(6): p. 1524-33.
538. Schwartz, G.J., *The role of gastrointestinal vagal afferents in the control of food intake: current prospects*. Nutrition, 2000. **16**(10): p. 866-73.
539. Izzo, A.A., et al., *Effect of vanilloid drugs on gastrointestinal transit in mice*. Br J Pharmacol, 2001. **132**(7): p. 1411-6.
540. Peeters, T.L., *Ghrelin: a new player in the control of gastrointestinal functions*. Gut, 2005. **54**(11): p. 1638-49.
541. Smith, K.B. and M.S. Smith, *Obesity Statistics*. Prim Care, 2016. **43**(1): p. 121-35, ix.
542. Gupta, N., et al., *Childhood Obesity in Developing Countries: Epidemiology, Determinants, and Prevention*. Endocrine Reviews, 2012. **33**: p. 48-70.
543. Venkatachalam, K. and C. Montell, *TRP channels*. Annu Rev Biochem, 2007. **76**: p. 387-417.

544. Ocobock, C., *Human energy expenditure, allocation, and interactions in natural temperate, hot, and cold environments*. Am J Phys Anthropol, 2016. **161**(4): p. 667-675.
545. Bhave, G., et al., *cAMP-dependent protein kinase regulates desensitization of the capsaicin receptor (VR1) by direct phosphorylation*. Neuron, 2002. **35**(4): p. 721-31.
546. Dhaka, A., et al., *TRPV1 is activated by both acidic and basic pH*. J Neurosci, 2009. **29**(1): p. 153-8.
547. Iwasaki, Y., et al., *A nonpungent component of steamed ginger--[10]-shogaol--increases adrenaline secretion via the activation of TRPV1*. Nutr Neurosci, 2006. **9**(3-4): p. 169-78.
548. De Petrocellis, L., et al., *The activity of anandamide at vanilloid VR1 receptors requires facilitated transport across the cell membrane and is limited by intracellular metabolism*. J Biol Chem, 2001. **276**(16): p. 12856-63.
549. Vigna, S.R., et al., *Leukotriene B4 Mediates Inflammation via TRPV1 in Duct Obstruction-induced Pancreatitis in Rats*. Pancreas, 2001. **40**(5): p. 708-714.
550. Rosenbaum, T., et al., *Ca²⁺/Calmodulin Modulates TRPV1 Activation by Capsaicin*. Journal of General Physiology, 2004. **123**: p. 53-62.
551. Vyklicky, L., et al., *Calcium-dependent desensitization of vanilloid receptor TRPV1: a mechanism possibly involved in analgesia induced by topical application of capsaicin*. Physiol Res, 2008. **57 Suppl 3**: p. S59-68.
552. Lu, Y. and H.D. Anderson, *Cannabinoid signaling in health and disease*. Can J Physiol Pharmacol, 2017. **95**(4): p. 311-327.

553. Natarajan, V., et al., *N-Acylation of ethanolamine phospholipids in canine myocardium*. Biochim Biophys Acta, 1982. **712**(2): p. 342-55.
554. Natarajan, V., et al., *Biosynthesis of N-acylethanolamine phospholipids by dog brain preparations*. J Neurochem, 1983. **41**(5): p. 1303-12.
555. Schmid, P.C., et al., *Metabolism of N-acylethanolamine phospholipids by a mammalian phosphodiesterase of the phospholipase D type*. J Biol Chem, 1983. **258**(15): p. 9302-6.
556. Bisogno, T., et al., *Cloning of the first sn1-DAG lipases points to the spatial and temporal regulation of endocannabinoid signaling in the brain*. J Cell Biol, 2003. **163**(3): p. 463-8.
557. Nicolussi, S. and J. Gertsch, *Endocannabinoid transport revisited*. Vitam Horm, 2015. **98**: p. 441-85.
558. Sanson, B., et al., *Crystallographic study of FABP5 as an intracellular endocannabinoid transporter*. Acta Crystallogr D Biol Crystallogr, 2014. **70**(Pt 2): p. 290-8.
559. Tsuboi, K., et al., *Predominant expression of lysosomal N-acylethanolamine-hydrolyzing acid amidase in macrophages revealed by immunochemical studies*. Biochim Biophys Acta, 2007. **1771**(5): p. 623-32.
560. Kaczocha, M., et al., *Lipid droplets are novel sites of N-acylethanolamine inactivation by fatty acid amide hydrolase-2*. J Biol Chem, 2010. **285**(4): p. 2796-806.
561. Wei, B.Q., et al., *A second fatty acid amide hydrolase with variable distribution among placental mammals*. J Biol Chem, 2006. **281**(48): p. 36569-78.

562. Pan, B., et al., *Alterations of endocannabinoid signaling, synaptic plasticity, learning, and memory in monoacylglycerol lipase knock-out mice*. *J Neurosci*, 2011. **31**(38): p. 13420-30.
563. Zhong, P., et al., *Genetic deletion of monoacylglycerol lipase alters endocannabinoid-mediated retrograde synaptic depression in the cerebellum*. *J Physiol*, 2011. **589**(Pt 20): p. 4847-55.
564. Howlett, A.C., *Reverse pharmacology applied to the cannabinoid receptor*. *Trends Pharmacol Sci*, 1990. **11**(10): p. 395-7.
565. Ibsen, M.S., M. Connor, and M. Glass, *Cannabinoid CB1 and CB2 Receptor Signaling and Bias*. *Cannabis Cannabinoid Res*, 2017. **2**(1): p. 48-60.
566. Khajehali, E., et al., *Biased Agonism and Biased Allosteric Modulation at the CB1 Cannabinoid Receptor*. *Mol Pharmacol*, 2015. **88**(2): p. 368-79.
567. Laprairie, R.B., et al., *Biased Type 1 Cannabinoid Receptor Signaling Influences Neuronal Viability in a Cell Culture Model of Huntington Disease*. *Mol Pharmacol*, 2016. **89**(3): p. 364-75.
568. Jarbe, T.U. and N.V. DiPatrizio, *Delta9-THC induced hyperphagia and tolerance assessment: interactions between the CB1 receptor agonist delta9-THC and the CB1 receptor antagonist SR-141716 (rimonabant) in rats*. *Behav Pharmacol*, 2005. **16**(5-6): p. 373-80.
569. Foltin, R.W., J.V. Brady, and M.W. Fischman, *Behavioral analysis of marijuana effects on food intake in humans*. *Pharmacol Biochem Behav*, 1986. **25**(3): p. 577-82.

570. Scheen, A.J., et al., *Efficacy and tolerability of rimonabant in overweight or obese patients with type 2 diabetes: a randomised controlled study*. Lancet, 2006. **368**(9548): p. 1660-72.
571. Shrestha, N., et al., *Peripheral modulation of the endocannabinoid system in metabolic disease*. Drug Discov Today, 2018. **23**(3): p. 592-604.
572. Ross, R.A., *Anandamide and vanilloid TRPV1 receptors*. Br J Pharmacol, 2003. **140**(5): p. 790-801.
573. Santha, P., et al., *The endogenous cannabinoid anandamide inhibits transient receptor potential vanilloid type 1 receptor-mediated currents in rat cultured primary sensory neurons*. Acta Physiol Hung, 2010. **97**(2): p. 149-58.
574. Matsuda, L.A., et al., *Structure of a cannabinoid receptor and functional expression of the cloned cDNA*. Nature, 1990. **346**(6284): p. 561-4.
575. Little, T.J., et al., *Plasma endocannabinoid levels in lean, overweight and obese humans: relationships with intestinal permeability markers, inflammation and incretin secretion*. Am J Physiol Endocrinol Metab, 2018.
576. Wahlqvist, M.L. and N. Wattanapenpaiboon, *Hot foods--unexpected help with energy balance?* Lancet, 2001. **358**(9279): p. 348-9.
577. Snitker, S., et al., *Effects of novel capsinoid treatment on fatness and energy metabolism in humans: possible pharmacogenetic implications*. Am J Clin Nutr, 2009. **89**(1): p. 45-50.
578. Inoue, N., et al., *Enhanced energy expenditure and fat oxidation in humans with high BMI scores by the ingestion of novel and non-pungent capsaicin analogues (capsinoids)*. Biosci Biotechnol Biochem, 2007. **71**(2): p. 380-9.

579. Baboota, R.K., et al., *Capsaicin-induced transcriptional changes in hypothalamus and alterations in gut microbial count in high fat diet fed mice*. J Nutr Biochem, 2014. **25**(9): p. 893-902.
580. Lee, G.R., et al., *Topical application of capsaicin reduces visceral adipose fat by affecting adipokine levels in high-fat diet-induced obese mice*. Obesity (Silver Spring), 2013. **21**(1): p. 115-22.
581. Yu, Q., et al., *Expression of TRPV1 in rabbits and consuming hot pepper affects its body weight*. Mol Biol Rep, 2012. **39**(7): p. 7583-9.
582. Song, J.X., et al., *Dietary Capsaicin Improves Glucose Homeostasis and Alters the Gut Microbiota in Obese Diabetic ob/ob Mice*. Front Physiol, 2017. **8**: p. 602.
583. Marshall, N.J., et al., *A role for TRPV1 in influencing the onset of cardiovascular disease in obesity*. Hypertension, 2013. **61**(1): p. 246-52.
584. Chaiyasit, K., W. Khovidhunkit, and S. Wittayalertpanya, *Pharmacokinetic and the effect of capsaicin in Capsicum frutescens on decreasing plasma glucose level*. J Med Assoc Thai, 2009. **92**(1): p. 108-13.
585. Chaiyata, P., S. Puttadechakum, and S. Komindr, *Effect of chili pepper (Capsicum frutescens) ingestion on plasma glucose response and metabolic rate in Thai women*. J Med Assoc Thai, 2003. **86**(9): p. 854-60.
586. Matsumoto, T., et al., *Effects of Capsaicin-containing Yellow Curry Sauce on Sympathetic Nervous System Activity and Diet-induced Thermogenesis in Lean and Obese Young Women*. Journal of Nutritional Science and Vitaminology, 2000. **46**(6): p. 309-315.
587. Yoshioka, M., et al., *Effects of red-pepper diet on the energy metabolism in men*. J Nutr Sci Vitaminol (Tokyo), 1995. **41**(6): p. 647-56.

588. Sato, T., et al., *Structure, regulation and function of ghrelin*. The Journal of Biochemistry, 2012. **151**(2): p. 119-128.
589. Smeets, A. and M. Westerterp-Plantnga, *The acute effects of a lunch containing capsaicin on energy and substrate utilization, hormones, and satiety*. European Journal of Nutrition, 2009. **48**: p. 229-234.
590. Kentish, S., et al., *Diet-induced adaptation of vagal afferent function*. J. Physiol., 2012. **590**(1): p. 209-221.
591. Page, A.J., et al., *Ghrelin selectively reduces mechanosensitivity of upper gastrointestinal vagal afferents*. Am. J. Physiol. Gastrointest. Liver Physiol., 2007. **292**: p. G1376 –G1384.
592. Arnold, M., et al., *Gut vagal afferents are not necessary for the eating-stimulatory effect of intraperitoneally injected ghrelin in the rat*. J Neurosci, 2006. **26**(43): p. 11052-60.
593. Date, Y., et al., *The role of the gastric afferent vagal nerve in ghrelin-induced feeding and growth hormone secretion in rats*. Gastroenterology, 2002. **123**(4): p. 1120-1128.
594. Sobhani, I., et al., *Leptin secretion and leptin receptor in the human stomach*. Gut, 2000. **47**(2): p. 178-183.
595. Zsombok, A., et al., *Regulation of leptin receptor-expressing neurons in the brainstem by TRPV1*. Physiol Rep, 2014. **2**(9): p. e12160.
596. Baggio, L.L. and D.J. Drucker, *Biology of incretins: GLP-1 and GIP*. Gastroenterology, 2007. **132**(6): p. 2131-57.

597. Torekov, S.S., S. Madsbad, and J.J. Holst, *Obesity – an indication for GLP-1 treatment? Obesity pathophysiology and GLP-1 treatment potential*. *Obesity Reviews*, 2011. **12**: p. 593-601.
598. Ryan, D. and A. Acosta, *GLP-1 receptor agonists: Nonglycemic clinical effects in weight loss and beyond*. *Obesity*, 2015. **23**(6): p. 1119-1129.
599. Hameed, S., W.S. Dhillon, and S.R. Bloom, *Gut hormones and appetite control*. *Oral Dis*, 2009. **15**(1): p. 18-26.
600. Page, A.J. and S. Kentish, *Plasticity of gastrointestinal vagal afferent satiety signals*. *Neurogastroenterol Motil*, 2016. **29**: p. e12973.
601. Page, A.J. and L.A. Blackshaw, *An in vitro study of the properties of vagal afferent fibres innervating the ferret oesophagus and stomach*. *J. Physiol.*, 1998. **512**: p. 907-916.
602. Page, A.J., C.M. Martin, and L.A. Blackshaw, *Vagal mechanoreceptors and chemoreceptors in mouse stomach and esophagus*. *J. Neurophysiol.*, 2002. **87**: p. 2095-2103.
603. Kentish, S.J., et al., *Gastric vagal afferent modulation by leptin is influenced by food intake status*. *J Physiol*, 2013. **591**(7): p. 1921-1934.
604. Kentish, S.J., et al., *Nesfatin-1 modulates murine gastric vagal afferent mechanosensitivity in a nutritional state dependent manner*. *Peptides*, 2017. **89**: p. 35-41.
605. Zhao, H., L.K. Sprunger, and S.M. Simasko, *Expression of transient receptor potential channels and two-pore potassium channels in subtypes of vagal afferent neurons in rat*. *Am. J. Physiol. Gastrointest. Liver Physiol.*, 2009. **298**(2): p. G212-G221.

606. Tan, L.L., J.C. Bornstein, and C.R. Anderson, *Neurochemical and morphological phenotypes of vagal afferent neurons innervating the adult mouse jejunum*. *Neurogastroenterology & Motility*, 2009. **21**(9): p. 994-1001.
607. Wang, X., R.L. Miyares, and G.P. Ahern, *Oleoylethanolamide excites vagal sensory neurones, induces visceral pain and reduces short-term food intake in mice via capsaicin receptor TRPV1*. *J Physiol*, 2005. **564**(Pt 2): p. 541-7.
608. Daly, D.M., et al., *Impaired intestinal afferent nerve satiety signalling and vagal afferent excitability in diet induced obesity in the mouse*. *The Journal of Physiology*, 2011. **589**(11): p. 2857-2870.
609. Burdyga, G., et al., *Expression of Cannabinoid CB1 Receptors by Vagal Afferent Neurons Is Inhibited by Cholecystokinin*. *The Journal of Neuroscience*, 2004. **24**(11): p. 2708-2715.
610. Partosoedarso, E.R., et al., *Cannabinoid1 receptor in the dorsal vagal complex modulates lower oesophageal sphincter relaxation in ferrets*. *J Physiol*, 2003. **550**(Pt 1): p. 149-58.
611. Longhurst, J.C., et al., *Effects of bradykinin and capsaicin on endings of afferent fibers from abdominal visceral organs*. *Am J Physiol*, 1984. **247**(3 Pt 2): p. R552-9.
612. Watanabe, T., et al., *Adrenal sympathetic efferent nerve and catecholamine secretion excitation caused by capsaicin in rats*. *Am J Physiol*, 1988. **255**(1 Pt 1): p. E23-7.
613. Watanabe, T., et al., *Capsaicin, a pungent principle of hot red pepper, evokes catecholamine secretion from the adrenal medulla of anesthetized rats*. *Biochem Biophys Res Commun*, 1987. **142**(1): p. 259-64.

614. Kawada, T., et al., *Capsaicin-induced beta-adrenergic action on energy metabolism in rats: influence of capsaicin on oxygen consumption, the respiratory quotient, and substrate utilization*. Proc Soc Exp Biol Med, 1986. **183**(2): p. 250-6.
615. Spiegelman, B.M. and J.S. Flier, *Adipogenesis and obesity: rounding out the big picture*. Cell, 1996. **87**(3): p. 377-89.
616. Feldmann, H.M., et al., *UCP1 ablation induces obesity and abolishes diet-induced thermogenesis in mice exempt from thermal stress by living at thermoneutrality*. Cell Metab, 2009. **9**(2): p. 203-9.
617. Nedergaard, J., D. Ricquier, and L.P. Kozak, *Uncoupling proteins: current status and therapeutic prospects*. EMBO Rep, 2005. **6**(10): p. 917-21.
618. Baboota, R.K., et al., *Capsaicin induces "brite" phenotype in differentiating 3T3-L1 preadipocytes*. PLoS One, 2014. **9**(7): p. e103093.
619. Kida, R., et al., *Direct action of capsaicin in brown adipogenesis and activation of brown adipocytes*. Cell Biochem Funct, 2016. **34**(1): p. 34-41.
620. Bishnoi, M., et al., *Expression of multiple Transient Receptor Potential channel genes in murine 3T3-L1 cell lines and adipose tissue*. Pharmacol Rep, 2013. **65**(3): p. 751-5.
621. Sun, W., et al., *Gene expression changes of thermo-sensitive transient receptor potential channels in obese mice*. Cell Biol Int, 2017. **41**(8): p. 908-913.
622. Brondani, L.d.A., et al., *The role of the uncoupling protein 1 (UCP1) on the development of obesity and type 2 diabetes mellitus*. Arq Bras Endocrinol Metab, 2012. **56**(4): p. 215-225.

623. Okamatsu-Ogura, Y., et al., *Capsinoids suppress diet-induced obesity through uncoupling protein 1-dependent mechanism in mice*. Journal of Functional Foods, 2015. **19**(A): p. 1-9.
624. Kawabata, F., et al., *Non-pungent capsaicin analogs (capsinoids) increase metabolic rate and enhance thermogenesis via gastrointestinal TRPV1 in mice*. Biosci Biotechnol Biochem, 2009. **73**(12): p. 2690-7.
625. Rong, W., et al., *Jejunal afferent nerve sensitivity in wild-type and TRPV1 knockout mice*. J Physiol, 2004. **560**(Pt 3): p. 867-81.
626. Yoneshiro, T., et al., *Nonpungent capsaicin analogs (capsinoids) increase energy expenditure through the activation of brown adipose tissue in humans*. Am J Clin Nutr, 2012. **95**(4): p. 845-50.
627. Bamshad, M., C.K. Song, and T.J. Bartness, *CNS origins of the sympathetic nervous system outflow to brown adipose tissue*. Am J Physiol, 1999. **276**(6 Pt 2): p. R1569-78.
628. Madden, C.J. and S.F. Morrison, *Hypoxic activation of arterial chemoreceptors inhibits sympathetic outflow to brown adipose tissue in rats*. J Physiol, 2005. **566**(Pt 2): p. 559-73.
629. Cao, W.H., C.J. Madden, and S.F. Morrison, *Inhibition of brown adipose tissue thermogenesis by neurons in the ventrolateral medulla and in the nucleus tractus solitarius*. Am J Physiol Regul Integr Comp Physiol, 2010. **299**(1): p. R277-90.

630. Skibicka, K.P. and H.J. Grill, *Hypothalamic and hindbrain melanocortin receptors contribute to the feeding, thermogenic, and cardiovascular action of melanocortins*. *Endocrinology*, 2009. **150**(12): p. 5351-61.
631. Blouet, C. and G.J. Schwartz, *Duodenal lipid sensing activates vagal afferents to regulate non-shivering brown fat thermogenesis in rats*. *PLoS One*, 2012. **7**(12): p. e51898.
632. Madden, C.J., E.P. Santos da Conceicao, and S.F. Morrison, *Vagal afferent activation decreases brown adipose tissue (BAT) sympathetic nerve activity and BAT thermogenesis*. *Temperature (Austin)*, 2017. **4**(1): p. 89-96.
633. Krieger, J.P., et al., *Glucagon-like peptide-1 regulates brown adipose tissue thermogenesis via the gut-brain axis in rats*. *Am J Physiol Regul Integr Comp Physiol*, 2018.
634. Szolcsanyi, J., *Capsaicin-type pungent agents producing pyrexia*. In: *Handbook of Experimental Pharmacology*. Milton AS. ed; Springer Verlag, Berlin., 1982. **60**: p. 437-478.
635. Kobayashi, A., et al., *Capsaicin activates heat loss and heat production simultaneously and independently in rats*. *Am J Physiol*, 1998. **275**(1 Pt 2): p. R92-8.
636. Gram, D.X., et al., *Capsaicin-sensitive sensory fibers in the islets of Langerhans contribute to defective insulin secretion in Zucker diabetic rat, an animal model for some aspects of human type 2 diabetes*. *Eur J Neurosci*, 2007. **25**(1): p. 213-23.

637. Jancso, G., E. Kiraly, and A. Jancso-Gabor, *Pharmacologically induced selective degeneration of chemosensitive primary sensory neurones*. *Nature*, 1977. **270**(5639): p. 741-3.
638. Razavi, R., et al., *TRPV1+ sensory neurons control beta cell stress and islet inflammation in autoimmune diabetes*. *Cell*, 2006. **127**(6): p. 1123-35.
639. Diaz-Garcia, C.M., et al., *Role for the TRPV1 channel in insulin secretion from pancreatic beta cells*. *J Membr Biol*, 2014. **247**(6): p. 479-91.
640. Basu, S. and P. Srivastava, *Immunological role of neuronal receptor vanilloid receptor 1 expressed on dendritic cells*. *Proc Natl Acad Sci U S A*, 2005. **102**(14): p. 5120-5.
641. Szollosi, A.G., et al., *Transient receptor potential vanilloid-2 mediates the effects of transient heat shock on endocytosis of human monocyte-derived dendritic cells*. *FEBS Lett*, 2013. **587**(9): p. 1440-5.
642. Toth, B.I., et al., *Transient receptor potential vanilloid-1 signaling inhibits differentiation and activation of human dendritic cells*. *FEBS Lett*, 2009. **583**(10): p. 1619-24.
643. O'Connell, P.J., S.C. Pingle, and G.P. Ahern, *Dendritic cells do not transduce inflammatory stimuli via the capsaicin receptor TRPV1*. *FEBS Lett*, 2005. **579**(23): p. 5135-9.
644. Akiba, Y., et al., *Transient receptor potential vanilloid subfamily 1 expressed in pancreatic islet beta cells modulates insulin secretion in rats*. *Biochem Biophys Res Commun*, 2004. **321**(1): p. 219-25.

645. Zhang, S., et al., *Capsaicin Reduces Blood Glucose by Increasing Insulin Levels and Glycogen Content Better than Capsiate in Streptozotocin-Induced Diabetic Rats*. J Agric Food Chem, 2017. **65**(11): p. 2323-2330.
646. Kahn, S.E., R.L. Hull, and K.M. Utzschneider, *Mechanisms linking obesity to insulin resistance and type 2 diabetes*. Nature, 2006. **444**(7121): p. 840-6.
647. Fonseca, V.A., *Defining and characterizing the progression of type 2 diabetes*. Diabetes Care, 2009. **32 Suppl 2**: p. S151-6.
648. Ahuja, K.D., et al., *Effects of chili consumption on postprandial glucose, insulin, and energy metabolism*. Am J Clin Nutr, 2006. **84**(1): p. 63-9.
649. Kroff, J., et al., *The metabolic effects of a commercially available chicken peri-peri (African bird's eye chilli) meal in overweight individuals*. Br J Nutr, 2017. **117**(5): p. 635-644.
650. Festa, A., et al., *Chronic subclinical inflammation as part of the insulin resistance syndrome: the Insulin Resistance Atherosclerosis Study (IRAS)*. Circulation, 2000. **102**(1): p. 42-7.
651. Wu, T., et al., *Associations of serum C-reactive protein with fasting insulin, glucose, and glycosylated hemoglobin: the Third National Health and Nutrition Examination Survey, 1988-1994*. Am J Epidemiol, 2002. **155**(1): p. 65-71.
652. Gram, D.X., et al., *Plasma calcitonin gene-related peptide is increased prior to obesity, and sensory nerve desensitization by capsaicin improves oral glucose tolerance in obese Zucker rats*. Eur J Endocrinol, 2005. **153**(6): p. 963-9.

653. Pettersson, M., et al., *Calcitonin gene-related peptide: occurrence in pancreatic islets in the mouse and the rat and inhibition of insulin secretion in the mouse.* *Endocrinology*, 1986. **119**(2): p. 865-9.
654. Gomtsyan, A., et al., *TRPV1 ligands with hyperthermic, hypothermic and no temperature effects in rats.* *Temperature (Austin)*, 2015. **2**(2): p. 297-301.
655. Lehto, S.G., et al., *Antihyperalgesic effects of (R,E)-N-(2-hydroxy-2,3-dihydro-1H-inden-4-yl)-3-(2-(piperidin-1-yl)-4-(trifluoromethyl)phenyl)-acrylamide (AMG8562), a novel transient receptor potential vanilloid type 1 modulator that does not cause hyperthermia in rats.* *J Pharmacol Exp Ther*, 2008. **326**(1): p. 218-29.

Chapter 8 Appendix: Published Literature Review

Involvement of TRPV1 Channels in Energy Homeostasis

Stewart Christie¹, Gary A. Wittert^{1,2}, Hui Li^{1,2} & Amanda J. Page^{1,2}

¹Vagal Afferent Research Group, Centre for Nutrition and Gastrointestinal Disease, Adelaide Medical School, University of Adelaide, Adelaide, SA 5005, Australia

²Long Life Health Theme, South Australian Health and Medical Research Institute, Adelaide, SA 5000, Australia

Published in: *Frontiers in Endocrinology*, DOI: 10.3389/fendo.2018.00420

Published online: 31/07/2018

Statement of Authorship

Title of Paper	Involvement of TRPV1 Channels in Energy Homeostasis
Publication Status	<input checked="" type="checkbox"/> Published <input type="checkbox"/> Accepted for Publication <input type="checkbox"/> Submitted for Publication <input type="checkbox"/> Unpublished and Unsubmitted work written in manuscript style
Publication Details	Journal of Endocrinology, DOI: 10.3389/fendo.2018.00420

Principal Author

Name of Principal Author (Candidate)	Stewart Christie			
Contribution to the Paper	Wrote and edited the paper			
Overall percentage (%)	70%			
Certification:	This paper reports on original research I conducted during the period of my Higher Degree by Research candidature and is not subject to any obligations or contractual agreements with a third party that would constrain its inclusion in this thesis. I am the primary author of this paper.			
Signature	<table border="1" style="width: 100%;"> <tr> <td style="width: 60%;"></td> <td style="width: 10%;">Date</td> <td style="width: 30%;">14/11/2019</td> </tr> </table>		Date	14/11/2019
	Date	14/11/2019		

Co-Author Contributions

By signing the Statement of Authorship, each author certifies that:

- i. the candidate's stated contribution to the publication is accurate (as detailed above);
- ii. permission is granted for the candidate to include the publication in the thesis; and
- iii. the sum of all co-author contributions is equal to 100% less the candidate's stated contribution.

Name of Co-Author	Hui Li			
Contribution to the Paper	Edited the paper			
Signature	<table border="1" style="width: 100%;"> <tr> <td style="width: 60%;"></td> <td style="width: 10%;">Date</td> <td style="width: 30%;">14/11/2019</td> </tr> </table>		Date	14/11/2019
	Date	14/11/2019		

Name of Co-Author	Gary Wittert		
Contribution to the Paper	Edited the paper		
Signature		Date	20/11/2019

Name of Co-Author	Amanda J Page		
Contribution to the Paper	Edited the paper		
Signature		Date	14/11/2019

Abstract

The ion channel TRPV1 is involved in a wide range of processes including nociception, thermosensation and, more recently discovered, energy homeostasis. Tightly controlling energy homeostasis is important to maintain a healthy body weight, or to aid in weight loss by expending more energy than energy intake. TRPV1 may be involved in energy homeostasis, both in the control of food intake and energy expenditure. In the periphery, it is possible that TRPV1 can impact on appetite through control of appetite hormone levels or via modulation of gastrointestinal vagal afferent signalling. Further, TRPV1 may increase energy expenditure via heat production. Dietary supplementation with TRPV1 agonists, such as capsaicin, has yielded conflicting results with some studies indicating a reduction in food intake and increase in energy expenditure, and other studies indicating the converse. Nonetheless, it is increasingly apparent that TRPV1 may be dysregulated in obesity and contributing to the development of this disease. The mechanisms behind this dysregulation are currently unknown but interactions with other systems, such as the endocannabinoid systems, could be altered and therefore play a role in this dysregulation. Further, TRPV1 channels appear to be involved in pancreatic insulin secretion. Therefore, given its plausible involvement in regulation of energy and glucose homeostasis and its dysregulation in obesity, TRPV1 may be a target for weight loss therapy and diabetes. However, further research is required to fully elucidate TRPV1's role in these processes. The review provides an overview of current knowledge in this field and potential areas for development.

Abbreviations

AC, adenylyl cyclase; AEA, anandamide; AMPK, adenosine monophosphate kinase; BAT, brown adipose tissue; BGL, blood glucose level; BMP, bone morphogenic protein; CAMK, calmodulin dependent kinase; CB, cannabinoid; DMV, dorsal motor nucleus of the vagus; GI, gastrointestinal; GLP, glucagon like peptide; PGC, PPAR gamma coactivator; PI3K, phosphatidylinositol 4-5 bisphosphate 3-kinase; PIP₂, phosphatidylinositol-4,5-bisphosphate; PKA, protein kinase A; PKC, protein kinase C; PLC, phospholipase C; PPAR, peroxisome proliferator activated receptor; PRDM, positive regulatory domain; SIRT, sirtuin; SNS, somatic nervous system; TRPV, transient receptor potential vanilloid; UCP, uncoupling protein; WAT, white adipose tissue.

1. Introduction

Obesity has become the fifth leading cause of death, and the second leading cause of preventable death worldwide, closely following tobacco smoking [541, 542]. There are multiple hormonal, neurotransmitter, and receptor systems involved in the regulation of energy balance. Pharmacological attempts to favourably modulate these systems to encourage weight loss have been somewhat effective, although not without adverse side effects. This has led to the search for more suitable targets. One such group of receptors/ion channels gaining attention for their possible role in energy homeostasis are the Transient Receptor Potential (TRP) channels.

TRP channels are a superfamily of about 28 non-selective cation channels divided into 7 subfamilies including TRP vanilloid (TRPV), and TRP ankyrin (TRPA) [543]. They were first identified in 1969 from an irregular electroretinogram in a mutant strain of the *Drosophila* fly [380]. The electroretinogram presented a short increase in retinal potential which gave rise to the name ‘transient receptor potential’ [381]. Since their discovery, TRP channels have been identified as osmo- and mechano-sensitive [379]. For example, TRPA1 is associated with pain sensations and inflammation [382], and TRPV1 is associated with pain and temperature regulation [383].

Endotherms use energy to create heat to maintain body temperature and in colder climates it has been shown that humans expend more energy for thermoregulation compared to warmer climates [544]. Given the high energy costs of generating heat to maintain an optimal cellular environment thermoregulation can also play an important role in energy homeostasis. TRPV1 channels are involved in thermoregulation, making them a possible target for the modulation of energy expenditure. Further, it is becoming apparent that

TRPV1 may be involved in the regulation of appetite via the modulation of appetite hormones and/or by acting on gastrointestinal vagal afferents. This is a process that may involve interaction with the endocannabinoid system considering that endocannabinoids such as anandamide (AEA), produced in the gastrointestinal tract are also endogenous TRPV1 agonists. In addition, there are suggestions that TRPV1 may be involved in the regulation of insulin secretion in the pancreas. Studies in obese individuals have suggested that TRPV1 may be dysfunctional or dysregulated due to loss of effect on energy homeostasis. For this reason TRPV1 may be a potential target for pharmacological manipulation to aid in weight loss with recent studies suggesting selective blockade or activation of specific functions of TRPV1. However, due to its complexity this may prove difficult. This review explores TRPV1 structure and modulation and will focus on its involvement in energy homeostasis, diabetes and possible pharmacological manipulation.

2. TRPV1 channels

TRPV1, the first channel in the vanilloid family, is highly permeable to calcium and was discovered in 1997 by cloning dorsal root ganglia expressed genes in human embryonic kidney cells [400]. It is expressed in a wide range of central and peripheral tissues. Centrally, TRPV1 is highly expressed in the brain stem, mid-brain, hypothalamus and limbic system [384]. Peripherally it is expressed in many tissues including the vagal and spinal sensory nerves [385], stomach [387] and adipose tissue [386].

2.1 TRPV1 structure

The TRPV1 channel consists of four identical subunits located in the plasma membrane with each subunit (Figure 1) consisting of an N-terminus, a transmembrane region, and a C-terminus [395, 396]. The N-terminus contains an ankyrin repeating domain consisting

of 6 ankyrin subunits [396] which in its tertiary structure forms six α -helices connected by finger loops [395]. Sites on the N-terminus are capable of phosphorylation by protein kinases with the S116 phosphorylation site being one of functionality [545]. A linker section connects the N-terminus to the transmembrane region via the pre-helical segment (pre-S1), and connects TRPV1 subunits together [395, 396, 398, 545].

The transmembrane region of each TRPV1 subunit comprises 6 helical segments (S1-S6), where S1-S4 contribute to the voltage-sensing domain, and S5-S6 contribute to the pore-forming domain [396]. S1-S4 are connected to S5-S6 by a linker segment, and act as a foundation which allows the linker segment to move, contributing to pore opening and TRPV1 activation. The transmembrane region also contains binding sites for several ligands. For example, vanilloids (e.g. capsaicin) are capable of binding to S3 and S4, and protons (H^+) are capable of binding to S5 and the S5-S6 linker (pore helix) [395].

Lastly, the C-terminus consists of a TRP domain (TRP-D) which interacts with pre-S1 suggesting a structural role [396]. Following the TRP domain are several protein kinase A (PKA) and protein kinase C (PKC) phosphorylation sites, and sites for binding calmodulin and phosphatidylinositol-4,5-bisphosphate (PIP₂) [395, 396].

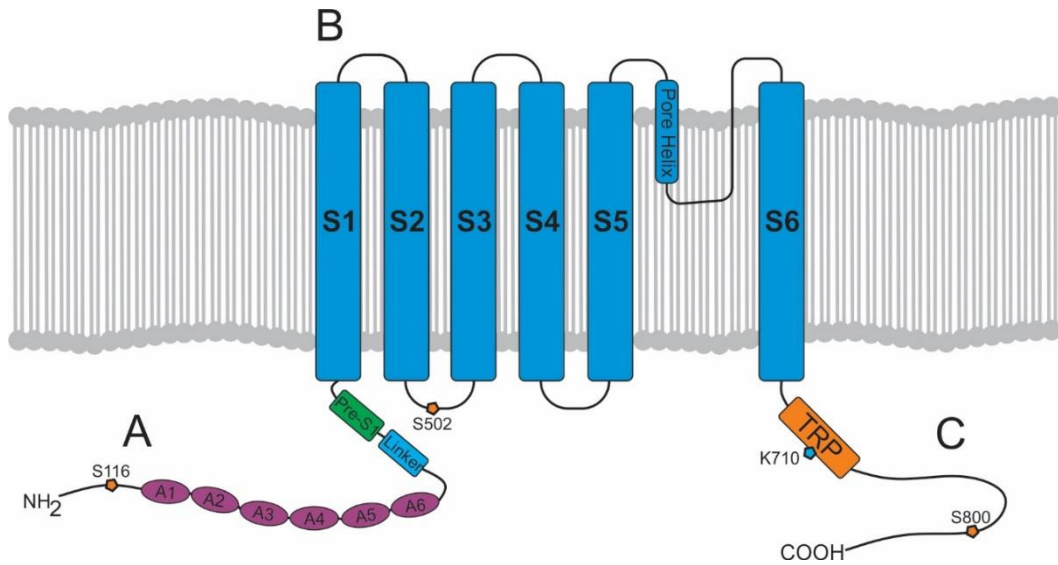


Figure 8.1: Structure of a TRPV1 subunit.

A) N-terminus containing 6 ankyrin subunits (A1-A6) and a linking region consisting of a linker and a Pre-S1 helix segment. B) transmembrane region with 6 helical segments (S1-S6). C) C-terminus containing a TRP domain and binding sites for PKA, PKC, PIP₂ and calmodulin.

2.2 TRPV1 channel activation or modulation

TRPV1 is activated by a wide variety of different stimuli including heat, protons (pH<5.9) [383, 546], capsaicin the irritant compound in hot chillies [400], allicin and diallyl sulphides from garlic [401, 402], piperine from black pepper [403] and gingerol from ginger [547]. Spider and jellyfish venom-derived toxins are also TRPV1 agonists [404, 405].

Endogenous agonists are referred to as endovanilloids. To qualify as an endovanilloid the compound should be produced and released in sufficient amount to evoke a TRPV1-mediated response by direct binding and subsequent activation of the channel. Further, to

permit regulation of the channel the signal should have a short half-life. Therefore, the mechanisms for synthesis and breakdown of the endovanilloid should be in close proximity to TRPV1. As the binding sites for endogenous ligands of TRPV1 are intracellular [407, 548] then the ligand could also be produced within the cell or there should be a mechanism to bring it into the cell. Three different classes of lipid are known to activate TRPV1 i.e. N-acyl-ethanolamines (NAEs, e.g. AEA [408]), some lipoxygenase products of arachidonic acid and N-acyl-dopamines (e.g. N-arachidonoyldopamine, N-oleoyldopamine) [411]. Further, adipose tissue B lymphocytes (B1 cells) that regulate local inflammatory responses produce leukotrienes including leukotriene B4 which is also a TRPV1 agonist [549].

Intracellularly, calmodulin, a calcium-binding messenger, mediates the negative feedback loop formed by calcium [550]. Calcium binds and activates calmodulin allowing it to bind to the N-terminus or C-terminus of TRPV1 inhibiting TRPV1 activity [395]. Other secondary messengers such as PKA, PKC, and PIP₂ are also capable of modulating TRPV1 activity. PKA can enhance or activate TRPV1 through phosphorylation of sites (S116 and T370) on the N-terminal [406] and may play a role in the capsaicin induced Ca²⁺ dependent desensitisation of TRPV1 activation, a phenomenon which has been extensively reviewed elsewhere [551]. PKC directly activates TRPV1 through phosphorylation of the S2-S3 linker region (S502) and C-terminal sites (S800), and also potentiates the effect of other ligands such as protons [412, 413]. PIP₂ is a negative regulator, inhibiting TRPV1 activity when bound to the C-terminal sites (TRP domain: K710) [414].

2.3 Interactions between TRPV1 and the endocannabinoid system

2.3.1 The endocannabinoid system

The endocannabinoid system consists of endocannabinoids, their receptors and the enzymes involved in endocannabinoid synthesis and degradation. This system is involved in many physiological processes including memory, mood and relevant to this review promotion of food intake [552]. Endocannabinoids are endogenous lipid messengers (e.g. AEA and 2-arachidonoyl-glycerol) which activate their receptors, cannabinoid receptor-1 (CB1) and cannabinoid receptor-2 (CB2) [236, 301].

These endogenous lipid messengers are synthesised on demand and degraded by cellular uptake and enzymatic hydrolysis (see review [319] and Figure 2). Briefly, the first step in the synthesis of AEA and NAEs is the transacylation of membrane phosphatidylethanolamine-containing phospholipids to N-acylphosphatidylethanolamines (NAPEs) [553, 554]. There are a number of ways that NAPEs are metabolised to their corresponding NAE including catalysed hydrolysis by the NAPE-hydrolysing enzyme phospholipase D (NAPE-PLD) [555]. In contrast, diacylglycerol lipase (DAGL) is responsible for the formation of 2-AG [556]. There is still some controversy on whether there is an endocannabinoid membrane transporter (See reviews [493, 557]). Nonetheless, endocannabinoids can be cleared from the extracellular space. Further, there are intracellular proteins that can shuttle these lipids to specific intracellular locations (e.g. TRPV1 for AEA) [324, 325], the best characterised of these are the fatty acid-binding proteins (FABP e.g. FABP5 and 7) [558]. The enzymes responsible for the breakdown of AEA and NAEs are fatty acid amide hydrolase (FAAH) and N-acylethanolamine-hydrolysing acid-amidase (NAAA). NAAA is predominantly located in the lungs where it is localised to the lysosomes of macrophages [312, 559]. FAAH is

more ubiquitous and FAAH-1 is located on the endoplasmic reticulum whereas FAAH-2 (not found in rodents) is located in the lipid rafts [560, 561]. Monoacylglycerol lipase (MAGL) is the enzyme responsible for the majority of 2-AG hydrolysis in most tissues [320, 562, 563].

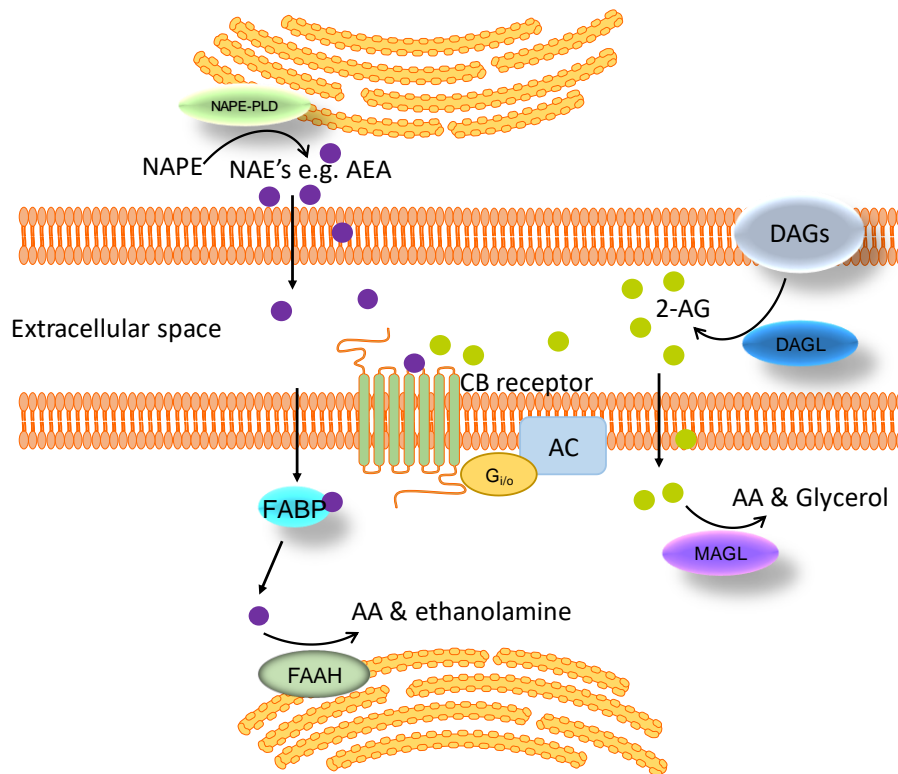


Figure 8.2: Schematic of the synthesis, degradation and action of endocannabinoids at cannabinoid receptors.

Endogenous lipid messengers, such as AEA and 2-AG, act on cannabinoid receptors. AEA and 2-AG are synthesised on demand and degraded by cellular uptake and enzymatic hydrolysis by FAAH and MAGL respectively. FABP carries AEA from the cell membrane to the endoplasmic reticulum where it is finally converted to AA by FAAH. Abbreviations: AA, arachidonic acid; AC, adenylate cyclase; AEA, anandamide; 2-AG, 2-arachidonoylglycerol; CB, cannabinoid; DAGs, diacylglycerols; DAGL, diacylglycerol lipase; FAAH, fatty acid amide hydrolase; FABP, fatty acid-binding

protein; MAGL, monoacylglycerol lipase; NAE, *N*-acylethanolamines; NAPE, *N*-acylphosphatidylethanolamine; NAPE-PLD, NAPE-specific phospholipase D.

The receptors for endocannabinoids, CB1 and CB2 are members of the G-protein coupled receptor family, being predominantly coupled to the $G_{i/o}\alpha$ proteins that inhibit adenylyl cyclase thereby reducing cellular cAMP levels [237, 564]. However, coupling to other effector proteins has also been reported, including activation of G_q and G_s proteins, inhibition of voltage-gated calcium channels, activation of inwardly rectifying potassium channels, β -arrestin recruitment and activation of mitogen-activated protein kinase (MAPK) signalling pathways [565]. As a result of CB receptor signalling through multiple effector proteins the probability of biased signalling (ligand-dependent selectivity for specific signal transduction pathways) increases. Biased signalling is thought to occur when different ligands bind to the receptor causing different conformational changes to the receptor enabling the receptor to preferentially signal one pathway over the other [566, 567]. This is attractive, in terms of development of pharmacotherapies for various diseases, as it suggests the possibility of being able to design a drug that will activate/inhibit a specific intracellular pathway.

The endocannabinoid system drives food intake via CB1 [469]. Administration of CB1 agonists induces feeding in rodents [568] and humans [569], while blocking CB1 reduces food intake [570]. Further, overactivity of the endocannabinoid system perpetuates the problems associated with obesity [469] and drugs targeting CB1 have been used therapeutically to manage obesity but withdrawn due to CNS side effects [571]. New evidence indicates the endocannabinoid system can control food intake by a peripheral

mechanism of action [571]. Peripherally-restricted CB1 antagonists, with no direct central effects, reduce food intake and body weight in rodents [470, 471].

2.3.2. The endocannabinoid system and TRPV1

Endocannabinoids, such as AEA, are also endogenous ligands for TRPV1 [572]. Capsaicin, an agonist of TRPV1, has an anti-obesity effect in rodents [386] and reduces food intake in humans [444]. Therefore, the effects of endocannabinoids on food intake will depend on the site of action (Figure 3). This is complicated further as effects may be mediated via cross talk between TRPV1 and CB1. It has been demonstrated that CB1 can enhance or inhibit TRPV1 channel activity depending on whether it activates the phospholipase C (PLC)-PKC or inhibits the adenylate cyclase (AC)-PKA pathways respectively [447] (Figure 3). This interaction appears to be dose-dependent. Moderate to high concentrations of AEA (1 μ M-10 μ M) have been shown to activate TRPV1 in a PKC dependent manner [412, 413]. Conversely, low doses of AEA (3nM-30nM) inhibit TRPV1 activity [450, 573], presumably through CB1 mediated inhibition of AC [574]. Therefore, enzymatic synthesis and breakdown of endocannabinoids are potentially important determinants of TRPV1 activity in tissue, such as neuronal tissue, that co-express TRPV1 and CB1 [447]. A clearer understanding of the role endocannabinoids play in food intake regulation in health and obesity is required to determine the physiological relevance of these different interactions. In mice, the levels of AEA in the small intestinal mucosa and plasma were elevated in high fat diet-induced obese mice compared to controls [470] but still within the low dose range (3nM-30nM) shown to inhibit TRPV1 [450, 573]. Consistent with these observations food intake was by treatment with a peripherally restricted CB1 antagonist [470]. Similar observations were made in humans with plasma anandamide levels elevated in obese compared to

overweight or lean individuals [575], again to levels consistent with TRPV1 inhibition. Therefore, the physiological significance of TRPV1 activation observed at moderate to high concentrations of AEA remain to be determined.

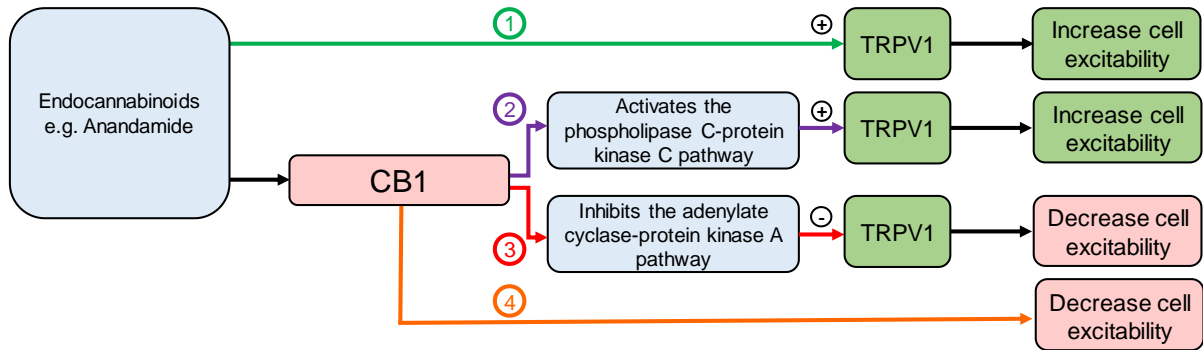


Figure 8.3: Interaction between endocannabinoids, TRPV1 and CB1.

Endocannabinoids can: 1) directly activate TRPV1 leading to cannabinoid receptor 1 (CB1)-independent effects; 2) activate CB1 leading to activation of the phospholipase C pathway enhancing TRPV1 activity; 3) activate CB1 leading to inhibition of the adenylyate cyclase pathway inhibiting TRPV1 activity; 4) activate CB1 leading to TRPV1-independent effects.

3. Involvement of TRPV1 in energy homeostasis

Reports on TRPV1 mediated regulation of energy intake and expenditure are conflicting. Nonetheless, epidemiological data indicate that consumption of food containing capsaicin is associated with a lower prevalence of obesity [433, 576]. Further, in a clinical trial capsinoid supplementation for 12 weeks decreased body weight in overweight individuals compared to the placebo control group [577]. In a separate trial, capsinoid supplementation for only 4 weeks resulted in a trend towards a decrease in body weight

[578]. Under laboratory conditions, dietary capsaicin supplementation had no effect on body weight [386] in mice fed a standard laboratory diet. However, in high-fat diet-induced obese mice, dietary supplementation of capsaicin significantly reduced weight gain [386, 473, 579]. Further, reduced weight gain was also observed in high fat diet mice after topical application of capsaicin [580]. This appears to be consistent across species as a study in rabbits, fed a standard laboratory diet supplemented with cholesterol and corn oil, demonstrated that dietary capsaicin reduced weight gain [581]. In contrast, it has been shown that a 6 week dietary capsaicin treatment had no effect on body weight in high fat diet mice [582]. Weight gain in TRPV1-knockout (KO) mice has been reported to be reduced [439], increased [438] or unchanged [235, 583] compared to wild type mice. This variability may reflect the study design. For example, TRPV1 channels can be activated by the endogenous ligand AEA [572]. The production of AEA is dependent on dietary fat and therefore even slight changes in diet will impact on research outcomes. A summary of the effect of TRPV1 on energy homeostasis in humans can be found in Table 1. The following sections integrate the data on energy intake and expenditure from human and animal studies in an attempt to draw some clear conclusions and directions for further study.

3.1 Role of TRPV1 in energy intake

The effects of capsaicin supplementation on satiety and food intake are illustrated in Table 1. In human studies, dietary supplementation of a TRPV1 agonist such as capsaicin, or the less pungent sweet form capsiate, caused a short-term trend or significant decrease in energy intake along with an increase in satiety [422, 423, 426, 435, 443]. These effects could at least in part be due to the effect of TRPV1 on appetite hormones and/or gastrointestinal vagal afferents. This will be discussed in detail below.

Conversely, other data from human [442, 443] and animal studies [428-430, 432, 581] suggest that dietary supplementation of capsaicin has no effects on energy intake. This could be due to capsaicin mediated TRPV1 desensitisation where food intake is initially reduced, due to capsaicin activation of the TRPV1 channel, but shortly returns to normal, due to a desensitisation of the channel following the initial transient activation [386]. In a Chinese adult cohort study, it has been shown that energy intake depends on the amount of chilli consumed with individuals with chilli consumption below 20g per day and above 50mg per day having reduced and increased energy intake respectively, compared to non-consumers [433]. Therefore, it is possible that at low levels of consumption capsaicin activates TRPV1 leading to a reduction in food intake and at high levels it could be desensitising TRPV1 leading to an increase in food intake. However, this is highly speculative and requires further investigation.

Dietary supplementation of capsaicin can also influence nutrient preference. It has been demonstrated that capsaicin ingestion reduced the desire for and subsequent intake of fatty foods [423, 435, 436], whilst also increasing the desire for and intake of carbohydrates [435, 443]. Conversely, in other studies, capsaicin ingestion reduced the desire for and consumption of carbohydrates, and increased the desire for salt rich foods [423, 437]. The sensory mechanisms responsible for the changes in food preferences remain to be determined.

Table 8.1: Effects of Capsaicin Supplementation on food intake and metabolism in Humans

Capsaicin Dosage	Duration	Appetite Effects	Metabolic Effects			Reference
			Energy Expenditure	RQ Value	Blood Glucose	
Capsaicin (7.68mg/day)	36 hours	↓ Energy Intake Trend ↑ Satiety	-	-	-	[422]
Chilli (1.03g/meal)	24 hours	↑ Satiety	↑ Thermogenesis	-	-	[426]
Capsaicin (7.68mg/meal)	24 hours	No Effects	↑ Energy Expenditure ↑ Fat Oxidation	↓	-	[442]
Chilli (1g/meal)	1 meal	↓ Energy Intake ↑ Satiety Trend	↑ Energy Expenditure	↓	-	[423]
Chilli (0.3g/meal)	5 meals	No Effects	-	-	-	[443]
Chilli (1.03g/meal)	1 meal	↑ Plasma GLP-1 ↓ Plasma Ghrelin Trend	No effect	-	-	[440]
Capsaicin 26.6mg	1 meal	-	-	-	↓	[584]
Capsaicin + green tea	3 weeks	↓ Energy Intake ↑ Satiety	-	-	-	[427]
Chilli 3g + caffeine 200mg	24 hours	↓ Energy Intake ↓ Fat Intake	↑ Energy Expenditure ↑ SNS Activity	-	-	[444]
Capsaicin 150mg	1 meal	-	↑ Fat Oxidation	↓	-	[425]
Chilli 0.9g/meal	2 days	↓ Energy Intake ↑ Satiety	-	-	-	[435]
Chilli with meal	1 meal	↓ Energy Intake Trend ↓ Fat Intake	-	-	-	[436]
Capsaicin 3.5mg with glucose drink	1 meal	-	-	-	↓	[585]
Capsaicin 135mg/day	3 months	↓ Plasma Leptin (likely)	↑ Fat Oxidation	↓	↓	[445]

			due to weight loss)			
Capsaicin 3mg/meal	1 meal	-	↑ Energy Expenditure ↑ SNS activity Effects lost in obesity	-	-	[586]
Chilli 6g in appetiser	1 meal	↓ Energy Intake ↓ Carbohydrate Intake	↑ SNS activity	-	-	[437]
Chilli 10g/meal	1 meal	↓ Energy Intake Trend ↓ Protein and fat Intake	↑ Thermogenesis ↑ Fat Oxidation	↓	-	[437]
Chilli 10g before meal	1 meal	-	No effect	↑	No effect	[431]
Chilli 10g/meal	1 meal	-	No effect	↑	-	[587]

3.1.1 TRPV1 and appetite hormones

There is evidence to indicate that TRPV1 interacts with appetite regulating hormones, most notably, ghrelin, leptin, and glucagon-like peptide-1 (GLP-1). Ghrelin is an orexigenic peptide mainly expressed in the stomach as an endogenous ligand for the growth hormone secretagogue receptor (GHSR) [483]. It is involved in many processes including appetite regulation, secretion of gastric acid, gastrointestinal motility, and regulation of energy storage [588]. It has been reported that TRPV1 activation reduced plasma ghrelin levels [589], which may account for the reduced food intake observed after capsaicin supplementation [422, 423, 426, 435, 443]. However, this requires more intensive investigation. Within the stomach ghrelin maybe involved in the interaction between the endocannabinoid system and TRPV1. CB1 receptors co-expressed with ghrelin in specialised cells within the stomach wall [249]. Ghrelin reduces gastric vagal

afferent mechanosensitivity, in a manner dependent on nutritional status, via action at GHSR expressed on vagal afferents [590-593]. Therefore, although the eating stimulatory effects of ghrelin are not thought to be mediated by vagal afferents [592], ghrelin acting on vagal afferents may impact on the amount of food consumed after the initiation of a meal. Inhibition of CB1 decreases gastric ghrelin secretion with subsequent, vagal afferent mediated, reductions in food intake [249]. Therefore, part of the effect of endocannabinoids on vagal afferent activity maybe mediated indirectly via the activation of CB1 on ghrelin-producing cells. It is conceivable that the inhibitory effects of ghrelin are mediated via TRPV1 considering that, in the CNS, ghrelin effects on supraoptic magnocellular neurones are mediated via TRPV1 [441]. Similar, interactions with the endocannabinoid system are observed centrally in areas associated with appetite regulation, including the hypothalamic arcuate and paraventricular nuclei [377]. A comprehensive investigation of the interactions between the endocannabinoid system, ghrelin and TRPV1 is required to fully understand their role in appetite regulation.

Leptin is a satiety hormone produced and secreted in proportion to the amount of white adipose tissue (WAT). Data suggests that it is also secreted by gastric cells [594]. There is evidence to suggest that TRPV1 and leptin may interact, since TRPV1 $-/-$ mice exhibit increased basal leptin levels, even when normalised to WAT mass [438]. Exogenous administration of leptin normally results in decreased food intake; however, this was not observed in TPRV1 $-/-$ mice [438]. Furthermore, there is evidence for direct interactions between leptin and TRPV1 in certain brain stem regions. For example, TRPV1 activation increased the frequency of miniature excitatory synaptic currents in leptin receptor containing neurons of gastric-related dorsal motor nucleus of the vagus (DMV) [595]. These data suggest that TRPV1 may mediate the effects of leptin; however, further

research is needed to substantiate these claims and to determine if leptin effects in the periphery are also mediated through TRPV1.

GLP-1 is a peptide hormone secreted by intestinal L-cells, pancreatic α -cells, and neurons in the brainstem and hypothalamus [596]. Evidence suggests it is involved in appetite regulation, gastric emptying, gastrointestinal motility [597], insulin secretion, and glucagon inhibition [598]. Capsaicin supplementation enhanced the increase in plasma GLP-1 levels observed after a meal [589] suggesting TRPV1 channel activation may play a role in GLP-1 secretion. This requires further investigation but has the potential to be a peripheral target for the treatment of obesity and/or diabetes.

3.1.2 TRPV1 and gastrointestinal vagal afferents

Gastrointestinal vagal afferents are an important link between the gut and brain. They relay information on the arrival, amount and nutrient composition of a meal to the hindbrain where it is processed and gastrointestinal reflexes are coordinated with behavioural responses and sensations such as satiety and fullness [79, 204, 599]. The role of gastrointestinal vagal afferents in the control of food intake has been extensively reviewed previously [600]. Briefly, as food is ingested the vagal afferents innervating the stomach respond to mechanical stimulation as undigested food enters, fills and distends the stomach wall. There are two fundamental classes of mechanosensitive vagal afferent ending in the stomach according to location and response to mechanical stimulation [601, 602]: mucosal receptors respond to fine tactile stimulation and tension receptors respond to distension and contraction of the stomach wall. Gastric mechanosensitive vagal afferents can be modulated by gut hormones and adipokines in a nutritional status dependent manner [591, 603, 604]. As gastric emptying occurs, nutrients enter the small

intestine and interact with nutrient receptors on the surface of specialised cells within the intestinal mucosa. This initiates an intracellular cascade that culminates in the release of gut hormones [600]. These hormones can act in a paracrine fashion on vagal afferent endings innervating the small intestine and/or act as true hormones by coordinating activities within the gut or by entering the circulation and acting in the brain.

It has been demonstrated that TRPV1 is expressed in rat duodenal [605], mouse jejunal [606] and mouse gastric vagal afferents [235, 387]. Activation of TRPV1, by oleoylethanolamide (OEA), caused depolarisation of nodose neurones and decreased short-term food intake [607]. Further, OEA increased gastric vagal afferent tension receptor mechanosensitivity in lean but not high fat diet-induced obese mice [235]. In standard laboratory diet fed TRPV1^{-/-} mice, the response of gastric vagal afferent tension (but not mucosal) receptors to mechanical stimulation was reduced compared to TRPV1^{+/+} mice [235, 387]. This was associated with an increase in food intake in the standard laboratory diet fed TRPV1^{-/-} mice [235]. However, the increase in food intake could also be due to the involvement of TRPV1 in gut hormone release [435, 440] or its interaction with leptin in central regions, such as the DMV [595], as described in detail above. Nonetheless, this data suggests that TRPV1 is involved in gastric vagal afferent signalling.

In high fat diet-induced obese mice the response of gastric tension receptors to distension was dampened [235] an effect also observed in jejunal vagal afferents [608]. Gastric tension receptor mechanosensitivity in high fat diet-fed TRPV1^{-/-} mice was not significantly different compared to standard laboratory diet fed TRPV1^{-/-} mice [235]. This suggests that disrupted TRPV1 signalling plays a role in the dampened vagal afferent signalling observed in high fat diet-induced obesity, however, this requires further

investigation. Interestingly, CB1 receptors are also expressed in vagal afferent neurons [609, 610] and therefore it is conceivable that there is an interaction between TRPV1 and CB1 in gastric vagal afferent signalling, however, this has yet to be confirmed.

3.2 Role of TRPV1 in energy expenditure

There is increasing evidence that capsaicin ingestion may have desirable metabolic outcomes such as increased metabolic rate and fat oxidation. It was reported that dietary capsaicin supplementation lowered the respiratory quotient indicating decreased carbohydrate oxidation and increased fat oxidation [423, 425, 442, 445]. In contrast, there is data demonstrating that dietary capsaicin increased the respiratory quotient [431, 587]. The differences in study design, which may account for the different outcomes, include method of ingestion (capsule vs meal), active ingredient (capsinoid vs capsaicin) and the population studied (habitual chilli consumers, non-habitual, normal weight, overweight, fitness level). For example, the study by Lim *et al.* specifically used ‘runners’ for their investigation [431]. There is some evidence that capsaicin can elevate energy expenditure by action on the sympathetic nervous system (SNS) or adipose tissue; this is discussed below.

3.2.1 TRPV1 and the sympathetic nervous system

The SNS is involved in many processes and is probably best known for its involvement in the ‘flight or fight’ response. Dietary supplementation of capsaicin increases postprandial SNS activity [437, 444, 586]. Capsaicin excites TRPV1 containing afferent nerves, carrying a signal to the spinal cord [611]. Efferent nerves are then excited by the central nervous system leading to elevated catecholamine (e.g. epinephrine, norepinephrine, and dopamine) release from the adrenal medulla [611-613].

Catecholamines can bind β -adrenergic receptors increasing expenditure and thermogenic activity [587, 614]. This suggests that TRPV1 may directly stimulate heat production. Further, these effects of TRPV1 on SNS activity are lost in obese subjects suggesting TRPV1 dysfunction in obesity [586].

3.2.2 TRPV1 and adipose tissue

Adipose tissue plays a key role in energy homeostasis [615]. WAT generally stores excess energy as lipids, and oxidises these stores when required, whereas, brown adipose tissue (BAT) is specialised for energy dissipation [616, 617]. TRPV1 has been shown to be expressed in 3T3-L1 and HB2 adipocyte cell lines, brown adipocytes, BAT and WAT [618-621]. Data indicate that TRPV1 may prevent the development of mature adipocytes from pre-adipocytes, and decrease their lipid content by increasing lipolysis [386]. This may partially explain the decreased lipid accumulation during dietary supplementation of capsaicin. Further, it has been demonstrated that capsaicin induces browning in differentiating 3T3-L1 preadipocytes [618]. Therefore, TRPV1 could be involved in the browning of WAT and the thermogenic activity of brown adipose tissue (BAT). The levels of TRPV1 mRNA in BAT and WAT are reduced in HFD-induced obesity and leptin receptor deficient mice [621] suggesting possible involvement in the development of obesity.

Browning is a process whereby WAT becomes thermogenic in nature, similar to BAT. The calcium influx from TRPV1 activation may mediate this process by activating the peroxisome proliferator-activated receptor gamma (PPAR γ) and positive regulatory domain containing 16 (PRDM16) pathways [429]. Calcium binds and activates

calmodulin-dependent protein kinase II (CaMKII) leading to the subsequent activation of adenosine monophosphate activated protein kinase (AMPK) and sirtuin-1 (SIRT-1). SIRT-1 deacetylates PRDM and PPAR γ causing browning events such as thermogenesis (Figure 4) [429].

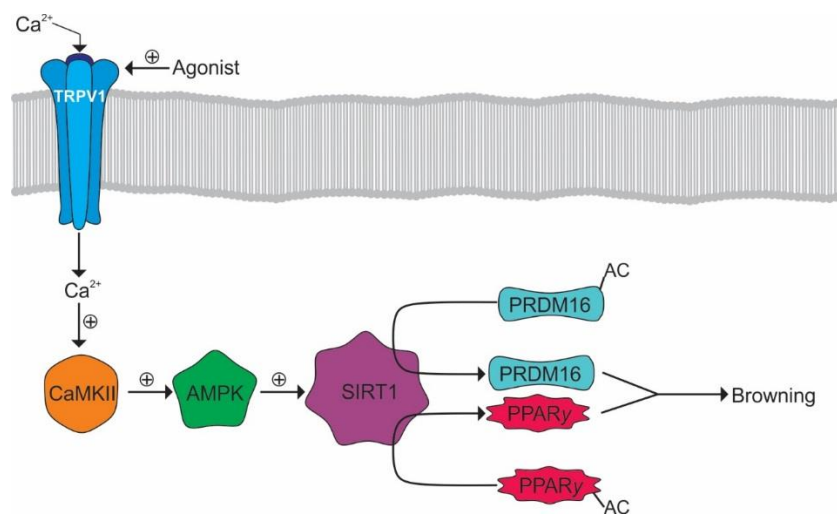


Figure 8.4: Browning of WAT by TRPV1 activation.

Activation of TRPV1 results in Ca²⁺ influx and the subsequent activation of CaMKII. CaMKII facilitates the subsequent activation of AMPK and SIRT1 allowing the deacetylation of PRDM16 and PPAR γ allowing their interaction and promotion of WAT browning.

TRPV1 activation may also promote BAT thermogenesis either through modulation of the SNS or via direct activation of BAT. However, research in this area is limited. The PPAR γ and PRDM16 pathway, previously mentioned in WAT, has been shown to be activated by TRPV1, via SIRT1, in BAT [428, 429]. Further, SIRT1 also activates peroxisome proliferator-activated receptor gamma coactivator 1- α (PGC-1 α). PGC-1 α

transcriptionally activates PPAR α subsequently leading to the production of uncoupling protein-1 (UCP-1) [428]. UCP-1 is a mitochondrial protein that uncouples the respiratory chain triggering a more efficient substrate oxidation and thus heat generation [622]. Lastly, TRPV1 activates bone morphogenic protein 8b in BAT, which also contributes to thermogenesis (Figure 5) [428].

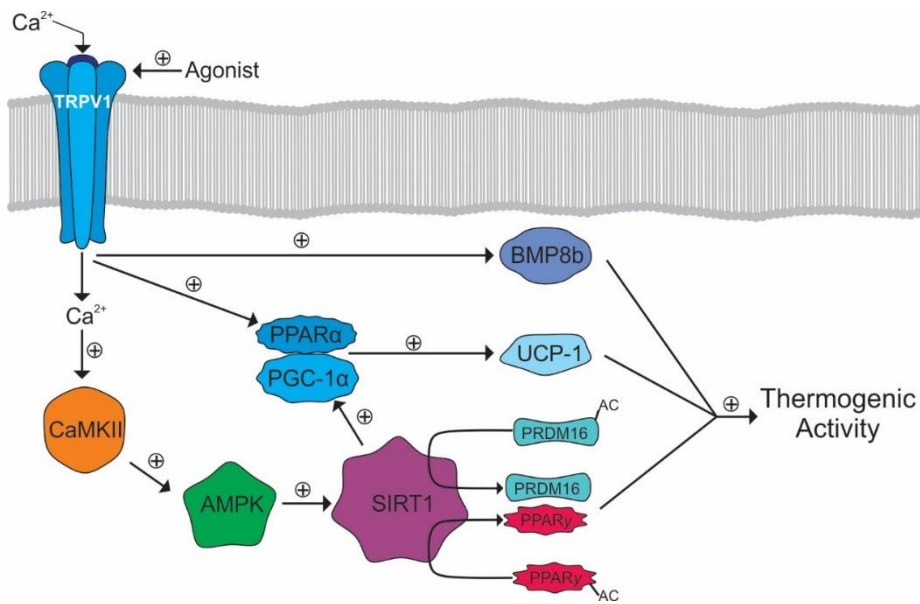


Figure 8.5: TRPV1 mediated activation of thermogenic activity in BAT.

The calcium influx activates CaMKII leading to the eventual activation of SIRT1 and deacetylation of PRDM16 and PPAR γ . SIRT1 also activates PGC-1 α leading to the activation of PPAR α . PGC-1 α and PPAR α transcriptionally activate UCP-1. TRPV1 also activates BMP8b which, along with UCP-1, PRDM, and PPAR γ , cause increased thermogenic activity.

Regulation of BAT by TRPV1 can also be via an indirect mechanism through modulation of the SNS. Activation of TRPV1 in the gastrointestinal tract, by capsaicin or its analogues, has been shown to enhance thermogenesis and activate UCP-1 in BAT in mice

[623, 624] via a mechanism mediated via extrinsic nerves innervating the gastrointestinal tract [624]. This is consistent with reports that TRPV1 ligands (capsaicin and acid) increase gastrointestinal afferent activity [460, 625] via TRPV1 [625]. Further, it has been demonstrated that ingestion of capsinoids increases energy expenditure through activation of BAT in humans [626]. Gastrointestinal vagal afferents have central endings in the nucleus tractus solitaries (NTS). The NTS has projections to BAT [627] where it regulates the sympathetic tone to BAT [628] and has been directly implicated in the control of thermogenesis [629, 630]. Lipid activation of duodenal vagal afferents has been shown to increase BAT temperature via a cholecystokinin dependent mechanism [631]. In contrast, it has been reported that vagal afferent activation decreases BAT sympathetic nerve activity and BAT thermogenesis in rats [632]. Further, glucagon-like peptide-1 activation of gastrointestinal vagal afferents leads to a reduction in energy expenditure and BAT thermogenesis in mice [633]. It is possible that different subtypes of gastrointestinal vagal afferent have different roles in the control of BAT thermogenesis, however, this requires further investigation along with the role of TRPV1 in this gut-brain-BAT pathway.

Capsaicin can also evoke a heat-loss response which could conceivably result in compensatory thermogenesis to maintain thermal homeostasis. Capsaicin evoked complex heat-loss responses have been shown in various mammals including the rat, mouse, guinea-pig, rabbit, dog, goat and humans [634]. In humans, cutaneous vasodilation and sweating in response to hot chilli consumption is well recognised [634]. In the rat it has been demonstrated that capsaicin elicited cutaneous vasodilation resulting in a reduction in core body temperature [635]. Simultaneously, capsaicin also enhanced heat production [635]. In these experiments, it appeared that capsaicin independently

activated pathways for heat production and heat loss and therefore the observed thermogenesis may not be a simple compensatory mechanism in response to heat loss, however, this requires further investigation.

4. Involvement of TRPV1 in diabetes

4.1 Type 1 diabetes

Insulin is a hormone, secreted by β -cells of the pancreatic islets, which regulates blood glucose levels. Type 1 diabetes is an autoimmune disease involving T cell-targeted destruction of pancreatic β -cells. TRPV1 is expressed in sensory nerves innervating the pancreas. Chemical denervation of these TRPV1 containing pancreatic afferents, using high doses of capsaicin (approximately 150mg/kg body weight), significantly reduced blood glucose levels and increased plasma insulin [636], suggesting that TRPV1 containing pancreatic afferents negatively regulate insulin secretion. Further, chemical destruction of TRPV1 expressing neurons in neonatal mice [637] was able to protect the mice from autoimmune diabetes [638]. Chemical denervation of TRPV1 containing pancreatic afferents significantly reduced the levels of pre-type 1 diabetes immune markers such as CD4⁺ and CD25⁺ T-regulatory cells in pancreatic lymph tissue and reduced the infiltration of CD8-CD69 positive effector T-cells [638, 639]; immune cells implicated in the destruction of pancreatic islets in type 1 diabetes. However, as the afferents are destroyed and the treatment is not selective for TRPV1, it is plausible that the observed effects have nothing to do with TRPV1. Pancreatic islets also include resident dendritic cells which are generally believed to express TRPV1 [640-642] although there is some controversy [643]. Activation of TRPV1 channels on dendritic cells could activate cell function including antigen presentation to CD4⁺ T cells. Further,

TRPV1 channels have been shown to be expressed on rat pancreatic β -cells where they control the release of insulin leading to reduced blood glucose levels [644] and capsaicin has been shown to reduce blood glucose by increasing insulin levels in a streptozotocin-induced diabetic rat model [645]. Taken together, these data suggest that TRPV1 may influence insulin secretion and type 1 diabetes acting via a number of different cell types within the pancreas

4.2 Type 2 diabetes

Insulin resistance, closely linked to obesity [646], occurs when cells are less responsive to insulin. As a consequence there is reduced blood glucose uptake leading to increased blood glucose levels. Pancreatic β -cells normally respond to this by increasing output of insulin to meet the needs of the tissues. Development of type 2 diabetes stems from a failure of the β -cells to adequately compensate for insulin resistance [647]. It has been demonstrated that postprandial insulin levels were lower after the consumption of a standardised meal seasoned with cayenne pepper [648]. As the plasma glucose levels were not significantly different from the control group the authors suggested that glucose clearance occurred similarly with lower levels of insulin, implying increased insulin sensitivity after the consumption of the hot meal. Further, consumption of chilli has been shown to decrease postprandial insulin levels in obese subjects [649]. In support of these studies, TRPV1^{-/-} mice have been shown to be more insulin resistant than wild type mice [438].

Type 2 diabetes is believed to be associated with inflammation [650, 651]. It is believed that inflammation in the pancreas leads to an increase in the activity of TRPV1 which contributes to increasing levels of calcitonin gene-related peptide (CGRP) [652]. CGRP

is known to promote insulin resistance and obesity by decreasing insulin release from β -cells [653].

5. TRPV1 as a pharmacological target for obesity and diabetes

Behavioural interventions (e.g. diet and exercise) alone are seldom sufficient for the intervention of obesity and diabetes. Combining behavioural and pharmacological approaches is becoming increasingly more attractive. However, pharmacological interventions can have hard to access targets and/or adverse side effects. TRPV1 is present in the periphery making it an easily accessible target compared to drugs that target the central nervous system. However, TRPV1 interacts with other systems and shares pathways commonly used by other signalling molecules. Therefore, without a clear understanding of the interactions of TRPV1 with other systems, the targeting TRPV1 for the treatment of obesity and diabetes is unlikely to be successful, as evident from the numerous contradictory studies looking at the effect of capsaicin analogues on food intake and weight gain. Data suggest that manipulation of TRPV1 may be possible in such a way to reduce or eliminate any unwanted side effects. For example, three different TRPV1 ligands known to antagonise TRPV1 had different effects on thermoregulation (e.g. hyperthermia, hypothermia, or no effect) [654]. In fact, TRPV1 can be manipulated in such a way, by action at different domains, to eliminate some functions of the TRPV1 channels without affecting others. For example, some antagonists block activation by capsaicin and high temperatures but not activation by low pH [537], and other antagonists block activation by capsaicin but not the activation by high temperature [655]. However, this raises further questions on whether, for example, the observed effects are cell type specific. Again, this highlights the lack of fundamental knowledge on the role of TRPV1

in energy homeostasis and therefore the current challenges of targeting TRPV1 for the treatment of obesity.

6. Conclusion

TRPV1 appears to be involved in energy homeostasis at a number of levels. In the periphery, TRPV1 activation or inhibition can have an impact of appetite and food intake through the control of appetite hormone levels or via the modulation of gastrointestinal vagal afferents, important for determining meal size and meal duration. In addition, TRPV1 plays a role in energy expenditure via heat production, either via direct thermogenesis or as a compensatory mechanism in response to TRPV1 induced heat-loss. Dietary supplementation with TRPV1 analogues, such as capsaicin, has yielded conflicting results with some studies demonstrating a decrease in food intake and increase in energy expenditure and others indicating the converse. This is probably reflective of the involvement of TRPV1 in a multitude of processes regulating food intake and energy expenditure. The story is complicated further by the interaction TRPV1 has with other systems involved in energy homeostasis, such as the endocannabinoid system. In addition, TRPV1 appears to be dysregulated in obesity, possibly due to alterations in the interaction with other systems. Therefore, although it is clear that TRPV1 plays a role in energy homeostasis without improved knowledge of the fundamental physiological mechanisms involved and the interactions with other systems it is impossible to target this system for the treatment of obesity, the maintenance of weight loss and the metabolic diseases associated with obesity.